Early Science at the Upgraded Advanced Photon Source

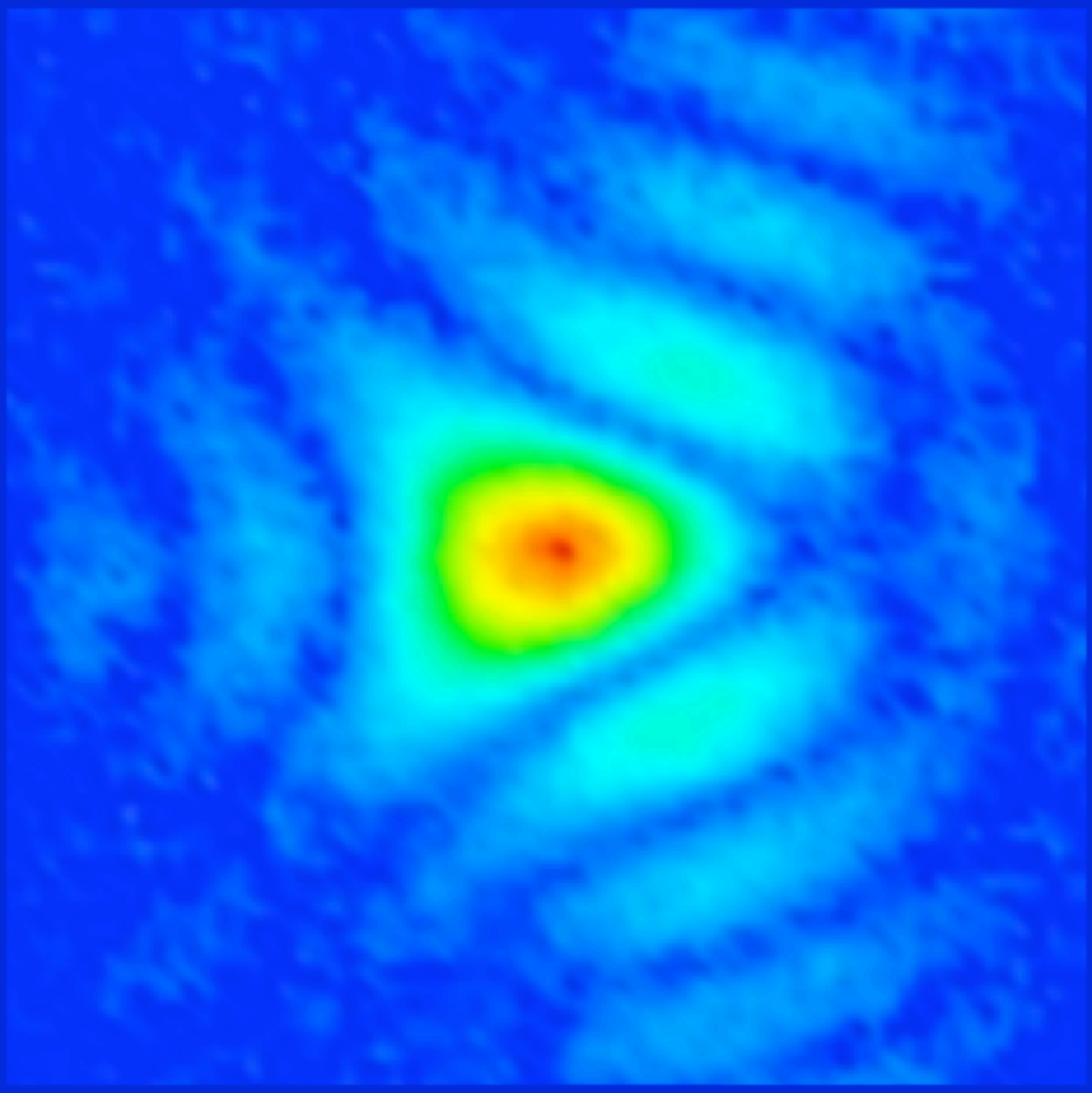

October 2015

Acknowledgments

In addition to the organizers and contributors to the body of this document, listed at the beginning of each chapter, we are deeply indebted to individuals that provided critical reviews and comments on this report:

Ercan Alp, Samuel Bader, Francesco DeCarlo, Kamel Fezzaa, Ross Harder, Chris Jacobsen, Byeongdu Lee, Jörg Maser, Ruben Reiniger, Yang Ren, Gopal Shenoy, Xianbo Shi, Tao Sun, David Vine, Jin Wang, Xianghui Xiao, Linda Young; Argonne National Laboratory.

Roger Falcone, Lawrence Berkeley National Laboratory; Steve Kevan, Lawrence Berkeley National Laboratory; Janos Kirz, Lawrence Berkeley National Laboratory; Richard Leapman, National Institutes of Health, National Institute of Biomedical Imaging and Bioengineering; John Sarrao, Los Alamos National Laboratory; Mark Sutton, McGill University; Paul Voyles, University of Wisconsin-Madison

We also wish to thank Elizabeth Austin for her enormous contributions and sustained effort in managing the assembly and production of this report, and Richard Fenner for assistance with the final version. We must thank Lorenza Salinas, Kerri Schroeder, Elizabeth Stefanski, and Katherine Obmascik for editorial support.

Cover Image

Coherent scattering pattern at the (200) reflection from a 2μm × 1.5μm × 0.7μm ZSM-5 aluminosilicate zeolite particle after heating to 200°C in nitrogen. Data were collected using unfocused coherent x-rays with a wavelength of 0.1380 nm at the 34-ID-C beamline at the Advanced Photon Source. Adapted from W. Cha, N. C. Jeong, S. Song, H.-J. Park, T. C. T. Pham, R. Harder, B. Lim, G. Xiong, D. Ahn, I. McNulty, J. Kim, K. B. Yoon, I. K. Robinson, and H. Kim, Nat. Mater. **12**, 729 (2013), DOI: 10.1038/NMAT3698.

Table of Contents

Preface

A new era is approaching in science and engineering, one that promises a revolutionary understanding of complex materials and chemical processes across the entire hierarchy of lengthscales and timescales. This understanding demands that we move beyond exploration of equilibrium phenomena and beyond models based on idealized materials and systems, so as to be able to create new states and achieve extraordinary new functions. The insights necessary to achieve these goals will be made possible by the extreme brightness of next-generation, accelerator-based x-ray sources. By harnessing the unique properties of light to interrogate realistic systems, we can obtain the dynamic structural, chemical, electronic, and magnetic information needed to progress beyond the current frontiers in the physical and biological sciences.

After decades of continuous development that has yielded enormous scientific impact, storage ring lightsources are on the brink of yet another transformational advance: the multi-bend achromat (MBA), which replaces lattice segments containing a few strong dipole magnets with segments incorporating a larger number of shorter dipole magnets with interspersed magnetic focusing. MBA lattice technology makes it possible for synchrotron x-ray lightsources to approach the diffraction limit at photon energies well into the hard x-ray regime (>20 keV), driving orders-of-magnitude increases in brightness and coherent x-ray flux. These vast improvements in photon beam properties, combined with rapid, ongoing advances in x-ray optics, insertion devices, detectors, computing, and theory will make it possible for researchers at x-ray lightsources to explore a new landscape of scientific problems that previously were completely inaccessible.

As the U.S. Department of Energy Office of Science's Advanced Photon Source (APS) at Argonne National Laboratory considers an upgrade centered on MBA lattice technology, diverse teams of researchers drawn from the APS, its users, and the broader scientific community have come together to study the experimental opportunities that would be enabled by this next-generation storage ring. These ideas have been explored through a series of workshops held at Argonne National Laboratory in 2013, 2014, and 2015 that have drawn tremendous interest and engagement from the scientific community.

Working groups have formed to articulate, in detail, the scientific opportunities that a high-energy lightsource approaching the diffraction limit would enable in six crucial areas: Mesoscale Engineering and Advanced Materials, Soft Materials, Biology and Life Sciences, Chemistry and Catalysis, Environmental Science and Geoscience, and Condensed Matter Physics. Individual workshops focused on these topics were held in May 2015, followed by a summary workshop in July 2015, bringing together nearly 200 researchers from national laboratories, academia, and industry to consider the early science that the APS Upgrade will enable.

This *Early Science* report documents a selection of the most compelling ideas explored in these workshops and captures the scientific community's enthusiastic support of an upgraded APS as an essential investment in the future of science and technology in the United States.

1 Introduction: Early Science at the Upgraded APS

Stephen Streiffer, *Argonne National Laboratory*
Stefan Vogt, *Argonne National Laboratory*
Paul Evans, *University of Wisconsin-Madison*

1.1 Executive Summary

Since the early discoveries of Laue, Compton, Moseley, and the Braggs, the insights derived from x-ray scattering, diffraction, and spectroscopy have been essential in solving challenging scientific problems. X-ray techniques have transformed our scientific understanding of the world around us and have been central to our ability to create new materials with the potential for enormous impacts in engineered structures, pharmaceuticals, electronics, and a host of other applications.

The scientific advances enabled by x-ray techniques have been tremendous and continuous, driven both by discoveries of new fundamental ways to derive insight from the interaction of x-rays with matter and by the evolution of lightsources themselves. As the generation of x-rays has evolved, from the earliest sealed tubes to electron storage rings and free-electron lasers, each new source has yielded transformational levels of insight.

Now a new set of scientific and engineering challenges faces us as we move beyond the study of idealized materials and systems largely in equilibrium. These new challenges are epitomized by questions such as:

- *Can we determine pathways that lead to novel states and non-equilibrium assemblies?*
- *Can we observe and control nanoscale chemical transformations in macroscopic systems?*
- *Can we map and ultimately harness dynamic heterogeneity in complex correlated systems?*
- *Can we understand physical and chemical processes in the most extreme environments?*
- *Can we unravel the secrets of biological function across length scales?*
- *Can we create new materials with extraordinary properties by engineering defects at the atomic scale?*

To answer these questions, it is essential to develop new tools that will provide the means to image heterogeneity across lengthscales and timescales, to explore non-equilibrium structures

and processes and non-stationary phenomena, and to unravel transport in complex systems and observe synthesis in action. A highly multiplexed, continuous source of highly energy-tunable, extremely stable, bright, and coherent hard x-rays will provide the capabilities to realize these objectives.

Although today's lightsources are unable to provide these capabilities, a revolution in accelerator technology stands poised to deliver them. For more than 40 years, electron storage rings have provided hard x-ray radiation with wavelengths roughly comparable to the lengths of atomic bonds and crystalline lattice spacings. Now, further improvements in storage ring design promise to expand their impact by extending performance and capabilities into previously inaccessible regimes.[1] Recent developments in accelerator technology, particularly the multi-bend achromat (MBA) lattice, offer orders-of-magnitude improvement in key parameters, such as coherence and brightness, that are directly relevant to almost all hard x-ray imaging, scattering, and spectroscopy experiments.[2]

With vastly improved coherence, nearly all techniques can become microscopies. The brightness and penetrating x-ray energy of photon beams produced by advanced undulators in an MBA lattice allow one to probe *in situ* and *operando* and to sample vast regions of experimental phase space with sufficient time resolution to capture rare events. Brightness and tunability enable spectroscopies that elucidate chemical, magnetic, and electronic states. For the first time, frontiers inaccessible today will be opened by x-ray instruments that provide 3D resolution from angstroms to centimeters, with time resolution from picoseconds to days, and with the ability to perform ultrasensitive trace element analysis, to the level of a few atoms. The coherence of light produced by such a source in itself represents a grand new frontier of scientific inquiry, and promises the highest spatial resolution even in non-periodic materials, with resolution down to below 1 nm, allowing atoms to be localized. Dramatic improvements in coherence also provide the foundation to explore novel time and space correlations, opening up the possibility of observing continuous, atomic-scale dynamics down to nanoseconds and of obtaining deterministic insight into phenomena as diverse as growth mechanisms and stability of materials, deformation and diffusive motion, and stick-slip motion in microfluidic flow. In the high-energy regime (x-ray energies above 20 keV) the APS Upgrade (APS-U) will improve unfocused flux density by an order of magnitude, greatly enhancing the majority of high-energy techniques. Even more exciting is the prospect of conducting coherence- and brightness-driven experiments at high x-ray energies. Today, nearly all such experiments are carried out at energies below 10 keV; coherent flux is simply insufficient at the higher energies required to penetrate deep into materials or systems with complex/extreme sample environments. The orders-of-magnitude increase in brightness in the harder x-ray regime afforded by the APS-U will at last enable application of coherence-based methods in the energy range well above 20 keV.

With such a lightsource, the scientific and engineering community will have the tools necessary to map all of the critical atoms in a cubic millimeter, bridging the length spectrum from atoms to nanostructure to grains deep within real materials under realistic conditions. Imaging continuous processes down to the 100-ps timescale makes it possible to explore phenomena ranging from fast chemical reactions to diffusive dynamics to lifetime failure mechanisms. New approaches will be enabled that have sufficient sensitivity to spatially resolve the extraordinarily weak scattering or absorption from inhomogeneous collective excitations that

produce novel electronic and magnetic states. Furthermore, the MBA technology can be deployed through a significant upgrade of an existing electron storage ring, leveraging the nation's substantial investments in existing infrastructure.

The proposed upgrade to the U.S. Department of Energy (DOE) Office of Science's Advanced Photon Source (APS) at Argonne National Laboratory will create a synchrotron x-ray lightsource optimized to produce hard x-rays with a high degree of spatial coherence. The upgraded source will exceed the capabilities of today's synchrotrons by two to three orders of magnitude in brightness and coherent flux in the hard x-ray range, enabling a transformational range of new probes for structure, properties, and functionality of matter. A greatly increased flux of spatially coherent x-rays will provide an unprecedented level of understanding (and a crucial step toward control) of nanometer-scale heterogeneity and fluctuation dynamics in matter ranging from "soft" biomolecules to "hard" structural materials.

The APS Upgrade's increase in coherence will particularly benefit three specific types of x-ray science techniques: (1) Intensely focused and coherent x-ray beams will dramatically advance nanoscale imaging, nanospectroscopies, and nanodiffraction; (2) coherent diffractive imaging and ptychography will reach spatial resolution approaching atomic lengthscales and permit time-resolved studies; and (3) the statistical information derived from photon correlation spectroscopy will open up previously inaccessible timescales and lengthscales. These advances in the capabilities of x-ray science will prove crucial in meeting the series of challenges the scientific community has articulated in a range of recent studies. Addressing the grand challenges identified by the DOE Basic Energy Sciences Advisory Committee (BESAC) requires understanding and controlling matter at a level that is not possible with the present generation of experimental tools.[3] The more recent and more detailed set of critical scientific challenges that have been identified as transformative opportunities by the BESAC demonstrate the critical importance of heterogeneity, interfaces, and disorder, and the need for thorough, real-time, multi-scale studies of heterogeneous populations.[4] These challenges include the need to create non-equilibrium states of matter, to harness coherence in light and matter, to improve the precision and versatility of synthesis, and to understand correlated electron systems. As the early experiments presented here demonstrate, it is precisely challenges at this level that the APS-U addresses.

The development of the upgraded APS is being accompanied by simultaneous advances in data analysis, theory, and computation that will yield new combinations of simulation and experiment. Fundamentally, the lengthscales and timescales of theory and experiment are converging with significant gains from both ends. The rapid expansion in the size and time ranges of the systems that can be considered using computational techniques will make it possible to perform precise first-principles simulations of nanoscale objects identical to those probed experimentally at new lightsources. X-ray methods will be used to extract new parameters that can then be incorporated into thermodynamic and statistical mechanics models. Similarly, rapid advances in detectors and optics, together with the far higher fluxes provided to imaging techniques, will make it possible to carry out multi-modal experiments spanning vast ranges of characteristic times and spatial scales.

As computational techniques and technologies progress, new methods for extracting insight from massive volumes of data will make it possible to use the upgraded APS to probe complex

hierarchical systems that previously have been impossible to study with precision. There is a tremendous synergy between the very high rate of data acquisition at the APS-U and the ongoing national investments in computational resources, including leadership-class computing facilities and field-specific computational science programs. In addition to providing the means to create more precise large-scale simulations, advances in computation promise to bring rapid multidimensional data analysis to three-dimensional microscopy measurements, to provide simulations that can be conducted during the course of experimental studies (simulation-in-the-loop), and to offer new tools that integrate near-real-time modeling, data acquisition, and advanced analysis methods.

This *Early Science* document presents both an overview of the capabilities of the APS-U and a selection of detailed studies of exemplary areas in which those capabilities will enable solutions to challenging problems in science and engineering. The directions presented here reflect the continuing development of ideas that recognize the scientific importance of highly coherent x-ray beams. (In particular, a report on diffraction-limited storage rings in both the soft- and hard-x-ray regimes was developed in 2013 in response to a request from BESAC for a study of the potential scientific impact of improvements in storage ring technology.[5]) The first experiments detailed in this report are divided into six areas: Mesoscale Engineering and Advanced Materials, Soft Materials, Biology and Life Sciences, Chemistry and Catalysis, Earth and Environmental Sciences, and Condensed Matter Physics. Key ideas in each of these areas were developed and quantitatively documented by working groups chaired by scientific leaders and involving participants from a wide range of institutions. This multi-year process, which drew on the insights and expertise of hundreds of individuals, included: an October 2013 APS workshop to introduce the lightsource user community to the scientific directions enabled by an MBA-lattice-based hard x-ray source;[6] an international workshop held at the APS in 2014 on the broad range of diffraction-limited lightsource;[7] six topical workshops at the APS in May–June 2015;[8] and a summary workshop held at the APS in July 2015.[9]

1.2 A Nearly Diffraction Limited Hard X-ray Source: Capabilities of the Upgraded Advanced Photon Source

A series of recent advances in the technology of electron storage rings have allowed the scientific community to reconsider the ways in which hard x-rays can be used to solve challenging scientific problems. Most notably, new magnet and vacuum technologies have made possible tightly-packed MBA lattices.[10,11] Further advances include the highly successful development of top-up operation (i.e., the maintenance of an essentially fixed storage ring current via frequent injection of electrons) and the prospect of swap-out injection, which make it possible to accommodate the shorter beam lifetime and corresponding higher losses that result from an aggressive lattice design. Additional improvements in simulation, optimization, and alignment make it possible to predict, with an extremely high degree of confidence, that a lightsource incorporating these advances can be built and operated successfully.[12] This prediction has been supported by the initial success of projects to construct smaller, 3-GeV sources based on MBA technology, such as MAX-IV in Sweden, which was able to first store beam in August of 2015.

The development of the MBA lattice addresses a longstanding challenge in electron storage ring design: the comparatively large electron beam emittance in the horizontal direction. The large horizontal electron beam emittance of present storage ring lightsources is caused by the bending magnets used to deflect the electrons to maintain their closed orbit. In this direction, the electron beam emittance is given by:[13]

$$\varepsilon_x = C_L \frac{E^2}{N_D^3} \quad (1)$$

Here C_L is a parameter termed the lattice constant, N_D is the total number of dipole magnets, and E is the electron energy.

Storage rings have conventionally operated under conditions for which improvements in electron emittance lead to improved photon brightness. At very small electron emittances, however, the storage ring reaches the diffraction limit, the point at which reducing the emittance of the electron beam cannot further reduce the emittance of the photon beam. The electron emittance at which the diffraction limit is reached is termed the diffraction-limited emittance ε_r, given by the product of the size σ_γ and divergence σ_γ' of the emitted photon beam.

$$\varepsilon_r = \sigma_\gamma \sigma_\gamma' = \frac{\lambda}{4\pi} \quad (2)$$

The spectral brightness of the resulting radiation depends on the convolution of the electron beam emittance and the diffraction-limited photon emittance. At a photon energy of 10 keV (wavelength λ = 1.24 Å), the diffraction limit is reached at a horizontal emittance of 10 pm, indicating that an electron storage ring with an emittance of tens of pm will be in the regime of the diffraction limit for this photon energy. The fraction of photons in a single coherent mode, f_{coh}, is given by the ratio of the coherent flux in a single transverse mode at a particular wavelength $F_{coh,T}(\lambda)$ divided by the total flux at that wavelength $F(\lambda)$. Equivalently, the coherent fraction can be estimated using the ratio of the true emittance of the emitted radiation (the convolved electron beam and diffraction limited photon emittance) in the horizontal x and vertical y directions, given by $\sigma_{Tx}\sigma_{Tx}'$ and $\sigma_{Ty}\sigma_{Ty}'$, to the diffraction-limited emittance $\sigma_\gamma\sigma_\gamma'$:

$$f_{coh} = \frac{F_{coh,T}(\lambda)}{F(\lambda)} = \frac{\sigma_\gamma \sigma_\gamma'}{\sigma_{Tx}\sigma_{Tx}'} \frac{\sigma_\gamma \sigma_\gamma'}{\sigma_{Ty}\sigma_{Ty}'} \quad (3)$$

Through the APS Upgrade, the existing double-bend achromat lattice of the APS storage ring will be replaced with a seven-bend achromat; the increase in N_D will result in a significant decrease in the emittance of the APS. Additionally, the storage electron energy will be lowered from 7 GeV to 6 GeV. In combination, these two changes will reduce horizontal emittance by a factor of 50 in comparison to the present APS. A further increase of brightness (x-ray flux per unit area per unit solid angle in a specified bandwidth) will be accomplished by increasing stored current to 200 mA, and additional gains will be achieved by optimized insertion devices. The key features of the upgraded APS storage ring are summarized in Table 1.

Table 1. Technical Features of the Upgraded APS Storage Ring

6 GeV, 200 mA, swap-out injection
Multi-bend achromat (7 bend) lattice
High-brightness, ultra-low emittance (ε_x, ε_y): 50-70 pm, 5-50 pm

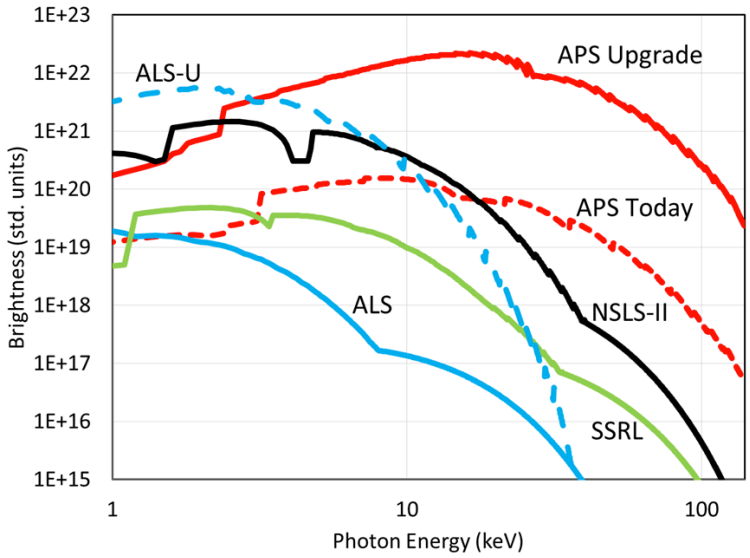

Fig. 1. Brightness as a function of x-ray photon energy at top beamlines among synchrotron radiation sources operated by the U. S. Department of Energy. Units are photons s^{-1} $mrad^{-2}$ mm^{-2} in 0.1% energy bandwidth.

At the upgraded APS, the electron beam emittance will approach the diffraction limit in the hard x-ray energy range, with a predicted horizontal emittance of approximately 60 pm. At a photon energy of 10 keV, the APS-U thus provides a coherent fraction of approximately 10%, a factor of 100 better than the present APS. The trend continues and actually improves across all photon energies, so that the coherent flux at a photon energy of 50 keV at the upgraded APS will equal the coherent flux at 10 keV today. In comparison with other present and planned synchrotron radiation lightsources in the United States, the APS Upgrade uniquely provides high brightness at very high photon energies of 20 keV or more, as shown in Fig 1.

The emittances in the vertical and horizontal can be made approximately equal at the upgraded APS, a situation that is termed “fully coupled.” As a result, photon beams will be much rounder in this mode than at the present APS. Fully coupled beams will be available for all fill patterns and operational modes, and will provide approximately spatially symmetric photon beam properties that will be particularly useful for imaging experiments. Alternative operation schemes with lower coupling (e.g., 0.10) will be available in 324-bunch mode to provide the highest possible brightness. In addition to installation of the MBA lattice and the increase in stored current, the plans for the APS Upgrade include a major modification of the injection system to allow on-axis injection, which is believed to be necessary given the small dynamic aperture of the MBA lattice and the short lifetime inherent in operating modes with small numbers of bunches.

The brightness also depends on the magnetic insertion devices serving as sources of x-ray radiation. The APS Upgrade will include development and application of new magnetic insertion devices that act as the source points for the x-ray emission. Superconducting undulators are expected to be the technology of choice for use above 20 keV. Permanent magnet revolver undulators (with up to three different magnetic periods) will be available for some beamlines. Specialized undulators (e.g., horizontal undulators and helical devices) are being studied for possible implementation.

The APS Upgrade will include a suite of new and upgraded beamlines designed for best-in-class performance with the high-brightness source. Additionally, optics and detector improvements to remaining beamlines will take full advantage of the MBA source properties. Stability

improvements will be made throughout. Nearly all of the existing conventional facilities (including buildings and utilities) will remain and be reused.

The APS Upgrade maintains the key advantages of a storage ring-based lightsource. Storage rings provide stable photon beams with excellent positional stability and essentially perfect photon energy stability. The turn-to-turn intensity stability is at the shot noise limit. The energy and polarization of photons delivered to experiments can be varied rapidly and easily. Storage ring lightsources also can serve more than 50 instruments simultaneously, with full stability and independent tunability of key photon parameters.

The international community has recognized the tremendous scientific potential of these new lightsource technologies and capabilities. Around the world, diffraction-limited capabilities are being incorporated into upgrades of existing facilities and construction of new lightsources. The world's first MBA-based lightsource is under construction at a medium-electron energy storage ring at MAX–IV (Sweden). Sirius (Brazil) will employ similar technology. Upgrades involving MBA storage rings at higher electron energies, similar to the APS Upgrade, are planned or in progress for the European Synchrotron Radiation Facility (France) and SPring-8 (Japan). An MBA storage ring also is planned for the new Beijing High Energy Photon Source (China) and for the upgrades of the Swiss Light Source (Switzerland) and Advanced Light Source (LBNL, USA).

1.3 Coherence and Brightness in Hard X-ray Science

The high coherent flux resulting from the APS Upgrade vastly expands the range of problems that can be addressed using x-ray microscopy, coherent x-ray scattering, and x-ray photon correlation spectroscopy. An orders-of-magnitude increase in the flux of coherent x-ray photons will enable these techniques to reach length- and timescales that are impossible to attain with present x-ray sources. In addition, the reduced horizontal emittance of the x-ray beam will allow new, highly efficient optical designs enabling advances in other techniques, such as inelastic scattering methods, in which the interaction with the sample is not based on coherent scattering. A cross-section of the APS-U's experimental capabilities is shown in Table 2 below.

Table 2. Highlights of Experimental Capabilities of the Upgraded APS

Highest resolution hard x-ray scanning probe imaging, down to 5 nm (20 nm in complex *in situ / operando* sample environments)
Ptychography and coherent imaging with spatial resolutions down to the localization of single atoms, as well as the ability to follow dynamic processes in close to real time.
High energy, highest-resolution 3D imaging, down to 100 nm at 80 keV
Extension of coherence techniques to high energies (E>20 keV), for instance allowing combination of ptychography with high-energy diffraction microscopy measurements to yield local ~10-nm resolution in global fields of view
Trace element sensitivity down to below 10 atoms
X-ray photon correlation spectroscopy down to 10s of ns correlation times, and higher order correlation spectroscopies
High-pressure science at TPa and high temperature, with sensitivity to 10-nm objects

New Methods in X-ray Microscopies

APS-U's brightness will allow generation of nanofocused hard x-ray beams with increased flux densities. At present, nanofocusing optics based on mirrors, Fresnel zone plates, and multi-layer Laue lenses can produce focal spots with sizes as small as 10 nm but can focus only a small fraction of the total x-ray flux.[14] APS-U will make it possible to use highly efficient x-ray mirror optics to focus the full x-ray flux into sub-micron spots and to produce nanofocused beams with intensity two to three orders of magnitude higher than at present sources. Increased coherence also will directly leverage more advanced optics, including encoding of phase or intensity information into the focused beam and introduction of beams with non-zero photon orbital angular momentum.[15,16]

The use of focused beams is particularly important for spectroscopic techniques for which the interaction with the sample is fundamentally inelastic. The APS-U will lead to a new regime of scattering and spectroscopy with nanobeams via the full realization of nanobeam x-ray absorption spectroscopy, x-ray fluorescence and x-ray emission spectroscopies, and nanobeam inelastic scattering methods.

There are numerous highly relevant applications of the improved nanobeam techniques. These include x-ray fluorescence nanotomography for the 3D elemental mapping of functional mesostructures, biological materials, and geological materials, as well as more precise fluorescence microscopy allowing direct study of nano-toxicity or catalysis in complex, active environments. Intense, focused x-ray beams uniquely enable studies that employ structural, chemical, magnetic, and electronic contrast mechanisms and require the combination of large two- or three-dimensional fields of view at high spatial resolution (rare events or needle-in-a-haystack problems), as well as time resolution. In addition to fluorescence spectroscopy, other methods based on spectroscopic signatures that previously have been too weak to use with focused beams now become suitable for microscopy, allowing fluctuations and correlations as well as magnetic, electronic, and plasmonic excitations to be mapped with nanometer resolution. Nanoscale inelastic spectroscopies will reveal the electronic texture and coupled excitations in heterogeneous materials and nanostructures. The combination of nanobeam techniques with timing techniques will permit ultrafast microscopy probes in the picosecond/nanometer scale, which is highly relevant to the propagation of excitations. Microscopy can be readily combined with coherent scattering, as illustrated in Fig. 2, to further enhance the achievable spatial resolution via lensless imaging approaches such as ptychography.

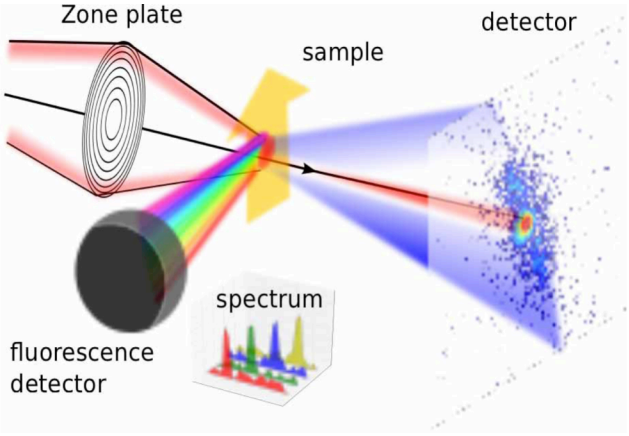

Fig 2. Orders-of-magnitude increases in nanofocused flux directly enable studies using inelastic probes, for example, x-ray fluorescence and related techniques, and lensless imaging approaches based on the combination of scanning probe microscopy with scattering, including ptychography. Figure courtesy Y. Shvyd'ko.

A range of challenges in nanobeam techniques also must be addressed before their full scientific opportunities can be realized. A more fundamental understanding of the cascades of effects resulting from the interaction of x-rays with soft and hard materials will be required to fully understand radiation damage and to develop strategies for its mitigation. Such studies of the fundamental mechanisms of radiation damage in increasingly complex systems are being carried out in both hard and soft materials. The use of nanobeam spectroscopies will require complex methodology development and will impose stringent engineering requirements on mechanical and environmental stability and sampling speed, among other factors. Important future advances in instrumentation include eV-scale energy resolution at the detector, combined with large solid angles and high dynamic range, to enable routine x-ray emission spectroscopy at the nanometer scale, as well as optics permitting nanometer-scale focusing of hard x-rays with high efficiencies.

X-ray Coherent Imaging Techniques

The high coherent flux provided by the APS Upgrade will enable significant advances in coherent imaging techniques, which provide quantitative 3D images of the real and imaginary contributions to scattering, yielding information about magnetization, composition, bonding configuration, and strain. Key systems for which coherent imaging will be essential include surfaces and interfaces, disordered materials, and heterogeneous bulk materials.

In the far field, the intensity of coherently scattered x-rays is distributed in a complex interference pattern, termed a speckle pattern.[17] Smooth intensity distributions in diffuse scattering or small-angle x-ray scattering are formed when speckle patterns are summed incoherently over large regions of the sample or created with incoherent x-ray beams. With spatially coherent sources of x-rays, however, the speckle pattern is preserved, as shown in Fig. 3(a).[18,19] Crucially, the distribution of intensity in the scattering pattern of coherent x-rays reflects the exact structure of the sample rather than an incoherent average over many configurations. The information in coherent diffraction patterns can be used in two ways: first, the distribution of scattered intensity can be inverted to obtain an image of the sample, in a process known as coherent diffractive imaging (CDI). A second series of methods, termed x-ray photon correlation spectroscopy (XPCS), is based on a statistical analysis of the variation of the speckle pattern as a function either of elapsed time or of an externally varied quantity, such as magnetic field, electric field or temperature. (XPCS is discussed further in Section 3 below.)

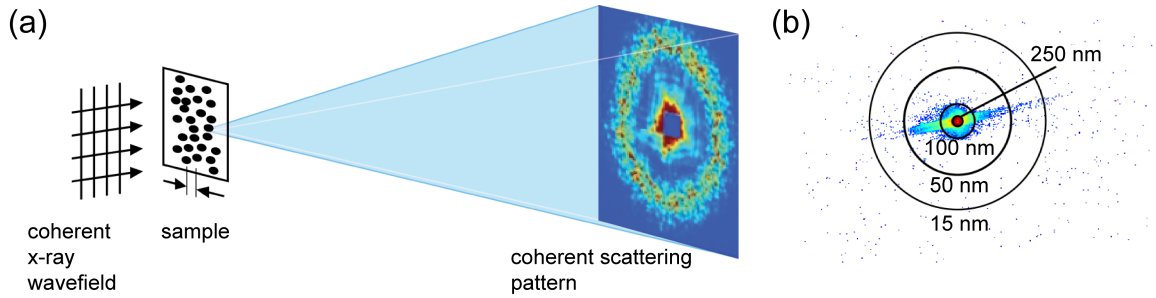

Fig. 3. (a) Coherent x-ray scattering, shown schematically at angles near the transmitted x-ray beam. Similar scattering patterns arise at structural Bragg reflections.[19] (b) Scaling of the resolution of reconstructed images with the volume of reciprocal space over which the coherent diffraction pattern can be recorded. High-resolution images require recording weak signals over large volumes and thus benefit from high coherent x-ray flux.[18]

Imaging methods based on coherent diffraction ultimately provide resolution limited by wavelength and sample stability, not by the optics used to form the image. The APS Upgrade will extend CDI to higher resolution, enable the visualization of fast dynamics using coherent imaging methods, expand the maximum size of objects that can be imaged with nanoscale resolution by increasing the dynamic range of experimental measurements, and widen the range of phenomena that can be studied by increasing the coherent flux at high photon energies.

As shown in Fig. 3(b), achieving high spatial resolution in coherent diffractive imaging requires sampling coherent scattering intensity distributions at large wavevectors.[18] The high coherent flux of the APS Upgrade will allow coherent diffraction patterns to be sampled at sufficiently high wave vectors to provide high-resolution images within experimentally relevant timescales.

For those familiar with present third-generation lightsources, some key quantitative comparisons are useful in understanding the designs of experiments to be done at the upgraded APS facility. The APS Upgrade will allow coherent surface/interface scattering with fluxes that are comparable to the intensities of Bragg reflections at the present APS. For example, it will be possible to probe the surface reconstructions of individual nanoparticles (NPs) via crystal truncation rod analysis. Resonant magnetic scattering intensity will be comparable to the present intensity of Bragg reflections from nanoparticles, making possible 3D CDI maps of magnetic structure within nanomaterials. Similar resonant scattering techniques will allow imaging of spin and orbital ordering near domain boundaries.

Further significant advances in the application of CDI techniques will be made by extending coherent diffraction techniques to far higher photon energies than are possible today. As was mentioned briefly above, the APS Upgrade will provide a coherent flux at 50 keV that is comparable to the current coherent flux at 10 keV, extending coherent techniques to address a new frontier of complex 3D samples with particular relevance to *in situ* deformation and function of structural and electrochemically active materials.

Ptychography, a variant of coherent diffractive imaging, adapts CDI to continuous samples by using a series of coherent diffraction patterns collected as the beam is scanned across the sample. The spatial resolution available via ptychography is better than the focused spot size and resolution limit imposed on present scanning techniques by x-ray optics, and is, like CDI, fundamentally limited only by coherent flux and x-ray wavelength. Ptychographic images can be formed in either two or three dimensions, allowing 3D imaging of internal states and of surfaces.[20,21,22,23,24] As in conventional coherent diffractive imaging, the mathematical methods used to create ptychographic images naturally combine transmission or scattering contrast mechanisms to recover both absorption and phase contrast. In addition, the technique can recover the point-spread function of the instrument, which can be used to increase the native contrast mechanisms (e.g., x-ray fluorescence for visualization of elemental content) via deconvolution techniques.[25] Challenges in imaging and ptychography include radiation damage, in particular for soft materials. Rapid advances in data analysis and computation will make ptychographic methods far more accessible in the future.

Near the Bragg condition, the imaginary part of the scattering pattern depends on the relative positions of atoms; thus strain can be imaged via variations in the imaginary part of the scattering factor. The APS Upgrade's improvement in coherent flux creates opportunities to

employ CDI and ptychographic techniques near the Bragg condition that will offer exquisite sensitivity to the positions of atoms—perhaps even reaching the atomic resolution limit, as discussed in Chapter 3 below.

X-ray Photon Correlation Spectroscopy

The time evolution of complex systems is reflected by variations in their coherent x-ray scattering patterns. Statistical analysis of the time dependence of coherent scattering patterns (e.g., x-ray photon correlation spectroscopy, or XPCS), provides insight into the dynamics. Rigorous statistical mechanical methods relate the dynamical evolution of scattering patterns to fluctuations, allowing quantitative comparisons with theory. The contrast leading to coherent diffraction can arise from chemical, magnetic, and structural features, so XPCS provides insight into the time dependence of a multitude of complex phenomena. This document describes applications to self-assembly, domain wall motion, and the fluctuation of complex order parameters.

XPCS provides insights into dynamical phenomena that cannot be obtained via pump-probe techniques. This distinction is important because many physical processes cannot be selectively and reproducibly driven by external stimuli and are thus fundamentally un-clocked. Examples of such random or un-clocked processes, described extensively in the following chapters, include the nucleation of new phases, the fluctuation of magnetic and electronic domains, and the reconfiguration of macromolecules. These processes are inaccessible at their fundamental timescales because of the limitations of present x-ray lightsources.

In practical terms, the time resolution of XPCS measurements is determined by the acquisition time required to reduce the statistical uncertainty in the measurement of the correlation functions used in the analysis of the data. Because measurements are required at two separate times, the ultimate accessible time resolution is proportional to the square of the coherent flux, which scales as the square of the brightness. The APS Upgrade increases coherent flux by factors of up to nearly three orders of magnitude and thus improves time resolution by up to five to six orders of magnitude. Based on this scaling consideration, the APS Upgrade will enable nanosecond-resolution studies of nanometer-scale fluctuations and, potentially in certain instances, time resolution to 100 ps for correlations detected within the duration of a single x-ray pulse.

The importance of matching the timescale of XPCS measurements to the physics of the system is illustrated by the ensemble of diffusing particles shown in Fig. 4(a).[26] Measurements with the present APS have time resolution that effectively convolves multiple times in order to achieve sufficient counting statistics in the diffraction pattern, as is apparent in the smearing of particle positions and the loss of the speckle diffraction pattern. Higher coherent flux captures the speckle pattern corresponding to the instantaneous positions. The impact of the coherent flux on the dynamic range of XPCS is further illustrated in Fig. 4(b), which shows correlation functions from a gel-forming colloidal suspension of nanoparticles at two points near the gel transition.[27]

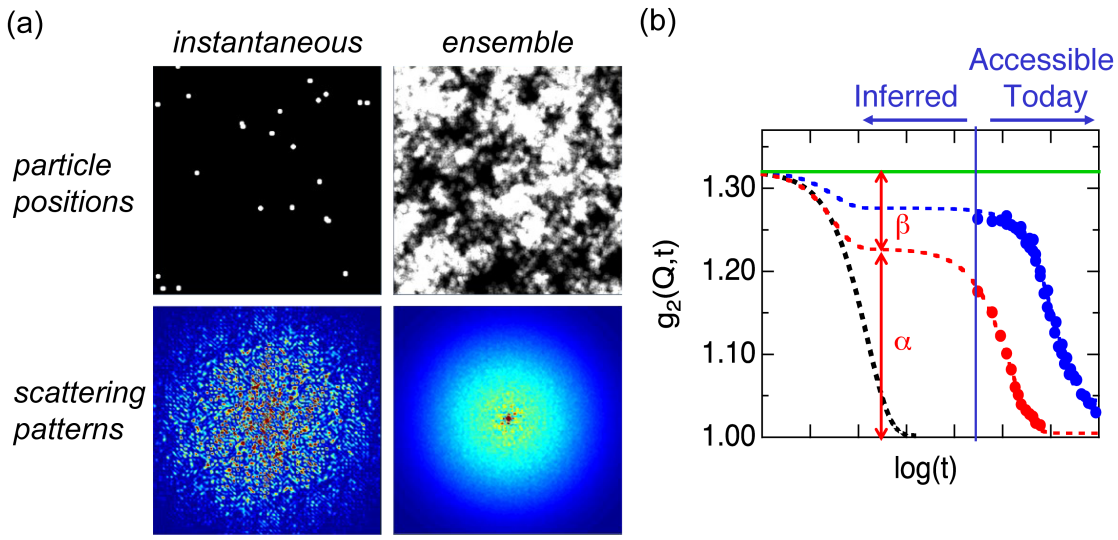

Fig. 4. (a) Coherent diffraction patterns of diffusing particles captured with sufficient time resolution (left) reflect effectively instantaneous positions of the particles and thus capture the diffusion process. Scattering experiments average over the dynamics when acquired with poor time resolution (right).[26] (b) Correlation functions $g_2(Q,t)$ measured on a soft glassy material (nanocolloidal gel) at existing (solid circles) and proposed (dashed) U.S. sources of synchrotron radiation. Insight into short-time dynamics is not available at present sources.[27]

Entering the gel phase, the colloidal dynamics are characterized by an increasing separation between fast, localized motions that cause a partial decay in the correlation function and slow modes that lead to its terminal decay. At present, only the long-timescale dynamics are observable, and features of short time effects can only be inferred. The APS Upgrade will permit access to the entire range of the dynamics.

The APS Upgrade also will permit XPCS studies to be conducted at far higher photon energies, providing, for the first time, access to the interiors of complex materials and to resonant edges.

Advanced X-ray Optical Design, Experimental Design, and Methods Development

The designs of x-ray optics, including mirrors, monochromators, and other basic beamline-optical building blocks, are intimately connected to the brightness of the x-ray source. The APS Upgrade will drive fundamental redesign of x-ray optics; as a result, x-ray scattering methods that do not rely directly on beam coherence for scattering or focusing also will benefit directly from the APS Upgrade. With respect to inelastic spectroscopy, for example, the high brightness of the APS Upgrade will permit higher spectral and momentum-transfer resolution and will simultaneously increase count-rates through the use of imaging broadband 0.1-meV-resolution inelastic x-ray scattering monochromators and spectrometers.[28]

Development of sources based on the MBA lattice will require a significant reconsideration of experimental designs in order to understand and, where possible, mitigate the effects of beam-induced changes in the structure and chemistry of samples. These issues are discussed in detail below in the context of the Soft Matter and Biology & Life Sciences chapters, in part because soft materials have proven most sensitive to intense x-ray beams. Experimental design issues, such as limiting exposure, cryogenic sample temperatures, rapid sample exchange, and efficient post-sample optics and detectors, have been raised very frequently throughout the APS-U

science planning process. Also critical to optimized performance of the upgraded APS is the development and integration of optimized data acquisition and analysis strategies that take advantage of recent and ongoing developments in the field. This is needed to effectively deal with rapidly increasing data volumes (especially after the Upgrade) and also to enable targeted measurements that will provide exactly (and only) the information required to address the scientific problem at hand, thus minimizing exposure.

Experiments at the upgraded APS will make full use of these ongoing developments in both instrumentation and methods, through beamlines engineered to provide comprehensive "systems" solutions. For example, the vastly improved brightness will be paired with significantly improved nano-focusing optics, faster detectors, and advanced data acquisition strategies (e.g., dose fractionation) to not only provide significantly improved acquisition speed (source and detectors), but also simultaneously improved spatial resolution (source and optics), increased field of view (source), and in 3D as opposed to 2D sampling (methods).

1.4 Early Scientific Opportunities

Mesoscale Engineering and Advanced Materials

The increasingly rapid development of novel materials has been driven by improved synergies between synthesis techniques, theory, and characterization, which have created a cycle of increasing knowledge and greater opportunities to create advanced materials by design. The APS Upgrade plays a key role in this cycle by providing unique, non-destructive characterization tools to probe the structure, topology, electronic configuration, and dynamics under operational conditions. This document highlights three particularly important scientific challenges: the nanoscopic origins of turbine blade dwell fatigue, mesoscale complexity in batteries, and structure and dynamics during materials synthesis. These areas offer scientific, technological, and industrial relevance; each serves to highlight specific key aspects of the APS Upgrade's capabilities.

Soft Matter

Soft matter concerns materials and related phenomena at the juncture of physics, chemistry, biology, and engineering; it is a discipline that spans polymers, liquid crystals, colloidal suspensions, and much of living matter. Unlike simple liquids or solids, soft materials are highly correlated many-body systems with complex internal structures that extend across a wide range of lengthscales. The presence of these structures—and, importantly, their tendency to interact and to self-organize in a hierarchical manner—instill these materials with properties unlike any others seen in nature. Progress in soft materials depends greatly on development of experimental tools that can probe new spatial and temporal domains. Given that processing of soft matter for technology often involves exotic conditions, such as simultaneous flow and electromagnetic fields, engineering of new materials often requires the ability to interrogate them *in situ*.

The APS Upgrade will provide tremendous opportunities for soft matter discovery by leveraging existing imaging techniques across lengthscales and timescales—especially in XPCS, which will see capabilities increase by up to six orders of magnitude, as noted above. Improved

characterization provides a fuller picture of soft matter assembly and dynamic response and will lead to a much deeper understanding of soft matter processes ranging from disease modalities to development of next-generation microelectronics.

Biological and Life Sciences

Living systems have developed highly efficient and effective structures, materials, and approaches that provide useful templates for innovations in engineering, materials science, medicine, and other fields. These living systems typically involve highly complex hierarchical structures composed of weakly coupled building blocks, ranging from molecules and molecular complexes to organelles, cells, and tissues. These building blocks exhibit emergent behavior expressed as self-organization and collective, sometimes chaotic activities that can be explained only by the complex interactions between these components rather than by their individual properties.

Due to the characteristics of today's lightsources, synchrotron studies of biological systems to date have largely been limited to static, reductive studies epitomized by experimental approaches such as crystallography of a purified crystallized protein or the imaging of an isolated single cell. Improving our understanding of hierarchical biological systems will require a spectrum of new capabilities—in particular, penetrating x-rays with adequate intensity and resolution to access both structural and chemical information across all relevant lengthscales and timescales. The APS Upgrade will enable diffraction, scattering, imaging, and spectroscopy of biological systems across multiple building-block length scales, from molecules to tissues, with unprecedented temporal resolution. These new capabilities will revolutionize our understanding of biological systems and the structures of both healthy and diseased biological machinery.

Chemistry and Catalysis

Discovery in chemistry and catalysis is driven by the need to resolve structure and electronic states at the atomic scale, as a function of reaction-specific environments and across timescales related to chemical functionality. Methods that resolve these features down to the atomic scale, including x-ray diffraction (XRD), x-ray absorption spectroscopy (XAS), and pair distribution function (PDF) analysis, push our understanding of these important chemical and catalytic processes. The APS Upgrade will drive new discoveries in chemistry and catalysis by extending time resolution of these tools to match the rates at which atom-atom bonds are made and broken, by enhancing the local structural information that can be obtained in general (not just periodic) systems from spherically-averaged 1D to multi-dimensional real-space information, and by exploring coupling of processes across multiple lengthscales and/or characterization modalities. The selected examples discussed in detail below, which demonstrate both the scientific and technological importance of these new capabilities, include the use of fluctuation x-ray microscopy to understand structure direction in zeolite synthesis, atomic-resolution studies of early-stage self-assembly during materials synthesis using total x-ray scattering, dissecting catalysis in the artificial leaf, and enhancing our understanding of strain-engineered catalysts using coherent diffractive imaging.

Environmental Sciences and Geosciences

The investigation of new phases of matter at the extremes of pressure, temperature, and electromagnetic fields provides a route to transforming our understanding of a large array of fundamental problems in environmental and geoscience systems. However, this type of research is highly challenged by the extremely heterogeneous nature of materials studied by the Earth, Environmental, and Extreme Conditions Science (E^3) community. Today's most pressing challenge in environmental science and geoscience is to develop integrated characterization and modeling of these inherently complex, multi-component systems at multiple lengthscales, ranging from atomic to meso- and macroscopic.

Although efforts to understand these systems have benefited enormously from the continued improvement in brightness afforded by x-ray storage rings and free-electron lasers, dynamic, *in situ*, and multimodal analyses of heterogeneous E^3 materials and systems remain out of reach by currently available instruments. For example, recent breakthroughs in diamond anvil cell (DAC) technology allow the highest attainable static pressures to increase to 1 TPa. Although these pressure studies open up new frontiers of research that take us beyond the terrestrial geotherm to regimes of giant planet interiors and studies of exotic states of matter, these pressures are now attainable only by using a two-stage DAC that requires confined samples and heating with a laser spot of about 1 µm. The APS Upgrade will uniquely provide x-ray brightness that will allow *in situ* analysis at high energies within novel, ultrasmall-volume, submicron DAC tips that will reach terapascal pressures. At 30 keV, the APS Upgrade will more than double the current range of "parameter space" for pressure and temperature studies.

The impact of the APS Upgrade on important scientific problems in the E^3 community is discussed below within the context of several example problems: probing materials at the extremes of pressure and temperature; using early condensates to understand the conditions under which the solar system formed; imaging heterogeneous materials and interfaces in natural systems to link molecular to mesoscale transport phenomena in the environment; understanding bacterial metabolic function; evaluating long-term environmental impacts of engineered nanomaterials; and unraveling controls on ocean productivity by trace-metal micronutrients.

Condensed Matter Physics

The competition arising from correlations between multiple degrees of freedom in condensed matter systems can lead to the emergence of new states of matter with beneficial properties. Unanticipated behavior can emerge on the nanoscale and mesoscale, giving rise to novel correlated electronic and magnetic phases, phase transitions, self-organization, and phase separation. Such phenomena are at the heart of condensed matter research. Major scientific challenges include creating new states of matter and exploring their emergent properties to understand and potentially tailor controlled responses over a wide range of temporal and spatial lengthscales. The mesoscale represents a broad crossover region from the quantum realm of nano-systems to the classical realm of macro-systems. Classical physics primarily governs macroscopic equilibrium behavior, while quantum physics governs the complex behavior of correlated electron systems. A thorough grasp of the fundamentals of all three regimes—nano, meso, and macro—is needed to develop a new generation of (i) energy-

efficient materials and processes to extend the information technology revolution; (ii) motors for transportation applications that do not require fossil fuel; (iii) generators for renewable, wind-powered alternative energy sources; and (iv) instrumentation that ranges from biomedical applications to astrophysical telescopes. The condensed matter physics chapter that follows highlights the likely impacts of the APS Upgrade in exploring fundamentals that underpin the world around us. Examples include achieving new perspectives on quantum criticality and phases under extreme conditions, fluctuations in correlated electron systems, and dynamic manipulation of novel polarization phases.

1.5 References

[1] R. Hettel, J. Synchrotron Rad. **21**, 843 (2014).

[2] M. Eriksson, J. F. Van der Veen and C. Quitmann, J. Synchrotron Rad. **21**, 837 (2014).

[3] "*Directing Matter and Energy: Five Challenges for Science and the Imagination*," BESAC Subcommittee on Grand Challenges for Basic Energy Science, G. Fleming and M. Ratner, U. S. Department of Energy (2007).

[4] "*Challenges at the Frontiers of Matter and Energy: Transformative Opportunities for Discovery Science," http://science.energy.gov/~/media/bes/besac/pdf/201507/Sarrao_BESAC_July.pdf.*

[5] BESAC Subcommittee on Future Light Sources, *Grand Challenge Science on Diffraction Limited Storage Rings,* (2013).

[6] "*Workshop on new science opportunities provided by a multi-bend achromat lattice at the APS*," held at Argonne National Laboratory, October 21–22, 2013. Program available at: http://www.aps.anl.gov/Upgrade/Workshops/2013/MBA-Technology/.

[7] "*4th Diffraction Limited Storage Ring (DLSR) Workshop,*" held at Argonne National Laboratory, November 19–21, 2014. Program available at: http://dlsr-workshop-2014.aps.anl.gov/.

[8] "*Early Experiments with the Upgraded APS*," held at Argonne National Laboratory, May–June, 2015. Program available at: http://www.aps.anl.gov/Upgrade/Meetings_Workshops/Early-Experiments-with-the-Upgraded-APS.html.

[9] "*Emerging Opportunities in High Energy X-ray Science: The Diffraction Limited Storage Ring Frontier*," held at Argonne National Laboratory, July 13–14, 2015. Program available at: http://aps.anl.gov/News/Conferences/2015/ANL-SRI-2015/index.html.

[10] M. Borland, G. Decker, L. Emery, V. Sajaev, Y. Sun, and A. Xiao, J. Synchrotron Rad. **21**, 912 (2014).

[11] E. Al-Dmour, J. Ahlback, D. Einfeld, P. Fernandes Tavares, and M. Grabski, J. Synchrotron Rad. **21**, 878 (2014).

[12] M. Borland, V. Sajaev, L. Emery, and A. Xiao, "*Multi-objective Direct Optimization of Dynamic Acceptance and Lifetime for Potential Upgrades of the Advanced Photon Source*," ANL/APS LS-319 (2010).

[13] J. Murphy, "*Synchrotron Light Source Data Book*," BNL-42333 Version 4, Brookhaven National Laboratory (1996).

[14] K. Yamauchi, H. Mimura, T. Kimura, H. Yumoto, S. Handa, S. Matsuyama, K. Arima, Y. Sano, K. Yamamura, K. Inagaki, H. Nakamori, J. Kim, K. Tamasaku, Y. Nishino, M. Yabashi, and T. Ishikawa, J. Phys.: Condens. Mat. **23**, 394206 (2011).

[15] S. Sasaki and I. McNulty, Phys. Rev. Lett. **100**, 124801 (2008).

[16] M. van Veenendaal and I. McNulty, Phys. Rev. Lett. **98**, 157401 (2007).

[17] M. Sutton, S. G. J. Mochrie, T. Greytak, S. E. Nagler, L. E. Berman, G. A. Held, and G. B. Stephenson, Nature **352**, 608 (1991).

[18] D. Vine, private communication (2015).

[19] F. van der Veen and F. Pfeiffer, J Phys. Condens. Matter **16**, 5003 (2004).

[20] R. Hegerl and W. Hoppe, Ber. Bunsenges. Phys. Chem. **74**, 1148 (1970).

[21] J. M. Rodenburg and H. M. L. Faulkner, Appl. Phys. Lett. **85**, 4795 (2004).

[22] P. Thibault, M. Dierolf, A. Menzel, O. Bunk, C. David, and F. Pfeiffer, Science **321**, 379 (2008).

[23] I. Peterson, B. Abbey, C. T. Putkunz, D. J. Vine, G. A. van Riessen, G. A. Cadenazzi, E. Balaur, R. Ryan, H. M. Quiney, I. McNulty, A. G. Peele, and K. A. Nugent, Opt. Express **20**, 24678 (2012).

[24] C. Zhu, R. Harder, A. Diaz, V. Komanicky, A. Barbour, R. Xu, X. Huang, Y. Liu, M.S. Pierce, A. Menzel, and H. You, Appl. Phys. Lett. **106**, 101604 (2015).

[25] D. J. Vine, D. Pelliccia, C. Holzner, S. B. Baines, A. Berry, I. McNulty, S. Vogt, A. G. Peele and K. A. Nugent, Opt. Express **20**, 18287 (2012).

[26] Z. Jiang, private communication (2015).

[27] R. Leheny, private communication (2015).

[28] Y. Shvyd'ko, Phys. Rev. A **91**, 053817 (2015).

2 Mesoscale Engineering and Advanced Materials

Robert Suter, *Carnegie Mellon University*

Dillon Fong, *Argonne National Laboratory*
Peter Chupas, *Argonne National Laboratory*
Paul Shade, *Air Force Research Laboratory;* John Almer, Meimei Li, Sharvit Shastri, Xianbo Shi, *Argonne National Laboratory;* Karl Ludwig, *Boston University;* Anthony Rollett, Paul Salvador, *Carnegie Mellon University;* Conal Murray, *IBM;* Todd Hufnagel, *Johns Hopkins University;* Joel Bernier, *Lawrence Livermore National Laboratory;* Michael Sangid, *Purdue University;* William Chueh, *Stanford University;* Randall Headrick, *University of Vermont;* Paul Voyles, *University of Wisconsin-Madison*

2.1 Executive Summary

The increasingly rapid development of novel structural materials has been driven by improved synergies between synthesis, theory, and characterization, which have created a virtuous cycle of increasing knowledge and greater opportunities to create advanced materials by design. Unfortunately, progress in both science and technology has been impeded by a limited ability to probe and understand heterogeneities of these materials at the 1-100-nm lengthscale. In the past, these heterogeneities were broadly characterized as defects; now, however, features ranging from secondary phases and phase boundaries to dislocations and point defects are understood as key components of the systems, providing the strength and ductility of structural materials,[1] determining the electronic properties of semiconductors, and forming the active sites of heterogeneous catalysts. Improved scientific understanding of these heterogeneities, with a focus on their atomic structure, their controlled synthesis, and their evolution under conditions of use, is needed to enable further understanding and control of these structural and chemical heterogeneities. Access to this nanoscale information is crucial to achieve improved mechanical strength and toughness in alloys, sustained efficiency in electrochemically functional materials, and advances across the full spectrum of novel materials.

Previous models of structural phenomena at the 1-100 nm lengthscale have been based largely on *ex situ* techniques, such as using electron microscopy to examine thin specimens cut from the sample after operation and performing *a posteriori* analysis of defect dynamics and microstructural evolution. Today, however, the advent of diffraction-limited hard x-ray sources,

such as the APS Upgrade, promises to allow observation of defect behavior at crucial lengthscales in materials under realistic conditions—for example, during chemical reactions, under applied fields, and at high pressures and temperatures. These new experimental capabilities will make it possible to examine how defects and nanostructures form, move, and interact. Similar studies of materials synthesis at these lengthscales will provide insight into their growth processes, including the development of metastable phases that will significantly advance our ability to design and synthesize materials with hierarchical microstructures and dramatically improved performance.

The challenges and opportunities involved in creating materials with optimized mesoscopic order have been recognized in a number of influential publications. For example, a recent report from the Mesoscale Science Subcommittee of the BESAC identified "mastering hierarchical architectures" through *in situ* characterization of synthesis and "understanding the critical roles of heterogeneity, interfaces, and disorder" through real-time, multi-scale "epidemiological studies of heterogeneous populations" as priority research directions, central both to the advancement of science and to our national interest.[2] The U.S. Materials Genome Initiative, [3] a multi-agency initiative launched in 2011 with the goal of discovering, manufacturing, and deploying advanced materials "twice as fast, at a fraction of the cost," has stressed the importance of reducing the duration of the design-synthesis-application cycle through application of advanced research techniques, including *in situ* characterization. Numerous professional societies across multiple disciplines have demonstrated great and growing interest in this field; for example, the 2015 World Congress on Integrated Computational Materials Engineering alone drew 200 participants, up more than 10% from the previous year.[4] The APS Upgrade's new experimental capabilities are tailored to enable probes at this lengthscale, with the promise of profound impacts throughout materials science.

2.2 New Opportunities for Mesoscale Engineering and Advanced Materials at APS-U

The improved brightness and coherence of the APS Upgrade, particularly at the high photon energies required for *in situ* studies, will dramatically expand our understanding of synthesis, operation, and other complex processes within materials across a wide range of lengthscales. As noted above, our understanding of the nanoscale structural and chemical states of materials to this point has been based almost entirely on experiments using *ex situ* techniques, which introduce sample modifications during preparation and in interactions with the electron beam. While x-ray characterization using present third-generation lightsources can provide insight into important model systems, such as large areas of 2D interfaces, it cannot support crucial *operando* and *in situ* interrogations with nanoscale precision. The APS Upgrade will make it possible for experimentalists to directly observe material behavior over a wide range of lengthscales under realistic conditions, allowing us to examine how defects (point, line, or interface) form, move, and interact in real time. This capability will have a profound impact on our ability to design and synthesize hierarchical materials with near-ideal microstructures and will afford dramatically optimized device performance.

The three experiments described here are examples of how the x-ray coherence of the APS Upgrade can be used to attack pressing questions in our quest to master the mesoscale; they

illustrate how mesoscale engineering and advanced materials research will be transformed by the new capabilities provided by the APS Upgrade. These experiments also highlight critical new capabilities provided by the APS Upgrade: (1) high-energy (>40 keV) coherent diffraction x-ray imaging, (2) tightly focused high-energy x-rays (with photon energy higher than 50 keV, to a focus smaller than 100 nm) and (3) high-flux coherent x-ray scattering probing dynamic processes. The experiments discussed in detail are as follows:

1) *Nanoscopic origins of turbine disk dwell fatigue behavior*. Structural materials, such as those employed at extremely high temperatures in turbine engines, are critical to our energy and transportation infrastructure. However, the mechanisms of their underlying failure—including fracture, crack propagation, and plastic deformation via dislocation motion and/or mechanical twinning—remain poorly understood. Additional (and currently inaccessible) experimental data are needed to test hypotheses about polycrystalline materials deformation at the crucial nanoscopic lengthscale. The APS Upgrade will make it possible to combine three powerful measurement techniques—high-energy diffraction microscopy (HEDM), CDI, and high-energy computed tomography (CT)—to span the required lengthscales and provide unique tests for predictive theory and modeling.

2) *Mesoscale complexity in batteries*. Batteries are archetypical mesoscale heterogeneous systems. Although their basic operation derives from local atomic-scale phenomena, the most important device performance metrics, such as high charge/discharge rate capability and long lifetime, are predicated on control of mesoscale effects such as changes in phase and microstructure. Understanding the architecture of composite electrodes is critical to understanding the mobility of ions and charges within the device and to developing long-term battery stability. The APS Upgrade will allow us to close the existing information gaps between reciprocal space techniques that elucidate atomic-scale structure and real-space imaging methods that are able to map evolving heterogeneity, making it possible to fully comprehend how mesoscale structure determines electrochemical performance.

3) *Structure and dynamics during materials synthesis*. The solutions to many of our current energy and environmental challenges will require development of new advanced materials. Although there are now significant opportunities in advanced semiconductors, catalysts, energy storage, and other systems comprised of highly desirable materials and architectures, it remains very difficult to synthesize important materials with hierarchical structures far from equilibrium. The APS Upgrade, with its combination of high brightness and hard x-rays, will be the ideal tool for probing synthesis *in situ*. Techniques such as XPCS will, for the first time, enable direct monitoring of crystal growth dynamics with the time resolution necessary to probe atomic-level details of the synthesis process.

2.3 Early Mesoscale Engineering Experiments at APS-U

2.3.A. Nanoscopic Origins of Turbine Disk Dwell Fatigue Behavior

Background and Motivations

Polycrystalline materials serve as the backbone of the U.S. energy, transportation, and defense infrastructures. Yet, despite the critical importance of structural materials, their underlying

failure modes—including fracture, crack propagation, and plastic deformation—remain poorly understood due to the lack of experimental data needed to test predictive models of polycrystal deformation at the appropriate lengthscale and to develop useful hypotheses regarding the incorporation of new materials in complex systems. Such predictive models are crucially important in understanding failures of structural alloys that result from mechanical fatigue due to repeated loading, which is frequently combined with chemical interaction with the environment. Bridge collapses and in-flight airplane fuselage ruptures[5] are but the most extreme examples of these types of failures, which create chronic, widespread concerns throughout the manufacturing and applied materials sectors. The present inability to correctly predict failure modes under realistic conditions necessitates redundant inspections, costly over-design, and premature replacement of expensive equipment, such as jet engine turbine blades or disks, well before the end of their useful life, with economic costs that can be measured in the billions of dollars every year.[6,7]

The development of accurate models that predict microstructure-based heterogeneity evolution and its impact on material failure depends on gaining accurate hierarchical information on responses to mechanical loading, from the nanoscopic level to the macroscale. Most crucially, experimental insights are lacking on the rapid and irreversible evolution of defects immediately preceding and following crack formation. Because crack initiation is a rare event within the microstructure, it is extremely challenging to image and quantify the motion of individual dislocations and the stress fields that drive them, and present experimental technologies cannot access the lengthscales and timescales of defects under relevant *in situ* mechanical loading. The APS Upgrade will provide the precise tool required to observe dislocation slip at the nanoscale in realistic geometries that allow development and validation of micro-mechanical models.

The ability to test hypotheses for crack formation (such as the singular importance of long straight twin boundaries in nickel superalloys[8]) will enable development of proven, predictive, physics-based models of failure mechanisms in materials. Such models would serve as formidable tools for failure prevention, allowing more accurate prediction of the properties of newly synthesized materials and guiding development of complex structures with graded properties designed for specific system parts.[9] For example, detailed knowledge and control of local properties in polycrystalline materials would be a tremendous boon to additive manufacturing (3D printing) of metal parts for critical applications, which has the potential to force a paradigm shift in design. Computational models derived from detailed experimental measurements of materials responses could greatly reduce uncertainties about performance *operando,* which would allow use of lighter, more efficient systems throughout our infrastructure.

By definition, polycrystals are complex systems in which local internal stress distributions deviate markedly from macroscopically imposed forces.[10] Each crystal has anisotropic properties that are acted upon by a unique anisotropic neighborhood. Unlike the well-defined elastic and plastic properties of individual grains or single crystals, the properties of polycrystals depend on nanoscopic defects (primarily dislocations) that migrate in response to local forces interacting with other features, such as grain boundaries between crystals, impurities, and second-phase particles. The emergent behaviors of mesoscopic and macroscopic volumes of material are generated by this complex set of interactions, which include rare events that result

in material failure. Gaining a quantitative and predictive understanding of materials properties thus requires multi-scale characterization of the structure of highly complex materials under realistic conditions.

The high energy, coherence, and brightness of the APS Upgrade will allow for the first time two powerful characterization techniques, HEDM[11,12,13] and CDI,[14,15] to be extended and combined to span the required lengthscales and provide unique datasets for predictive modeling of polycrystals. HEDM uses highly penetrating x-rays, with a photon energy higher than 40 keV, to generate spatially resolved maps of grain orientation, strain distributions, secondary phases, and density variations with micron resolution over millimeter sample dimensions. Metallic structural materials are sufficiently radiation-hard that HEDM is non-destructive, and the response and evolution of these quantities can thus be tracked *in situ* (for example, under thermo-mechanical loading conditions). HEDM precisely measures emergent behavior that can be compared directly to continuum models.[16,17,18] The second approach, CDI, promises resolution at the 10-nm scale of density variations within individual crystals, so dislocation-level responses can be tracked. The application of CDI to characterize evolution and propagation of defects such as dislocations deep inside polycrystalline materials, combined with concurrent HEDM measurements of the evolution of the surrounding microstructure, will be truly revolutionary. This combination of techniques will provide a new understanding of local defect physics and emergent meso- and macroscopic phenomena necessary to reduce uncertainties, control defect propagation, and facilitate development of new structural materials.

Combining HEDM and CDI in studies of structural materials requires the high photon energy, high brightness, and high coherence of the APS Upgrade. Currently feasible HEDM measurements that probe structure on the micron to millimeter lengthscales will be accelerated by the increased brightness at high energies and by new detector systems that will allow, for example, sampling of states in synchronism with application-relevant cyclic loading. CDI measurements with high-energy x-rays (which can penetrate bulk samples) simply have not been possible with current APS beams, because the spatially coherent fraction of the total beam intensity is on the order of 10^{-5} at the high energies required for HEDM, yielding insufficient coherent flux for such applications. With the APS Upgrade, sufficient coherent flux for CDI measurements will be available up to x-ray energies approaching 50 keV.

Scientific Objectives

Aerospace gas turbine engines continue to push the upper limits of operating temperatures, increasing engine efficiency and resulting in remarkable fuel savings.[19] The limiting factor in engine operating temperatures is the structural integrity of the materials within the hot-section path of the turbine. At increased temperatures, there emerges a distinct failure mechanism, known as dwell fatigue. For example, in Ni-base superalloys,[20] this is the primary failure mode at temperatures above 700 °C, whereas Ti alloys[21] undergo cold dwell even at room temperature. This distinction is not as clear in the case of magnesium; however, making such a clarification is critical, since this is a material of interest for structural applications because of its light weight.[22] At present, the scientific understanding of dwell fatigue is provided through experiments in which cyclic loading is combined with long hold times, resulting in characterizations that are complicated by artifacts known as creep-fatigue interactions.[23]

Despite its great relevance to materials performance, dwell fatigue remains poorly understood. Past probes of dwell fatigue at the fundamental single-defect level have employed specific model systems, thus providing limited insight. Microscopy studies of single crystals of pure metals do not capture the complex interactions between grains during polycrystalline deformation.[17] Large-scale mechanical tests result in a correlation of behavior to the processing steps employed in the preparation of the materials, but they do not elucidate the causes of the pertinent failure mechanisms or the role of the microstructure.

Careful consideration of the dwell fatigue problem has yielded hypotheses for which there are no existing experimental tests. For example, it is widely believed that crack initiation is due to strain localization near grain boundaries. Current capabilities at the APS, including far-field HEDM, allow measurements of elastic strains averaged over the volume of each grain, but they cannot capture the accumulation of strain at a grain boundary. It is apparent from present measurements that the distortion of grains is heterogeneous, as illustrated for a Ni superalloy in Fig. 1, but far-field HEDM smears out this response due to spatial averaging.[24] HEDM/CDI measurements will make it possible to observe the development of strain fields due to complex interactions between dislocations, and between dislocations and grain boundaries and second-phase particles. Ultimately, sub-grain-resolution measurements of strain in polycrystalline structural materials using the APS Upgrade will test the predictions of strain localization at grain boundaries and allow creation of the models and materials required to prevent failures caused by dwell fatigue. Images of the motion of dislocations in applied stress fields will address the question of why some slip systems are effectively in creep mode, while others are effectively responding in a low-temperature pinned mode. This distinction is now hypothesized to be critical to developing a fundamental understanding of dwell fatigue. [20,21,25] Further studies of specially prepared samples with intentionally created voids or cracks are needed to understand the response of dislocations to the strong gradient in the elastic field around such defects prior to crack formation.

Experimental Details

A new understanding of the mechanisms of creep, crack formation, and fatigue in structural materials can be gained through a series of experiments of increasing complexity. Important insights can be gained via *in situ* fatigue loading at room temperature, using a specifically chosen Mg specimen. Magnesium can be prepared with 10-μm-diameter grains[26] and an overall cross-section of 200 μm, yielding roughly 10^5 grains in the specimen. This geometry provides a system that exhibits the structural complexity of high-temperature materials while allowing tests of structural hypotheses under less challenging experimental conditions. A second set of

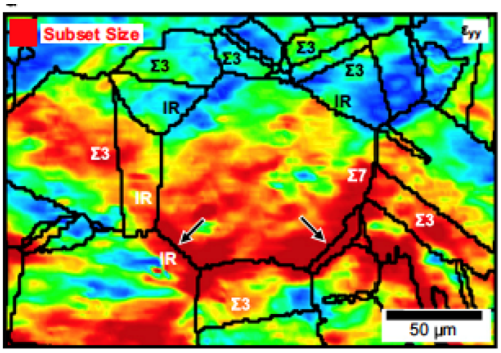

Fig. 1. A surface strain map measured by digital image correlation of optical microscope images in a nickel superalloy specimen after cyclic (fatigue- inducing) loading. Note that the information is derived entirely from the surface and over an extremely long lateral scale. A highly non-uniform strain distribution results from macroscopic loading, and there is a correlation of large strains with many of the grain boundaries.[24]

experiments will probe dwell fatigue at elevated temperatures in polycrystalline Ni-based superalloys, a system relevant to turbine disk applications.[27,28] Superalloy experiments will employ samples with average grain sizes of approximately 20 μm, similar to the case of Mg discussed above, but will be conducted at elevated temperatures requiring development of an *in situ* furnace.

At the largest lengthscale, the orientation and average strain states of grains will be obtained by using near-field HEDM to map a volume with many grains (on the order of 1,000) and using far-field HEDM to map out the elastic strain field over the same 3D volume. This measurement set currently requires 24 hours, but the APS-U's brightness and detector improvements are expected to reduce this by a factor of 5 to 10. The neighborhoods of particularly important grains will then be mapped at the nanometer scale with CDI to reveal the distribution of dislocations and other structural defects. Successive measurements will observe defect generation and defect motions, which will then be directly compared to model computations based on the initial state of the specific microstructure. Advanced loading schemes can be used to derive the necessary information about dislocation motion using elastic stress distributions, without necessarily having to induce macroscopic plasticity.[10,29] HEDM measurements will be carried out during load cycling, at both peak and minimum stress conditions and during dwell. Relevant timescales are broadly distributed, from sub-second imaging of sub-spaces of the experimental range to timescales of one hour during dwell periods.

The CDI measurement yields resolution of sub-nanometer-scale strain displacement fields surrounding individual crystal defects with spatial resolution of 10 nm or less. While CDI studies of individual defects are possible with the capabilities of third-generation lightsources, as illustrated by results obtained at the APS and shown in Fig. 2, the required coherent flux for CDI is available only at x-ray photon energies lower than 10 keV, restricting studies to objects of sub-micron dimensions. The APS Upgrade will allow CDI measurements to probe larger polycrystalline grains embedded in samples of far larger overall dimensions. CDI measurements of sets of nearest-neighbor grains will elucidate interactions of defects within and between grains in the full context of their surrounding environments.

Local CDI measurements can be expected to be slower than the global HEDM, since high dynamic range is required, as are a large number of images as the sample is rotated through one or more Bragg peaks. For the results shown in Fig. 2 (measured at the APS), Ulvestad *et al.* acquired 51 images at 10 min each, a total of 8.5 hours of data collection.[14,15] At present, however, CDI measurements require low photon energies to ensure sufficient coherence, and cannot be applied to the interior of structural materials. The APS Upgrade represents a significant advance in that it allows CDI measurements at the high photon energies required for

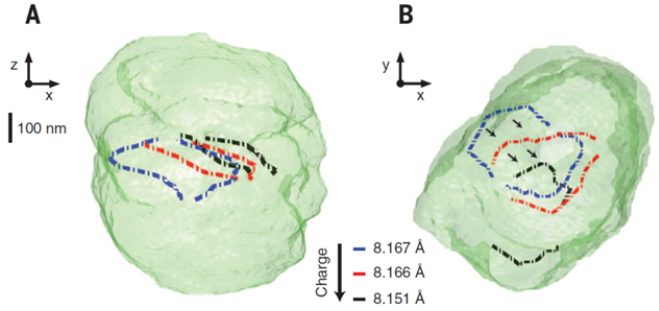

Fig. 2. 3D CDI images of dislocations inside a spinel-structure battery electrode nanoparticle. Entire dislocation lines and their motions can be tracked during electrochemical charging. These measurements used 9-keV x-rays, which provided sufficient coherence, flux, and penetration for this particle size.[14]

interior grains in dense materials. The comparison between previous low-photon-energy measurements and those at the APS-U is favorable. We expect the MBA-based flux at 50 keV to be within a factor of two of the fluxes currently used for low-energy measurements, but we also expect a reduced quantum efficiency of the detector at high photon energies. With compromises, we expect an initial CDI data collection time of around 24 hours, sufficiently short to allow the CDI experiment to be conducted.

Straightforward estimates demonstrate the feasibility of the extension to imaging of buried structures at the APS Upgrade. Approximately 20 grains across each linear dimension of the sample are required for a sufficient population fraction that is far from the surface and that can be considered to experience a bulk environment. A 20 × 20 array of grains contains 400 grains in a cross-section, with 80% in the interior. With grain sizes of approximately 10 μm, the sample side dimensions are 0.2 mm. Using x-rays with a photon energy of 42 keV, transmission geometry measurements will be practical for light elements (e.g., Mg and Al) through the first row of the periodic table. Heavier element materials require higher photon energies and will require longer counting times. The continuing rapid pace of development in numerical methods for coherent scattering and in computational power will allow 3D images to be examined as the data are taken, so that analysis codes can search for regions and signals of particular interest for more detailed studies.

2.3.B. Mesoscale Complexity In Batteries

Background and Motivations

Functional materials find application in a wide range of applications, including energy conversion, storage, and nanoelectronics.[3,30] The continued drive toward higher-density energy storage, for both grid and transportation applications, and toward increasing miniaturization of energy technologies has heightened the need to develop energy storage materials that maintain their functionality in extreme conditions, e.g., under large electrochemical potentials or in reactive environments at elevated temperatures. These materials are typically heterogeneous, with a high density of heterophase boundaries and distinct phases with sizes spanning several orders of magnitude, from angstroms to millimeters. Future technology developments depend on greater understanding of the operating behaviors of these materials and the devices formed from them, with a particular focus on how phenomena occurring at the atomic scale can affect performance on the macroscopic scale.

Basic battery operation derives from local atomic-scale phenomena in well-defined chemical reactions. The practical functional materials in battery applications, however, are predicated on mesoscale effects. Although simple schematics depict battery operation as ion transfer between monolithic, homogeneous electrodes, real battery electrodes are complex composite heterostructures that include electronic and ion conduction paths, cathode and anode, electrolyte, and other constituents that are critical to both functionality and failure, as illustrated in Fig. 3.[31] As synthesized, the heterostructure includes the electrochemically active material, additives such as electrically conductive carbon and binder, and included porosity to accommodate fluid electrolyte.

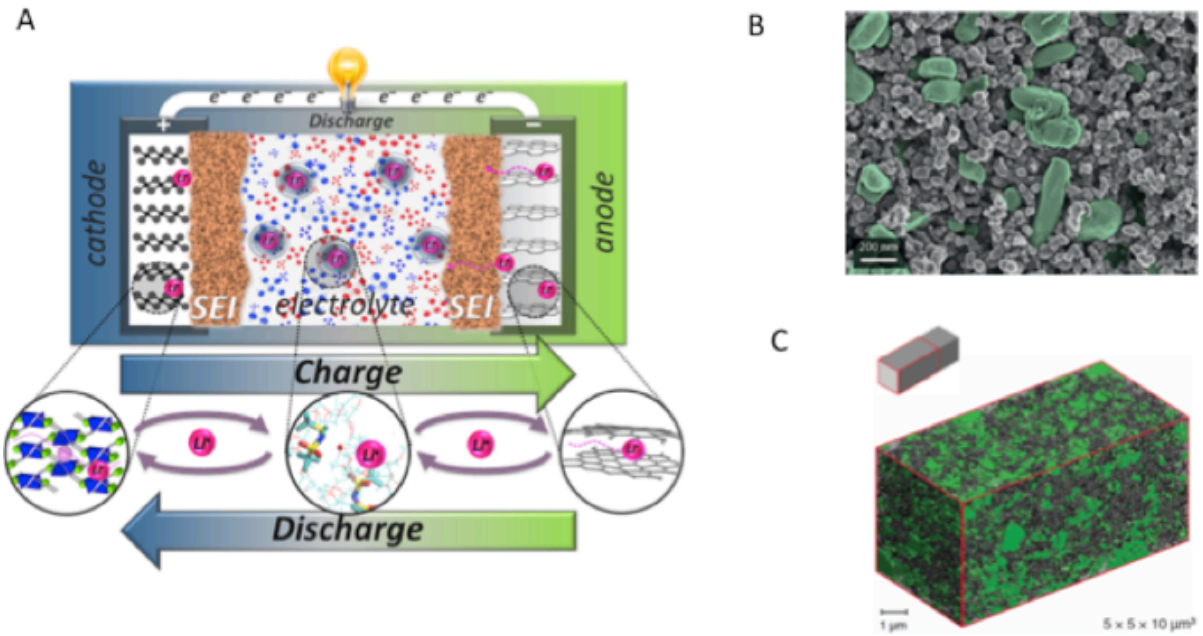

Fig. 3. (a) Schematic of a lithium-ion battery, showing the relationship between anode, separator and cathode, and local environment of lithium in each. (b) Scanning electron microscope (SEM) image of the surface of the lab-scale composite electrode (active material: $LiFePO_4$), with the active material grains highlighted in green. The smaller particles in between are carbon black added for good electronic conductivity.[31] (c) Graphic of a composite electrode and visualization of a 5 × 5 × 10- μm^3 segment of the reconstructed volume of a $LiFePO_4$ composite electrode, from SEM measurement. The distribution of the carbon black (gray) among the $LiFePO_4$ grains (green) and the pores (semitransparent) is clearly visible. The image in (c) was obtained through destructive focused ion beam milling and scanning electron microscopy methods, which preclude further cycling.[31]

In addition to the components created during the construction of the battery, a range of crucial interphases can develop during the charge/discharge cycling. The structural inhomogeneity and complexity only intensify with further cycling, as gradients in electric field, composition, and phase fronts develop across interfaces and the electrode. The characteristics of this electrode composite have a significant impact on the performance of a given active material. Changing the composite electrode structure by tuning the primary and secondary particles (size, size distribution, and interfacial structures), the porosity, and the connectivity can alter the percolation pathways for ion mass and charge transport. It is well understood that the size ofthe active material particles can impact rate capabilities and the potential for side reactions, but it remains unclear why dilution of active material can boost performance, or how different types of carbons change cyclability. Understanding the architecture of the composite electrodes is critical to understanding the mobility of ions and charges through a device and its long-term stability. Ultimately, this knowledge will underpin our ability to design better batteries.

Scientific Objectives

The key issue in studying complex battery materials is to characterize reactivity and structural changes over lengthscales that cover many orders of magnitude in order to disentangle mesoscale effects from fundamental chemical reactivity in battery systems. Highly focused high-energy x-rays will allow both small-angle x-ray scattering (SAXS) and PDF tomography to probe mesoscale heterogeneities in battery systems and to examine how these heterogeneities

evolve during charge/discharge cycling. PDF will characterize materials based on their local atomic structure (0-10 nm), including amorphous components to which diffraction methods are blind. SAXS characterizes the size and shapes of nanostructures in the 2- to 400-nm region. Combining these techniques will reveal the structural and chemical gradients that develop across the electrode. Focused high-energy x-ray beams will be used to enable higher-resolution measurements that match the features in the electrode microstructure. The PDF/SAXS methods can be applied in 3D with a tomography voxel resolution that is set by the size of the beam.

For the first experiment, we will study the evolution of mesoscale structure in $LiFePO_4$ under operating conditions to understand the cycling of batteries across lengthscales that allow us to model all diffusion constants related to transport and reactivity. The results can be compared with *in continuum* models of transport and reaction processes.

Experimental Details

Because high-resolution reciprocal space methods (PDF and SAXS) yield information at sizes as large as the x-ray beam diameter, conducting scattering and diffraction experiments simultaneously with a focused beam, as in Fig. 4(a), allows spatial information to be acquired over a continuous series of lengthscales. Diffraction tomography, in which each individual volume element of a 3D grid has an associated reconstructed diffraction pattern, has been employed to study inherently heterogeneous systems.[32] Extension beyond analysis of crystalline components also has been demonstrated, in which both SAXS and PDF analysis modalities have been applied to the reconstructed scattering patterns.[33, 34] The major limitations in these studies thus far have been the large gaps between the lengthscales that are probed. In the case of PDF tomography, for example, the volume elements are on the order of 100 μm in dimension.[35] Fundamentally, however, there is no gap between the atomic-resolution structural information that reciprocal-space techniques provide (e.g., PDF analysis) and the capabilities of improved real-space imaging approaches, which can probe lengthscales that reach up to millimeters. A schematic of the range over which different techniques provide experimental insight is shown in Fig. 4(b).

The APS Upgrade makes microscopy and scattering experiments practical at high photon energies for the first time. High energies, greater than approximately 50 keV, provide two critical capabilities: (1) the ability to access high wave vectors, thus providing atomic-scale

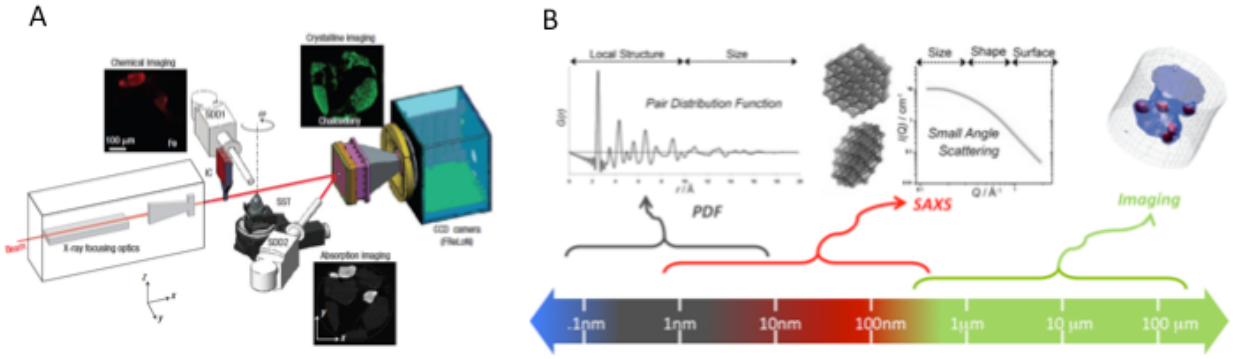

Fig. 4. (a) Experimental arrangement for diffraction tomography.[32] This experiment requires high photon energies and two detectors, one each for PDF and SAXS. (b) Lengthscales that the proposed experiment would cover by using both reciprocal- and real-space modalities.

resolution in PDF measurements; and (2) the ability to penetrate complex sample environments. Multiple analysis modalities of data from a singular measurement strategy will be used to access the different lengthscales. This approach will be widely used to study multi-scale structure in heterogeneous systems, including catalysts, batteries, geological materials (such as shale), and nanoelectronics.

Diffraction tomography has been used to study 3D heterogeneity through distributions in crystalline structure, with an ultimate volume resolution correlated to the available beam size.[32] In the case of high-energy x-rays, the limiting factor is the ability to achieve sub-micron beam sizes with adequate working distances. At present, tightly focused, high-energy x-ray beams with sufficient intensity are not available; as a result, the current imaging grid is rather coarse, on the order of tens of microns. The application of multimodal tomography will be vastly expanded by the APS Upgrade because small, intense, high-photon-energy x-ray beams enable a decrease of voxel (volume element) size while maintaining an adequate field of view, providing a robust platform for *operando* multimodal tomography measurements.

2.3.C. Understanding Structure & Dynamics During Materials Synthesis

Background and Motivations

Materials researchers have a toolbox containing 76 non-radioactive non-noble elements for the construction of new materials. Thus far, only a tiny subset of the many possible combinations of these elements has been studied, and detailed information is sorely lacking for more complex, multicomponent systems. Given the many recent developments in high-precision materials fabrication, there is now an opportunity to create truly novel forms of matter that could have a transformative impact on how our society is able to manipulate, transport, and store both energy and information. Computational studies are rapidly expanding the materials database by virtually exploring many combinations, with the goal of designing materials having the properties we desire. The principal bottleneck in this process has been the physical realization of these new materials, which requires the ability to control how atoms assemble, often across multiple lengthscales, to form materials systems that may be hierarchical in structure and far from thermodynamic equilibrium. This level of control is unachievable without dramatic improvement in our understanding of the fundamental processes involved in materials creation.

Perhaps the simplest and best-studied processes of crystal growth are those involved in the deposition from the vapor phase onto a solid. The seminal work in this field was published by Burton, Cabrera, and Frank in 1951.[36] As schematically shown in Fig. 5(a) for a material having low-coverage, θ_1, prior to nucleation, adsorbed atoms (adatoms) can diffuse on the surface, react and bond with each other, or re-evaporate, with the rate of each process dependent on a thermal activation barrier.[37] Fig. 5(b) shows another surface configuration that may appear at a second instant in time. Possible configurations at a larger coverage, θ_2, are displayed in figures 5(d) and (e), where stable nuclei (islands) compete with each other for unattached adatoms, and incoming atoms may condense atop the existing islands. Coherent x-ray scattering produces scattering patterns in which the island statistics and dynamics can be resolved, as illustrated in Figs. 5(c) and 5(f).[38] Fig. 5 represents only a small number of the many possible processes taking place during crystal growth. In reality, there may be a wealth of other

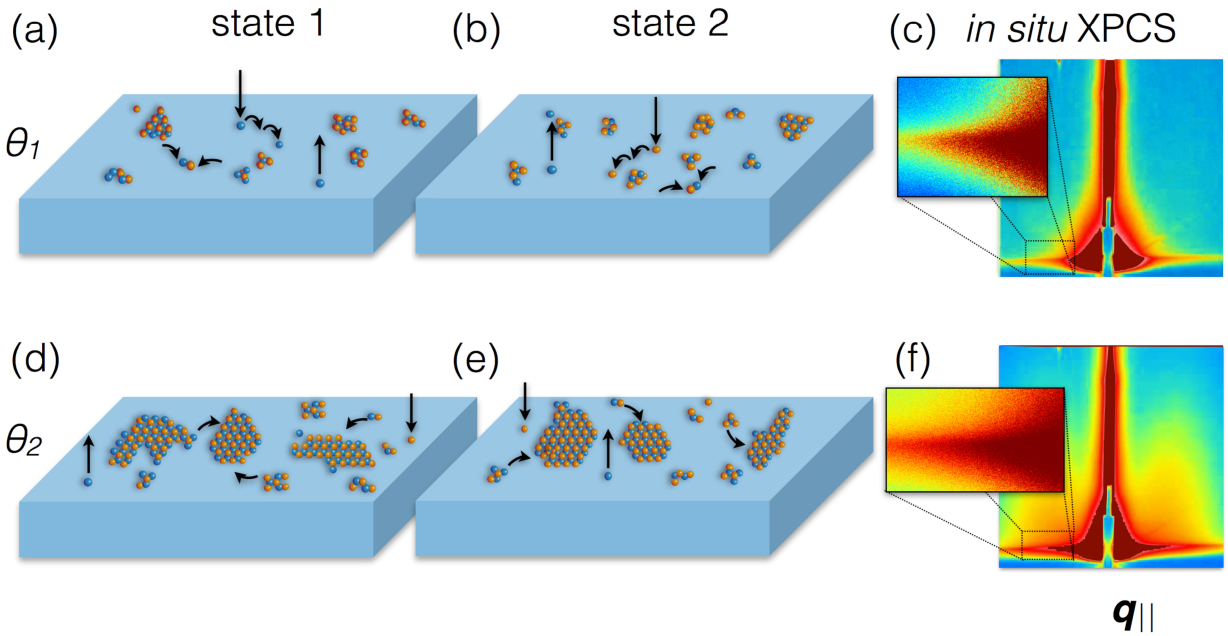

Fig. 5. Schematic depiction of processes on growing surfaces. (a, b) Two distinct configurations of the surface prior to the development of stable nuclei, resulting in coverage θ_1. (c) *In situ* coherent x-ray experiment showing speckle in the diffuse scatter from the deposit. (d, e) Two configurations of the surface after the nucleation stage, resulting in larger 2D islands and a coverage θ_2. (f) *In situ* coherent x-ray experiment showing speckle and the development of an interisland correlation length.[37]

considerations, such as interactions with point defects and foreign species, surface termination and reconstructions, interdiffusion, structural polymorphs, and chemical non-stoichiometry—any and all of which may ultimately dictate crystal growth behavior and thus the structure and phase of the resulting material.

Scientific Objectives

Although simplistic, crystal growth models such as the ones in Fig. 5 continue to form the basis of our understanding of this process because of the inherent experimental difficulties involved in observing atomic motion at a growing surface. Advances require *in situ* probes able to penetrate into the reactive growth environment and directly monitor crystal growth over wide ranges in spatial and temporal scales. Although some *in situ* techniques already are being developed and applied to challenging problems,[39,40] the APS Upgrade offers a singular opportunity to create a new generation of *in situ* probes. X-rays at the upgraded APS will have the penetrating power, the brightness, and the timing structure to access details of the growth process in ways that have never before been achievable. Below, we describe an experiment exploiting the dramatically improved coherence of the beam for *in situ* XPCS studies of the deposition of van der Waals heterostructures. XPCS allows the study of material dynamics: for instance, fluctuations between different microstates, e.g. Fig. 5(a) vs. Fig. 5(b), can be observed, permitting detailed investigations into the atomic-scale processes taking place at certain coverages even when the macroscopic system is observed to be static. Dynamical information is obtained by measuring a speckle pattern, as in Fig. 5(c,)[41] and tracking its evolution with time, typically with a correlation function. The auto-correlation function of the intensity, $I(\mathbf{Q},t)$, is $g_2(\mathbf{Q},t)=1+A(\mathbf{Q})|f(\mathbf{Q},t)|^2$ where $A(\mathbf{Q})$ is the optical contrast, which depends on the degree of

beam coherence (ranging from 0 to 1), and $f(\mathbf{Q},t)$ is the normalized intermediate scattering function, which typically reflects the time constant of the process in question via $exp(-[t/\tau(\mathbf{Q})]^{\beta})$.[42] Due to its dependence on $\mathbf{Q}$, g_2 can be used to identify processes occurring at different lengthscales with distinct correlation times. As shown by Falus *et al*., an improvement in coherent flux by a factor of N implies a reduction of the shortest measurable correlation time $\tau(\mathbf{Q})$ by a factor of N^2.[43] Thus, the APS Upgrade will lead to the measurement of time constants that are many orders of magnitude (10^4 to 10^6) shorter than today, pushing into the nanosecond time regime.

In terms of synthesis science, the consequences of this improvement are profound. Our aim is to conduct direct measurements of $\mathbf{Q}$-dependent dynamics at the elevated temperatures necessary for growth, removing the need for model-dependent investigations (which often rely on observations of quenched surfaces) and permitting discovery of unexpected processes that may take place on the growing surface.[44, 45] This further allows the possibility of observing a wide range of different correlation times (across 10 orders of magnitude) as a function of $\mathbf{Q}$, which could be a means of distinguishing between the many various surface interactions. Because these mechanisms vary strongly with temperature, and because the processes change with coverage and are history-dependent, it is crucial to conduct such studies *in situ* during a single growth experiment. Such XPCS experiments will prove invaluable to the thin-film community and will mark the beginning of a new era in the science of synthesis.

Experimental Details

We consider here in more detail the synthesis of layered 2D materials, such as the van der Waals heterostructures of interest in valleytronics.[46] The construction of artificial crystals from layered materials such as graphene or WSe_2, much like "sheets" of toy blocks as in Fig. 6(a), are interesting in that one can imagine new materials that can be made to exhibit either 2D or 3D behavior by tuning the spacing between the sheets.[47] However, as implied by the name, van der Waals solids are highly unnatural and difficult to synthesize, as they are usually constructed through exfoliation and reassembly.[48] Interface contamination and poor lateral ordering has prompted others to attempt direct growth of van der Waals solids by chemical vapor deposition (CVD) techniques.[49] While this is an extremely promising synthesis route, much is unknown about the growth process, as CVD of multicomponent systems and other reactive deposition techniques involves a number of complex processes and reaction steps.

Synthesis of these 2D materials typically proceeds by island growth, which produces diffuse x-ray scattering such as that shown in Figs. 5(c) and 5(f) and in Fig. 6(b). This particular *in situ* scattering result for an oxide ultrathin film was measured with 15 keV x-rays that were sufficient to penetrate into the reactive growth environment, but the incoherence of the incident beam under these conditions prevented measurement of island dynamics. With APS-U, we will be able to observe dynamics that are a factor of 10^4 to 10^6 faster with sub-nanometer resolution, even at high temperature and in highly reactive growth environments.

For non-equilibrium processes such as growth, correlation functions other than g_2 may be more informative. For example, two-time correlation function maps such as those depicted in Figs. 6(c) and 6(d) show that it will be possible to easily distinguish and quickly determine the key transport mechanisms governing the growth process.[50] Further, coherent diffraction and

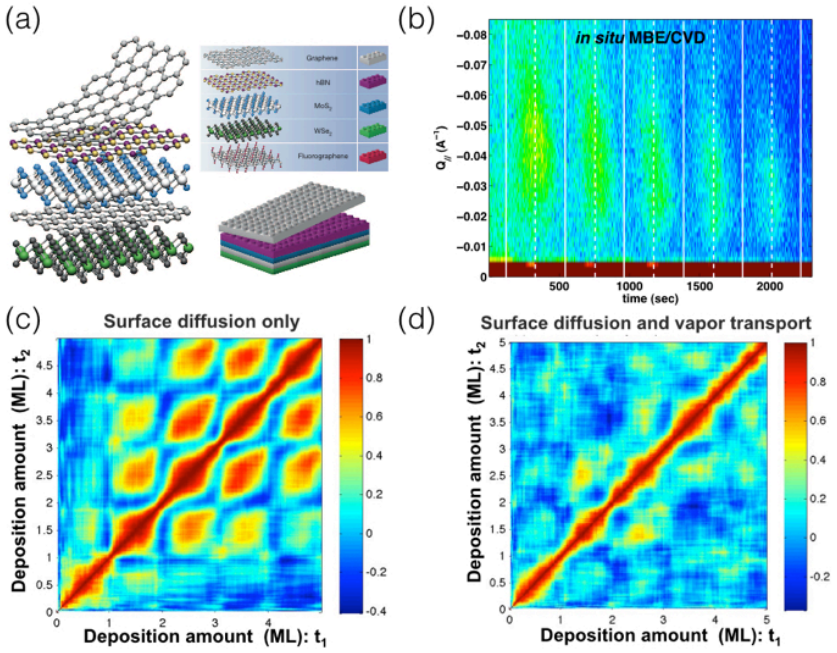

Fig. 6. Dynamic studies of 2D layer growth. (a) Schematic of a van der Waals heterostructure composed of different 2D crystals.[47] (b) Diffuse scattering adjacent to the specular rod during epitaxial growth by oxide MBE. (c-d) Calculated two-time correlation function maps for the layer-by-layer growth of an epitaxial thin film in which island dynamics are governed by surface diffusion only (c) or by both surface diffusion and transport in the vapor phase (d).[50]

resonant CDI will permit the imaging of nanoscale islands, allowing studies of morphological and chemical evolution.

Insight into the synthesis of 2D materials requires the coherent flux of the APS Upgrade. With the current capabilities of the APS, scattering from a single monolayer of WSe_2 gives 10 coherent photons/sec per detector pixel with an appropriately focused beam.[51] Conservatively, achieving sufficient signal with XPCS requires ~1 photon per pixel per correlation time, limiting the current time resolution to 0.1 sec. A 10^2 to 10^3-fold increase in coherent flux will yield a 10^4 to 10^6 improvement in time resolution, allowing interrogation of correlation times ranging from 100 ns to 10 µs.

These studies use the parameters from the 324-bunch mode of the APS Upgrade with 55-ps bunches and 11-ns bunch spacing. Even higher time resolution will be possible with the development of more advanced techniques, such as split and delay with single bunches.[42]

2.4 Operational and Instrumentation Needs

The advanced materials/mesoscale engineering community will benefit substantially from the APS Upgrade, especially in concert with related improvements that can exploit the improved coherence for *in situ* and *operando* studies, such as high-resolution x-ray optics, scattering instrumentation including large mechanically robust goniometers, and advanced detectors with improved readout rates and pixel sizes.

X-ray Optics

The APS Upgrade will allow the creation of fully coherent, sub-micron-focused, high-energy x-ray beams (with photon energies greater than 50 keV) that retain a high flux (>1e^{12} ph/s/0.1% energy bandwidth), a key requirement for the materials research studies described in the preceding sections. Table 1 presents the coherent flux expected at high energies at the APS Upgrade for three different spot sizes achievable using currently proven optics design principles.[52] In the direct focusing case (case 1 in Table 1: <200 × 60-nm focus), the focal spot is obtained for a regular-length beamline at the APS with a working distance of 100 mm. The other two cases are based on the optical design of the 180 m *in situ* nanoprobe,[53] which requires intermediate focusing with a Kirkpatrick-Baez (K-B) pair onto slits to control the coherent flux. Focusing onto the sample achieves a 20 × 20-nm^2 spot using K-B mirrors, or a 5 × 5-nm^2 spot using multilayer Laue lenses (MLLs). The working distance in the second case is 55 mm; in the third, it is only 2 mm. It should be noted that even a 100-mm working distance could be too short for some measurements; in these cases, the working distance could be increased by providing slightly larger beam sizes of, for example, 300 nm. Flux numbers also would correspondingly increase by a small amount relative to those in Table 1.

The *in situ* XPCS growth studies, which require a coherent beam and a relatively large growth chamber, would benefit from the use of long-focal-length optics with working distances on the order of 2 m. Compound x-ray refractive lenses with such a long focal length could collect the full coherent beam and provide a micron-sized spot. Smaller beams also would permit use of detectors with larger pixel sizes for XPCS.

Table 1. Potential spot sizes achievable at 20, 50 and 100 keV, with the MBA lattice in the projected 324-bunch mode, and an optimum insertion device.[52] [52] The fluxes and spot sizes are given for three optical arrangements, denoted 1, 2, and 3.

	MBA 324 bunch mode, fully coherent spot sizes		
Energy (keV)	**20**	**50**	**100**
Coherent Flux (ph/s/0.1% BW)	3.0 × 10^{13}	1.4 × 10^{12}	3.7 × 10^{10}
1. KB pair[1] (nm × nm) **Flux (ph/s/0.1% BW)**	<200 × 60 2.4 × 10^{13}	<200 × 60 1.1 × 10^{12}	<200 × 60 3.0 × 10^{10}
2. KB pair[2] (nm × nm) **Flux (ph/s/0.1% BW)**	20 × 20 1.3 × 10^{12}	20 × 20 1.0 × 10^{11}	20 × 20 2.0 × 10^{9}
3. MLLs[3] (nm × nm) **Flux (ph/s)**	5×5 6.2 × 10^{11}	5×5 7.0 × 10^{10}	5×5 2.3 × 10^{9}

[1] Direct focusing with one KB pair. Source to sample 70 m, working distance 100 mm.
[2] Secondary focusing with two KB pairs. Source to sample 180 m, working distance 55 mm.
[3] Secondary focusing with MLLs and KB pair. Source to sample 180 m, working distance 2 mm. The MLL requires a BW of 0.01%.

The small emittance of the upgraded machine also will make it possible to obtain high incoherent flux (> 10^{14} ph/s/0.1% BW) on a 1 μm^2 spot at 50 keV with relatively short mirrors (250-mm long) and a working distance > 0.5 m. The small spot and high flux will significantly improve photon-hungry experiments that do not require coherent flux.

The small emittance of the upgraded APS also will make it possible to obtain high incoherent flux (> 10^{14} ph/s/0.1% BW) on a 1-μm^2 spot at 50 keV with relatively short mirrors (250 mm long) and a working distance > 0.5 m. The small spot and high flux will significantly improve photon-hungry experiments that do not require coherent flux.

Detectors

Detectors that can efficiently collect scattering at higher x-ray energies are a key requirement for meeting the scientific goals described above. Coherent scattering applications such as CDI and XPCS require fine spatial resolution as well as sensitivity. XPCS requires high frame rates but little dynamic range, while higher dynamic range is considerably more important than frame rate for CDI. Each of the examples above benefits from some combination of reduced pixel size, increased frame rate, and improved detector quantum efficiency; the exact balance among the three will be dictated by the specific use case.

- For CDI at 42 keV, the reciprocal space calibration is ~ 0.05 radian (in 2θ) / $Å^{-1}$ or 200 μm $Å^{-1}$ at 4 m. Roughly 1% of the Brillouin zone, which corresponds to ~ 0.02 $Å^{-1}$ or a 4-mm field of view, needs to be observed. At a sample-to-detector distance of 4 m, a detector with a 1-μm pixel pitch and a 4 x 4 mm^2 field of view with high quantum efficiency would be ideal. The principal challenge here is obtaining sufficient quantum efficiency to allow the measurement to be done within a practical experimental time. Current detectors using a scintillator optically coupled to a charge-coupled device camera have the required pixel pitch. Increased collection efficiency is possible through the use of heavier-element scintillators and optical coatings that reduce internal reflection of the scintillation light. Additionally, thick scintillators can be used, since the camera can be oriented normal to the chosen Bragg scattering so as to minimize parallax-induced smearing of the signals.
- For the multimodal tomography example, PDF data require a large area detector that ideally has readout rates of 1–2 kHz and an active area of 40 cm x 40 cm with pixels on the order of 100-200 μm^2. The current commercial pipeline is poised to deliver such detectors within the timeframe of the APS Upgrade. The second detector required for SAXS must provide enhanced resolution, decreasing pixel sizes while maintaining sensitivity at high energies; these requirements parallel many of those in the HEDM/CDI example.
- *In situ* XPCS crystal growth measurements on fast timescales will require vastly improved detectors with readout rates higher than 10 MHz and small pixels. For XPCS, the pixel size should be approximately the size of a speckle, which scales $\lambda d / L$. Here λ is the x-ray wavelength, d is the sample-to-detector distance, and L is the size of the illuminated region, which increases with lower incidence angles. Thus, larger footprints lead to more scatterers but smaller speckles. For a detector ~1 m away, pixel sizes ≤ 50 μm would be highly desirable.

Goniometers, Sample Environment, Data Analysis

Full realization of the powerful new capabilities of the APS Upgrade and success in all of these proposed measurements will require improved goniometers, advanced sample environments, and efficient analytical tools.

For *operando* studies on the deformation of structural materials, the experiment requires a goniometer mount to bring the coherent beam-imaging detector perpendicular to (semi-) arbitrary diffracted beams so as to minimize smearing of rapidly oscillating signals. In the case of electrochemical energy storage, advanced sample environments allow *operando* measurements, and numerous proven examples exist. However, it is expected that engineering effort will be needed to modify existing designs or create suitable new designs for the proposed measurement modalities. The *in situ* crystal growth studies will naturally require a growth chamber mounted on a diffractometer.

The large volume of 2D detector images that will be collected requires significant computational and storage capacity. Rapid data reduction and analysis is needed to provide real-time feedback to inform experimental decision-making. Coupling beamlines to high-performance computational facilities such as the Argonne Leadership Computing Facility will be essential. Large data storage systems will be required since, in many cases, multiple passes through data analysis procedures will be used to extract as much information as possible from these expensive and unique datasets.

2.5 References

[1] C. A. Handwerker and T. M. Pollock, J.O.M. **66**, 1321 (2014).

[2] BESAC (Basic Energy Sciences Advisory Committee) Subcommittee on Mesoscale Science, J. Hemminger, chair, "From Quanta to the Continuum: Opportunities for Mesoscale Science," U.S. Department of Energy (2012).

[3] The White House, "*Materials Genome Initiative*," https://www.whitehouse.gov/mgi.

[4] See, for example, "*3rd World Congress on Integrated Computational Materials Engineering (ICME 2015)*," available at: http://www.tms.org/meetings/2015/icme2015/home.aspx.

[5] See, for example, http://www.ntsb.gov/investigations/AccidentReports/Pages/AAB1302.aspx and http://www.ntsb.gov/investigations/AccidentReports/Pages/AAB1302.aspx

[6] National Science and Technology Council Committee on Technology Subcommittee on the Materials Genome Initiative, "*Materials Genome Initiative Strategic Plan*," National Science and Technology Council, Washington, D.C. (2014).

[7] National Research Council, "*Integrated Computational Materials Engineering*," National Academies Press, Washington, D.C. (2008).

[8] A. Cerrone, C. Stein, R. Pokharel, C. M. Hefferan, J. Lind, H. Tucker, R. M. Suter, A. D. Rollett, and A. Ingraffea, Mater. Sci. Eng. **23**, 035006 (2014).

[9] W. J. Sames, K. A. Unocic, R. R. Dehoff, T. Lolla, and S. S. Babu, J. Mater. Res. **29**, 1920 (2014).

[10] J. C. Schuren, P. A. Shade, J. V. Bernier, S. F. Li, B. Blank, J. Lind, P. Kenesei, U. Lienert, R. M. Suter, T. J. Turner, D. M. Dimiduk, and J. Almer, Curr. Opin. Solid State Mater. Sci. **19**, 235 (2015).

[11] M. Miller, R. Suter, U. Lienert, A. Beaudoin, E. Fontes, J. Almer, and J. Schuren, Synchrotron Radiat. News **25**, 18 (2012).

[12] U. Lienert, S. F. Li, C. M. Hefferan, J. Lind, R. M. Suter, J. V. Bernier, N. R. Barton, C. Brandes, M. J. Mills, M. P. Miller, C. Wejdemann, and W. Pantleon, J. O. M. **63**, 70 (2011).

[13] H. F. Poulsen, "*Three-Dimensional X-ray Diffraction Microscopy*," Springer, Berlin (2004).

[14] A. Ulvestad, A. Singer, J. N. Clark, H. M. Cho, J. W. Kim, R. Harder., J. Maser, Y. S. Meng, and O. G. Shpyrko, Science **348**, 1344 (2015).

[15] I. K. Robinson and R. Harder, Nat. Mater. **8**, 291 (2009).

[16] J. Lind, S. F. Li, R. Pokharel, U. Lienert, A. D. Rollett, and R. M. Suter, Acta Mater. **76**, 213 (2014).

[17] R. Pokharel, J. Lind, A. K. Kanjarla, R.A. Lebensohn, S. F. Li, P. Kenesei, R. M. Suter, and A. D. Rollett, Annu. Rev. Condens. Matter Phys. **5**, 317 (2014).

[18] R. Pokharel, J. Lind, S. F. Li, P. Kenesei, R. A. Lebensohn, R. M. Suter, and A. D. Rollett, Int. J. Plasticity **67**, 217 (2015).

[19] J. H Perepezko, Science **326**, 1068 (2009).

[20] H. Y. Li, J. F. Sun JF, M. C. Hardy, H. E. Evans, S. J. Williams, T. J. A. Doel, and P. Bowen, Acta Mater. **90**, 355 (2015).

[21] F. P. E. Dunne, D. Rugg, and A. Walker, Int. J. Plast. **23**, 1061 (2007).

[22] K. Kubota, M. Mabuchi, and K. Higashi, J. Mater. Sci. **34**, 2255 (1999).

[23] M. R. Bache, Int. J. Fatigue **25**, 1079 (2003).

[24] W. Abuzaid, M. D. Sangid, J. Carroll, H. Sehitoglu, and J. Lambros, J. Mech. Phys. Sol. **60**, 1201 (2012).

[25] J. Telesman, T. P. Gabb, Y. Yamada, L. J. Ghosn, D. Hornbach, and N. Jayaraman, pp. 853-862 in: E. S. Huron, R. C. Reed, M. C. Hardy, M. J. Mills, R. E. Montero, P. D. Portella, and J. Telesman (editors), "*Superalloys 2012,"* John Wiley & Sons, Inc., New York (2012).

[26] S. K. Sahoo, R. K. Sabat, S. Panda, S. C. Mishra, and S. Suwas, J. Mater. Eng. Perform. **24**, 2346 (2015).

[27] Y. Tjiptowidjojo, C. Przybyla, M. Shenoy, and D. L. McDowell, Int. J. Fatigue **31**, 515 (2009).

[28] T. P. Gabb, J. Gayda, J. Telesman, L. J. Ghosn, and A. Garg, Int. J. Fatigue **48**, 55 (2013).

[29] P. Shade, private communication (2015).

[30] Office of Basic Energy Sciences, "*Basic Research Needs for Electrical Energy Storage: Report of the Basic Energy Sciences Workshop on Electrical Energy Storage, April 2–4, 2007*," U.S. Department of Energy (2007).

[31] M. Ender, J. Joos, T. Carraro, and E. Ivers-Tiffee, J. Electrochem. Soc. **159**, A972 (2012).

[32] P. Bleuet, E. Welcomme, E. Dooryhée, J. Susini, J.-L. Hodeau, and P. Walter, Nat. Mater. **7**, 468 (2008).

[33] S. Huotari, T Pylkkanen, R. Verbeni, G. Monaco, and K. Hamalainen, Nat. Mater. **10**, 489 (2011).

[34] S. D. M. Jacques, M. Di Michiel, S. A. J. Kimber, X. H. Yang, R. J. Cernik, A. M. Beale, and S. J. L. Billinge, Nat. Commun. **4**, 2536 (2013).

[35] S. D. M. Jacques, M. Di Michiel, A. M. Beale, T. Sochi, M. G. O'Brien, L. Espinosa-Alonso, B .M. Weckhuysen, and P. Barnes, Angew. Chem. Int. Edit. **50**, 10148 (2011).

[36] W. K. Burton, N. Cabrera, and F. C. Frank, Philos. T. Roy. Soc. A **243**, 299 (1951).

[37] P. Zapol and D. Ford, private communication (2015).

[38] F. Leroy, J. Eymery, D. Buttard, G. Renaud, and R. Lazzari, J. Cryst. Growth **275,** 2195 (2005).

[39] J. Z. Tischler, G. Eres, B. C. Larson, C. M. Rouleau, P. Zschack, and D. H. Lowndes, Phys. Rev. Lett. **96**, 226104 (2006).

[40] R.-V. Wang, G. B. Stephenson, D. D. Fong, F. Jiang, P. H. Fuoss, J. A. Eastman, S. K. Streiffer, K. Latifi, and C. Thompson, Appl. Phys. Lett. **89**, 221914 (2006).

[41] J. G. Ulbrandt, M. G. Rainville, C. Hoskin, S. Narayanan, A. R. Sandy, H. Zhou, K. F. Ludwig, and R. L. Headrick, arXiv:1507.03694 (2015).

[42] O. G. Shpyrko, J. Synchrotron Rad. **21**, 1057 (2014).

[43] P. Falus, L. B. Lurio, and S. G. J. Mochrie, J. Synchrotron Rad. **13**, 253 (2006).

[44] J. Tersoff, A. W. Denier van der Gon, and R. M. Tromp, Phys. Rev. Lett. **72,** 266 (1994).

[45] F. M. Ross, R. M. Tromp, and M. C. Reuter, Science **286,** 1931 (1999).

[46] K. Behnia, Nat. Nanotechnol. **7**, 488 (2012).

[47] A. K. Geim and I. V. Grigorieva, Nature **499**, 419 (2015).

[48] G. Gao, W. Gao, E. Cannuccia, J. Taha-Tijerina, L. Balicas, A. Mathkar, T. N. Narayanan, Z. Liu, B. K. Gupta, J. Peng, Y. Yin, A. Rubio, and P. M. Ajayan, Nano Lett. **12**, 3518 (2012).

[49] Y.-C. Lin, N. Lu, N. Perea-Lopez, J. Li, Z. Lin, X. Peng, C. H. Lee, C. Sun, L. Calderin, P. N. Browning, M. S. Bresnehan, M. J. Kim, T. S. Mayer, M. Terrones, and J. A. Robinson, ACS Nano **8**, 3715 (2014).

[50] G. B. Stephenson, private communication (2015).

[51] H. Wen, private communication (2015).

[52] X. Shi, private communication (2015).

[53] J. Maser, X. Shi, R. Reininger, B. Lai, S. Vogt, "*HYBRID Simulations of Diffraction-Limited Focusing with Kirkpatrick-Baez Mirrors for a Next-Generation In-Situ Hard X-ray Nanoprobe*", submitted (2015).

3 Structure, Dynamics, and Functionality of Soft Materials

Robert Leheny, *Johns Hopkins University*
Alec Sandy, *Argonne National Laboratory*
Byeongdu Lee, David Vine, Jin Wang, *Argonne National Laboratory;* Oleg Gang, Benjamin Ocko, *Brookhaven National Laboratory;* Samuel Sprunt, *Kent State University*; Robert Macfarlane, *Massachusetts Institute of Technology*; Laurence Lurio, *Northern Illinois University*; Wes Burghardt, *Northwestern University*; Tonya L. Kuhl, Oleg Shpyrko, *University of California-Davis*; Paul Nealey, *University of Chicago*; Norman Wagner, *University of Delaware*; Mark Schlossman, *University of Illinois at Chicago;* Thomas Russell, *University of Massachusetts-Amherst;* Andrea Liu, *University of Pennsylvania*; Nicholas Abbott, *University of Wisconsin-Madison*

3.1 Executive Summary

Soft matter refers to a class of materials that includes polymers, liquid crystals, colloidal suspensions and much of living matter. Soft materials differ from simple liquids or solids due to internal structures at the nanometer or micrometer scales. The presence of these structures, and importantly, their tendency to interact and to self-organize in a hierarchical manner, instills soft materials with highly unusual properties of deformation and flow. Because of the potential applications these properties promise, improved understanding of soft matter is crucial to development of high-impact technologies across a wide array of sectors, from energy and transportation to health, agriculture, and national defense. In addition, much of the life sciences relates fundamentally to soft matter, so improving our understanding of soft matter helps to answer critical questions of health and disease.

The organization and dynamics of the internal structure within soft matter reflect a delicate balance of microscopic interactions, such as entropic, electrostatic, and interfacial forces. It is this balance that makes soft matter "soft", because it instills the structure with a strong sensitivity to external stimuli and to perturbations in temperature, composition, and other variables. Studies of soft matter provide fundamental insights into how collective behavior at the microscale drives complex macroscopic phenomena. These attributes make soft materials ideal for emerging nano- and microtechnologies that require design and manipulation of matter and devices on molecular and macromolecular lengthscales. Soft materials also create new opportunities for applications that demand multifunctional static and dynamic properties involving reconfigurability, programmability, and/or autonomous behavior in response to external stimuli.

Because soft materials are highly correlated many-body systems with complex structures and dynamics that can span a wide range of lengthscales and timescales, progress in this field goes hand-in-hand with the development of experimental tools that can probe new spatial and temporal domains. Additionally, because the processing of soft matter for technological applications often involves specific, complex environmental conditions such as simultaneous flow and electromagnetic fields, engineering new materials often requires the ability to

interrogate the materials *in situ* within challenging environments. The novel capabilities that MBA lattice-based hard x-ray sources will deliver are particularly suited to address these issues and introduce significant opportunities for transformational soft matter studies.

3.2 New Opportunities for Soft Matter Science at APS-U

The APS Upgrade will transform soft matter discovery by extending existing imaging techniques across increasingly broad lengthscales and timescales—especially in XPCS, which will see capabilities increase by up to six orders of magnitude. This transformative improvement will enable us to develop a fuller picture of soft matter assembly and dynamic response, leading to a much deeper understanding of soft matter processes ranging from disease modalities to development of next-generation microelectronics. For example, the gentle energy landscapes of soft matter that enable spontaneous and directed hierarchical order also make such materials highly prone to defects, including "functional defects" that perform important roles. The small, highly coherent, high-energy x-ray beams of the upgraded APS will enable interrogation of the local structure and temporal response of these defects, making it possible to understand these structures and advance the application of engineered defects.

Understanding the importance of defects in next-generation materials also is critical to directed assembly of nanoparticle arrays. Such strategies already have produced a remarkable variety of structures with numerous possible applications. However, the soft energy landscape of these assemblies makes them prone to defects that are very slow to anneal, limiting their technological potential. Understanding and controlling their energy landscape and defect behavior will be key to advancing applications in these novel materials. The greatly enhanced time-resolved coherent scattering techniques enabled by APS-U will make it possible to probe the collective excitations of these materials, measure their stability, and observe how they soften as they transform from one structure to another.

The APS Upgrade promises to revolutionize our understanding of the structural and dynamical properties of nanoparticles in confined geometries, hastening their application to a wide variety of technical problems. Although XPCS is being used today to explore this problem with coarse spatial sensitivity, for slow dynamics under idealized experimental conditions, current lightsources do not allow access to the localized knowledge about the structural, kinetic, and dynamical properties of nanoparticles at or near interfaces that is required for further technical advances. The APS Upgrade will provide the dramatic increases in spatial and dynamic sensitivity needed to fully explore these properties.

Similarly, XPCS and CDI at the upgraded APS will enable new insights into the temporal and spatial heterogeneity of fluctuations that are central to out-of-equilibrium behavior in soft materials, such as responses to mechanical stress. In principle, XPCS can provide crucial information about stress-induced structural dynamics in complex fluids, but studies to date have been limited by the inability to observe samples in challenging environments at high temporal resolution. Likewise, any solid subjected to applied stress possesses an elastic limit, above which it fails. Amorphous solids (such as metallic and polymer glasses) fail by yielding; however, their intrinsic disorder makes it difficult to identify the microstructural changes associated with those failures. CDI at the upgraded APS will offer high-impact opportunities to better understand failure in amorphous solids, providing near-atomic-scale resolution in high-Z

amorphous materials and creating an unprecedented opportunity to probe structural changes associated with yielding events in metallic glasses.

Here we describe several key experiments that illustrate the fundamental advances in soft matter research that will be driven by the APS Upgrade. These experiments include:

1) Nanoparticles confined at or near interfaces. An ensemble of nanoparticles can be confined at liquid-liquid or liquid-solid interfaces, providing a highly relevant model for understanding the technical and fundamental scientific questions noted above. Using the APS Upgrade's high coherent fraction of x-rays and enhanced coherent flux, researchers will achieve unprecedented measurements of the structure and dynamics of nanoparticles confined to the interface of a single suspended droplet in a water-oil emulsion under controllable conditions. For example, the sizes of the droplet and nanoparticles can be varied to investigate the effects of interface curvature and capillary interactions at the nanoscale. Although x-ray investigations of these properties have been attempted in the past, previous studies have been limited by the lack of a higher-energy, highly coherent beam of appropriate size and flux. The APS-U will finally make these crucial experiments possible.

2) *Nanoparticle arrays produced by directed assembly.* Nanoparticles can be assembled into periodic three-dimensional crystals through the action of linker molecules such as DNA, yielding a remarkable variety of structures with a large number of possible applications. The gentle free-energy landscapes of these assemblies make them prone to defects that are very slow to anneal and that limit their use for novel technological applications. The highly coherent x-ray beams produced by the APS Upgrade will address a key need in these investigations, enabling exact CDI reconstructions of nanoparticle arrangement in micron-sized crystals of DNA-assembled materials and leading to precise characterization of the nature of their defects. Additionally, XPCS experiments will make it possible to characterize the energy landscapes that dictate the formation and stability of self-assembled crystals, particularly near structural transitions.

3) Yielding in amorphous metals. The mechanical properties of metallic glasses are imperfectly understood because their intrinsic disorder makes it difficult to identify the microstructural changes associated with such behavior using currently available experimental technologies. Current theories regarding yielding in amorphous solids, such as metallic glasses, have identified local regions of approximately 100 atoms, known as shear transformation zones (STZs), that can act collectively to form shear bands. The APS Upgrade will drive advances in CDI that are expected to provide atomic-scale resolution in high-Z amorphous materials, creating opportunities to gain heretofore unavailable information and, ultimately, to test predictive models of yielding in this system with relevance to the mechanical properties of many other soft materials.

3.3 Early Soft Matter Experiments at APS-U

3.3.A. Nanoparticles Confined at or Near Interfaces and Other Quasi 2D Systems

Background and Motivations

The properties of surface-active species at or near liquid-liquid and liquid-solid interfaces have considerable technical and scientific importance. Typically, these systems involve the assembly and ordering of monolayers or sub-monolayers that are buried between two fluids or between a fluid and solid, making characterization of their structure and dynamics intrinsically difficult. Although present x-ray techniques can provide some microscopic information in this case, the APS Upgrade's small, bright, high-energy beams will be able to penetrate surrounding fluid phases to interrogate interfaces with limited background scattering, opening opportunities to address currently inaccessible problems. Improved understanding of these interfacial phenomena and the nature of nanoscale dynamical processes [1] could have important applications, such as the use of surfactant-based solvent extraction methods to clear toxic metals and other impurities from water. Surface-sensitive scattering combined with spectroscopy at the oil-water interface will provide key information about the poorly understood molecular-scale processes that drive extraction. Another example involves the ability to probe freezing transitions in amphiphiles at the oil-water interface. Although indirect evidence for such transitions exists, grazing incidence diffraction (GID) from such buried interfaces enabled by the APS Upgrade will provide information about the in-plane order needed to understand the phase behavior. A third example addresses the structure and dynamics of room-temperature ionic liquids (RTILs) in the vicinity of an interface (electrode) after a potential step. Time-resolved studies using highly coherent, higher-energy x-ray beams from the upgraded APS will lead to understanding of the microscopic behavior of RTILs that should enable improved design of energy-related technology such as supercapacitors.[2]

Lipid bilayer studies are another important interfacial system for which the APS Upgrade promises significant new insight. Lipid bilayers form the basic structural unit for the membranes of eukaryotic cells. At present, finely resolved measurements of single membranes are very challenging due to weak contrast and large background scattering from the surrounding water. However, such measurements, which the APS Upgrade will make possible, are crucial to understanding lipid membranes as soft matter systems and their properties in biological contexts. For example, the APS Upgrade will enable grazing incidence x-ray scattering (GIXS) studies of both the

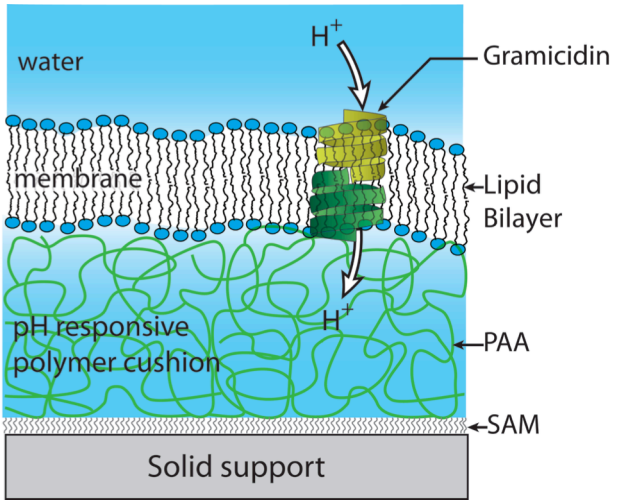

Fig. 1. Schematic of a lipid bilayer containing an antibiotic polypeptide (gramicidin) that acts as an ion channel. The bilayer is supported on a polymer gel (PAA) whose viscoelasticity mimics that of the cytoskeleton.

structure and most especially, the dynamics of increasingly more complex bilayers that successively approximate living membranes. Experiments that probe the lipid composition-dependent functionality of membrane proteins are of particular interest.[3] An example is shown schematically in Fig. 1. X-ray studies of in-plane correlations within membranes will allow detailed probes of fluctuations that would be particularly relevant to membranes with mixed lipid compositions. Such studies will provide insight into phenomena such as membrane rafting, a mechanism postulated to significantly enhance interactions between components within a membrane by segregating them into locally phase-separated regions. XPCS studies of biomembranes also will provide information on the viscoelastic properties of the membranes at the nanoscale. As a specific example of an enabling approach to address the weak signals present in experiments targeting such phenomena, by using APS-U's high coherent flux and small focal spots, a coherent x-ray beam could be coupled into nanoscale wave guides that enclose membranes, reducing the otherwise large water background present in a traditional experimental geometry. In addition, lipid membranes are closely related to lyotropic liquid crystals, and x-ray studies could provide ways to link the well-established theoretical framework of liquid crystals to biological systems. In addition to exploring this link between liquid crystals and membranes, layered liquid crystals display interesting behavior of their own that can be probed using APS-U beams. For instance, XPCS extended to very fast timescales should be able to investigate the dynamic character of so-called cybotactic (locally smectic) domains in nematic liquid crystals.

Another frontier area in interfacial science concerns nanoparticle ordering and assembly at fluid-fluid interfaces. While considerable information about micrometer-scale colloids at fluid-fluid interfaces has been obtained by confocal microscopy, the energy scales of adsorption and interactions of nanoparticles at fluid interfaces are typically much smaller, making their behavior qualitatively different and much more difficult to characterize. In the case of emulsions stabilized by nanoparticles, the ability of interfaces to change morphology depends sensitively on the nanoparticle mobility and desorption properties; small changes in conditions can lead to widely varied behaviors. Current hard x-ray lightsources lack the brightness and coherence needed to interrogate the structure, flow, and dynamics of nanoparticle assemblies at buried interfaces.

From a technological perspective, the behavior of nanoparticles at interfaces is central to development of important new applications, such as boosting the energy storage capacity of nascent flow-cell batteries.[4] Similar advances in accessing localized knowledge about the structural, kinetic, and dynamical properties of nanoparticles at or near interfaces of various types are required for further technical advances across a wide range of industries, including food, personal care, and pharmaceuticals. The APS Upgrade will make it possible to study the flow and dynamics of suspended nanoparticles at the nanoscale in varying conditions.

Scientific Objectives

As a first experiment, we consider how the APS Upgrade's high coherent fraction of x-rays and enhanced coherent flux will enable measurements of the structure and dynamics of nanoparticles confined to the interface of a single suspended droplet in a water-oil emulsion. Such a system is an excellent model for understanding the technical and fundamental scientific questions described above. An electric field, for instance, may readily distort a suspended

droplet to tune the area fraction of nanoparticles and thereby move the particles between various structural and dynamical regimes, such as through the jamming transition. In addition, the adsorbate interactions can be varied via different surface chemistries, and the relative sizes of the droplet and nanoparticles can be varied to investigate in a controlled fashion the effects of interface curvature and capillary interactions at the nanoscale.

Experimental Details

A geometrically well-defined liquid-liquid interface can readily be created by using a single micrometer-sized pendant drop of oil in water. The single-drop geometry will enable the investigation of salient phenomena, such as interfacial jamming and the coupling to drop morphology. It also will enable studies of the relationship between concentration-dependent dynamics and adsorption/desorption processes in well-controlled experiments. Here we consider first experiments based on the interfacial confinement of Au nanoparticles, which provide both excellent scattering contrast and facile tuning of surface energetics via molecular functionalization.

In a first series of experiments, schematically illustrated in Fig. 2, a highly coherent x-ray beam from the upgraded APS is incident on the pendant droplet from the lower left. A high-speed photon-counting detector, with sufficient spatial resolution to resolve individual speckles, collects scattering in transmission from the nanoparticle monolayers in a small-angle scattering geometry.

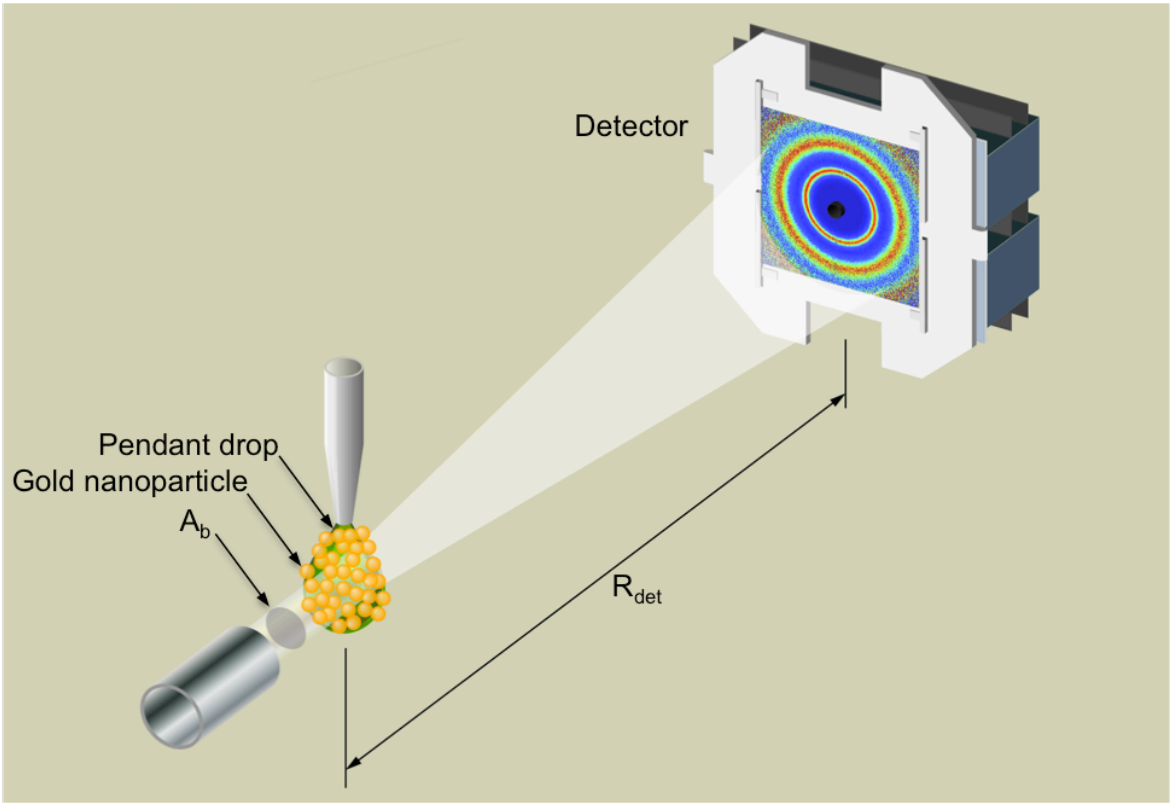

Fig. 2. Schematic of an experiment to study the structure and dynamics of nanoparticles confined to the interface of a micron-scale pendent droplet.

To evaluate the feasibility of coherent x-ray scattering measurements from such systems, we determine the expected scattering rates for APS-U beams. Since we are studying nanometer-sized particles, our measurements will be in the small-angle scattering regime. Accordingly, the absolute number of photons per unit time (J/t) recorded by a detector with pixels each subtending a solid angle Ω is given by:

$$J/t = J_0 \Omega \epsilon T \frac{d\sigma}{d\Omega}$$

where J_0 is the incident flux in photons per second per unit area, ϵ is the detector efficiency, T is the sample transmittance, and $\frac{d\sigma}{d\Omega}$ is the differential scattering cross-section in units of area divided by solid angle. We have ignored any background signals, which by careful experiment design can be made nearly negligible, and we assume that the droplet and surrounding medium are small (with dimensions on the order of 10 to 50 μm)) so $T \approx 1$. For J_0, we assume that a single coherence area from an optimized APS-U undulator beam, monochromatized to the relative bandwidth produced by a Si(111) monochromator, is incident on the droplet. For 10-keV x-rays and an APS-U source brightness of 2×10^{22} ph/s/0.1%bw/mm^2/mrad^2/s, we find the total incident coherent flux to be 4×10^{13} ph/s. This flux will be focused to a beam area of A_b that is incident on the droplet normal to its surface. We assume gentle de-magnification of the source with $A_b \cong \pi R_b^2$, where R_b = 5 μm is the radius of the focused coherent x-ray beam at the sample position and we assume, for concreteness, that the beam is smaller than the droplet.

For the detector, we assume $\epsilon = 1$. The solid angle subtended by a detector pixel is $(d_{pix}/R_{det})^2/4\pi$, where d_{pix} is the detector pixel size and R_{det} is the sample-to-detector distance. This solid angle should be made equal to the angular speckle size by placing the detector at an appropriate distance from the sample. The angular speckle size is $\lambda/(2R_b)$ so for d_{pix} = 75 μm, which seems to be emerging as a lower limit for the pixel size on the next generation of relevant high-performance area detectors, we find $R_{det} \approx 6$ m, which is reasonable.

The differential scattering cross section is given by

$$\frac{d\sigma}{d\Omega}(q) = r_e^2 \left(\rho_p - \rho_{solv}\right)^2 N_p V_p^2 P(q) S(q)$$

where $q = 2k\sin(2\vartheta/2)$ is the wave-vector transfer with $k = 2\pi/\lambda$, $\lambda \approx 1.2$ Å is the x-ray wavelength, 2ϑ is the scattering angle, r_e is the Thomson radius of the electron, ρ_p and ρ_{solv} are the electron densities of the nanoparticles and solvent, respectively, N_p is the number of nanoparticles in the illuminated volume, V_p is the volume of a nanoparticle, $P(q)$ is the form factor of the nanoparticles (spheres), and $S(q)$ is the interparticle structure factor. We assume gold nanoparticles of radius R_p = 50 nm. The number of nanoparticles in the illuminated volume is $\phi \frac{2A_b}{\pi R_p^2}$ where ϕ is the area fraction of the interface covered by particles.

We are interested in cases where the adsorbed nanoparticles significantly affect interfacial properties and where interparticle interactions at the surface are appreciable, so $\phi > 0.1$; for this calculation, we assume $\phi = 0.5$. This also means that $S(q)$ will include salient information about the nanoparticle packing at the interface, and, in fact, $S(q)$ and its dynamic counterpart

S(q,t) contain the science in this problem. We note, however, that *S(q)* for a disordered material varies little from 1. Therefore, the dependence on *S(q)* introduces only a small perturbation in expected scattering rates. For example, *S(q)* is approximately equal to 2 at the interparticle peak for dense disordered packings.

Using these relations and the quantities itemized above, we compute the scattering rate into a detector pixel at a wave-vector transfer corresponding to the mean separation of the nanoparticles and find a count rate of approximately 30,000 photons/s/pixel. Using a standard figure of merit for XPCS wherein resolving dynamics on a timescale τ requires count rates of approximately $1/\tau$ per pixel, we expect with this rate to be able to measure correlation times as small as ~ 1/30,000 ≈ 30 μs.[5] The correlation decay time at this wave vector calculated on the basis of unhindered Brownian diffusion of the nanoparticles in a medium with a viscosity ≈ 10^{-3} Pa s is ~ 50 μs, just within reach of our proposed experiment. However, since we are by design in a regime where interparticle interactions are significant and hinder diffusion, this value for free diffusion should be considered a lower limit. In contrast, today's sources, which are constrained by lower count rates, are restricted to highly jammed regimes where particle diffusion is essentially arrested.

On the more technical side, we note that some of the above assumptions are conservative, and that practical measurements likely will be even more favorable when other factors are considered. Specifically, the radiation bandwidth can be relaxed in the small-angle scattering geometry,[6] i.e., by a factor of 3 with a Ge(111) monochromator instead of Si(111), and the number of coherence areas illuminating the sample and the solid angle subtended by each pixel can be increased[7] with little penalty. On the other hand, losses in the optics and the sample will reduce the yields quoted above. In short, we conclude that challenging XPCS experiments performed using the extremely bright x-ray beams produced by the APS Upgrade will be capable of probing the diffusion of nanoparticles at a liquid-liquid interface and will provide valuable fundamental insight into a host of scientific phenomena.

3.3.B. Dynamics of Nanoparticle Arrays Produced by DNA-Guided Assembly

Background and Motivations

The understanding and control of mesoscale defects represent key opportunities in condensed matter. The recent DOE BESAC report, *From Quanta to the Continuum: Opportunities for Mesoscale Science*,[8] concludes: "Delivering value from the nanoscale requires mastery of defects at the mesoscale." Although the BESAC report focuses primarily on hard materials, the gentle energy landscapes of soft matter, which enable a wide range of spontaneous and directed hierarchical orders, also make such materials prone to defects. In some cases, so-called functional defects perform important roles and warrant detailed structural and dynamic understanding. For instance, topological defects in liquid crystals serve as extremely sensitive "detectors," so that picograms-per-milliliter quantities of toxins can be readily identified by optical microscopy.[9] But defects also challenge our ability to produce large-scale self-assembled materials, whether as templates for high-density structured materials relevant to information storage or as technologically useful self-assembled materials in themselves. For example, block copolymers and lithographic techniques are used in directed self-assembly (DSA) to achieve well-ordered templates for cost-effective nanoscale engineering. Whether defects are

performing functional roles or hindering material performance, the types of local information about their structure that APS-U will provide is sorely needed for progress in this area.

Although considerable success in reducing defects in the desired order has been achieved by a combination of fundamental and combinatorial materials science,[10,11,12] these approaches become inefficient as the defect density becomes increasingly dilute. Coherent imaging of a surface structure has been demonstrated at the APS today, under highly idealized circumstances.[13] CDI with highly transversely coherent x-ray beams enabled by the APS-U will reveal the three-dimensional structure of isolated defects, such as those present in lamellar block copolymer structures relevant to DSA, thereby guiding the development of more perfect templates. As another example, the ability to apply XPCS to the study of soft material defects at the nanoscale is crucial to understanding the complex energy landscape that facilitates (but also limits) the programmable assembly of nanoparticle arrays tethered by DNA linkers.

Scientific Objectives

As illustrated schematically in Fig. 3,[14,15] directed assembly of nanoparticle arrays by DNA linkages has produced a remarkable variety of structures and an even larger number of possible applications. Given the soft energy landscape of nanoparticle assemblies and their resultant tendency to exhibit very small defect energies, and thus slow defect-annealing kinetics, understanding and controlling the free energy landscape (and specifically, defect behavior) is key to advancing applications in these novel materials. Coherent x-ray beams produced by the APS Upgrade will enable exact CDI reconstructions of the arrangement of nanoparticles in micron-sized crystals of (DNA) assembled materials, leading to precise characterization of the nature of their defects. The enhanced coherent flux also will create opportunities to characterize the energy landscapes that dictate the formation and stability of the self-assembled crystals, particularly near structural transitions, through XPCS experiments.

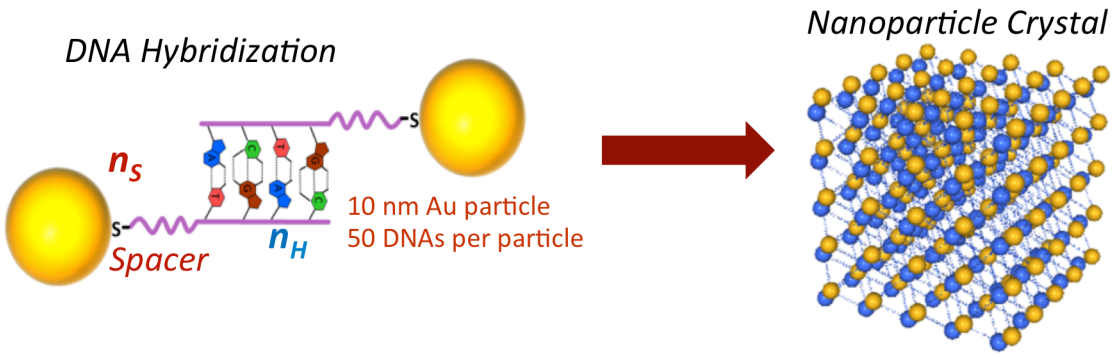

Fig. 3. Nanoparticles form bonds though the hybridization of attached DNA strands and assemble into crystal lattices with tunable symmetry.[15]

Experimental Details

Key insights into the free energy landscape of nanoparticle crystals stabilized by DNA tethers can be obtained by probing collective excitations, i.e., those involving collective coherent motion of many nanoparticles. Given the timescale of these excitations, their experimental characterization will be enabled by the greatly enhanced time-resolved coherent scattering

techniques (e.g., XPCS) at the upgraded APS. To provide a concrete assessment of the feasibility of such characterization, we consider an XPCS experiment on crystals of the type reported recently by O. Gang and coworkers.[15] The crystals are composed of 10-nm Au spheres functionalized with complementary DNA strands that form interparticle bonds. Based on the specific DNA sequences and the possible introduction into the solution of additional complementary strands that hybridize with the attached DNA to alter the bonding, the researchers find that they can drive the crystals through structural transitions between several lattice types, including hexagonal close packed (HCP), face-centered cubic (FCC), and body-centered cubic (BCC). This feature introduces the intriguing possibility of using XPCS to track the softening of modes as the crystals transform between different lattice types. Here, in the interest of specificity, we focus on the BCC lattice.

The theory for XPCS studies of nanoparticle crystals follows directly from methods developed for the interpretation of dynamic light scattering studies on crystals formed from micrometer-sized colloids.[16] Unlike phonons in ordinary solids, in colloidal crystals all but the lowest-frequency, longest-wavelength shear modes are strongly overdamped; as a result, the intermediate scattering function in a one-phonon approximation decays exponentially,

$$g_1(\Delta\vec{q},t) \sim exp\left[-\frac{\omega^2(\Delta\vec{q})}{\lambda(\Delta\vec{q})}t\right],$$

where $\omega(\Delta\vec{q})$ are the eigenvalues of the elastic matrix, $\lambda(\Delta\vec{q})$ are the eigenvalues of the dissipation matrix, and $\Delta\vec{q}$ is the scattering wave vector measured with respect to the nearest reciprocal lattice point q_{Bragg}. For instance, for a BCC lattice in which nearest neighbor interactions are dominant (as expected for the DNA-mediated nanoparticle crystals), the elastic eigenvalues along the [110] direction are given by

$$m\omega^2(\Delta\vec{q}) = \frac{16}{3}\kappa sin^2\alpha$$

where κ is the effective spring constant of the interparticle interaction, m is the particle mass, and $\alpha = \pi(\Delta q/q_{\text{Bragg}})$ is the wave-vector position in the Brillouin zone.

To estimate κ and hence ω, we note that the strength of the nanoparticle interactions can vary significantly through the choice of specific DNA linkers and temperature, and the corresponding rigidity of bonds can be manipulated by almost two orders of magnitude.[17] Based on previous direct measurements and modeling of DNA-mediated colloidal interactions[18] and the length of the DNA strands and the typical number of links involved in bonds in the Au-nanoparticle crystals,[15] we estimate that the effective spring constant is tunable over at least the range

$$\kappa = 10^{-4} - 10^{-3}\ \text{J/m}^2.$$

To first approximation, the dissipation eigenvalues can be taken to be independent of Δq and estimated as $\lambda \approx 6\pi\eta\beta R/m$, where $\eta \approx 2\text{x}10^{-3}$ Pa s is the solvent viscosity, R is the nanoparticle hydrodynamic radius, and β corrects for hydrodynamic interactions between the particles.[16] Typically, the hydrodynamic interactions in colloidal crystals are large and need to be taken into account in quantitative descriptions of the lattice dynamics (e.g., $\beta \approx 55$ in hard-sphere colloidal crystals).[19] For the purposes of obtaining an estimate of the XPCS correlation time, we take β =

10 and R = 20 nm, to account for the contribution from the attached DNA strands to the nanoparticle hydrodynamic radius.

Because typical crystal sizes are several micrometers across,[20] we further assume that the beam is focused with radius $R_b \approx 5$ μm and, for concreteness, that the beam is smaller than the crystal. We also assume that a single coherent area from an optimized APS-U undulator beam monochromatized to the relative bandwidth produced by a Si (111) monochromator is incident on the crystal. For x-rays with a photon energy of 10 keV and an APS-U source brightness of 2×10^{22} ph/s/0.1%bw/mm^2/mrad^2/s, we find the total incident coherent flux to be 4×10^{13} ph/s. As in the case of the interfacial monolayer of nanoparticles considered above, the scattering will be at small angles in transmission, and we again take the sample-to-detector distance to be 6 m and the detector pixel size to be 75 μm. The scattering intensity from the BCC nanoparticle crystal includes a robust [110] peak,[15] and we consider phonon dispersions in the vicinity of this peak. We further assume that the thermal (phonon) contribution to diffuse scattering away from the peak is significant as compared to that from first-order defects such as polydispersity and orientational disorder.[21] Specifically, we consider measurements over the range $\alpha = 0.025\pi$ – 0.1π (which corresponds approximately to wave-vector ranges 0.238 – 0.248 nm^{-1} or 0.253 – 0.263 nm^{-1}, depending on whether one is in the 1st or 2nd Brillouin zone). Based on previous SAXS studies of these crystals,[15] we estimate that the count rates at these wave vectors will be in the range 2×10^4 to 5×10^4 photons/s/pixel. With these count rates, we expect to be able to measure correlation times as small as 20 μs. Further, over this range of wave vectors and using the numerical values for the various parameters given above, we arrive at a range of values for the correlation time of g_1 of $\lambda/\omega^2 \approx 1.5\text{x}10^{-5} - 2\text{x}10^{-3}$ s, indicating that the experiments should indeed be feasible at the upgraded APS. Tracking these modes near the structural transitions in these DNA nanoparticle crystals would provide important insights toward understanding and ultimately controlling these transitions in this class of promising metamaterials.

3.3.C. Yielding in Amorphous Metals

Background and Motivations

Many soft-matter systems are far from equilibrium because they are driven by non-thermal excitations, because they possess intrinsically slow dynamics, or because they consume energy locally. As a result, they cannot be understood using standard statistical mechanics. Far-from-equilibrium behavior differs strikingly from that in equilibrium and represents largely uncharted intellectual territory that offers exciting opportunities for major breakthroughs. Out-of-equilibrium behavior also forms the basis for novel processing strategies for soft materials, since material properties generally depend not only on present conditions, such as temperature or pressure, but also on their history. Further, many out-of-equilibrium systems are characterized by spatially and temporally heterogeneous dynamics. In the case of polymeric glasses, the spatial scale of the heterogeneity is believed to be several nanometers; however, direct information is scarce due to the lack of probes that can resolve slow dynamics on such scales. XPCS with the highly focused beams of the APS Upgrade promises a new strategy to map heterogeneous dynamics and gain new insights into the temporal heterogeneity of fluctuations that are central to out-of-equilibrium behavior.

A further area in which soft materials display rich out-of-equilibrium behavior is in their strongly nonlinear response to mechanical stress. Examples include shear thinning, shear thickening, and thixotropic behavior of dense suspensions and pastes. These nonlinear responses originate in stress-induced microstructural changes, but the identification of connections between the microscopic and macroscopic behavior remains a central challenge. In principle, XPCS can provide crucial information about such stress-induced structural dynamics, but studies to date have been limited by the inability to conduct these studies in challenging sample environments with high temporal resolution.

Principles such as jamming and descriptions of the glass transition in terms of kinetic parameters provide a framework for understanding non-equilibrium mechanical properties for which experimental insight will be extremely valuable. Beyond testing predictions arising from these concepts, the directions described here for research enabled by the APS-U will facilitate validation of emerging theoretical work that ultimately will enable rational design of new soft materials and new applications for these materials. One of the highest-impact inquiries, which is the topic of the APS-U first experiment described below, concerns failure in amorphous solids under applied stress.

Scientific Objectives

Any solid subjected to applied stress possesses an elastic limit, above which it fails. Amorphous solids such as metallic and polymer glasses fail by yielding; however, their intrinsic disorder makes it difficult to identify the microstructural changes associated with yielding. Specifically, theories for yielding in amorphous solids such as metallic glasses identify local regions (containing approximately 100 atoms) known as shear transformation zones (STZs) that preferentially undergo atomic rearrangement. Under sufficient yielding, STZs can act collectively to form shear bands, as shown in the electron micrograph in Fig. 4.[22] Advances in CDI with the APS-U, where atomic-scale resolution in high-Z amorphous materials is expected, will create an opportunity to test these ideas and gain unprecedented information about the structural changes associated with yielding events in metallic glasses. Specifically, by comparing exact before and after atomic arrangements to map the rearrangements that occur during a yielding event in a metallic glass nanopillar, CDI will provide atomic-scale characterization of yielding, enabling tests of recent theoretical advances[23] that will allow the first-ever prediction of failure location in amorphous materials based solely on atomic structure.

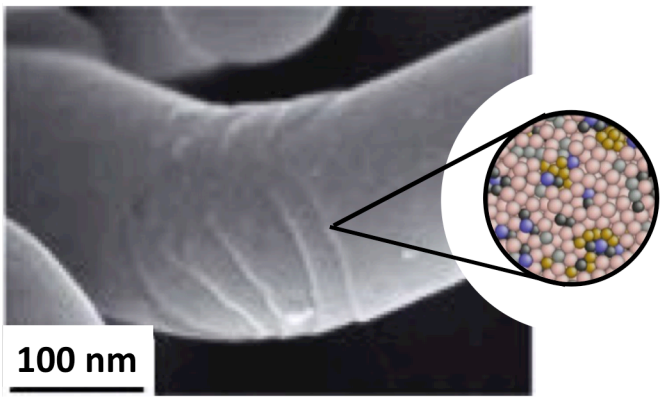

Fig. 4. Scanning electron microscopy image of a metallic glass ($Pt_{57.5}Cu_{14.7}Ni_{5.3}P_{22.5}$) nanorod displaying shear bands following plastic deformation by bending.[22]

Experimental Details

APS Upgrade-enabled CDI measurements with atomic (or near-atomic) resolution have the potential to characterize the atomic rearrangements associated with yielding of an amorphous metal. As envisioned here, samples will be cylindrical, with diameters and lengths of 20 nm and 50 nm, respectively. The glass will be subjected to applied strain that is either in compression, using a nanopillar of the type commonly employed in stress-response measurements of amorphous metals, or that is in tension, where "dog bone-shaped" samples would isolate the failure region to a desired cylindrical segment. In either case, CDI reconstructions would be performed as a function of fixed strain, as the stress is simultaneously monitored so that rearrangement events can be directly connected to nonlinear mechanical response.

As an assessment of the feasibility of such measurements, we have calculated the expected scattering intensities in coherent diffraction patterns from a sample of amorphous metal, based on molecular dynamics simulations.[24] The simulation results contain the positions of 96,000 atoms within an approximately 8 × 8 × 26 nm^3 specimen of the widely studied metallic glass composition $Cu_{64}Zr_{36}$ before and after yielding under an applied shear stress. Fig. 5 shows the coherent diffraction patterns calculated from Monte Carlo simulations of the scattering from the glass for two configurations of the atoms, one before and one after the application of stress that has caused atomic rearrangements.

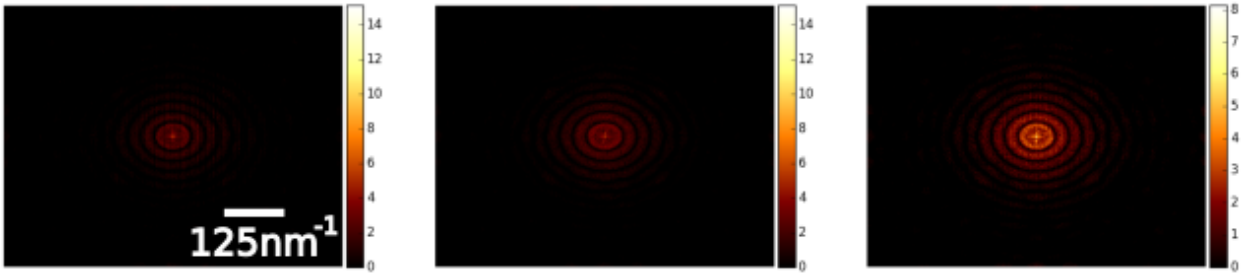

Fig. 5. Simulated coherent scattering[25] from an amorphous metal[24] before (left panel) and after (center panel) a yielding event. The right panel shows the difference between the two scattering patterns.

The diffraction patterns, which are shown on a log scale and extend to a maximum wave-vector q_{max} = 1.26 $Å^{-1}$, were calculated based on a 20 × 26 nm^2 incident beam on the specimen with a total dose of 10^{13} photons/nm^2. Patterns with such scattering intensity to this q_{max} can be used to reconstruct the real-space atomic configuration with a precision of 0.1 Å in the atomic positions. Assuming that the top half of a cylindrical sample is being imaged, so that the beam and sample size approximately match (and so that the total number of atoms being imaged is about six times the number in the simulation), and using the expected coherent flux at APS-U that can be focused into a 20 x 26 nm spot of $2x10^{12}$ photons/sec (0.01% BW), we estimate that the total exposure time needed to collect such a dataset from the nanopillar will be approximately 7 min. Further, assuming one obtains roughly 10 such datasets from different orientations to make a tomographic 3D reconstruction, the total time for a measurement at each strain position will be about 1 h. Thus we expect that atomic-resolution images of the amorphous metal nanopillar at multiple strain amplitudes, and hence at multiples stages of yielding, should be feasible. In contrast, based only on considerations of the coherent flux available today at the APS (i.e., not factoring in the low efficiency of available high-

demagnification optics), we estimate that a single dataset would require an exposure exceeding 12 h, implying that several days would be needed for a single 3D reconstruction; this is infeasible due to the measurement's stringent requirements for sample and beam stability. More practical and technical considerations suggest the difference in accumulation times between the APS today and APS-U could be at least another factor of 5 to 10 greater.

We note several factors that could influence the measurements of the diffraction pattern. The first is radiation damage, which for a metallic glass we expect to take the form primarily of beam heating. Assuming a nanopillar sample geometry with the dimensions given above, in which the pillar is in good thermal contact with a temperature-controlled substrate, we estimate that the sample temperature will increase by roughly 20 K during the measurements, an amount that should not create significant complications.

Another consideration is slow glassy creep, (anelasticity), which amorphous metals can display under some circumstances following step changes in stress or strain.[26] Even if the global strain is held fixed during this relaxation, creep could nevertheless involve slow local atomic motions that potentially complicate the CDI measurements. However, the detection and characterization of such slow dynamics through time-resolved coherent scattering (i.e., XPCS) would provide alternative, unique information about the atomic-scale response of amorphous metals to stress that today is inaccessible.

Finally, we note that, under ideal conditions, electron microscopy techniques can achieve near-atomic-scale resolution of amorphous metal structure; however, constraints on sample geometry and sample environment that are intrinsic to electron microscopy experiments would preclude measurements under the *in situ* applied strain that we envision here. In particular, the ability to obtain scattering images from multiple perspectives for full 3D reconstructions on a sample that is under *in situ* strain is likely to remain outside the current and anticipated capabilities of electron microscopy.

3.4 Operational and Instrumentation Needs

The experiments described here primarily require advances in instrumentation, but there are some operational requirements that must be met:

- There is a key need for positioning stability of focusing optics, samples, and detectors. The capability to scatter horizontally without reduced intensity due to polarization would greatly facilitate advances in mechanical stability by simplifying the mechanical design problem. Accordingly, beamlines that perform the types of experiments listed above will benefit from either a superconducting helical undulator or a horizontal gap undulator. Detailed calculations and comparisons are required, but the superconducting helical undulator seems especially favorable in this regard because the on-axis heat load is less for brightness similar to that from a planar device. Reduced on-axis heat load helps with regard to improving the stability of the beam delivered to the sample.
- An approximately symmetric source is preferred largely because it greatly simplifies focusing with little loss of coherent flux.

We note that none of the experiments we have described require beamlines that extend beyond the existing experiment hall floor of the APS.

Instrumentation needs

Significant advances in instrumentation, especially in detectors, are required to achieve the scientific goals described in this document. Before describing our requirements in this regard, however, it is important to consider the issue of x-ray beam damage. Soft materials can be especially prone to damage, because the properties that make these materials interesting often depend sensitively on molecular-scale structure that is significantly modified by photoelectron-induced changes in chemical bonding. Since x-ray damage effects already are significant at current third-generation sources, it seems reasonable to wonder whether the APS Upgrade will cause even more serious beam damage problems. In fact, however, the source properties of the APS Upgrade will provide opportunities to reduce beam damage in several ways.

Most importantly, the MBA lattice will significantly increase the x-ray beam's coherent flux with only a modest increase in the overall flux. The current APS provides a partially coherent beam, which reduces the contrast available for CDI and XPCS. To compensate for relatively poor coherence while achieving sufficient counting statistics at a desired temporal resolution, it usually is necessary to expose the sample to a higher number of x-ray photons, but this reduces signal fidelity. Starting with a higher-coherence source will provide a tremendous advantage in reducing radiation damage while increasing temporal resolution and sensitivity.

It also should be noted that the effect of x-ray damage is reduced at higher energies. For example, the absorbed dose for carbon decreases approximately as E^{-2}, (the absorption changes as E^{-3} while the energy deposited changes as E), where E is the x-ray energy, for energies up to about 20 keV, while the scattered signal can be kept roughly constant by increasing the sample thickness. Above approximately 20 keV, Compton scattering begins to contribute significantly to the background and there is no further advantage to increasing energy to reduce damage. Moreover, detector efficiency and spatial resolution are increasingly incompatible with efficient speckle resolution above these energies. The current APS has insufficient coherent flux at 20 keV for most coherent applications, preventing high-energy, high-coherence experiments. The dramatically increased coherent flux of the upgraded APS will make it possible to carry out experiments at higher energies. For higher Z materials, the potential gains extend to even higher energies, and the impact of reduced beam damage at the APS-U will be even more pronounced.

Additionally, the APS Upgrade will make it possible to perform XPCS measurements at much faster timescales, which are necessary for advances in soft-matter science. Recall that the fastest relaxation time (τ) that can be resolved with XPCS scales as I^{-2}, where I is the coherent flux. Several aspects of experimental design can be used to mitigate radiation damage effects in coherent scattering studies of dynamics. For example, a previously unexposed region of the sample can be moved through the beam, so long as the motion is smaller than the motion due to the dynamics under study. If the rate at which the new sample can be exposed to the beam is inversely proportional to the relaxation time, then the damage actually will decrease with increased coherent flux, assuming that the increased coherent flux is used specifically to allow access to faster dynamics.

Advanced Detector and Instrumentation Needs

Advanced detectors will be key to meeting the scientific goals described above. For measurements of soft matter at the upgraded APS, it will be important to collect the scattering quickly and efficiently, and at higher x-ray energies. For coherent scattering applications such as CDI and XPCS, fine spatial resolution is required as well as single-photon sensitivity. For XPCS, high frame rates are required but limited dynamic range is acceptable; for CDI, higher dynamic range or pixel-specific gain is considerably more important than extreme frame rates. Some specific requirements and desired features for XPCS and CDI-relevant detectors are summarized in Table 1.

Table 1. Detector Requirements for XPCS and CDI

Item	XPCS Requirement	CDI Requirement
Pixel size	≤ 75 μm	≤ 75 μm
Number of pixels	≥ 1,000 × 1,000	≥ 1,000 × 1,000
Dynamic range	2 bits	12 bits
Frame rate	$\geq 10^6$ frames per sec	$\approx 10^3$ frames per sec for on-the-fly acquisition
Controls and firmware	Sparse dead-time-less readout. Onboard 'droplet' algorithms	Dead-time-less readout. Adaptive per-pixel gain

In additional to detectors, improvements in the following instrumentation will greatly advance the state of the art in XPCS and CDI measurements.

1. Zoom K-B optics[27] for controlled variation of the spot size versus the field of view
2. Extremely stable goniometers with active registration between the sample and the beam
3. Vastly improved small-offset monochromators for rapidly switching between broad and narrow bandpass beams without changing optics
4. Temperature-controlled hutches and better thermal design of beamline stages and supports to improve stability
5. High-performance computing data analysis pipelines to facilitate rapid reduction and understanding of large datasets and to efficiently integrate data from a variety of sources, such as fluorescence and Compton scattering

Soft matter studies also require development of advanced sample environment capabilities, such as flow cells, combination acoustic and laser tweezers, and manipulators to position or translate samples in ways that maximize signal and minimize damage.

Finally, improvements are required in coherence-preserving optics to ensure that the brightest x-ray beams are efficiently delivered to the sample in a stable manner. Advances in coherence-based modeling of beamlines and optics[28] should be made and applied so that the most important areas of focus can be quantitatively identified and addressed.

3.5 References

[1] W. Bu, H. Yu, G. Luo, M. K. Bera, B. Hou, A. W. Schuman, B. Lin, M. Meron, I. Kuzmenko, M. R. Antonio, L. Soderholm, M. L. Schlossman, J. Phys. Chem. B **118**, 10662 (2014).

[2] A. Matic and B. Scrosati, MRS Bull. **38**, 533 (2013).

[3] G. T. Tietjen, Z. Gong, C.-H. Chen, E. Vargas, J. E. Crooks, K. D. Cao, J. M. Henderson, C. T. R. Heffern, M. Meron, B. Lin, B. Roux, M. L. Schlossman, T. L. Steck, K. Y. C. Lee, and E. J. Adams, Proc. Natl. Acad. Sci. USA **111**, E1463 (2014).

[4] See, for example, "*ARPA-E awards IIT-Argonne team $3.4 million for breakthrough battery technology*," Argonne National Laboratory Press Release, August 30, 2013. http://www.anl.gov/articles/arpa-e-awards-iit-argonne-team-34-million-breakthrough-battery-technology or "*Nanoparticle Networks Promise Cheaper Batteries for Storing Renewable Energy,*" http://www.technologyreview.com/news/526811/nanoparticle-networks-promise-cheaper-batteries-for-storing-renewable-energy

[5] D. Lumma, L.B. Lurio, S.G.J. Mochrie, M. Sutton, Rev. Sci. Instrum. **71**, 3274 (2000).

[6] F. van der Veen and F. Pfeiffer, J. Phys.: Condens. Matter **16,**5003 (2004).

[7] P. Falus, L. B. Lurio, and S. G. J. Mochrie, J. Synchrotron Rad. **13**, 253 (2006).

[8] Basic Energy Sciences Advisory Committee Subcommittee on Mesoscale Science, J. Hemminger, chair, "*From Quanta to the Continuum: Opportunities for Mesoscale Science*," U.S. Department of Energy, Washington, D.C. (2012).

[9] I. H. Lin, D. S. Miller, P. J. Bertics, C. J. Murphy, J. J. dePablo, and N. L. Abbott, Science **332**, 1297 (2011).

[10] L. Van Look, P. Rincon Delgadillo, Y. Lee, I. Pollentier, R. Gronheid, Y. Cao, G. Lin, and P. F. Nealey, Micro. Eng. **123**, 175 (2014).

[11] T. Segal-Peretz, J. Winterstein, J. Ren, M. Biswas, J. A. Liddle, J. W. Elam, L. E. Ocola, R. N. S. Divan, N. Zaluzec, and P. F. Nealey, Proc. SPIE **9424**, 94240U (2015).

[12] M. Doxastakis, H. S. Suh, X. Chen, P. A. Rincon Delgadillo, L. Wan, L. Williamson, Z. Jiang, J. Strzalka, J. Wang, W. Chen, N. Ferrier, A. Ramirez-Hernandez, J. J. de Pablo, R. Gronheid, and P. Nealey, Proc. SPIE **9424**, 94241N (2015).

[13] T. Sun, Z. Jiang, J. Strzalka, L. Ocola and J. Wang, Nat. Photon. **6,** 586 (2012).

[14] M. B. Ross, J. C. Ku, V. M. Vaccarezza, G. C. Schatz, and C. A. Mirkin, Nat. Nanotechnol. **10**, 453 (2015).

[15] Y. Zhang, S. Pal, B. Srinivasan, T. Vo, S. Kumar, and O. Gang, Nat. Mater. **17**, 840 (2015).

[16] A. J. Hurd, N. A. Clark, R. C. Mockler, and W. J. O'Sullivan, Phys. Rev. A **26**, 2869 (1982).

[17] O. Gang, private communication (2015).

[18] W. B. Rogers and J. C. Crocker, Proc. Natl. Acad. Sci. USA **108**, 15687 (2011).

[19] Z. Cheng, J. Zhu, W. B. Russel, and P. M. Chaikin, Phys. Rev. Lett. **85**, 1460 (2000).

[20] M. N. O'Brien, M. R. Jones, B. Lee, and C. A. Mirkin, Nat. Mater. **14**, 833 (2015).

[21] A .J. Senesi and B. Lee, J. Appl. Cryst. **48**, 1172 (2015).

[22] G. Kumar, A. Desai, and J. Schroers, Adv. Mater. **23**, 461 (2011).

[23] E. D. Cubuk, S. S. Schoenholz, J. M. Rieser, B. D. Malone, J. Rottler, D. J. Durian, E. Kaxiras, and A. J. Liu, Phys. Rev. Lett. **114**, 108001 (2015).

[24] M. Falk and D. Alix-Williams, private communication (2015).

[25] D. Vine, private communication (2015)

[26] J. D. Ju, D. Jang, A. Nwankpa, and M. Atzmon, J. Appl. Phys. **109**, 053522 (2011).

[27] T. Kimura, S. Matsuyama, K. Yamauchi, and Y. Nishino, Opt. Express **21**, 9267 (2013).

[28] X. Shi, R. Reininger, M. Sanchez Del Rio, and L. J. Assoufid, J. Synchrotron Radiat. **21**, 669 (2014).

4 Biology and Life Sciences

Gayle Woloschak, *Northwestern University*
Robert Fischetti, *Argonne National Laboratory*
Lee Makowski, *Northeastern University*

Michael Becker, Andrzej Joachimiak, Stefan Vogt, Xiaobing Zuo, *Argonne National Laboratory*; Andre Hoelz, *California Institute of Technology*; Steve Soisson, *Merck Research Laboratories;* Tom O'Halloran, *Northwestern University*; Rajiv Chopra, *Novartis Institutes for BioMedical Research*; Keith Moffat, *University of Chicago*; Jim Penner-Hahn, Janet Smith, *University of Michigan*; Peter Lay, *University of Sydney*

4.1 Executive Summary

Biological systems are complex, both in the colloquial sense of being complicated and in the mathematical sense of being built from a large number of weakly-coupled building blocks. In biological systems, such blocks can be single molecules, molecular complexes, organelles, whole cells, and tissues. These building blocks exhibit emergent behavior expressed as self-organization and as collective (and in some instances chaotic) activities that can be explained only by the interactions between the building blocks rather than by the properties of the individual building blocks alone. Systems that are complex in this mathematical sense require a systematic approach, but synchrotron studies of biological systems largely have been limited to reductionist approaches, such as crystallography of a purified protein or 2D imaging of an isolated single cell or thin tissue section. The APS Upgrade will enable diffraction, scattering, imaging, and spectroscopy to be brought to bear on biological systems, providing diverse information across multiple building-block lengthscales, from molecules to tissues and everything in between. The APS Upgrade also will allow the addition of temporal resolution where only static measurements are now possible, as well as greatly increasing the capacity of 3D imaging of such complex systems. The APS Upgrade will provide high-intensity, high-energy (~30-keV) x-rays that can be focused to sub-micron sizes to maximize the amount of data that can be collected from a single crystal. Some milestones enabled by the new capabilities of the APS Upgrade are already clear. The upgraded APS will revolutionize pharmaceutical research, for example, by allowing thousands of potential drug-target structures to be determined in a single day. It also will provide the imaging capabilities to better address intra- and extracellular signaling processes that are central to physiological processes in disease and in health, as well as the roles and toxicities of metals in the environment.

4.2 New Opportunities for Biology and Life Sciences at APS-U

Biological sciences are a vast field whose impact ranges from human health to agriculture to energy. The complexity of biological systems means that qualitative studies have great

prominence; therefore, the use of parallel, complementary techniques is very important. Because many such complementary techniques depend on synchrotron radiation, advances in x-ray science have immense importance in biology. The program of biology and life sciences research at synchrotron lightsources reflects this diversity and has had a major impact across the entire range of biological sciences. For the purposes of the development of x-ray techniques, biological research at hard x-ray lightsources can be thought of as comprising four categories: macromolecular crystallography to determine the structure of proteins and various macromolecular assemblies in 3D at near-atomic resolution; direct imaging of specimen structure over the entire range of lengthscales from molecules to organisms; real-space mapping of trace elemental content and chemical state of specimens; and studies of less-ordered systems by structural and spectroscopic approaches. Grand challenges at the frontiers of structural biology address such questions as how complex molecular machines embedded in cell membranes work, exactly how drugs interact with their targets, how side effects arise, and how drugs can be improved. Macromolecular crystallography is currently the most powerful tool to determine structure at the atomic level, but studies are limited by the need to prepare crystals of sufficient size and quality. For many grand challenge questions, it often is possible to grow only tiny crystals. Present experimental capabilities generally provide structural information for crystals as small as 5 μm, but even these can be hard to prepare. The APS Upgrade will extend structural capabilities dramatically by creating a powerful opportunity to study even smaller (0.5-μm) microcrystals that are likely to be easier to obtain in a well-ordered form. A particularly exciting advance is the introduction of statistically rigorous techniques that combine data from many small crystals to retrieve molecular structure.[1,2]

Local chemistry and functionality complement purely structural considerations. About one-third of all proteins require a metal co-factor for proper regulatory or catalytic function. Understanding the role that trace metals play in fundamental questions of biology is therefore critically important. Scanning x-ray microscopy and microspectroscopy allow both the amount of trace metals and their local chemistry to be visualized at the subcellular level. Today these microscopies are largely limited to moderate spatial resolution (typically 100 nm) of systems where a high concentration of metals is present, and to 2D imaging of 3D objects. The significant increase in focused x-ray flux available in nanobeam techniques will dramatically enhance the capability to probe trace metal concentrations and chemistry. The realistically achievable spatial resolution and elemental concentration sensitivity will be increased by approximately two orders of magnitude. For example, nanocomposites are being developed to effectively combine diagnosis and therapy for diseases such as cancer.[3,4] To assess the functionality and potential side effects of nanocomposite therapies requires visualizing the interaction of individual nanocomposites with tissues, cells, and organelles in three dimensions.[5,6] The APS Upgrade will enable rapid acquisition of information because of greater brightness and shorter dwell time. This will allow investigators to take full benefit from the highest spatial resolution, 10 nm and below, even across the large fields of view of tissue sections, and will thus for the first time enable direct visualization of nanostructures in the broader context of larger tissue sections. The greatly increased speed of data acquisition will enable evaluation of statistically significant populations of biological samples (the lack of which is a common criticism of synchrotron-generated data today) and will greatly increase access to tomographic studies. In addition, the APS Upgrade will unlock a series of multi-modal approaches ranging from the complementation of trace elemental mapping by simultaneous

visualization of ultrastructure using lensless imaging approaches to complementation with simultaneously acquired nanodiffraction data in order to characterize local architecture.

Functions in biological systems invariably require motion across all lengthscales and timescales ranging from that of fundamental chemistry to the generation time of an organism. Most synchrotron studies have concentrated on static techniques, which give a highly informative but ultimately limited picture. The APS Upgrade will extend hitherto static measurements into dynamics, where possible, and thus will offer a new view of biological function.

4.3 Early Biology and Life Sciences Experiments at APS-U

4.3.A. Molecular Pathology: Structure of Healthy and Diseased Tissues

Background and Motivation

Human disease generally involves disruption of the function of cells, degeneration of important molecular structures, and dysregulation of physiological processes.[7] At the molecular level, disease expresses itself in alterations in the structure and dynamics of systems constituting the substructures of the cells and the polymeric extracellular scaffolding within which the cells are arranged. The study of molecular pathology (a term that has been applied to cancer for several years[8]) is an excellent example of a crossover discipline because it employs an extremely wide range of cell and molecular biology techniques, from imaging to genomics, proteomics, and metabolomics. Maps of molecular constituents and their architectures in healthy and pathological tissues are needed at the finest spatial resolution to understand the disruptions of tissues that are expressions of disease. Linking molecular architecture to tissue anatomy will often require information at sub-micron resolution, as low as hundreds or even tens of nanometers. A detailed understanding of pathological molecular processes and their temporal progression is necessary to create relevant therapies. Adding elementomics (the study of metals and their functions in biological systems) to the toolkit of molecular pathology would be an important breakthrough in this field. With increased brightness and consequently increased scanning speeds, x-ray fluorescence microscopy could make this possible.

As a concrete and dramatic example, Alzheimer's disease involves the slow buildup of amyloid plaques in the brain and the progressive cell death associated with amyloid constituents.[9] The medical and economic impacts of this disease in an aging population are enormous,[10] and improved understanding of the molecular events underlying its genesis and progression is a very high societal priority. Recent work has demonstrated the existence of distinct strains of fibrils in Alzheimer's disease plaques.[11] At present, a pathologist using current post mortem clinical tools can identify plaques and map their distribution in the brain. Current x-ray scattering technology provides only relatively low-resolution information about individual plaques, as shown in Fig. 1. Use of a much smaller, higher-brightness beam will enable production of images at much higher resolution, providing detailed characterization of plaque architecture, insights into the process of plaque assembly, and an understanding of the relationship of plaque structure to cellular milieu, amyloid oligomers and mechanisms of cellular toxicity.

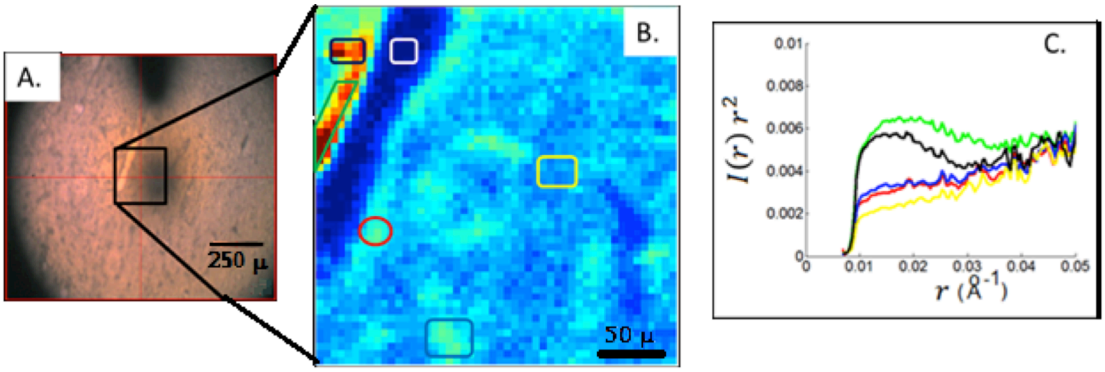

Fig. 1: Scanning microdiffraction of brain tissue from a subject with Alzheimer's disease detects cerebral amyloid angiopathy (CAA).[11] (a) Optical micrograph of the tissue as viewed by a microscope whose optical axis is coincident with the x-ray beam path. (b) Map of the intensity of small-angle scattering from the region outlined in A using a 5 μm diameter beam. The buildup of amyloid around small blood vessels (indicated in red) corresponds to the highest intensity in the small-angle scattering pattern. (c) Colored boxes in B are coded to the plots, which are the circularly averaged, wave vector-weighted, small-angle intensity $I(r)r^2$ as a function of wave vector r from the different regions, including empty blood vessel (white – not shown in plot), tissue debris (yellow), diffuse amyloid deposits (blue and red), perivascular amyloid (green), and heavy amyloid deposit (black).

Scientific Objectives

Molecular pathology is an emergent field that studies the nature of disease by examining molecules in organs and tissues.[8] It expands the rationale of cell biology to cellular systems, tissues and organs, seeking to characterize the relationship between molecular structures and function at multiple lengthscales. Molecular pathology also will be able to probe the phenotype of certain classes of genetic disorders. For example, there are many disorders of connective tissue in which the point mutations in relevant collagen genes have been identified but the exact mechanism by which the defective collagen affects overall structure remains unknown.[12] It exemplifies an approach amenable to studies of any nanostructured biomaterial, including plant-based biomass, biofilms, and synthetic hybrid materials or biopolymers, and may provide insights into disease mechanisms and new potential therapeutic targets.

Experimental Design

A foundation for the design of therapies to slow or halt the progression of AD can be provided by developing the means to map the progression of lesions within brain tissue. The APS Upgrade will enable the production of nanoscale (10-100-nm) x-ray beams with far higher intensity than is presently available. Diffraction data derived from these beams will be capable of providing detailed information about the molecular architecture of amyloid plaques.

The structures of individual strains of amyloid may be distinguished and the molecular relationship of plaques within distinct regions of the brain identified. The higher x-ray brightness in these nanoscale beams will vastly increase the sensitivity (because of reduced background due to a smaller focus size) and spatial resolution at which diffraction data can be acquired. For example, the scanning microdiffraction image shown in Fig. 1 required approximately 1 hour to record over a 250 × 250 μm^2 area with 5-μm resolution and a focused

flux of 10^{11} photons/s. To visualize individual fibrils at the required resolution and sensitivity for the experiments proposed here, in the context of 2-3 cells embedded in tissue, one would need to probe an area of about 50 × 50 μm^2 at a spatial resolution of 100 x 100 nm. With available instrumentation at the APS today, this would require 5,000 hours, assuming a focused flux of 2 x 10^9 photons/s, making the experiment impossible for practical purposes. The APS-U is anticipated to provide more than 10^{12} photons/s focused into a 100-nm spot size, due to the improved source as well as more advanced focusing optics; this would permit imaging a 50 × 50 μm^2 area with 100-nm resolution in only about 10 hours, rendering the experiment feasible.

Studies of specific sub-cellular structures will also be enabled by the use of 10 nm x-ray beams that generate the greatest level of detail in scanning images. Such detail is impossible today because the required scattered intensity cannot be generated from such small spots. Correlation of structural diversity among and within neighboring plaques and those in different parts of the brain will yield a deeper understanding of the process of coalescence, fragmentation, diffusion, and dispersion of fibrils during disease progression, providing important insights into the design of possible therapies. For example, small collections of amyloid fibers/oligomers interact with different proteins compared to interactions inside large structures such as plaques.[13] Structural and elemental changes associated with amyloid size increase may be observable by high-brightness x-rays.

4.3.B. Integral Membrane Proteins, Disease and Drug Discovery

Background and Motivation

Integral membrane proteins are structurally and functionally diverse and comprise about one-third of the estimated 20,000 to 25,000 human proteins.[14] According to the Membrane Proteins of Known 3D Structure database,[15] structures have been determined for only about 550 unique membrane proteins; this number includes similar proteins from different species. Membrane proteins play critical roles in biological processes such as ion conduction (e.g., voltage-gated ion channels), the regulation of biochemical pathways (e.g., protein kinases), and physiological function (e.g., through G-protein coupled receptors). These proteins have been implicated in many diseases, including cystic fibrosis, epilepsy, infertility, diabetes, hypertension, cardiovascular illness, neurodegeneration and Alzheimer's disease. They also play a role in the development of many known cancer types. Given their central role in so many biological processes and their ready accessibility from extracellular space, integral membrane proteins are the targets of more than 50% of all new small-molecule drugs. The biomedical importance of determining the 3D structures of such molecules has been recognized by three Nobel Prizes in Chemistry, in 1988, 1998, and 2012.

Despite their importance, less than 3% of the > 110,000 structures in the Protein Data Bank are of integral membrane proteins. These proteins and functional protein complexes are notoriously difficult to produce in a quantity and purity sufficient to crystallize. If the proteins do crystallize, they tend to yield either small, micron-sized crystals or larger, structurally heterogeneous crystals.

Such crystals diffract poorly, due either to small size or lack of internal order. In many cases, partial data sets from many micron-sized crystals must be merged to overcome the effects of

radiation damage.[16] Recent advances in crystallization techniques such as use of the lipidic cubic phase and advances in micro-crystallography techniques have enabled the structural determination of important integral membrane protein complexes, such as the β2-adrenergic receptor-Gs protein complex shown in Fig. 2.[17] However, the structures of only 30 of the estimated 800 G protein-coupled receptors (GPCRs) have been determined, and most are in an inactive form without the G protein. To fully understand the structure/function relationship of the many diverse GPCRs, one needs to determine the structures of GPCRs with a bound ligand and G protein, which are likely to yield only micron-sized crystals that diffract weakly.

Fig. 2. Ribbon representation of the β2 adrenergic receptor-Gs protein complex. This integral membrane receptor is shown in green with an agonist bound (yellow), and the heterotrimeric Gs protein components (Gα - orange, Gβ - cyan, and Gγ - purple).[17]

Although the nuclear pore complex (NPC) is not an integral membrane protein, it represents an even larger class of membrane spanning complexes, and a prime example of the broadening range of systems amenable to structural analysis through the APS-U. The NPC is the sole gateway that allows bi-directional macromolecular exchange across the nuclear envelope and thus functions as a key regulator of the flow of genetic information from DNA to RNA to protein.[18] The NPC is a massive transport channel; in vertebrates, the NPC has an extraordinarily high molecular mass of approximately 120 MDa and is 120 nm in diameter and 50 nm thick. The NPC transport channel is constructed of approximately 35 distinct proteins, which assemble into six subcomplexes that further assemble with 8-fold symmetry to form the full NPC. The size and flexibility of the NPC presently preclude the crystallographic determination of the structure of the entire intact NPC. However, the structures of large subcomplexes up to 400 kDa in mass have been determined by a multimodal approach using cryoelectron tomography[19,20] x-ray crystallography[21,22,23] and super-resolution microscopy[24]. Larger subcomplexes or the intact NPC most certainly will yield small crystals due to the particle's flexibility. The APS-U will allow structure determination using serial x-ray crystallography from crystals as small as 0.5 µm. Furthermore, the methodologies developed to determine the structure of the NPC will push the current boundaries of structural cell biology and when developed, will be more generally applicable to other supramolecular complexes.

The pharmaceutical industry has a long history at the APS of applying synchrotron radiation to enable pre-clinical drug discovery research. Macromolecular crystallography has been at the forefront of this interaction. Approximately 30% of therapeutically relevant protein targets are routinely studied at the APS. The remaining 70% do not currently benefit from extensive structural guidance because the crystals are too small or diffract too poorly with current x-ray capabilities. These include some of the most important protein target classes listed above, including GPCRs, ion channels, and multi-protein complexes.

Scientific Objectives

The APS-U's new, more tightly focused x-ray beam will create the capability to collect and merge data from hundreds of crystals in a short period of time and to examine thousands of crystals in a day. This greatly expanded throughput of excellent crystallographic data will significantly increase the number of drug targets amenable to crystallographic analysis, creating explosive growth in structure-guided drug discovery and transforming the pharmaceutical industry's search for and optimization of drugs that target these important classes of molecules.

Experimental Design

Radiation damage to protein crystals is an increasing concern with an x-ray beam as small as 0.5 μm; new data acquisition strategies and instrumentation are needed to minimize its effects. By extrapolating from recent radiation damage studies, we anticipate that each crystal will have a lifetime in the x-ray beam as short as 10 μs.[25] Synchrotron structural studies thus will require (and benefit from) development of technologies for rapid and efficient delivery of crystals, similar to those being developed for the free-electron lasers. One such delivery system used at the SLAC Linac Coherent Light Source, the lipidic cubic phase (LCP) injector, extrudes a ~50 μm-diameter stream of LCP-containing microcrystals.[26] This technology is rapidly being adapted to synchrotron applications. Experiments at the European Synchrotron Radiation Facility with bacteriorhodopsin crystals of sizes varying from 20 to 50 μm demonstrate the potential broader application to storage ring-based beamlines of this sample delivery technology.[27]

In collaboration with the developers of the LCP injector from Arizona State University (John Spence, Petra Fromme, Wei Liu, and Uwe Weierstall) and the University of Southern California (Vadim Cherezov), an APS-based team has demonstrated that, at present, a minimum crystal size of ~5 μm is required to collect useful data from human A_{2A} adenosine receptor (a GPCR). Figure 3 shows a sum of thousands of diffraction patterns from A_{2A} microcrystals delivered using the LCP arrangement. By comparison, the structure of A_{2A} was previously determined to 1.8-Å resolution on the same APS beamlines using a 10-μm beam and data from the 55 best crystals, with typical sizes of 60-80 μm.[28] The high brightness of the APS-U, coupled with appropriate focusing optics, will allow at least a 100-fold intensity increase and a reduction of the beam size to 0.5 μm. The combination of optimizing sample delivery (flow rate to match crystal and beam size) and reducing background scattering (smaller diameter jet and He or vacuum in the beam path) will allow structure determination from crystals as small as 0.5 μm.

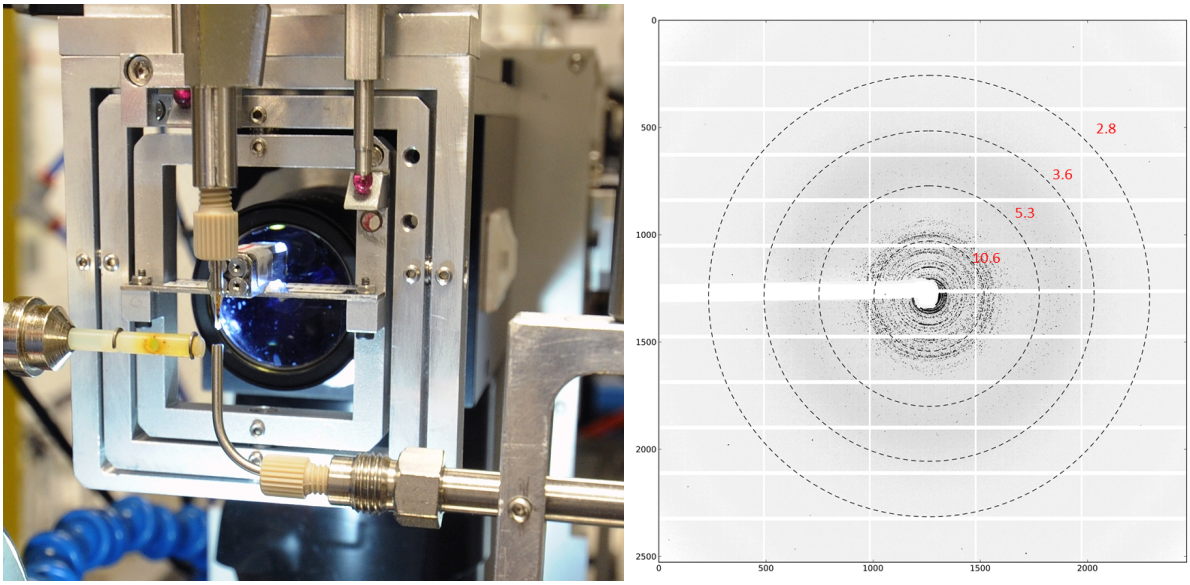

Fig. 3. (left) The LCP injector on APS beamline 23-ID-D. (right) A composite diffraction pattern of A_{2A}-adenosine receptor from 1,648 frames that showed diffraction of > 5 spots. A total of 17,654 frames were recorded at a 10-Hz frame rate in shutterless mode of data collection with a 10-µm beam. The hit rate was less than 1%, which is indicative of the density of crystals in the stream and the flow rate. The composite image is similar to a powder pattern, since the crystal orientation is random. The majority of the reflections fall within 3.6 Å. Several strong reflections can be seen at much higher resolution, but they may be salt crystal diffraction.

Studies with highly intense x-ray beams are improved by considering the fundamental mechanisms through which radiation damage occurs. Damage from x-rays is caused by photoelectrons and Auger electrons (primary damage) and diffusion of free radicals (secondary damage). Cryo-cooling samples during data collection can minimize or even prevent secondary damage but has limited effect on primary damage. To limit secondary damage, most data using x-rays in the energy range of 12 to 13 keV is collected today at cryogenic temperatures; however, recent experiments performed at 18.5 keV with a 1 µm beam have demonstrated the benefit of using higher-energy x-rays to reduce radiation damage to protein crystals.[29,30] Similar reductions in radiation damage are expected for crystals as large as 5 µm when diffraction data are collected at even higher x-ray energies (~30 keV) that are accessible at a high energy electron storage ring such as the APS.[31] The lengthy process of cryo-protecting (removing the crystal from its crystallization medium and mounting it suitably for data collection) and then cryo-cooling the crystal often degrades the crystal quality. It has recently been shown that, with very high dose rates (>1 MG/s) and very short exposure times, secondary damage can be "outrun" even at room temperatures.[32] The high brightness of the APS-U over a wide energy range will provide a unique opportunity to discover how best to collect data from submicron-sized crystals with minimal radiation damage. The combination of submicron-sized crystals, optimized sample delivery methods, and a high-intensity hard x-ray beam whose size is matched to the crystal size will allow thousands of structures to be determined in a single day.

In addition to enabling static and dynamic structural studies on submicron 3D crystals, the high brightness of the APS-U also will enable structure determination from weakly scattering 2D crystals of engineered protein and nucleic acid arrays on surfaces, and proteins in membranes. The high coherence will expand the range of options for phasing of 3D crystals to include CDI

ptychography and Fourier transform holography, which could become efficient and routine. High coherence also will provide detailed structural information in localized regions of membranes and engineered 2D arrays, possibly enabling structure determination of virtually any biomolecule of interest without the constraint of growing 3D crystals via traditional methods.

The APS-U will provide the exciting capability to observe time-resolved structural changes of proteins in crystals. Biological processes are fundamentally dynamic. For example, much of the physiology of cells is driven by the formation or breakdown of complexes, ranging from the capture of the substrate molecule by an enzyme, to the serial recruitment of proteins, to a complex regulatory assembly. Envisioning such processes as "molecular movies," in which each frame is underpinned by important structural physical knowledge, suggests a powerful paradigm for understanding and prediction.

Many of the new capacities of the upgraded APS, such as x-ray fluorescence spectroscopy, have important potential applications in various types of dynamical studies. The ability to examine crystals as small as 0.5 μm may well enable new regimes of time-resolved x-ray crystallography. In a crystal of such dimensions, diffusion time of a small ligand into the interior of the crystal can be on the order of 10 μs or less. Coupled with use of aqueous phase viscous jets for crystal delivery, it is easy to visualize a mode of serial crystallography at room temperature and in water, carried out as a function of time after the initiation of the diffusion process. Such a process would be a unique contribution from the APS-U to important problems in mechanistic and structural biology.

4.3.C. Microvesicles, and Cellular Protrusions: Nanomedical Frontiers in Intracellular and Extracellular Signaling

Background and Motivation

Extracellular signaling is essential in normal physiological functions; aberrant forms are widespread in disease pathologies, including cancers, cardiovascular disease, diabetes, and neurodegeneration. Molecules involved in extracellular signaling thus offer new targets for treatment of diseases. Extracellular signaling is controlled in large part by extracellular microvesicles—particles in the micron-to-submicron size range that are released from all cells—that carry DNA, RNA, proteins, lipids, and other biomolecules from one cell to another.[33,34] The target cell could be of the same type or of different origin. Recent reviews on microvesicles and exosomes indicate that this area of biology offers new ways to study topics as diverse as infection, cancer, and multiple sclerosis.[35,36]

There are four types of microvesicle particles that are physiologically distinct and of quite different sizes. Apoptotic particles are released from cells undergoing apoptosis (programmed cell death). Although their functions are unclear, these relatively large microvesicles, with sizes greater than 1 μm, are readily taken up by other target cells. Somewhat smaller microparticles (100 nm to 1 μm in diameter) are released by blebbing of the cell membrane and are essential for cell-cell signaling. Even smaller exosomes (10-100 nm in diameter) are equally critical for cell-cell signaling, but they are produced inside the cell and then exported. A newly discovered

type of microvesicles, known as oncosomes (1-10 μm in diameter), are released from amoeboid tumor cells; their function in tumorigenesis is unclear.[36]

With current x-ray imaging capabilities, microvesicles are either too small to map with sufficient resolution in the context of a whole cell or tissue area, they provide too little contrast to identify boundaries, or they cannot be imaged at all.[33,34] Even if microvesicles could be imaged, it is not possible at present to sample a sufficiently large set to offer meaningful statistical insight in an experiment of realistic duration, or to identify and characterize discrete phenotypic disease-induced sub-populations that differ from those that are released from control cells and that may confer different aspects of disease pathology. This is extremely important in the identification of new potential drug targets. The vesicle sizes and the composition of their populations are simply too heterogeneous, given the current limited statistics. Finally, the spatial resolution currently available is insufficient to obtain vesicular ultrastructure in the context of a whole cell or tissue area.

Rough, initial insight into the interaction of pharmaceuticals with microvesicles is obtainable with currently available x-ray techniques. Figure 4 shows a micro-x-ray fluorescence (micro-XRF) map of a metastatic lung cell in the presence of a Ru-complex drug.[37] The map shows that Ru is concentrated where the microvesicle interacts with the filipodia,[38] but the details of the interaction are unresolvable with current x-ray capabilities.

Scientific Objectives

All of the above classes of microparticles play important roles in cancer progression. When metastatic cancer cells are exposed to microparticles from primary tumors, they increase their transformation to more aggressive phenotypes that transfer multidrug resistance genes,[39,40,41,42] which may help to explain why metastasis is difficult to treat with chemotherapy.[43] The cancer microvesicles also "infect" a range of other cells in ways that support future tumor growth, for example by prompting vascularization or forming pre-metastatic niches. All of these processes lead to the life-threatening pathologies associated with multi-organ cancer involvement. Advanced x-ray approaches at the APS Upgrade will address many of the gaps in our knowledge of these processes, potentially leading to new treatments—or even prevention—of cancer metastases.

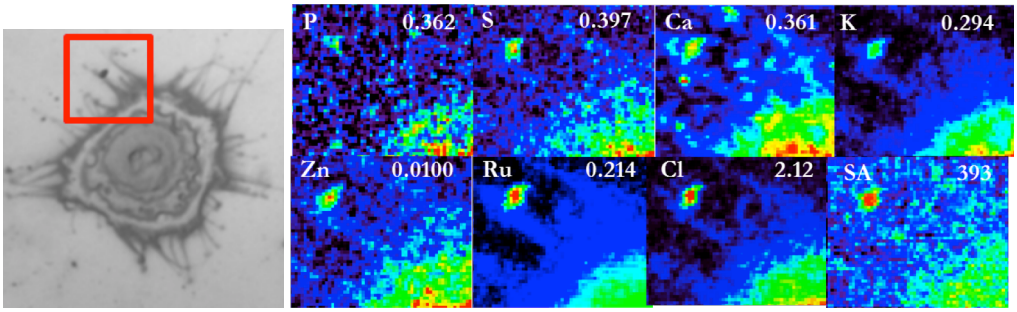

Fig. 4. Micro-XRF elemental mapping of Ru complexes with A549 metastatic lung cells. (left) Optical image showing a cancer cell and filipodia. (right) Cancer microvesicles bind the drug and interact with the filipodia. The Ru content is high in the microvesicle; the high P level also shows the high level of RNA/DNA. The concentration of Ru is high in the filipodia compared to other elements. The numbers in each image indicate the maximum concentration in μg/cm^2.[37]

Experimental Design

The questions laid out above can be addressed with high-resolution hard x-ray microscopy. The APS Upgrade will enhance x-ray fluorescence (XRF) imaging experiments and permit visualization of trace metal content with absolute sensitivities down to a few atoms. Image deconvolution techniques will further improve the spatial resolution of elemental content maps and facilitate 3D imaging of internal structures. Lensless imaging methods such as ptychography will be able to visualize structural detail at resolutions as low as 10 nm, and the higher brightness provided by the Upgrade will allow simultaneous registration of elemental content of microvesicles and exosomes. Preliminary low-resolution studies to 50 nm resolution for larger microvesicles show the presence of different elemental distributions suggestive of internal organelles or other local structures, which will be resolvable by such techniques.[44] Other studies focusing on (possible) exosomes, for instance, are suggestive of RNA/DNA cargoes being contained within particular ultrastructures, which appear to be of appropriate size. By investigating a statistically relevant number of cancer cells with 10 nm spatial resolution, we will be able to examine the production and extrusion of microvesicles from their parent cells, as well as the structures—including surface characteristics— of the very heterogeneous types of microvesicles. Conversely, we may also be able to follow (due to their elemental content) isolated exosomes and their fates as we deliver them to cancer cells or even tumors. High-resolution imaging will allow us to observe how microvesicles interact with the surfaces of the target cells, and how and where they are internalized and deliver their cargoes to the target cells.

4.3.D. Transforming Our Understanding of Cell Biology

Background and Motivation

A major challenge in the field of cell biology is mapping and following the dynamic molecular concentrations and concentration gradients that are essential for cellular functions. The problem is complicated by the crowded nature of the intracellular milieu—millions of macromolecular complexes and hundreds of organelles and vesicular compartments. While many subcellular compartments maintain their own innate elemental composition (e.g., Mn is present at higher concentrations in mitochondria than in the cytoplasm), mapping these elements quantifiably in 2D at the spatial and chemical resolution required for such studies is nearly impossible with current nanobeam intensities at the APS. Similarly, tomography of elemental content at the required spatial resolution is at present completely impractical.[45]

Scientific Objectives

The enhanced brightness offered by APS-U will provide unprecedented tomographic imaging capabilities that will distinguish between many different molecular populations and place these within a high level of ultrastructural definition. These imaging capabilities will open new doors to an understanding of how subcellular components operate together to maintain living processes. With APS-U's 100-fold increase in sensitivity to detect low elemental content, x-ray fluorescence microscopy will allow precise concentration measurements and sensitive mapping of more than 15 essential and important elements at extremely small lengthscales (*i.e.* P, S, Cl, K, Na, Ca, V, Mn, Fe, Co, Ni, Cu, Zn, Se, I, Br, Mo). Today's experiments are limited to spatial

resolution of a few microns over a moderate 3D field of view that cannot resolve underlying heterogeneous distributions, as illustrated in the left panel of Fig. 5.[46] Cells employ these elements in a number of structural and catalytic biopolymer complexes. The APS Upgrade will offer a spatial resolution of tens of nm and sensitivity capable of detecting tens of atoms of a specific element, over a large field of view. The expanded spatial lengthscale, at both the long- and short-distance scales is illustrated in the right panel of Fig 5.

The spatial and concentration information can be combined with another advantage of the higher brightness planned in the APS-U, namely lensless imaging combined with scanning probe imaging (ptychography). This modality provides an ultrastructural context for determining the spatial distribution of the biopolymers with fixed elemental ratios. For example, the relative P and Zn content of chromatin varies within a narrow range, which is different from the P to Zn ratio characterizing mitochondria. With detailed elemental information, we may be able to gain better insight into the fundamental structural architecture of cells. The ptychographic ultrastructural approach, in combination with cryo-preservation, avoids the need to fix, embed, and stain cells as required by traditional electron microscopy, which is not compatible with the visualization of native structural content. These combined imaging modalities will allow interrogation of subcellular spatial domains in ways that will open entirely new chapters of intracellular and extracellular communication events that are essential in signaling, development, differentiation, and embryonic development.

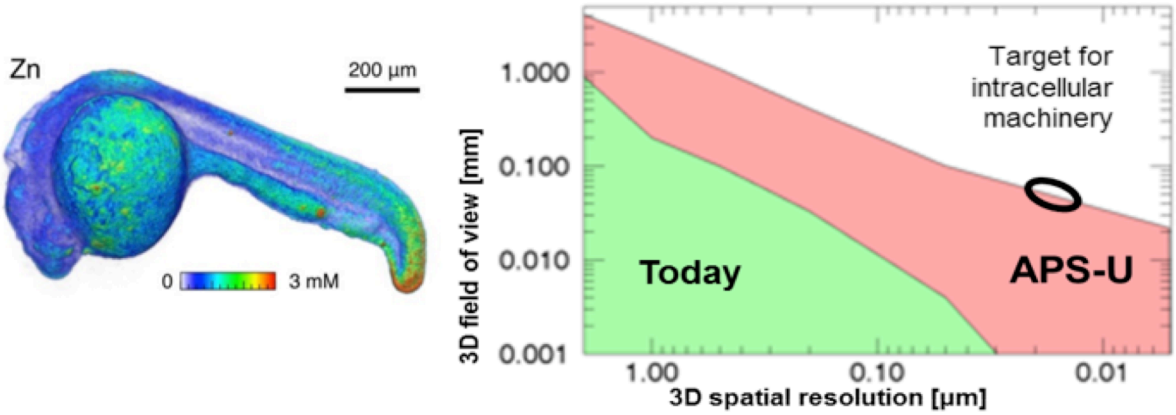

Fig. 5. (left) Tomographic visualization of the Zn distribution in a Zebrafish embryo.[46] (right) Estimate of the 3D spatial resolution achievable in a given observation volume at the APS today (green) versus an upgraded APS. Today, achievable 3D spatial resolution is largely limited by the time required to acquire a tomographic dataset at a given spatial resolution. In the case of the Zebrafish embryo, the dataset was acquired as a series of 60 projections of 840 x 1562 μm^2 each with 2 μm steps and 10-ms-per-pixel integration time, for a net data acquisition time of >50 hours. With the upgraded APS, we anticipate per-pixel integration times with identical statistics down to 100μs, so a single projection taken at 100 nm spatial resolution could be acquired within 3-4 h. Using dose fractionation approaches[49,50,51] and advanced reconstruction methods,[52] a 3D dataset of this object at vastly improved spatial resolution could be acquired in 8h of beam time. For smaller samples, the upgraded APS will enable visualization of intracellular machinery in the context of elemental content down to 10 nm in volumes as large as 100 × 100 × 100 μm^3, well-matched to multi-cell structures.

Experimental Design

Advances in x-ray fluorescence microscopy enabled by the APS Upgrade can be used to examine metal distribution in order to cross-reference elemental maps with cellular changes occurring during *Caenorhabditis elegans* development. *C. elegans* is an ideal model system for developmental studies because the entire process and cell lineage of each cell in the adult organism has been completely mapped. Further, an impressive and comprehensive set of genetic mutations has been identified that alter developmental processes.[47, 48] These mutations could be used to better understand cellular and elemental changes occurring in these altered or disrupted developmental states. Moreover, *in situ* x-ray diffraction experiments and high-resolution x-ray fluorescence microscopy (identifying subcellular compartments) with the same samples could lend further molecular understanding to the developmental process and cellular differentiation. For example, longevity in *C. elegans* is regulated by a series of genes, many of which are involved in regulation of stress-reducing biological thiols (e.g., glutathione).[48] Turning on and off the gene cascades that redistribute sulfur could perhaps be observed by high-throughput screening of worms frozen at different stages of this process.

A logical extension of microscopy techniques would exploit the ability to detect metals using x-ray fluorescence microscopy to follow metal-labeled drug molecules as they diffuse through and interact with tissues, cells, and specific molecular targets in those cells. The ability to spatially map drug interactions in natural tissue and organ environments could lead to significant advances in our understanding of complex pharmacology, the treatment of the disease state, and the possible mechanisms for undesirable off-target drug actions.

4.4 Operational and Instrumentation Needs

X-ray Microscopy and Microspectroscopy

The high-brightness MBA lattice storage ring at the APS-U is crucial to achieve the advances in biological science described here. To reach the full experimental gains, key developments in experimental facilities must occur in parallel with the lattice upgrade. Of particular importance are the development, installation, and commissioning of high-resolution x-ray optics to achieve the desired spatially resolved datasets. Achromatic mirror-based optics are required for high precision nano-spectroscopy down to the 50-100-nm level. Diffractive x-ray optics are required to push the resolution to 10 nm and below for imaging applications, to visualize both sample structure and local elemental content. To maximize the information content of acquired datasets and mitigate radiation damage issues, methods must be developed or refined to effectively apply approaches such as dose fractionation,[49, 50, 51] advanced tomographic reconstruction routines,[52] and advanced approaches to phasing and coherent diffractive imaging.

Advanced Macromolecular Structure Methods

We will build on the technology and software being developed for serial femtosecond crystallography and apply them to storage ring-based data collection. New sample delivery methods will be developed and adopted to provide a steady stream of micron or submicron crystals. These could be based on the LCP injector or the acoustic drop ejection (ADE) being

developed at Brookhaven National Laboratory, which has been tested at the APS in preparation for experiments at the LCLS.[53] Coupling ADE with one or more optical traps will allow one or more crystals to be trapped and presented to the x-ray beam for a particular exposure time. Another approach might be to use surface acoustic waves to generate or pattern crystals in solution.[54] The APS has recently developed "spot-finder" software that can detect diffraction in images at live frame rates of up to 100 Hz, but increased speed will be needed to keep up with anticipated rates of sample exchange. The structure determination approaches outlined for macromolecular crystallography will require an x-ray diffraction beamline with the following characteristics: (1) a very intense parallel x-ray beam with a 0.5 µm diameter; (2) high-speed, high-sensitivity, detectors with small (50-µm) pixels; and (3) fast sample delivery methods.

4.5 References

[1] K. Ayyer, H. T. Philipp, M. W. Tate, J. L. Wierman, V. Elser, and S. M. Gruner, IUCRJ **2**, 29 (2015).

[2] S. M. Gruner and E. E. Lattman, Ann. Rev. Biophys. **44**, 33 (2015).

[3] M. Ferrari, Nature Rev. Cancer **5**, 161 (2005).

[4] M. S. Muthu, D. T. Leong, L. Mei, and S. S. Feng, Theranostics. **4**, 660 (2014).

[5] Y. Yuan, S. Chen, T. Paunesku, S. C. Gleber, W. C. Liu, C. B. Doty, R. Mak, J. Deng, Q. Jin, B. Lai, K. Brister C. Flachenecker, C. Jacobsen, S. Vogt, and G. E. Woloschak, ACS Nano. **7**, 10502 (2013).]

[6] L.-S. Lin, Z. X. Cong, J. B. Cao, K. M. Ke, Q. L. Peng, J. H. Gao, H. H. Yang, G. Liu and X. Y. Chen, ACS Nano **8**, 3876 (2014).

[7] V. Kumar, A. K. Abbas, and J. C. Aster, *Robbins and Cotran Pathological Basis of Disease*, Saunders (2014).

[8] T. J. Harris and F. McCormick, Nat. Rev. Clin. Oncol. **7**, 251 (2010).

[9] Y. S. Gong, L. Chang, K. L. Viola, P. N. Lacor, M. P. Lambert, C. E. Finch, G. A. Krafft, and W. L. Klein, Proc. Nat. Acad. Sci. USA **100**, 10417 (2003).

[10] A. Wimo, L. Jonsson, J. Bond, M. Prince, and B. Winblad, Alzheimer's & Dementia **9**, 1 (2013).

[11] J.-X. Lu, W. Qiang, W.-M. Yau, C. D. Schwieters, S. C. Meredith, and R. Tycko, Cell **154**, 1257 (2013).

[12] K. Vahedi and S. Alamowitch, Curr. Opin. Neurology **24**, 63 (2011).

[13] M. C. Dinamarca, M. Di Luca, J. A. Godoy, and N. C. Inestrosa, Biochem. Biophys. Res. Commun. in press (2015).

[14] International Human Genome Sequencing Consortium, Nature **431**, 931 (2004).

[15] Membrane Proteins of Known 3D Structure, http://blanco.biomol.uci.edu/mpstruc/.

[16] D. L. Akey, W. C. Brown, J. R. Konwerski, C. M. Ogata, J. L. Smith, Acta Cryst. D **70**, 2719 (2014).

[17] S. G. Rasmussen, B. T. DeVree, Y. Zou, A. C. Kruse, K. Y. Chung, T. S. Kobilka, F. S. Thian, P. S. Chae, E. Pardon, D. Calinski, J. M. Mathiesen, S. T. Shah, J. A. Lyons, M. Caffrey, S. H. Gellman, J. Steyaert, G. Skiniotis, W. I. Weis, R. K. Sunahara, and B. K. Kobilka, Nature **477**, 549 (2011).

[18] A. Hoelz, E. W. Debler, and G. Blobel, Annu. Rev. Biochem. 80, 613-643 (2011).

[19] M. Eibauer, M. Pellanda, Y. Turgay, A. Dubrovsky, A. Wild, and O. Medalia, Nature Comm. 6, 1-8 (2015)

[20] K. H. Bui, A. von Appen et al., Cell 155, 1233-1243 (2013).

[21] T. Stuwe et al., Science 347, 1148-1152 (2015).

[22] T. Stuwe, C. J. Bley, K. Thierbach, S. Petrovic, S. Schilbach, D. J. Mayo, T. Perriches, E. J. Rundlet, Y. E. Jeon, L. N. Collins, F. M. Huber, D. H. Lin, M. Paduch, A. Koide, V. Lu, J. Fischer, E. Hurt, S. Koide, A. A. Kossiakoff, and A. Hoelz. Science 350, 56-64 (2015).

[23] H. Chug, S. Trakhanov, B. B. Hülsmann, T. Pleiner, and D. Görlich, Science 350, 106-110 (2015)

[24] A. Szymborska, A de Marco, N. Daigle, V. C. Cordes, J. A. G. Briggs, and J. Ellenberg. Science 341, 655-658 (2013).

[25] O. B. Zeldin, M. Gerstel, and E. F. Garman, J. Appl. Cryst. **46**, 1225 (2013).

[26] U. Weierstall, D. James, C. Wang, T. A. White., D. Wang, W. Liu, J. C. H. Spence, R. B. Doak, G. Nelson, P. Fromme, R. Fromme, I. Grotjohann, C. Kupitz, N. A. Zatsepin, H. Liu, S. Basu, D. Wacker, G. W. Han, V. Katritch, S. Boutet, M. Messerschmidt, G. J. Williams, J. E. Koglin, M. M. Seibert, M. Klinker, C. Gati, R. L. Shoeman, A. Barty, H. N. Chapman, R. A. Kirian, K. R. Beyerlein, R. C. Stevens, D. Li, S. T. A. Shah, N. Howe, M. Caffrey and V. Cherezov, Nat. Comm. **5**, 3309 (2014).

[27] P. Nogly, D. James, D. Wang, T.A. White, N. Zatsepin, A. Shilova, G. Nelson, H. Liu, L. Johansson, M. Heymann, K. Jaeger, M. Metz, C. Wickstrand, W. Wu, P. Bath, P. Berntsen, D. Oberthuer, V. Panneels, V. Cherezov, H. Chapman, G. Schertler, R. Neutze, J. Spence, I. Moraes, M. Burghammer, J. Standfuss and U. Weierstall, IUCrJ **2**, 168 (2015).

[28] W. Liu, E. Chun, A.A. Thompson, P. Chubukov, F. Xu, V. Katritch, G.W. Han, C.B. Roth, L.H. Heitman, A.P. IJzerman, V. Cherezov and R.C. Stevens, Science **337**, (2012).

[29] R. Sanishvili, D. W. Yoder, S. B. Pothineni, G. Rosenbaum, S. L. Xu, S. Vogt, S. Stepanova, O. A. Makarov, S. Corcoran, R. Benn, V. Nagarajan, J. L. Smith, and R. Fischetti, Proc. Natl. Acad. Sci. USA **108**, 6127 (2011).

[30] Y. Z. Finfrock, E. A. Stern, Y. Yacoby, R. W. Alkire, K. Evans-Lutterodt, A. Stein, A. F. Isakovic, J. J. Kas, and A. Joachimiak, Acta Crys. D **66**, 1287 (2010).

[31] J. A. Cowan and C. Nave, J. Synchrotron Rad. 15, 458-462 (2008).

[32] R. L. Owen, N. Paterson, D. Axford, J. Aishima, C. Schulze-Briese, J. Ren, E. E. Fry, D. L. Stuart and G. Evans, Acta Cryst. D **70**, 1248 (2014).

[33] K. Denzer, M. J. Kleijmeer, H. F. Heijnen, W. Stoorvogel, and H. J. Geuze, J. Cell Sci. **113**, 3365 (2000).

[34] P. D. Stahl and M. A. Barbieri Sci. Signal. **2002**, pe32 (2002).

[35] T. Carandini, F. Colombo, A. Finardi, G. Casella, L. Garzetti, C. Verderio, and R. Furlan, Front. Neurol. **6**, 111 (2015).

[36] V. R. Minciacchi, M. R. Freeman, and D. Di Vizio, Semin. Cell Dev Biol. **40**, 41 (2015).

[37] P. Lay, private communication (2015).

[38] P. K. Mattila and P. Lappalaienen, Nat. Rev. Mol. Cell Biol. **9**, 446 (2008).

Biol. **9**, 446 (2008). | ure, and G. E. R. Grau, Leukemia **23**, 1643 (2009).

[40] J. Gong, R. Jaiswal, J. M. Mathys,V. Combes, G. E. R. Grau, and M. Bebawy, Cancer Treat. Rev., **38**, 226 (2012).

[41] J. Gong, F. Luk, R. Jaiswal, A. M. George, G. E. R. Grau, and M. Bebawy, Eur. J. Pharmacol. **721**, 116 (2013).

[42] R. Jaiswal, F. Luk, P. V. Dalla, G. E. R. Grau, and M. Bebawy, PLoS One **8**, e61515 (2013).

[43] J. Gong, R. Jaiswal, P. Dalla, F. Luk, and M. Bebawy, Sem. Cell Develop. Biol. **40**, 35 (2015).

[44] J. Deng, D. J. Vine, S. Chen, Y. S. Nashed, Q. Jin, N. W. Phillips, T. Peterka, R. Ross, S. Vogt, C. J. Jacobsen, Proc. Natl. Acad. Sci. USA **112**, 2314 (2015).]

[45] T. Paunesku, S. Vogt, B. Lai, J. Maser, N. Stojićević, K. T. Thurn, C. Osipo, H. Liu H, D. Legnini, Z. Wang, C. Lee, and G. E. Woloschak, Nano Lett. **7**, 596 (2007).

[46] D. Bourassa, S. C. Gleber, S. Vogt, H. Yi, F. Will, H. Richter, C. H. Chen, and C. J. Fahrni, Metallomics **6**, 1648 (2014).

[47] J. Lowry, J. Yochem, C. H. Chuang, K. Sugioka, A. A. Connolly, and B. Bowerman, G3 (Bethesda) in press (2015).

[48] A. T. Chen, C. Guo, O. A. Itani, B. G. Budaitis, T. W. Williams, C. E. Hopkins, R. C. McEachin, M. M. Pande, A. R. Grant, S. Yoshina, S. Mitani, and P. J. Hu, Genetics **115**, 177998 (2015).

[49] R. Hegerl and W. Hoppe, Z. Naturforschung **31a**, 1717 (1976).

[50] B. F. McEwen, K. H. Downing, and R. M. Glaeser, Ultramicroscopy **60**, 357 (1995).

[51] P. Y. Hong, S. C. Gleber, T. V. O'Halloran, E. L. Que, R. Bleher, S. Vogt, T. K. Woodruff and C. Jacobsen, J. Synchrotron Rad. **21**, 229 (2014).

[52] D. Gürsoy, F. De Carlo, X. Xiao, and C. Jacobsen, J. Synchrotron Rad. **21**, 1188 (2014).

[53] A. S. Soares, M. A. Engel, R. Stearns, S. Datwani, J. Olechno, R. Ellson, J. M. Skinner, M. Allaire, and A. M. Orville, Biochem. **50**, 4399 (2011).

[54] F. Guo, W. Zhou, P. Li, Z. Mao, N. H. Yennawar, J. B. French, and T. J. Huang, small **11**, 2733 (2015).

5 Structures & Dynamics Defining Reactivity in Chemistry & Catalysis

Angus Wilkinson, *Georgia Institute of Technology*
Karena Chapman, *X-ray Science Division, Argonne National Laboratory*
David Tiede, *Chemical Sciences Division, Argonne National Laboratory*

Stephen Streiffer, Ross Harder, Eric Dufresne, Tao Sun, *Argonne National Laboratory;* Younan Xia, *Georgia Institute of Technology;* Joseph Hupp, Mike Wasielewski, Lin Chen, *Northwestern University;* Michael Toney, *Stanford Synchrotron Radiation Lightsource;* Michael Tsapatsis, *University of Minnesota;* Mark Newton, *University of Warwick*

5.1 Executive Summary

Discovery in chemistry and catalysis is driven by the need to resolve structure and electronic states at the atomic scale, as a function of reaction-specific environments, and across timescales related to chemical functionality. Critical challenges revolve around understanding how chemical reactivity is tuned by local structure and how these local interactions evolve over the timescales of a reaction. X-ray science has had a profound impact on our understanding of these processes and the development of fundamental concepts in chemistry by probing the structure of crystalline materials through diffraction and the electronic structures through x-ray spectroscopy. However, major challenges remain in correlating structure with chemical function for fluid, aperiodic, and heterogeneous systems, and in resolving processes throughout the duration of chemical reactions.

The coherence, brilliance, and nanometer-scale focus of the APS-U, particularly at high photon energies, will lead to breakthroughs in our understanding of the relationship between structure and chemical function and of the evolution of structure across the timescales of rate-limiting steps in chemical reactions. The increase in brightness at high photon energies (approximately 60 keV) will enable 1) *in situ* atomic resolution structural studies of a material's self-assembly at short times (microseconds to milliseconds), thereby revealing key steps in its formation, and 2) time-resolved structural studies of catalysts relevant to solar fuels production that can characterize individual intermediates in a catalytic cycle. The increase in coherent flux will enhance our understanding of how strain can be used to tailor catalytic activity, using Bragg coherent diffraction measurements of strain in nanoparticles, and will allow x-ray fluctuation microscopy studies designed to reveal how structure-directing agents control the formation of zeolitic frameworks.

5.2 New Opportunities for Chemistry and Catalysis at APS-U

Chemistry and catalysis touch all aspects of modern life, from fine chemical production to harvesting energy from sunlight in order to generate renewable fuels. Breakthroughs in chemistry and catalysis that lead to new capabilities, enhance efficiency, and reduce costs can be achieved only by understanding and controlling the reactivity and functionality of molecules and materials at the atomic scale and beyond. Understanding and controlling reactions during synthesis are critical in discovering of new phases and in optimizing the preparation and properties of known systems. Such optimization can include manipulating the composition, nanostructure, and morphology of functional materials to enhance their performance in specific applications. For chemical transformations and catalyzed reactions, identifying and controlling the molecular transition states and, rate-limiting steps, and understanding how these are impacted by a catalytic species are fundamental to achieving efficient energy and molecular conversions.

Understanding reactivity and functionality in molecules and materials is a universal and persistent challenge that limits advances in chemistry and catalysis. To address this challenge, we must be able to probe and correlate the complex interplay between the chemistry, structure, and electronic state of atoms within molecules and materials, and how these couple across multiple length scales, at timescales that match the chemical function/reactions (from nanoseconds to days). While interactions and bonding occur at the atomic scale, functionality often ultimately relies on cooperative multi-scale mesoscopic effects. For example, size- and shape-selective molecular separations in porous framework solids, or "molecular sieves," are based on the geometry and flexibility of apertures defined by multi-atom architectures. While catalytic sites often are localized on individual atoms or defects, their critical electronic states are coupled to a larger-scale local environment. In addition to considerations of the static structure, the processes underlying reactions are inherently dynamic, with timescales varying across a wide range. The structural and dynamic hierarchies relevant to functional chemical systems are illustrated in Fig. 1.[1]

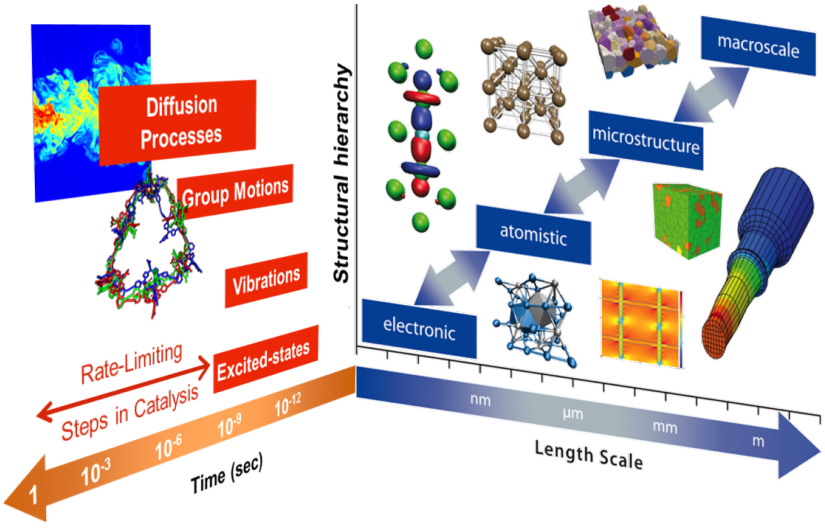

Fig. 1. Illustration of the multiple lengthscales and timescales impacting chemistry and catalysis in functional materials. Image adapted from the Interdisciplinary Centre for Advanced Materials Simulation (ICAMS).[1]

The highly diverse set of challenges in chemistry and catalysis typically requires that a wide variety of different characterization tools be applied, including optical/vibrational spectroscopies, thermal analysis, and chemical analysis of reaction products. The dynamic structural and electronic evolution of these systems can only truly be explored *in situ*, under realistic operating or reaction conditions, which poses a significant challenge to characterization techniques. In many cases, the required experimental conditions cannot be produced without complex high-temperature, liquid, or gaseous sample environments. As a result, synthetic reactions and materials discovery often proceed by a procedure that can best be termed "cook-and-look." In this approach, the products of a reaction are examined only in a few steady-state samples that have been removed to ambient conditions, for example following conclusion of a reaction. The APS-U provides the opportunity to obtain highly precise insight into previously hidden intermediate configurations in crucial chemical processes.

X-rays provide outstanding precision and sensitivity in characterizing atomic structure and have played a leading role in understanding chemistry and catalysis through history. One-third of all Nobel Prizes in Chemistry have been awarded for work involving x-ray structure characterization and crystallography. At present, x-ray characterization methods are sensitive to diverse aspects of structure, chemistry, electronic state, and functionality. Reciprocal space methods that resolve these features on the angstrom (i.e., atomic) scale, including diffraction, XAS, and PDF analysis, have advanced our understanding of important chemical and catalytic processes in bulk materials. Local structure probes such as PDF and XAS allow local atom-atom distances in non-crystalline systems, if well-defined, to be resolved as a spherical average for the sample. The long penetration lengths and high flux of hard x-ray beams from the present generation of synchrotron x-ray lightsources have enabled structural studies during the time course of chemical reactions under applications-relevant *operando* conditions. New scientific challenges lie in characterizing interfacial, thin-film, and spatially localized catalyst materials. The coherent, focused, high-energy x-ray capabilities of the APS Upgrade will have direct impacts on these challenges.

Similarly, time resolution for measurements of chemical structural dynamics is ultimately limited by x-ray brightness. For reactions that cannot be examined in a repetitive or stroboscopic fashion, time resolution on the order of 0.1 sec represents a typical present limit for scattering measurements on solids and nanocrystalline powders. More signal-limited experiments, such as XAFS measurements on dilute solution of molecular catalysts, presently require times on the 1-min scale. Higher time resolution in chemical dynamics is currently achieved by repetitive, gated, or pump-probe experiments. These experiments require fast sample exchange rates to achieve the kHz to MHz repetition rates needed for effective signal averaging. The APS Upgrade's focused high-energy beams will enable first-of-a-kind, high time resolution, pump-probe measurements to be extended to the PDF technique. More generally, the focused x-ray probe capabilities of the APS-U will reduce the probe volume by more than an order of magnitude. The reduced probe volume will proportionally reduce sample fluid-flow or film translation rates to levels at which they are experimentally tractable and can be routinely employed for a range of catalytic materials, initiated by light or rapid-mixing chemistries.

The APS-U will drive new discoveries in chemistry and catalysis by extending the time resolution of x-ray tools to match the rate-limiting steps at which atom-atom bonds are made and broken, by enhancing the local structural information that can be obtained in general (not just periodic)

systems from spherically-averaged 1D to multi-dimensional real-space information, and by exploring coupling of processes across multiple lengthscales and characterization modalities. With new opportunities to better understand the structures of solids, liquids, solutions, and even gases using the gains delivered by the APS-U, chemistry and catalysis represents an important growth area for the APS. The community of chemistry and catalysis researchers is large; with expanded capabilities in this area made possible by the APS-U, there is enormous potential to increase this community's engagement in synchrotron x-ray science.

A. Understanding and Controlling Materials Synthesis Across Lengthscales and Timescales

Chemical synthesis is of broad fundamental and applied importance. Synthesis and self-assembly are key to new materials discovery and to tuning functionality by controlling polymorphism, defects, particle/grain/cluster size, morphology, and hierarchical architectures. Interactions between atoms, ions and molecules at short lengthscales can lead to materials with simple geometrical shapes or very complex functional architectures structured on multiple length scales. Inspiration can be drawn from remarkable self-assembled structures found in nature, such as the micron-scale architectures of calcite single crystals, which compose the exoskeleton of single-cell phytoplankton, as shown in Fig. 2(a),[2] while Fig. 2(b) illustrates precisely controlled metal nanocages.[3]

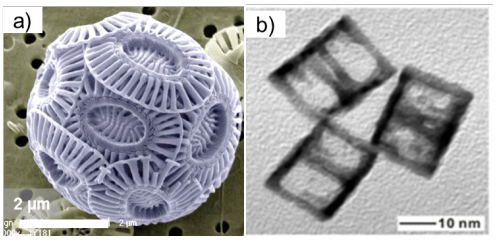

Fig. 2. a) Calcium carbonate exoskeleton from phyto-plankton *Emiliania huxleyi.* b) Synthetic metallic nanoparticle cage.

However, our understanding of how short-lengthscale chemical processes involving competing interactions lead to a particular material, structure, and architecture is far from predictive. We are limited by our ability to characterize directly the local structures and geometries of pre-crystalline molecular aggregates on timescales that capture their dynamics. The time resolution and precision of the experiments are limited not only by the raw data rates, but also by additional uncertainty associated with the sample environment; probe volumes that provide acceptable sample signal can include a distribution of reaction states.

At present, our understanding of materials synthesis and self-assembly relies heavily on indirect observations. Mechanistic models have been developed that describe the observed changes in concentration of, for example, a known reagent or the bulk crystalline product, and attempts have been made to correlate reaction parameters with the structure of the eventual product. All of these approaches reflect the limitations of the "cook-and-look" approach.

To target and control the formation of a particular material requires understanding of the processes occurring along the path from starting materials to final product, beginning with the molecular-scale aggregates that may exist before nucleation and growth of a bulk product. Figure 3 illustrates conceptual stages in coordination-driven assembly. Reversible coordinating forces between reaction precursors, which can

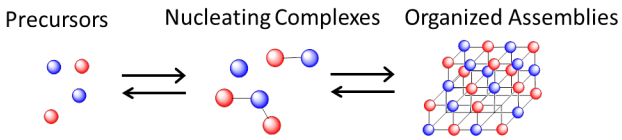

Fig. 3. Generalized scheme for dynamic, coordination-driven assembly of organized assemblies

be either atomic or molecular, lead to the nucleation of complexes, which is followed by the subsequent growth of larger assemblies. The dynamics of the solutions and clusters are critical in determining the resulting structures. The reversible coordination-driven associations at each step in the assembly reaction can be expected to create local, microscopically non-uniform, fluctuating concentration gradients and dynamics which function in determining assembly pathways. At present, direct information on the character of these structures and dynamic fluctuations leading to product assemblies is not available. The unknown configurations represent the "missing structures" in materials and chemical self-assembly.

The increase in x-ray beam brightness and coherence associated with the APS Upgrade will provide new opportunities to examine many critical points along this path. The following examples illustrate some of the gains that will be realized in synthetic chemistry as a consequence of the APS-U:

1) Structure-directing agents and the nucleation of specific zeolite frameworks

Zeolitic materials are crystalline porous framework materials, also known as “molecular sieves,” that are of critical importance to many fields, including heterogeneous catalysis, separations, and ion exchange. Their utility for a given application strongly depends upon their framework topology and chemical composition. While an effectively infinite number of different porous frameworks can in principle be built up from the simple tetrahedral building blocks (TO_4, T = Si, Al, P, Ti, Ge, Sn) that constitute the lattice, only approximately 210 different structures are currently well-established.[4] The synthesis of a particular zeolitic framework is typically accomplished by adding an organic or inorganic structure-directing agent (SDA) to the gels used for its hydrothermal synthesis and then heating the aqueous gel for periods of up to several days. While there has been significant progress towards the rational design of SDAs for zeolite synthesis,[5] the complex dissolution-reprecipitation process by which a particular framework nucleates and grows in the presence of an SDA remains unresolved after decades of work. In particular, it is not yet possible to characterize the local structural order that develops within the reaction mixture, for example around the SDA, in the lead-up to nucleation and crystallization. Diffraction methods can only probe the structure of the crystalline precipitates that follow nucleation. PDF methods probe the local atomic structures that form within the reaction mixture in the non-crystalline state before nucleation, but because the structural insights are provided as 1D averages, insights into the local geometries lack sufficient structural specificity to provide guidance in designing synthetic methods. Experiments designed to reveal, in 3D atomic-scale detail, how SDAs modify the gel structure prior to nucleation and to direct the formation of a particular framework could significantly advance our ability to access “missing zeolites”—materials with energetically feasible framework structures that have not yet been synthesized.

2) Understanding and controlling early stage self-assembly during nanoparticle syntheses

The growth of crystals, nanocrystals, and nanoparticles with controlled compositions, structures and morphologies is of great technological importance. Vast new functionalities can arise from tuning the structure and chemical composition of nanostructures. For example, novel optical properties are accessible by virtue of quantum confinement in semiconductor nanoparticles,[6] and both strain in nanostructures and morphological control of metal nanocrystals can be used to tailor catalytic activity.[7,8] The field’s importance and growth are

reflected by the large and increasing number of studies over the last 20 years that examine nanomaterial formation while controlling crystal size, shape, and structure: In 1994, only 24 papers contained the terms "nanocrystal" or "nanoparticle" in their titles; by 2004, this number had grown to 1,100, and in 2014 there were 11,000 such papers. Despite this extensive body of work, however, the community's understanding of self-assembly in its earliest stages is far from complete. This is a significant blind spot, as the ability to fully control a material's properties by tuning key parameters is dependent on these first steps.

Nanocrystal nucleation and growth is often discussed in the context of the La Mer model, Fig. 4(a),[9] in which the concentration of the fundamental building blocks (e.g., monomer precursors) rises over time to a critical concentration, nuclei are then formed, and the growth of these nuclei proceeds with a concomitant decrease in monomer concentration. However, actual growth mechanisms are universally more complex than this simple scheme suggests, and can include intermediate clusters of defined size, aggregation, surface segregation, and ripening processes. The nature of the "monomer" and other species that may be present during the early stages of this nucleation and growth process is often obscure. For many materials of interest, the relevant processes take place very quickly, presenting a characterization challenge that the APS Upgrade will address.

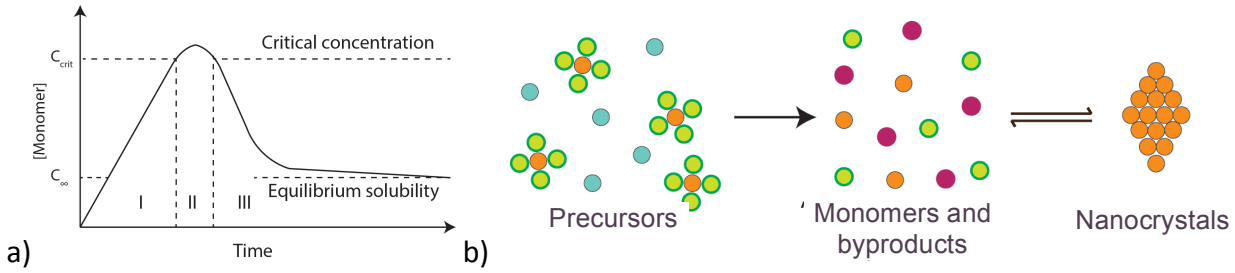

Fig. 4. a) The evolution of monomer concentration versus time during crystal nucleation and growth according to the La Mer model. b) Scheme showing the transformation of precursors to "monomers" and onto nanocrystals.

The great importance of understanding and controlling all stages of the self-assembly process in solution has motivated many *in situ* studies of nanocrystal growth using a wide variety of methods, but atomic-level structural detail at the earliest stages of this process has remained out of reach. Such detail would provide considerable insight into the self-assembly process. The dramatic increase in high-energy photon flux and brightness provided by the APS-U will provide a valuable opportunity to interrogate self-assembly processes *in situ*, over a wide range of timescales, using total scattering and PDF methods with efficiently focused high-energy x-rays.

3) Real-time observation of architecture development in hierarchical materials

The formation mechanisms of complex architectures, such as those shown in Fig. 5,[10] are often known at an intuitive rather than a quantitative level. *In situ* imaging of growth, on lengthscales and timescales that are relevant to their assembly and structure, will provide highly informative time-resolved structural maps of their formation. The dramatic enhancements in coherent flux associated with the APS Upgrade will enable the use of lensless imaging techniques, such as ptychography, with spatial and time resolutions that are well matched to the growth kinetics and lengthscales of architectures such as the self-pillared pentasil (SPP) or "house of cards" zeolite structure shown in Fig. 5. If it becomes possible to overcome the formidable challenges

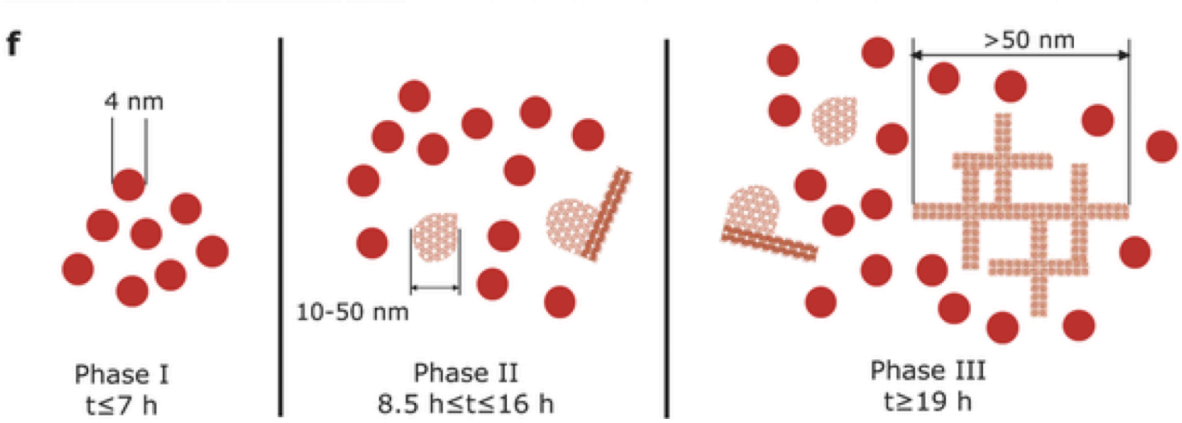

Fig. 5. The proposed mechanism involving time-evolving structures underlying formation of the SPP "house of cards" zeolites.[10]

associated with imaging under actual growth conditions (such as the positional stability of the sample and x-ray beam-induced chemistry), the imaging of such a growth process would represent an enormous advance. Rather than relying on "cartoon" mechanisms that have been inferred from a combination of rather indirect measurements,[10] the actual growth process could be followed directly. This type of experiment can provide insight into the formation of materials with hierarchical porosity, biomineralization (a process in nature whereby crystallization of single crystals with complex mesoscale architectures is triggered in a metastable amorphous polymorph), and size- and shape-controlled synthesis of catalytic nanoparticles.

B. Understanding Chemical Reactivity and Functionality

Resolving the structures of intermediates during multi-step catalytic processes is one of the central challenges in chemistry and catalysis. Reaction sequences and transition state landscapes underlying bond formation or breakage are fundamentally complex, typically involving both electron and atom-coordinate transfers mediated by reactant binding on transition-metal centers. The resolution of intermediate structures at the atomic scale is necessary to achieve a fundamental understanding of catalytic mechanisms and to develop theories that can enable the design of catalysts with tailored or enhanced reactivity.

Opportunities for the APS Upgrade can be illustrated by considering the multi-step reactions underlying water-splitting and CO_2 reduction to fuels. These reactions are of primary importance for national energy security and are current foci for both national and international research efforts.

At present, the most detailed level of understanding of a reaction sequence in multi-step catalysis is derived from investigations of the light-induced water oxidation in photosynthesis. The structure of the resting-state $CaMn_4O_x$ catalytic cluster has been determined in the photosystem II protein crystals;[11] single-electron oxidation state intermediates in the catalytic cycle have been investigated by laser flash-initiated reactions and probed by x-ray and electron paramagnetic spectroscopies.[12] A summary of the proposed reaction cycle is shown in Fig. 6(a). Similarly, Fig. 6(b) illustrates the sequence of intermediates produced by sequential two-electron reduction of CO_2 in the reaction leading to methanol production.[13] The schemes illustrate the complexity of multi-step catalytic reactions, requiring proton-coupled electron

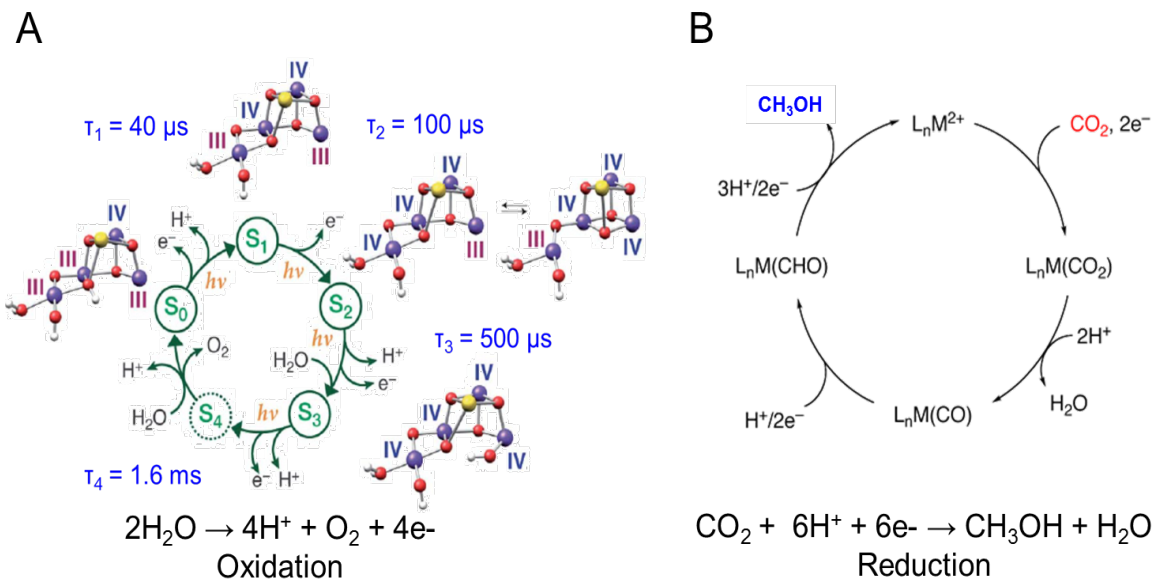

Fig. 6. Redox cycles in multi-step catalysis. a) Single-electron oxidation states proposed for the oxidation of water in photosynthesis for the $CaMn_4O_x$ catalytic cluster. The scheme shows the proposed structures and metal atom valence states for the $CaMn_4O_x$ cluster at each intermediate state, and the reaction time constants.[12] (b) Generalized sequence of two-electron reduced intermediate state in CO_2 reduction to methanol.[13]

transfer at each reaction step. In terms of reaction timescale, the photosynthetic water-splitting catalyst has the highest turnover frequency known for this type of four-electron, four-proton-coupled reaction. Photosynthetic water-splitting has a rate-limiting step of 1.6 ms for the final release of oxygen. Earlier reaction steps have time constants ranging from 40 µs to 500 µs.[14] These measurements provide a reference scale for gauging the time domains for rate-limiting steps in bond-making/breaking chemistry driven by an optimized multi-step catalyst. We note here that the timescales for these rate-limiting steps are readily addressed by the time-resolved structural and spectroscopic capabilities of the APS Upgrade.

Commensurate with the importance of these chemistries, there is an intense international research effort focused on developing high-performance catalysts for solar and electrochemically-driven water oxidation and fuels production. Catalysts under investigation span the full range from molecular[14,15] to amorphous[16,17] to nano- and micro-crystalline thin-film[15] materials. Ongoing advances in synthetic chemistry are developing catalytic materials that are coupled to light and electrochemical driving forces for activation as a path to enhanced reaction efficiencies. A fundamental barrier to achieving breakthroughs in the determination of reaction mechanisms for these solar fuels catalysts lies in the need to resolve structures for intermediate steps in multi-step catalytic reactions. New *in situ*, non-crystallographic x-ray characterization techniques are needed. Similarly, in the development of devices for artificial leaf applications,[16,17] amorphous thin-film catalysts are electrolytically grown on electrode and photovoltaic surfaces. However, their amorphous character precludes crystallographic characterization, and the sub-micron dimensions of the films have prevented *in situ* PDF analysis using high-energy x-rays. For nano- and micro-crystalline catalyst materials,[18] key issues include the need to understand the spatial distribution and sites for catalysis within the

polycrystalline film and to probe how catalytic function varies with respect to position relative to the electrode and charge conductor interfaces.

The APS Upgrade will have a major scientific impact on solar fuels research, providing new opportunities to resolve structures of intermediates in multi-step catalysts using spatially resolved high-energy x-ray diffraction and PDF techniques for *in situ*, light-activated and electrode-supported catalysts, measured across the full timescales of chemical reactivity. These new opportunities arise from the availability of focused high-energy x-ray beams for probing thin-film and spatially localized catalyst materials. For pump-probe time-resolved experiments that require fast sample exchange rates to achieve high signal-averaging, the focused high-energy beams will reduce the x-ray probe volume by more than an order of magnitude, which in turn will proportionally reduce sample fluid-flow or film translation rates to levels at which they are experimentally tractable and can be routinely and generally employed. The timescales for complex, multi-step reactions are well matched to the nanosecond-to-real-time resolution capabilities of the APS Upgrade, suggesting that the APS Upgrade will be positioned for leadership in hard x-ray analyses of complex catalysis.

5.3 Early Chemistry and Catalysis Experiments at APS-U

5.3.A. Structure Direction in Zeolite Synthesis

Structure-directing agents exert control over the crystallization of zeolite frameworks by organizing the inorganic material in the synthesis gel (Fig. 7).[19] The zeolite framework crystalizes around these SDAs, defining regular pores of several angstroms to several nanometers in diameter. An enhanced understanding of how different organic additives structure the gel before and during nucleation would aid efforts to prepare new zeolite frameworks with useful properties.

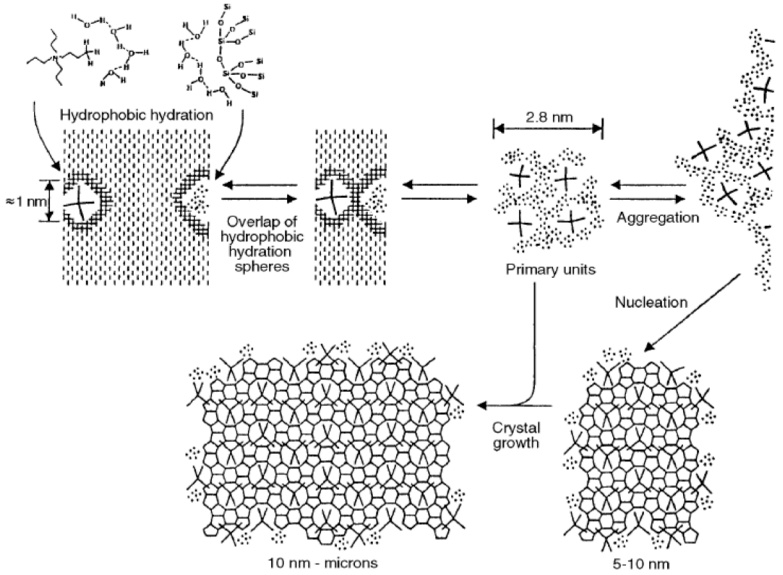

Fig. 7. Scheme for zeolite nucleation and growth in the presence of an organic structure-directing agent.

The APS-U will allow the role of SDAs in zeolite formation to be addressed by fluctuation microscopy, which probes medium-range order in non-crystalline systems by examining the spatial variation in coherent diffraction patterns. Fluctuation microscopy has been developed and most widely applied in electron microscopy, where it has been used to reveal the lengthscale of short/medium-range order in glassy systems including amorphous silicon.[20] When cross-correlation of the scattering domains from fluctuation microscopy data are further analyzed, the local geometry and symmetry of the ordered scattering domains can be determined.[21] Electron scattering is not readily applicable to *in situ* studies of wet zeolite synthesis gels under hydrothermal conditions, but the principles underlying the approach apply to all types of coherent scattering. Fluctuation x-ray microscopy with cross-correlation analysis, using coherent x-ray beams at x-ray energies high enough to penetrate an *in situ* synthesis cell and to access the momentum transfers needed to detect ordering of the gel, could provide considerable insight into the role of organic SDAs in zeolite synthesis.

Fluctuation microscopy examines the variance in scattering from different small areas within a thin sample. The momentum transfer dependence of this variance provides information on the nature of the medium-range order and the dependence of this variance on the size of the region probed, as determined by the lengthscale of the ordering. X-ray fluctuation microscopy experiments can be performed either by directly examining the spatial variation of scattering from thin samples, while using different-sized probe beams, or by the numerical analysis of ptychographic images.[22]

Prior work using x-ray fluctuation microscopy (Fig. 8)[23] has employed x-rays with low photon energy, on the order of 3 keV, and focal spot sizes on the order of 20 nm.[24] This work provides insight into medium-range ordering over distances of tens of nanometers. The APS Upgrade provides a dramatic increase in coherent flux at higher x-ray energies that will revolutionize the way fluctuation microscopy is applied. The increased coherent flux will allow fluctuation microscopy to be applied at high energies, i.e. at ~15 keV, which is required to obtain atomic-scale detail in scattering patterns. The lengthscales and momentum transfers will be vastly expanded, into the ranges (~2 nm and ~20 nm^{-1}, respectively) needed to study the formation of medium-range order in zeolite synthesis gels. Fluctuation microscopy examines the variance in

Fig. 8. Illustration of x-ray cross-correlation to determine local geometry.[23]

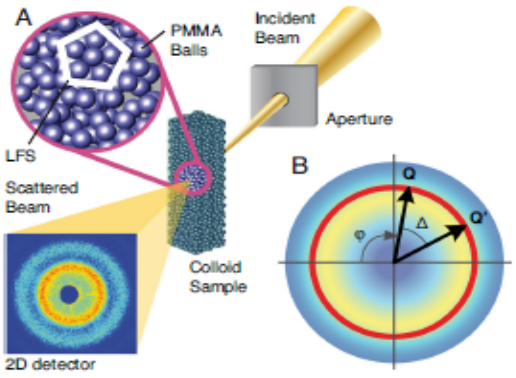

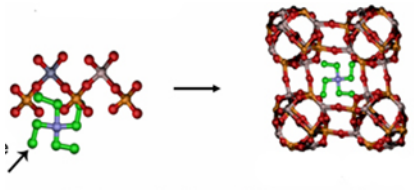

Fig. 9. Structure direction in the assembly of zeolites.[25]

scattering from different small areas within a thin sample. Snapshots of zeolite synthesis gels containing different SDAs can be recorded and analyzed at different lengthscales. X-ray cross-correlation analysis of the data at different wave vectors provides information on local symmetry.[23]

Zeolite syntheses are typically carried out by the hydrothermal treatment of silicate gels containing organic SDAs, as shown schematically in Fig. 9,[25] but framework compositions including higher-Z elements, such as germanium, can be employed.[26] In both cases, the scattering contrast required for *in situ* structural studies is provided by the density difference between the SDA and the aluminosilicate walls of the zeolite. The nucleation and crystallization process is, in general, not rapid and can take days to complete. For the proposed experiments, a sample stage will be developed suitable for high-resolution imaging of thin synthesis gel layers under hydrothermal conditions, using a ptychographic or variable-beam-size approach. Such a sample environment can be adapted from fluid-compatible sample holders originally developed for transmission electron microscopies. This stage ideally would hold an array of different gel compositions and would be designed to be readily moved on and off the beamline while continuously maintaining hydrothermal reaction conditions. The time needed to record an image on any particular gel will be short compared to the overall length of the crystallization process; thus the structure of each gel will be recorded at intervals over the duration of the syntheses. The resulting images will be used to reconstruct the scattering from different areas of the sample so that the location-to-location variance in scattering can be computed as a function of momentum transfer and size of the area on the image used in the analysis. The dependence of this variance on momentum transfer provides information on the nature of the medium-range order, and the dependence of this variance on the size of the region probed provides insight into the lengthscale of the ordering.

Several Intermediate steps will be required to develop fluctuation microscopy methods for the study of the nucleation and formation of zeolites. These are: 1) establishing whether the introduction of an SDA into a zeolite synthesis gel actually modifies the development of medium-range order, as seen by fluctuation x-ray microscopy; 2) establishing how SDAs, which already are known to lead to different zeolite frameworks, give rise to distinct signatures in the fluctuation x-ray microscopy experiment; and 3) determining whether closely related SDAs, which usually direct the formation of the same zeolite framework, give rise to similar or identical fluctuation x-ray microscopy signatures. The first step can be accomplished by comparing the structural evolution of gel compositions that would normally give rise to the well-known and industrially important zeolite ZSM-5, in the presence and absence of the commonly employed SDA tetrapropylammonium (TPA) hydroxide.

The discovery of how SDAs lead to the formation of medium-range order during the early stages of zeolite synthesis, and how this order correlates with the formation of a particular crystalline framework, would be highly significant and would help to enable the rational design of libraries of potential SDAs that match (i.e., template) the library of hypothetical zeolite structures.

5.3.B. Atomic Resolution Studies of Early-Stage Self-Assembly During Materials Synthesis Using Total X-Ray Scattering

For many materials grown from solution, the formation of "monomers" and aggregates, prior to nucleation, occurs very shortly after the reactants are mixed. To study these events, sample environments that provide very rapid mixing are needed. Time resolutions as short as 20 μs already have been demonstrated in SAXS using microfluidic mixing devices and jet reactors.[27,28] Experimental approaches based on mixing or on jets essentially decouple the time required to obtain an x-ray data set of adequate statistics from the time resolution of the measurement. Very narrow liquid jets are employed to facilitate rapid mixing. While this small in-beam sample volume is not an obstacle to SAXS experiments, it effectively precludes atomic-resolution structural (e.g. PDF) studies using the present generation of x-ray lightsources. The APS Upgrade's dramatically enhanced high-energy brightness will enable such studies for the first time by allowing focusing of the high-energy x-rays required for PDF measurements without the substantial inefficiencies of present high-energy focusing optics.

The overall experimental scheme for the conceived total scattering studies of self-assembly in solution at short timescales (μs to ms) is shown in Fig. 10. This concept already has been demonstrated for SAXS studies of self-assembly in aqueous solution at near-ambient temperature and will be adapted for PDF studies using the APS-U.[27] The liquid jet arrangement is highly versatile and can, for example, be used to study the formation of metallic and non-metallic nanocrystals, the early stages of metal-oxide framework (MOF) formation from inorganic and organic precursor solutions, and the crystallization of molecular solids, such as different pharmaceutical polymorphs, after mixing an anti-solvent with a solution. A key experimental detail in developing such an instrument will be to develop a mixer (or mixers with different capabilities) compatible with a wide range of solvents, usable with both acids and bases, and capable of working at elevated temperatures. Many nanoparticle syntheses make use of a hot injection approach to start nucleation; this could be replicated by mixing solutions of different temperatures. When working at above-ambient temperature, the jet would need to travel through a heated space saturated with solvent vapor to avoid cooling and evaporative loss.

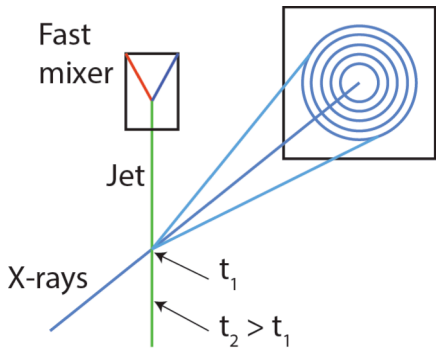

Fig. 10. Rapid mixing of reactants to generate a jet, combined with the interrogation of different points along the jet provide snapshots of the structures in solution at different (short) times.

Scattering studies will probe nucleation and self-assembly as a function of reaction conditions such as temperature, precursor type, and precursor concentration, in addition to reaction time. As the species resulting from early-stage reaction and self-assembly processes will be present at low concentrations along with unreacted precursor and solvent, data of very high statistical quality will be needed to extract small changes that occur as a function of time. The time resolution with which a chemical process can be studied is decoupled from the x-ray source characteristics when using the flow scheme shown in Fig. 10, but the time needed to record a good-quality scattering pattern at some point in the self-assembly process is dependent on

source characteristics. Such experiments benefit from enhanced flux at the required x-ray photon energy of approximately 60 keV because the jets under study are necessarily small when rapid mixing strategies are used. At 60 keV, the APS Upgrade using superconducting undulator insertion devices will provide an order-of-magnitude increase in flux and 2 to 3 orders of magnitude higher brightness than the current APS.

Insight into the experimental design of the proposed short-timescale experiments can be gained from the small number of pioneering studies looking at self-assembly processes in solution. The studies to date have probed longer timescales of seconds to hours using total scattering methods.[29] A recent *in situ* study of CeO_2 hydrothermal growth,[29,30,31] which is of interest for reversible oxygen storage and catalysis, required 3 sec exposures using precursor with a 1M in Ce^{4+} concentration. Recall, however, that the time resolution in such experiments is determined by the jet geometry rather than by the time required for the acquisition of the scattering pattern. With the experimental arrangement allowing smaller jets shown in Fig. 10, the illuminated solution volume will decrease by a factor of 500; this will be offset by the increased source brightness, which allows the full undulator flux to be more readily focused into the relevant region of the jet. Experiments with Ce-based materials are clearly feasible and can have impact on the formation of catalysts. Other nanocrystals of interest are grown using solutions with far lower concentrations than those employed for the CeO_2 particle growth experiments. A reduction in concentration to 10 mM would require at least a factor of 100 increase in exposure time, leading to an estimate of 300 s for each measurement; again, this is clearly beyond the capabilities of the present third-generation sources, but it will be well within the range of feasibility with the APS-U.

While the proposed approach is in principle applicable to the self-assembly of many different materials, studies of noble metal nanocrystal synthesis (Au, Ag and others) and II-VI or III-V semiconductors, such as CdSe or InP, are appropriate initial experiments. These systems are of considerable interest, are accessible using a variety of different synthetic approaches, and could provide opportunities to look at magic cluster formation in real time. They also contain high-Z elements that will help with the signal-constrained nature of the measurements.

5.3.C. Dissecting Catalysis in the Artificial Leaf

The enhanced x-ray capabilities of the APS Upgrade at high photon energies will create opportunities for breakthroughs in resolving mechanisms for multi-step catalysis. A particularly important impact will be on solar energy and solar fuels catalysis research. Artificial leaf devices couple light-driven water oxidation on anodes as a source of reducing equivalents for cathodic reduction of CO_2 to fuels following the reaction chemistries noted in Fig. 11.[32,33] Key challenges in this research lie in deciphering mechanisms for catalysis, developing theory for the design of optimized catalysts, and spatially resolving *in situ* catalyst function, including the resolution of activity with local electrical conductance and proton and ion transports within functional devices and under operating conditions.

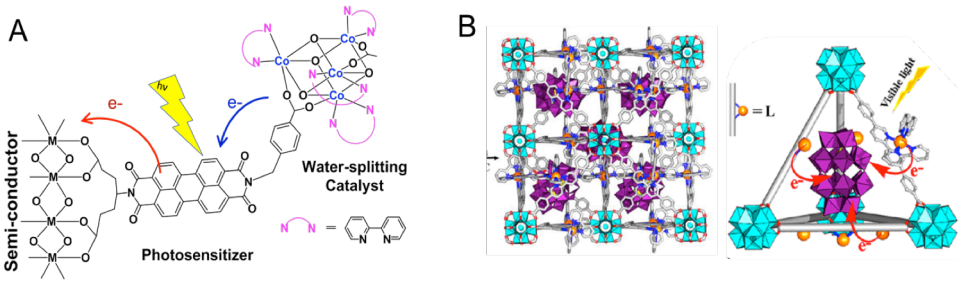

Fig. 11. Solar water oxidation catalysts linked to light harvesting. (a) Linked photosensitizer catalyst for multi-electron water-splitting.[32] The APs-U will allow this reaction to be followed one electron at a time. (b) Photoactive MOF, with an imbedded polyoxometalate catalyst for light-driven hydrogen evolution.[33]

New classes of synthetic materials are being developed that link discrete molecular and metal cluster catalysts to light-harvesting molecules and materials. These architectures offer opportunities to activate multi-electron, multi-step catalysts with light-generated excited states and to follow the sequence of steps in multi-electron catalysis using pulsed light, one electron at a time. Examples include the coupling of molecular light-absorbing photosensitizer molecules to molecular catalysts,[34] which are in turn linked to nanoparticle semiconductors that serve as sinks for multi-electron transfer, as shown in Fig. 11(a). This is an example of a rapidly expanding portfolio of catalyst materials linked to semiconductors and electrodes in porous, high-surface-area architectures. Further, post-synthetic modification of metal organic framework (MOF) materials has been developed for insertion of a broad range of molecular catalysts and metal cluster catalysts into precisely controlled positions in conductive and light-absorbing framework materials.[35,36,37,38,39] Fig. 11(b) illustrates an example of a light-harvesting MOF with polyoxometalate catalyst for solar fuels.[33] These designs are significant in providing approaches to investigate mechanisms using single-electron, single-turnover photochemistry in a manner comparable to the milestone achievements in photosynthesis, but now with a full range of synthetic catalysts that are designed for artificial leaf solar fuels applications.

A key challenge for resolving the structure and structural dynamics mechanisms underlying solar fuels catalysis lies in obtaining structure at the atomic scale for interfacial, electrode-supported, photocatalyst thin films. The APS Upgrade will provide unique capabilities for *in situ* characterization of catalyst thin films by providing high-energy x-rays with enhanced intensities using superconducting undulator insertion devices and with collimation characteristics permitting submicron focusing. In particular, PDF analyses will provide opportunities for atomic-scale structure resolution that can be directly linked to chemical reactivity. A proposed experiment is illustrated in Fig. 12,[40] for *in situ* structure resolution for a photocatalyst thin film to resolve structural intermediates during multi-step catalysis. PDF analyses measured with 0.1-Å real-space resolution, when combined with atomistic modeling, are capable of providing definitive structure identification for molecular coordination complexes and small metal clusters. By extending these capabilities to *in situ* thin film catalysts, the APS Upgrade provides the new possibility of following the structures of solar fuels catalysts as they are advanced through redox cycles, one electron at a time, using light or electrical pulses to trigger single-electron oxidation state changes. By using sequences of timed optical or electric field pulses, structural intermediates in complete reaction cycles can be mapped out.

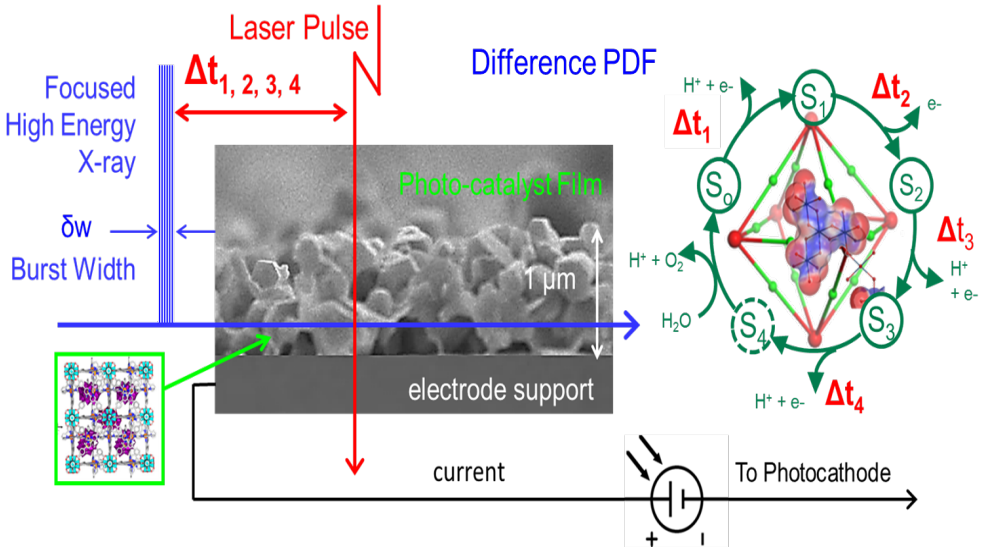

Fig. 12. Following solar fuels catalysis around the redox-cycle "clock" in artificial photosynthesis. Proposed experiment for *in situ* photocatalyst thin-film structure characterization by PDF analyses to resolve structure for intermediates in multistep catalysis

In the case of optical excitation, laser pulses are used to create photosensitizer excited states that trigger subsequent single-electron oxidation state changes on the linked catalysts. X-ray pulses synchronized to laser excitation are adjusted within a sequence of n different time delays, Δt_1, Δt_2, ..., Δt_n, to probe individual steps, S_1, S_2, ..., S_n, in the catalytic redox cycle. The timespan of interest for capturing intermediates associated with rate-limiting steps in multi-electron catalysis ranges from 1 ns to 1 s. This time domain is readily probed by the x-ray pulse characteristics of the APS Upgrade. With the APS Upgrade and upgraded high-energy detectors, we anticipate that data acquisition times for PDF will decrease by a factor of 10 to 50 compared to today. Difference PDF patterns at selected delay times could be acquired in 2 min for amorphous oxide film catalysts and in approximately 60 min for comparatively dilute, mono-nuclear molecular complexes as monolayers on nanoporous supports.

The proposed time-resolved PDF measurements on solar photocatalyst architectures in the artificial leaf will be critical, first-of-a-kind detection of structural intermediates during multi-step catalysis, followed one electron at a time. These would be milestone accomplishments. Structural data in difference PDF measurements provide quantitative, model-discriminating benchmarks for atomistic simulations. The combined use of time-domain PDF experiments with explicit atomistic modeling will enable fundamental mechanistic details of multi-step catalysis to be determined. These experiments will establish structural characterization approaches applicable to a broad range of applications in electro-catalysis and bond-making/breaking chemistries.

5.3.D. Strain-Engineered Catalysis

A critical concept in catalysis exploits the unique electronic environments for atoms at the surfaces of crystalline materials. Catalysis in nano-, micro-, and mesoporous crystalline materials is driven by the details of coordination numbers, geometries, and surface free energies for atoms at the crystalline interface. In particular for crystalline metal particles there are well-known correlations between crystal facets and chemical reactivity. Gaining control of the electronic structures for atoms at the surfaces through manipulation of the underlying lattice structure in metal nanoparticles has emerged as a powerful means to control surface catalytic activity and has led to the concept of strain-engineered catalysis.[7] Strain manipulation offers a means to modify the sorption energies of reactants and products and optimize catalytic performance. Recent advances in nanoparticle synthesis have enabled the syntheses of remarkable multi-metallic nanoparticles with precisely controlled core-shell structures. Twinning, core shell structures and complex architectures, such as those shown in Fig. 13, have all been demonstrated as effective in the tuning of catalysis through strain effects.[41] Such nanostructure designs offer routes to achieve advanced catalysts for more sustainable and zero-emissions technologies.[42] Tools enabling a detailed and precise characterization of the relationship between surface atom chemical reactivity and the underlying lattice strain and structure are needed.

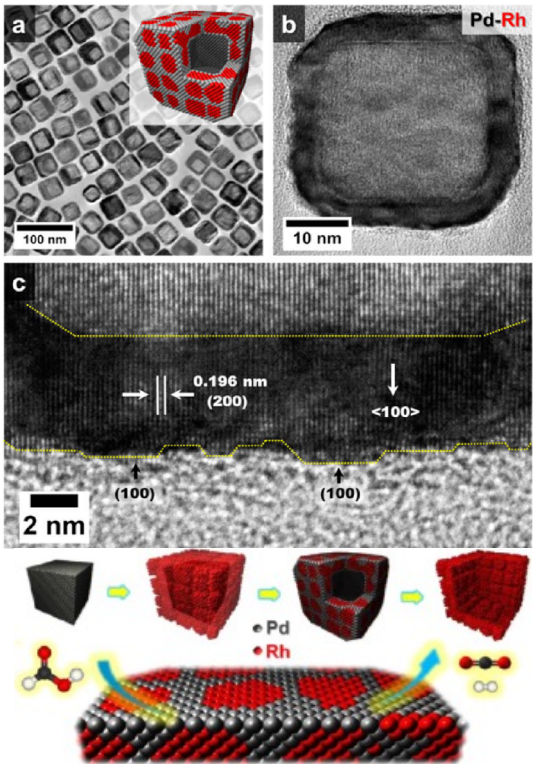

Fig. 13. Engineered strains in ~30 nm Pd-Rh nano-boxes lead to enhanced catalytic performance.[41]

CDI provides both images and volumetric (3D) quantification of strain in metal nanocrystals.[43,44] Compared with electron microscopy, x-ray CDI offers extended opportunities for the *operando* measurements required to establish direct correlations between strain and catalytic reactivity. In milestone experiments, CDI demonstrated pronounced strain effects due to monolayer thiol adsorption on 300 nm gold nanocrystals,[45] thermal expansion mismatch in zeolite crystals,[46] and the *operando* examination of dislocation dynamics in lithium batteries.[47] In the context of surface catalysis, the CDI spatial resolution of extended strain upon surface adsorption is particularly significant. Computational studies have demonstrated the ability to calculate models for electronic structure perturbation induced by adduct binding on metal particle surfaces for large, nanoscale clusters,[48,49] illustrated in Fig. 14, by the charge redistribution calculated upon oxygen adsorption to gold nanoparticles.[49] Charge redistribution underlies atomic displacements and lattice strain detected by CDI. Critically, CDI measurements provide unique experimental benchmarks for the development of quantitative theory for understanding surface atom reactivity. Even when the surface atoms cannot be resolved individually, the

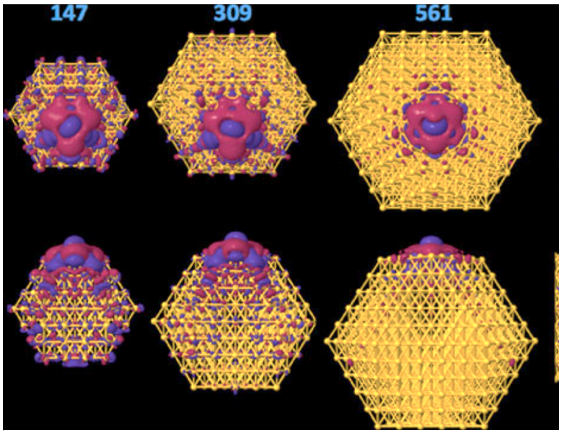

Fig. 14. Computational studies showing electronic charge redistribution upon oxygen binding to gold nanoparticle surfaces.[48]

phenomena of extended electronic structure and strain propagation can be measured and visualized. In this way, CDI measurements provide a unique, direct window for deducing the electronic properties of the surface atoms underlying catalysis to be modeled.

Currently, Bragg CDI experiments are viable only for crystals much larger than those typically used for catalysis, due to the limited coherent flux from third-generation synchrotron lightsources, although some preliminary work on the catalytic transformation of ascorbic acid has been performed using large gold nanocrystals. [50] Coherent diffraction analysis and imaging have been successfully demonstrated for 15-nm Pb nanoparticles using x-ray powder diffraction patterns.[51] The APS Upgrade will increase coherent flux by two orders of magnitude, driving a significant decrease in the size of nanostructures that can be studied individually and bringing the crystal sizes that can be studied by CDI much closer to those of interest for practical catalysts. Preliminary work already has demonstrated the feasibility of CDI experiments in electrochemical cells[47] and in aqueous[52] and reactive vapor environments.[45] We anticipate that quantitative volumetric strain measurements, using CDI, on strain-engineered catalytic nanostructures in virgin form, in the presence of reactants/products, and *operando* can be used to verify computational models used for the design and understanding of these nanostructures. For example, one could perhaps directly examine the response of oxygen reduction reaction (ORR) catalytic nanostructures in an electrochemical cell to changes in reaction conditions.

5.4 Operational and Instrumentation Needs

Insertion devices optimized for high energy: High-energy x-rays are a key strength of the APS and are pivotal to PDF measurements and other methodologies that, as described earlier, provide valuable insights into chemical transformations and reactivity. With the reduction in storage ring energy shifting the energy spectrum of existing insertion devices to lower energies, the development and optimization of specialized high-energy insertion devices must be a priority. The development of superconducting undulators will be critical to maintaining APS leadership in high-energy x-ray science.

Timing and the bunch structure of the ring: Time resolution will be limited by the x-ray bunch profile, 50 ps rms, in the standard operating 48-bunch mode.[53] Experiments exploiting single timing will require a fast chopper (e.g., the Jülich-type chopper) or electronically gated high-energy x-ray detectors to select single x-ray bunches. As discussed in the experimental section, rate-limiting steps in multi-step catalysis typically occur at or above microsecond timescales. These cases will enable the x-ray probe to consist of a sequence of x-ray pulses, framed using either slotted, rotating-wheel x-ray choppers or gated detectors. For a 1-μs x-ray burst probe, laser-activated experiments would be run with 1-kHz to 10-kHz repetition rates, with data

acquisition times increased by factors of 1,000 to 100 compared to continuous (non-pulsed) acquisition experiments.

Sample environments: The development of specialized sample environments will continue to be of principal importance in enabling discoveries in chemistry and catalysis. Sample environments that replicate conditions used for normal laboratory or industrial-scale processes are needed for *operando*/*in situ* studies. With higher-time-resolution measurements planned, higher-fidelity sample environments will be needed to ensure that the observed mechanisms and kinetics are intrinsic to the system being studied and are not artifacts of the sample environment. Additionally, coherent methodologies require thin samples and operando sample environments with excellent mechanical stability.

It will be important for the field as a whole to move from *ad hoc* solutions and one-offs put together from scratch for each experiment to more rigorously engineered higher-fidelity devices. Commercial sample environments are not generally available. Expertise and experience at the APS in the design of sample environments should be cultivated to ensure that APS-U's full potential to advance chemistry and catalysis is realized. For coherent methods that require thin samples and sample environments, devices being developed for transmission electron microscopies (e.g., with controlled temperatures and fluid flow capabilities) may be suitable for adaptation to APS Upgrade measurements. It also will be important to develop automated sample handling for high-throughput measurements, so that beam time can be used efficiently. This will enable high-throughput combinatorial synthesis efforts. As individual measurements may be made much more quickly than the rate at which changes occur in the sample, it also will enable multiple processes to be studied in parallel under *in situ/operando* conditions.

Infrastructure: Experimental set-ups for studies of synthesis and reactive processes are often complex. Cutting-edge science and successful experiments are heavily reliant on robust experimental infrastructure beyond the x-ray beam. Substantial investment and optimization of experimental infrastructure should be part of the path to the APS Upgrade, to make it possible to capitalize on the beam gains more immediately.

Data handling & analysis: With increased data rates provided by increased flux and more complex data sets provided by newly enabled methodologies, bottlenecks are created by data reduction, handling, storage and analysis. There has been much discussion of using high-performance computing capabilities to address this problem. However, the scale of computational problems associated with x-ray science, while they exceed the hardware and software readily available to lightsource users, are often too small to require the enormous capabilities of national computing facilities. A layered set of resources is required that will span local tools and capabilities for data handling and that will enable access to leadership-class computing for experiments with the most demanding computational science problems. Computation solutions also must be optimized for different experimental needs.

Detectors: As with x-ray brightness/flux limitations, detector sensitivity and read-out rates can equally limit or enable measurements and science. The APS-U will place even greater demands on detector performance. Advances in detector technologies have the potential to deliver gains of the same orders of magnitude as those provided by the accelerator upgrade. The variety and

performance parameters of the needed detectors require leveraged investment beyond the facility's in-house detector development programs. For example, the expected emergence of high-energy-optimized, gateable, photon-counting, large-area detectors, such as CdTe pixel array detectors, will be important to enabling nanosecond-resolution PDF measurements.

Beam-induced damage, reactivity, heating and sample motion: While the heat load on optics may not increase significantly, the increased x-ray doses on samples raise concerns for chemistry and catalysis research because they can impact chemical reactivity and kinetics. Shifting to higher beam energies, which is newly possible for coherent methods, will mitigate some effects. Otherwise, careful experimental design strategies (e.g., flowing fluids) will need to be considered.

High photon energy will be important in minimizing beam damage and accessing the highest resolution reciprocal space data (e.g., PDF). This will be a strength of the APS-U within the United States and, with the superconducting undulator technology, will be an area of advantage on the international stage.

5.5 References

[1] Image adapted from the Interdisciplinary Centre for Advanced Materials Simulation (ICAMS): http://www.icams.de/content/research/.

[2] Image based on: http://oceanworld.tamu.edu/resources/oceanography-book/microbialweb.htm

[3] S. F. Xie, N. Lu, Z. X. Xie, J. G. Wang, M. J. Kim, and Y. N. Xia, Angew. Chem. Int. Ed. **51**, 10266 (2012).

[4] Y. Li and J. H. Yu, Chem. Rev. **114**, 7268 (2014).

[5] M. Moliner, F. Rey, and A. Corma, Angew. Chem. Int. Edit. **52**, 13880 (2013).

[6] C. B. Murray, D. J. Norris, and M. G. Bawendi, J. Am. Chem. Soc. **115**, 8706 (1993).

[7] B. T. Sneed, A. P. Young, and C.-K. Tsung, Nanoscale **7**, 12248 (2015).

[8] T. S. Ahmadi, Z. L. Wang, T. C. Green, A. Henglein, and M. A. El-Sayed, Science **272**, 1924 (1996).

[9] R. Garcia-Rodriguez, M. P. Hendricks, B. M. Cossairt, H. T. Liu, and J. S. Owen, Chem. Mater. **25**, 1233 (2013).

[10] D. Xu, G.R. Swindlehurst, H. Wu, D.H. Olson, X. Zhang, and M. Tsapatsis, M. Adv. Funct. Mater. **24**, 201 (2014).

[11] M. Suga, F. Akita, K. Hirata, G. Ueno, H. Murakami, Y. Nakajima, T. Shimizu, K. Yamashita, M. Yamamoto, H. Ago, and J. R. Shen, Nature **517**, 99 (2015).

[12] N. Cox, D. A. Pantazis, F. Neese, and W. Lubitz, Interface Focus **5**, 20150009 (2015).

[13] Image adapted from D. A. Watson, http://www.udel.edu/chem/dawatson/research.html.

[14] C. X. Zhang, C. H. Chen, H. X. Dong, J. R. Shen, H. Dau, and J. Q. Zhao, Science **348**, 690 (2015).

[15] Q. Yin, J. M. Tan, C. Besson, C.; Y. V. Geletii, D. G. Musaev, A. E. Kuznetzov, Z. Luo, K. I. Hardcastle, and C. L. Hill, Science **328**, 342 (2010).

[16] M. W. Kanan and D. G. Nocera, Science **321**, 1072 (2008).

[17] R. D. L. Smith, M. S. Prevot, R. D. Fagan, Z. P. Zhang, P. A. Sedach, M. K. J. Siu, S. Trudel, and C. P. Berlinguette, Science **340**, 60 (2013).

[18] L. Jingshan, I. Jeong-Hyeok, M. T. Mayer, M. Schreier, M. K. Nazeeruddfn, P. Nam-Gyu, S. D. Tilley, F. Hong Jin, and M. Gratzel, Science **345**, 1593 (2014).

[19] L. Fan, I. McNulty, D. Paterson, M. M. J. Treacy, and J. M. Gibson, Nucl. Instrum. Meth. B **238**, 196 (2005).

[20] M. M. J. Treacy and K. B. Borisenko, Science **335,** 950 (2012).

[21] M. Altarelli, R. P. Kurta, and I. A. Vartanyants, Phys. Rev. B **82,** 104207 (2010).

[22] A. T. J. Torrance, B. Abbey, C. T. Putkunz, D. Pelliccia, E. Balaur, G. J. Williams, D. J. Vine, A. Y. Nikulin, I. McNulty, H. M. Quiney, and K. A. Nugent, Opt. Express **21**, 28019 (2013).

[23] P. Wochner, C. Gutt, T. Autenrieth, T. Demmer, V. Bugaev, A. D. Ortiz, A. Duri, F. Zontone, G. Grubel, and H. Dosch, P. Natl. Acad. Sci. USA **106**, 11511 (2009).

[24] M. M. J. Treacy, J. M. Gibson, L. Fan, D. J. Paterson, and I McNulty, Rep. Prog. Phys. **68**, 2899 (2005).

[25] Image adapted from http://www.esrf.eu/news/general-old/general-2006/catalyst.

[26] Z. P. Wang, J. H. Yu and R. R. Xu, Chemical Society Reviews **41**, 1729 (2012).

[27] B. Marmiroli, G. Grenci, F. Cacho-Nerin, B. Sartori, E. Ferrari, P. Laggner, L. Businaro, and H. Amenitsch, Lab Chip **9**, 2063 (2009).

[28] W. Schmidt, P. Bussian, M. Linden, H. Amenitsch, P. Agren, M. Tiemann, and F. Schuth, J. Am. Chem. Soc. **132**, 6822 (2010).

[29] D. Saha, K. M. O. Jensen, C. Tyrsted, E. D. Bøjesen, A. H. Mamakhel, A.-C. Dippel, M. Christensen, and B. B. Iversen, Angew. Chem. Int. Edit. **53**, 3667 (2014).

[30] C. Tyrsted, K. M. O. Jensen, E. D. Bojesen, N. Lock, M. Christensen, S. J. L. Billinge, and B. B. Iversen, Angew. Chem. Int. Edit. **51**, 9030 (2012).

[31] K. M. O. Jensen, M. Christensen, P. Juhas, C. Tyrsted, E. D. Bojesen, N. Lock, S. J. L. Billinge, and B. B. Iversen, J. Am. Chem. Soc. **134**, 6785 (2012).

[32] M. T. Vagnini, M. W. Mara, M. R. Harpham, J. Huang, M. L. Shelby, L. X. Chen, and M. R. Wasielewski, Chem. Sci. **4**, 3863 (2013).

[33] Z.-M. Zhang, T. Zhang, C. Wang, Z. Lin, L.-S. Long, and W. Lin, J. Am. Chem. Soc. **137**, 3197 (2015).

[34] M. T. Vagnini, M. W. Mara, M. R. Harpham, J. Huang, M. L. Shelby, L. X. Chen, and M. R. Wasielewski, Chem. Sci. **4**, 3863 (2013).

[35] M. C. So, M. H. Beyzavi, R. Sawhney, O. Shekhah, M. Eddaoudi, S. S. Al-Juaid, J. T. Hupp, and O. K. Farha, Chem. Commun. **51**, 85 (2015).

[36] P. Deria, J. E. Mondloch, O. Karagiaridi, W. Bury, J. T. Hupp, and O. K. Farha, Chem. Soc. Rev. **43,** 5896 (2014).

[37] M. C. So, S. Jin, H.-J. Son, G. P. Wiederrecht, O. K. Farha, and J. T. Hupp, J. Am. Chem. Soc. **135**, 15698 (2013).

[38] Z. M. Zhang, T. Zhang, C. Wang, Z. K. Lin, L. S. Long, and W. B. Lin, J. Amer. Chem. Soc. **137**, 3197 (2015).

[39] J. L. Wang, C. Wang, and W. B. Lin, ACS Catal. **2**, 2630 (2012).

[40] SEM image of an MOF film from: http://www.membrane.unsw.edu.au/wp-content/gallery/cmst-gallery/mof-sem-2.jpg. Insets on lower left and right show representative catalyst MOF architectures adapted from ref. 28 and from a slide provided by Prof. Wenbin Lin (University of Chicago).

[41] B. T. Sneed, C. N. Brodsky, C. H. Kuo, L. K. Lamontagne, Y. Jiang, Y. Wang, F. Tao, W. X. Huang, and C. K. Tsung, J. Am. Chem. Soc. **135**, 14691 (2013).

[42] M. Oezaslan, F. Hasche, and P. Strasser, J. Phys. Chem. Lett. **4**, 3273 (2013).

[43] R. Harder and I. K. Robinson, JOM US **65**, 1202 (2013).

[44] I. Robinson and R. Harder, Nat. Mater. **8**, 291 (2009).

[45] M. Watari, R. A. McKendry, M. Vogtli, G. Aeppli, Y. A. Soh, X. W. Shi, G. Xiong, X. J. Wang, R. Harder, and I. K. Robinson, Nat. Mater. **10**, 862 (2011).

[46] W. Cha, N. C. Jeong, S. Song, H. J. Park, T. C. T. Pham, R. Harder, B. Lim, G. Xiong, D. Ahn, I. McNulty, J. Kim, K. B. Yoon, I. K. Robinson, and H. Kim, Nat. Mater. **12**, 729 (2013).

[47] A. Ulvestad, A. Singer, J. N. Clark, H. M. Cho, J. W. Kim, R. Harder, J. Maser, Y. S. Meng, and O. G. Shpyrko, Science **348**, 1344 (2015).

[48] J. Kleis, J. Greeley, N. A. Romero, V. A. Morozov, H. Falsig, A. H. Larsen, J. Lu, J. J. Mortensen, M. Dułak, K. S.Thygesen, J. K. Nørskov, and K. W. Jacobsen, Catal. Lett. **141**, 1067 (2011).

[49] L. Li, A. H. Larsen, N. A. Romero, V. A. Morozov, C. Glinsvad, F. Abild-Pedersen, J. Greeley, K. W. Jacobsen, and J. K. Nørskov, J. Phys. Chem. Lett. **4,** 222 (2013).

[50] R. Harder, unpublished (2015).

[51] P. Scardi, A. Leonardi, L. Gelisio, M. R. Suchomel, B. T. Sneed, M. K. Sheehan, and C. K. Tsung, Phys. Rev. B **91**, 155414 (2015).

[52] A. Ulvestad, J. N. Clark, R. Harder, I. K. Robinson, and O. G. Shpyrko, Nano Lett. **15**, 4066 (2015).

[53] M. Borland, http://www.aps.anl.gov/Upgrade/Documents/multi-bend-achromat-lattice.pdf (2014).

6 Earth, Environmental, and Extreme Conditions Science

Antonio Lanzirotti, *University of Chicago*
John Parise, *State University of New York at Stony Brook*
Mali Balasubramanian, Chris Benmore, Vincent De Andrade, Paul A. Fenter, Dean Haeffner, Steve Heald, Michael Hu, Ken Kemner, Stefan Vogt, *Argonne National Laboratory*; Ben Twining, *Bigelow Laboratory for Ocean Sciences;* Jennifer Jackson, *California Institute of Technology;* Guoyin Shen, Jesse Smith, *Carnegie Institution for Science*; Andrew Campbell, Peter Eng, Matthew Newville, Vitali Prakapenka, Mark Rivers, Joanne Stubbs, Steve Sutton, *University of Chicago*; Brandy Toner, *University of Minnesota*; Lars Ehm, *State University of New York at Stony Brook*; Przemek Dera, *University of Hawaii*; Bhoopesh Mishra, *Illinois Institute of Technology*; Malcolm McMahon, *University of Edinburgh*; Kirk Scheckel, *U.S. Environmental Protection Agency*

6.1 Executive Summary

Scientists involved in earth, environmental, and extreme conditions science (E^3) research seek to understand the physics and chemistry of planetary bodies, including Earth, from crust to core. The nature of E^3 research requires the study of small samples, which additionally are often heterogeneous in composition or structure on the nanometer scale. For example, generating the static pressures required to investigate conditions deep in planetary interiors necessarily results in sample volumes below 1 μm^3. Studies of samples of extraterrestrial material returned to Earth by spacecraft provide unique insights into the origin and evolution of the solar system, but these one-of-a-kind, precious samples contain mineral grains and interfaces that are often only tens to hundreds of nanometers in size. The fluids and microorganisms that influence metal transformations and mobility in the environment and in the subsurface involve sub-micrometer-scale mineral interface reactions, posing a significant challenge to characterization techniques.

Increasingly, our ability to successfully model and understand chemically and physically heterogeneous global systems (Fig. 1) relies on access to methods that allow us to bridge these extreme length scales analytically and conceptually.[1,2,3,4] Nanoscale resolution, applied over mesoscopic lengthscales, will allow us to understand how the atomic, molecular, and nanoscale hierarchy of architectures organize to define their more familiar bulk macroscopic behavior.[5]

The APS Upgrade provides vastly improved precision and sensitivity in studies at the nanoscale, permitting techniques such as inelastic spectroscopy and powder diffraction to be used to probe far smaller sample volumes than has been previously possible. In addition, the increased focused flux of the APS Upgrade in nanoscale probes dramatically increases sample throughput,

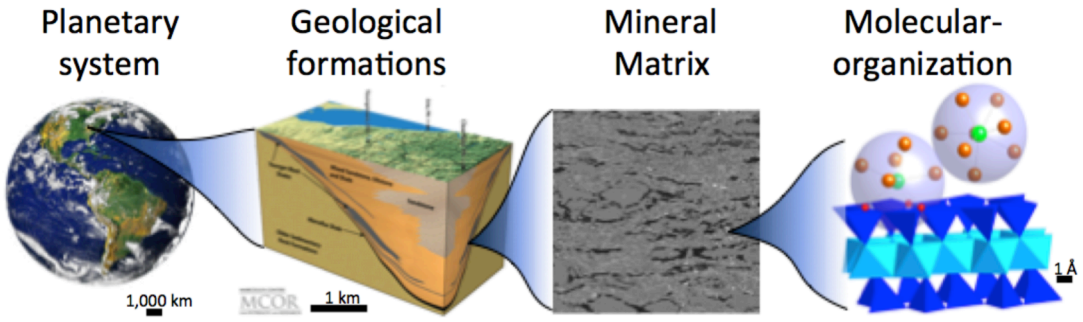

Fig. 1. Geosystems inherently display extreme inherent heterogeneity ranging from molecular to planetary lengthscales.[1,2,3,4] The use of coherent, high-brightness x-ray sources enables a robust understanding of the complex reactivity in these systems.

which provides more robust statistical characterization of Earth materials for experiments requiring large numbers of analyses, facilitating experiments that will allow atmospheric and marine scientists to generate more quantitative models of how element cycling in the atmosphere and oceans couples to climatic variations.

6.2 New Opportunities for E^3 Science at the APS Upgrade

The E^3 community benefits enormously from continued improvement in brightness afforded by next-generation hard x-ray lightsources, including the APS-U, because these facilities allow researchers to understand processes at their fundamental lengthscales. The unparalleled brightness and coherence of the APS Upgrade will allow dynamic, *in situ*, and multimodal analysis of heterogeneous Earth materials at spatial resolutions that are not currently possible.

An example of this is our ability to study materials under extreme conditions to understand large-scale planetary dynamics. APS-U opens up vast new areas of high-pressure research, since the smaller, brighter beams allow x-ray techniques to fully exploit new DAC developments that push the limits of attainable high pressures above 1 TPa. Experiments using the new cells are challenging because, at these pressures, sample sizes are limited to 1 μm^3 or smaller. Although laser heating using a 1 µm focused spot is possible, the focused x-ray beams must be at least a factor of 5 smaller than the laser spot to provide meaningful data without averaging over a temperature or pressure gradient. Studies in the TPa range thus would require a highly penetrating x-ray beam with a diameter of 100 to 200 nm at a photon energy of 40 keV or higher, while retaining sufficient flux for scattering, diffraction, and imaging. This source will be provided by the APS Upgrade.

Similarly, while advances in understanding and controlling the behavior of chemical species at complex rock-water interfaces in Earth's sub-surfaces are critical to developing enhanced energy production technologies and to minimizing the negative impacts related to unintentional release of contaminants to the environment, we are constrained by the spatial and temporal resolution of currently available x-ray sources.[6,7,8,9] *In situ* studies of reaction progress at the surfaces of submicron mineral grains will allow scientists to observe the real-time dynamics and evolution of heterogeneous reactivity (e.g., growth and dissolution) via

nanometer-scale spectroscopic probes. Further, the high coherent flux provided by APS-U will allow E^3 researchers to simultaneously use ptychographic approaches to image the full 3D structure of geomaterial matrices, providing the structure and reactivity of nanoparticles within the complex soil matrices that constitute their natural setting. The APS-U also offers unprecedented opportunities to image the structure and reactivity of buried interfaces in relevant subsurface geologic media (e.g., solid-fluid, solid-solid) *in situ*, directly, and dynamically.

In this document, we describe several key experiments that illustrate how E^3 research will take advantage of the new capabilities provided by APS-U. These experiments include:

1) *Determination of the melting curve and atomic arrangements of Fe to 1 TPa and 10,000 K*: An accurate determination of the structure of Fe under these conditions is the key piece of information required to define the thermal profile of terrestrial planetary cores possessing a magnetic field. Almost nothing is known at present about the melting and structural behavior of solid Fe above 300 GPa. APS-U will permit first-time measurements of scattering, trace-element partitioning, imaging of partial melts, 4D imaging with Mössbauer spectroscopy, and inelastic x-ray scattering measurements at 1 TPa. Ultimately, these data could significantly enhance our understanding of how planets generate magnetic fields, as well as the potential global impacts associated with geomagnetic reversals. Some calculations suggest that during magnetic reversals, Earth's dipole field may disappear entirely, leaving Earth highly susceptible to high-energy particles from solar wind, with serious potential consequences.

2) *The generation of models for the solar and extra-solar planets* (Fig. 2) requires high-pressure studies of the light, weakly-scattering constituents of giant planets (H_2, He, H_2O, CH_4, NH_3, etc.). Data on single-crystals of <3-μm size are desperately needed to resolve the crystal structure of hydrogen phase IV and of other, still-higher pressure-temperature (P-T) hydrogen phases. Bright, sub-μm x-ray beams need to be focused entirely inside the crystal to minimize the high background expected due to scattering from the sample environment. The enhanced nanobeam capability of the APS-U is ideal for this extremely challenging problem.

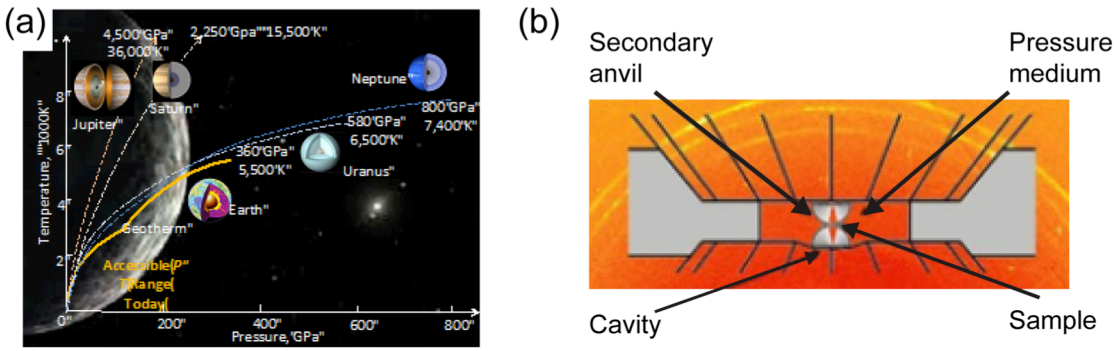

Fig. 2. (a) Pressure-temperature conditions in the interior of terrestrial and giant planets. (b) Recently developed double-stage diamond anvil cell allow collection of data of sufficient quality for structural refinement at pressures of 1 TPa and above, but require small samples (< 1 μm thickness) and high-photon-energy x-ray beams. The APS-U will allow precise imaging, spectroscopy, and elastic and inelastic scattering investigations of materials under these extreme conditions.

3) *The oxidation state (fO_2)*, which controls the compositions of condensed compounds in our solar system, can be inferred from x-ray absorption fine structure measurements of mineral phases and glasses to determine the valences of multivalent elements (Ti, V, Cr, Fe, and Eu) that can then be used as proxies for the oxidation states of the environments from which these mineral grains formed. This approach has been used on a variety of extraterrestrial materials at relatively coarse spatial scales,[10] but many of the most interesting and relevant specimens from which understanding early solar system evolution can be derived are at the micron scale and smaller. APS-U will allow focused beam x-ray absorption spectroscopy of these phases at nanometer spatial scales and at very low elemental abundance.

4) *Understanding the long-term health and environmental impacts of engineered nanomaterials (ENMs)* is a pressing need. For example, it has been reported that diesel exhaust deposition of a few ppm CeO_2 disrupts nitrogen fixation by legumes. Yet such controversial conclusions are based on studies of model systems where CeO_2 exposure doses are 4 to 5 orders of magnitude higher than found in nature, providing potentially unrealistic projected impacts of ENMs. The APS-U will allow nanoscale imaging over a large, mesoscale area with sub-ppm sensitivity to determine the speciation of ENMs in soils, sediments, biological organisms, and plants.

5) *Control of the heterogeneous reactivity of elements at mineral-fluid interfaces* requires going beyond imaging of nanoparticles after they form at a mineral surface and evaluating their relationship to observed surface heterogeneity, including nucleation sites, crystallographic orientation, structural phase, and structural defects.[11,12] The APS-U will enable the next generation of interfacial microscopy, which will include multiple imaging modalities in a single instrument to understand reactivity with sensitivities spanning from 10 nm to 10 μm. For example, full-field imaging with incoherent illumination will interrogate 10 μm × 10 μm fields of view, at 60 to 150 nm resolution with high photon energy to reduce perturbations caused by the x-ray beam to the chemical process of interest. Separate Bragg CDI/ptychography imaging of prototypical regions can then be used to reveal the structural basis for reactivity via 3D images at 10 nm spatial resolution using coherent illumination.[13,14] These new imaging capabilities are critical to understanding geological transport for repositories of energy-related materials such as CO_2 and radioactive waste.[15]

6) *Unraveling the effect on ocean productivity of trace metal micronutrients,* such as iron, zinc, cobalt, and manganese, is critical to developing a mechanistic understanding of how competition for metals by ocean phytoplankton will alter marine productivity and affect the ocean's role in the global carbon cycle. Little is understood about how some of the most abundant marine organisms in tropical and sub-tropical oceans impact oceanic and atmospheric elemental cycles because the organisms are too small, on the order of 500 nm, to be analyzed with existing x-ray lightsources. APS-U will provide high flux density in nanometer-focused spot sizes that will, for the first time, enable measurements of metal abundance and speciation in representatives of the vast microbial ecosystems which largely control the metabolism of our planet.[16]

6.3 Early E^3 Experiments at APS-U

6.3.A. Planets in a Laboratory Setting – Materials at the Extremes of P & T

Background and Motivation

Seismic tomography and remote planetary missions and observation are providing new information at unprecedented resolution of Earth's interior and planetary atmospheres, respectively. However, we have but a rudimentary understanding of the fundamental physics and chemistry of the materials that comprise Earth, solar, and extrasolar planets under extreme conditions; these data are critical for testing models for planetary formation, evolution, and likelihood of habitability. Figure 2 shows a plot of pressure-temperature (P-T) conditions along the depth of the planetary interiors. The current P-T range that is accessible using state-of-the-art static high-pressure technology and the current synchrotron source parameters spans a limited subset of the conditions indicated. Obtaining data at the extreme P-T regimes that exist within planets requires matching brighter, more coherent x-ray beams to the very much smaller volume that is necessary to generate pressures beyond 1TPa; APS-U provides that match.

Recent breakthroughs in the development of two-stage DACs provide a dramatic increase in pressure capability to about 1 TPa at room temperature,[17] which is more than three times the 0.3 TPa record established more than a generation ago.[18] Two-stage DACs are a transformative achievement that will herald a new generation of high-pressure science. The greatly enlarged P-T range that will be enabled by the smaller and brighter x-ray beam of the APS-U will allow scientists to probe materials representative of much deeper planetary depth. While x-ray diffraction at 1 TPa will be challenging, application of new techniques at high pressure becomes possible for the first time, including x-ray inelastic scattering, x-ray nuclear scattering, and spectroscopy. Exploring the application of these methods at high pressure will require significant research and instrumentation development to make full use of the capabilities of the APS-U.

Scientific Objectives

The melting, crystal structures, elasticity, and trace element partitioning associated with iron and iron-containing silicates, above 0.3 TPa and T > 4000 K, are especially important in understanding planetary composition. For example, the melting points of iron and its alloys define the thermal profile of terrestrial planetary cores possessing a magnetic field.[19] The APS-U facilitates combinations of x-ray scattering, high-resolution imaging, Mössbauer spectroscopy,[20] thermal diffuse scattering, and inelastic x-ray scattering measurements above 1 TPa that will provide the first essential information on planetary and exoplanetary interiors.

Experimental Details

In recent static-compression experiments on the melting of Fe,[21] the highest pressure at which melting was confirmed was 155 GPa, where the melting temperature was 4500 K. Although such a measurement is an outstanding experimental achievement, considerable extrapolation is required to reach higher pressures. There is for example, considerable uncertainty in the estimated melting temperature of 6000-7000 K at 330 GPa (Fig. 2), the pressure at the Earth's

inner-core boundary. For more massive Earth-like planets, which have masses that are a factor of 5 to 10 greater than that of the Earth, the melting curve of Fe up to at least 1 TPa is required for example, to determine whether they possess Earth-like liquid metallic cores and thereby to understand their internal dynamics. Such pressures have just been reached in micron-sized samples at room temperature in pilot experiments using the two-stage anvils at the APS. Coupled in the coming several years with pulsed laser heating, the new stages combined with the APS-U will open the way to determining the structures and melting curve of Fe, and Fe-alloys, to 1 TP and 10,000 K. Such a measurement would be transformative and would provide fundamental structural thermodynamic and transport property information for understanding exoplanet geodynamics.

Diffraction measurements at extreme P-T conditions allow us to derive information on phase stability, and atomic spatial arrangements. Progress also requires information about the Fe oxidation state, spin, and dynamic states, which control chemical transport, element partitioning, elastic, and melting properties of its host phase throughout planetary interiors. Mössbauer spectroscopy is a powerful probe to accurately determine such behaviors of iron in minerals. With the high-spectral brightness of APS-U and continued development of high-speed shutters (Fig. 3), new opportunities become available to perform 4D imaging of oxidation, spin state, phase stability and melting properties of iron-bearing minerals under multi-megabar pressures and thousands of kelvins.[22,23,24,25] Here developing a time structure for the x-ray bunches at APS-U that is compatible with nuclear resonant scattering is essential and must be supported by the design of storage-ring technologies.

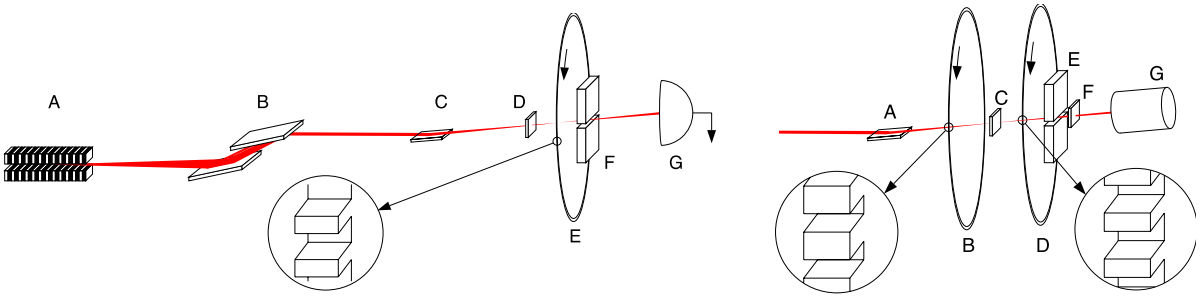

Fig. 3. Next-generation Mössbauer spectroscopy with high-speed shutters. Schematic of high-speed periodic shutters at Sector 3 of the APS.[20] Focused 2-eV-bandwidth photons on a sample containing a nuclear resonant isotope. A series of kHz shutters traverse the beam (left). The sample is placed between two shutters tailored for a particular fill mode (right), permitting Mössbauer spectroscopy while completely suppressing the electronic charge scattering. This permits collection of time domain Mössbauer spectra and diffraction without moving the sample, while a laser heats the sample to above 10,000 K.[20]

Of the light elements constituting the giant gaseous and icy planets, none is as important and difficult to study as hydrogen. As a result, the desire to compress solid hydrogen to extreme pressures and to study its properties *in situ* has long driven advances in high-pressure research at synchrotron facilities. The research conducted over the last five years has been particularly productive; hydrogen is now known to possess a rich and complex P-T phase diagram that consists of at least five different phases between 100 to 360 GPa as a function of temperature.[26,27,28,29] Much of the work on hydrogen to date is based on optical spectroscopy, given that its x-ray scattering cross-section is so low. But with the APS-U, the ultimate goal of characterizing the structures hydrogen adopts through its remarkable semiconductor,

semimetallic, metallic, and possibly superconducting states under pressure in the solid and fluid appears closer than ever. For the solid phases, critical information from single-crystal diffraction measurements is desperately needed to resolve the crystal structure of both hydrogen phase IV and the higher P-T phases; these experiments are not yet feasible. At ultrahigh pressures, the maximum size of hydrogen single crystals achievable by encasing them in a soft hydrostatic helium pressure medium is less than 3 μm. Sub-μm x-ray beams need to be focused entirely inside the hydrogen crystal to minimize the high background from the surrounding vessel. The enhanced nanobeam focused flux at the APS-U enables crystallographic studies of light elements in high P-T phases. Preliminary estimates of the count rates using the focused photon fluxes listed at the end of the Mesoscopic Engineering and Advanced Materials chapter show that diffraction from a $1\mu m^3$ H crystal will have sufficiently high intensity to be resolved in crystallographic studies.

As we build a knowledge base for pure elements at extreme conditions, it is important that we also study multi-element and highly heterogeneous samples, as illustrated in Fig. 4.[30] Such data will be used to address open questions regarding the dynamics of planetary interiors; e.g. rheology, the effects of partial melts, and trace element partitioning. For example, determining trace element fractionation between melt and solid phases, as a function of P and T, allows us to access the principal mechanism by which planets differentiated to form the structures contained within them today. Using samples quench-recovered from high P-T experiments, APS-U will provide 10-ppm sensitivity at 100-nm resolution, as well as the ability to identify major element compositions of grains 10 nm in size, using spectroscopic techniques pioneered by the E^3 community, highlighting the synergy between these groups of researchers. Ideally, 3D chemical mapping will be performed with the sample still in the DAC, which is potentially achievable with APS-U. Ultimately, the goal is to perform *in situ* 3D analysis at high pressure during laser heating of pure and multi-element samples, as a close approximation to small pieces of planets, in a laboratory setting.

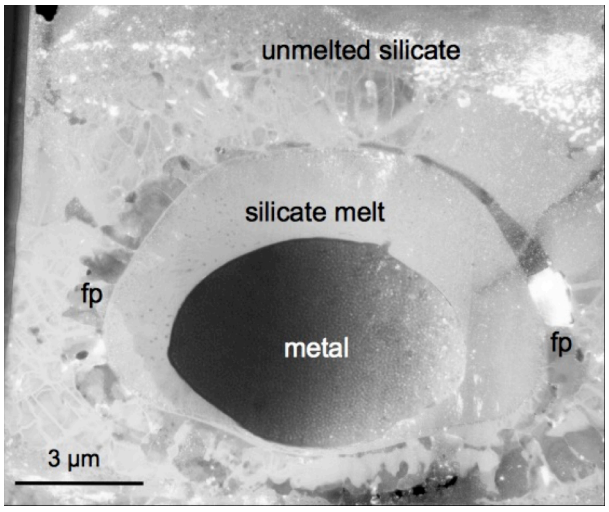

Fig. 4. Transmission electron microscope image of a laser-heated diamond anvil experiment recovered from 57 GPa, 4400 K.[30] The central rounded region includes quenched metal and silicate melts, reflecting the very high degree of melting of this sample at its peak temperature. The outer portions of the sample were subject to less extreme heating and show much finer grain size and heterogeneous texture; this presents analytical challenges, especially for trace element measurements. APS-U's high spatial resolution and sensitivity for synchrotron x-ray fluorescence tomography will allow dramatic improvements in the ability to measure trace element distributions in experiments like these.

6.3.B. Solar System Formation Conditions Recorded by Early Condensates

Background and Motivations

Mineral grains that comprise meteorites, comets, asteroids, and planets contain records of the conditions under which they formed. Deciphering these records can lead to improved understanding of the origin and evolution of our Solar System, guide the search for other life-compatible exoplanets, and provide new insights into the future of our home planet. Key information is locked within samples of the earliest condensates, so-called "refractory inclusion," predicted to be calcium and aluminum oxides, which exist as sub-micron components within rare, refractory inclusions in meteorites. Such early condensates also have been identified in particles returned by the Stardust spacecraft from the Wild-2 comet. These samples provide an extraordinary opportunity to define the conditions present during the earliest stages of Solar System formation.

Refractory inclusions are particularly important in understanding the conditions in the early Solar System, both because they are the oldest known objects[31,32,33] and because their bulk compositions are similar to those calculated for solid phase assemblages predicted to condense from a gas of solar composition.[34] Objects from meteorites have received extensive analytical study (see e.g., refs. 35, 36, and references therein).

Synchrotron analyses offer a direct means for characterizing the chemical and physical state of early condensates. However, such work is currently hampered by the difficulty in making highly sensitive measurements at the required nanoscale (Fig. 5). Much of the current work on these samples is being done by TEM or scanning transmission x-ray microscopy using microtomed slices, an approach that typically destroys the textural relationships of the grains, important information in defining crystallization sequences, for example. The APS-U will advance the capabilities for chemical characterization of these nanoscale building blocks by allowing analyses of un-sectioned samples and permitting the application of highly sensitive x-ray methods, such as x-ray absorption fine structure.

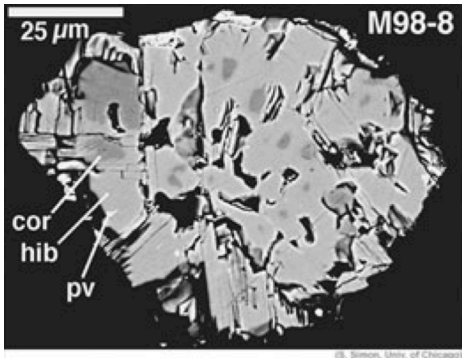

Fig. 5. A backscattered electron image of a refractory inclusion from the Murchison carbonaceous chondrite, consisting of corundum, hibonite, and perovskite, three minerals predicted to be some of the earliest condensates in the Solar System.[36]

In addition, the APS-U is likely to be well-timed with future sample return missions to primitive small bodies. The Hayabusa 2 mission to the Apollo asteroid (162173) 1999 JU_3 was launched in 2014 and is scheduled to return samples in 2020. OSIRIS-Rex will launch in 2016 and return samples in 2023 from asteroid Bennu, a carbon-rich asteroid specifically targeted to provide material from the earliest history of our Solar System.

Scientific Objectives

One of the most important properties to define for the early Solar System is its oxidation state, a parameter that controls the compositions of condensed compounds. Valences of multivalent elements (notably Ti, V, Cr, Fe, and Eu) in mineral grains can be used as proxies for oxygen

fugacity (fO_2); the valences can be determined using x-ray absorption fine structure techniques. This approach has been used on a variety of extraterrestrial materials at relatively coarse spatial scales, i.e., homogeneous volumes greater than 10^4 μm^3.[37] The APS Upgrade will allow these methods to be applied at much smaller spatial scales and at the very low concentrations that are likely to exist in some minerals, allowing extraction of oxidation state records from these nanoscale early condensates.

Experimental Details

The focus of first experiments will be on refractory inclusions in carbonaceous meteorites (notably Murchison) and refractory grains from cometary dust returned by the Stardust spacecraft.[38] Murchison refractory inclusions have been shown to contain mineral assemblages (Fig. 5) predicted from condensation theory,[39, 40] i.e., corundum (Al_2O_3), hibonite ($CaAl_{12}O_{19}$), and perovskite ($CaTiO_3$).[35] A refractory grain from Wild 2, a lower-temperature condensate collected from NASA's Stardust mission, is shown in Fig. 6.[41] This grain consists of a fine-scale intergrowth of fassaite (Ti-, Al-rich clinopyroxene), diopside, spinel, and anorthite with typical grain size in the ≤100-nm range.[42] Determining the valence of titanium in thsese systems will be the initial experimental target, based on the fact that the $Ti^{3+} \leftrightarrow Ti^{4+}$ oxygen buffer lies near the predicted fO_2 of the early solar gas and results from previous work on larger grains yielding mixtures of these species.[43] The results will define the oxidation state of early solar nebula at the time and place that these grains crystallized.

The proposed experiment requires an undulator insertion device source that can provide x-rays in the range from 2.3 to 20 keV, with approximately 100-nm achromatic focusing at all energies and with positional stability at the 10-nm scale. Advanced detectors that provide the highest possible output count-rate capability with excellent energy resolution are also required.

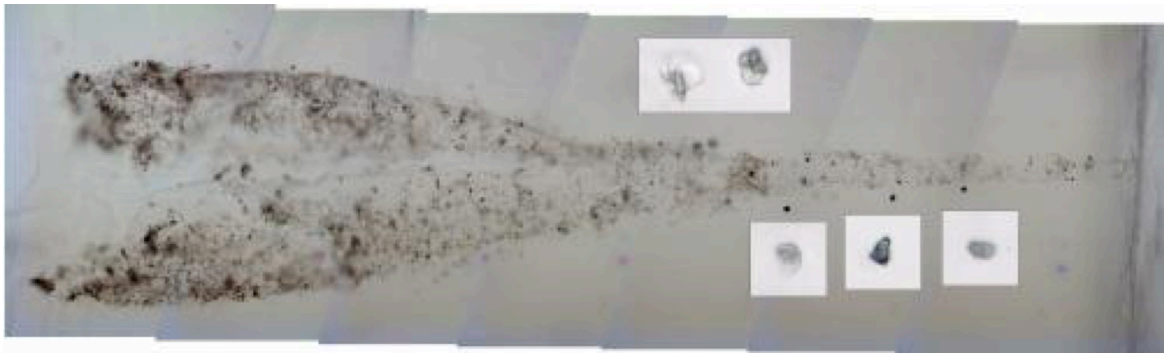

Fig. 6. Cometary dust particle track (~ 1 mm in length) in aerogel containing refractory inclusions (magnified in insets) returned from comet Wild 2 in 2006 by the Stardust spacecraft.[41] To visualize and probe high Ca and Ti grains (elements of key interest for identifying some of the oldest Solar System material), it is necessary to image the full track (approximately 1,000 μm x 300 μm) at a spatial resolution of 100 nm. With oversampling, this requires 20,000 x 6000 measurement points. Today, a dwell time of 100 ms per point is required to achieve sufficient sensitivities for the elements, meaning the complete measurement would require more than 3,000 hours of beam time; this would be impossible to carry out due to instrument instabilities over such a time period. With the upgraded APS, we anticipate being able to acquire sufficient statistics in just ~250 μs per point, so the experiment could be carried out in about 8 hours of beam time. Once identified, such grains can then be spectroscopically interrogated with an upgraded APS nanoprobe to generate x-ray absorption spectra in a 100 nm focus that are comparable to what is achievable now with a 1 μm focused beam, but 10x faster, making it possible to not only distinguish individual grains but also to probe a statistically relevant number of grains.

6.3.C. Bacterial Metabolic Function and Impacts of Engineered Nanomaterials (ENMs) in Soils and Organisms

Background and Motivation

As noted by Hooke: "For the limits, to which our thoughts are confined, are small in respect of the vast extent of Nature itself; some parts of it are too large to be comprehended, and some too little to be perceived."[44] The APS-U can change the scientific perception of the mesoscale, allowing better understanding of how the atomic, molecular, and nanoscale hierarchy of architectures organize to define their more familiar bulk macroscopic behavior.[5] Whether the challenge is microbial and biogeochemical interactions in soils or environmental release of nanoparticles (NPs), orders of magnitude increase in brightness and coherence at high energy will dramatically improve the ability to study smaller sample volumes with greater precision, spatial resolution, and throughput. Here we describe two examples in environmental science to illustrate the new science that will be possible at the APS-U in this area.

As an initial example, consider that the metabolic activities of soil microbes are the primary drivers of biogeochemical processes controlling the terrestrial carbon cycle, nutrient availability to plants, contaminant remediation, and other ecosystem services. However, our understanding of how microbes and microbial metabolism are distributed throughout soil aggregates[45] is limited, because no technique is available to image the soil pore network and the life that inhabits it. Soil is a highly complex network of pore spaces, minerals, and organic matter (e.g., roots, fungi, and bacteria). The size of soil aggregates can span lengthscales from tens of microns to a few millimeters. The size of fungal and root components can span length scales from microns to many meters, and the size of bacteria and their biomineralization products can span lengthscales from nanometers to microns. Thus, soil and its constituents can be physically, chemically, and biologically complex and heterogeneous over nano- to macro-scales.

Understanding the soil-microbe interaction in 3D is difficult because of experimental challenges. Imaging based on light or mass spectrometry can detect the location of organisms in relation to their biogeochemical environment, but these techniques cannot go beyond the surface of an opaque sample.[46,47] X-ray microtomography can provide highly detailed 3D renderings of soil structure [48,49,50] but cannot distinguish cells from other electron-light material, such as air or water. Nanometer-scale fiducial markers composed of high-Z elements (e.g., CdSe quantum dots) and placed preferentially into or on biological material could enable the contrast needed for XRF-based imaging of biological material in opaque media, but these would require x-ray imaging methods that will allow us to visualize them at the nanometer scale. The APS-U's high-brightness, high-spatial-resolution nanoscale hard x-ray beams will enable 3D imaging of the distribution of bacteria and their metabolism within soil through transmission, fluorescent, and ptychographic approaches.

As a second example, it is important to recognize that, although nanotechnology and the engineered nanomaterials (ENMs) it has produced hold the promise of revolutionizing many fields of science and technology, with prospective applications in medicine, sensing, and battery technology, the impacts of the release of such materials to the environment is poorly understood. As products enter the global market, there are still questions about the potential

risks and benefits of nanotechnology to consumers, workers, and, more generally, to human health and the environment. Responsible development of nanotechnology demands a balance between technological advancements that benefit society with environmental, health, and safety research to support science-based, real-world risk analysis and management to protect human health and the environment. Current models developed to measure the potential bioavailability of metal species in the environment assume a biotic ligand model (BLM) that relates metal toxicity to speciation and competition between environmental and biotic ligands.[51] Nanoparticulate metals may not be described well by the BLM because ENMs may (1) bind directly to cell surface receptors, (2) generate reactive oxygen species intracellularly or intercellularly, (3) bind directly to sensitive biotic ligands, and/or (4) be taken up into cells as intact metal particles with subsequent intercellular oxidation and release of free metal ions.

Some of the primary challenges in quantifying and characterizing the transport and binding behavior of nanoparticles in complex biological and environmental samples include truly low concentration of NPs in actual samples and identification of transformation products relative to the original NP. The concentrations of NPs in consumer products are often low and become more diluted when considering end-of-life scenarios such as disposal in a landfill or release of NPs to a wastewater treatment plant (WWTP). Biosolids from WWTPs are land-applied up to 10^4 kg per hectare, resulting in a minimum dilution factor of approximately 200. Despite available data on measured and predicted levels of NP concentrations entering the environment, many research studies utilize NP dose concentrations that are 3 to 5 orders of magnitude higher, with the justification that the level is required because analytical instruments have insufficient sensitivity to study more relevant concentrations. At present, real-world scenarios are often ignored, and experiments may have unreliable outcomes. Other exposure pathways of concern from a regulatory viewpoint include atmospheric deposition of CeO_2 and direct environmental exposure, such as CdSe NPs used in surface coatings and solar panels; however, research with relevant concentrations expected in the environment is necessary to make informed risk decisions and develop regulatory guidance. Much of the work to date on the evaluation of NP transformations has involved a variety of spectroscopic methods, including bulk x-ray absorption spectroscopy; however, a National Research Council report highlights the need for "greater spatial resolution and sensitivity to characterize and quantify [nanomaterials] at low environmental and *in vivo* concentrations." [52] The APS Upgrade will deliver exactly these needed capabilities.

Scientific Objectives

Imaging the 3D Distribution of Bacteria and Metabolic Function within Soil Pore Structure

The APS-U will allow high-resolution 3D imaging of bacterial communities coupled with their metabolic function in proximity to specific soil and pore structure. Soil microbes produce polysaccharides, acids, and other metabolites that can impact local water relations, glue soil minerals together, alter mineral surfaces, and affect the emission of carbon dioxide and methane into the atmosphere. At the same time, moisture gradients, redox conditions, nutrient concentrations, and gas fluxes produce a wide range of living conditions in soil pores,[53] leading to astounding genetic and functional diversity among soil microbes.[54] Three-dimensional imaging of bacteria and their metabolism within soil can enhance our understanding of the

terrestrial carbon cycle, nutrient availability to plants, contaminant remediation, and other ecosystem services.

Nanoparticles in the Environment: Investigating Real Concentrations and Transformation Products

The APS-U's increased brightness and coherence at high energy will dramatically improve detection sensitivity and spatial resolution to investigate ENMs at realistic concentrations in complex soil environments. Uncertainty persists about the potential implications of ENMs for consumers, workers, and ecosystems. Ecosystems are complex, heterogeneous natural systems consisting of biological, chemical, and physical properties influencing the fate, transport, and toxicity of NPs; however, our ability to probe the molecular-nano-meso continuum in heterogeneous media has limited our understanding of NPs in nature. Despite estimated knowledge of NP release concentrations, many research studies utilize concentrations 3 to 5 orders of magnitude higher than would be expected in the natural environment. Such concentrations can result in equilibrium scenarios far from reality, such as ZnO NPs causing phytotoxicity or agglomeration/precipitation of new phases due to solubility. Likewise, almost all regulatory and toxicological studies of NPs focus on the original, pristine material, not taking into account the multitude of research studies that indicate NPs will transform in the environment. Thus, perceived risk is based on the original material, not on the transformed by-product that results from environmental interaction.

Experimental Details

Imaging the 3D Distribution of Bacteria and Metabolic Function within Soil Pore Structure

Soil aggregates (0.1-1 mm in diameter) containing microorganisms with high-Z nanoscale elemental tags can presently be imaged in two dimensions with an x-ray nanoprobe via collection of transmission, fluorescence, and ptychographic data. We envision extending these datasets to three dimensions through application of next-generation tomographic techniques. The transmission data will provide the ability to image the soil pore structure while fluorescence data from the high-Z elemental tag will provide the ability to image the distribution of bacteria associated with the high-Z tag. Ptychographic data will provide the ability to image, with high spatial resolution, the inter- and intracellular biomineralization products resulting from microbial activity.

Nanoparticles in the Environment: Investigating Real Concentrations and Transformation Products

When real environmental concentrations are only a few parts per million or less, investigation requires high-resolution imaging and sensitivity over a large area to detect and determine the speciation of NPs in soils, sediments, biological organisms, and plants. As noted above, estimated exposure doses at present are often 3 to 5 orders of magnitude higher than predicted and measured, [55] which can result in unrealistic assessments of the impacts of NPs.[56] Studies that examine potential plant uptake of NPs from soil are of critical interest to several government agencies (USDA, FDA, USEPA) that are seeking to gauge risks and develop appropriate guidelines relative to human health. Land application of biosolids containing silver (Ag) and zinc oxide (ZnO) nanoparticles or diesel exhaust deposition of cerium oxide (CeO_2) may potentially be accumulated and taken up by edible crops. Of interest is the possible disruption

of nitrogen fixation by legumes caused by CeO_2. The scientific challenge also includes using hydrated plant samples and soil samples with sub-ppm concentrations of localized nanomaterials and submicron beam size for distribution of NPs, coupled with highly accurate positioning and stable detectors with fast readout. The study would need multi-modal, fast sampling to survey large areas with high resolution to find NPs, and then even higher-resolution distribution followed by spectroscopy to determine speciation–all while not damaging the sample, affecting redox, or introducing other potential artifacts.

6.3.D. Imaging Heterogeneous Materials and Interfaces in Natural Systems: Linking Molecular to Mesoscale Phenomena

Background and Motivation

The heterogeneity of natural materials presents an inherent challenge for understanding the structure and reactivity in Earth and environmental systems.[57,58] The current state of the art in geoscience studies has addressed this issue in two ways:

- The use of the present generation of synchrotron-based tools (e.g., x-ray diffraction and spectroscopy) to probe materials in microprobe and spatially-averaging modalities has enabled our understanding of the inherent heterogeneity of natural samples at micron lengths along with robust measurements of their spatially averaged molecular-scale behavior.[59] Such measurements probe the variation in elemental composition, oxidation states, and mineralogy, as well as the average size and distribution of particles and pores.
- Initial signs of future possibilities enabled by more advanced x-ray scattering techniques are available. For example, high-resolution interfacial studies at well-defined mineral-water interfaces (e.g., laterally homogeneous single-crystal surfaces) have demonstrated the ability to obtain a truly molecular-scale view of structure and reactivity, elucidating interfacial water organization, ion solvation/adsorption, growth, and dissolution.[59] These model studies, however, do not incorporate the full topological complexity of natural materials (e.g., rocks, soils) including the effects of confinement, interface curvature, or fluid flow patterns.

The broad separation of these two distinct modes of study is indicative of a significant gap in our understanding, dividing the meso- to macro-scale understanding of Earth materials from the ultimate molecular-scale behavior that can now only be understood with model materials (e.g., single crystals). Bridging this gap in our understanding is critical for establishing the scientific foundations for understanding the mobility and transport of elements in Earth's near-surface environment, and the control and management of subsurface porosity relevant to the production of energy (e.g., fracking, controlling porosity), as well as the sequestration of energy by-products (e.g., the geological storage of CO_2 and spent nuclear fuel).

The use of x-ray coherence opens a new opportunity to bridge between these two spatial regimes, so that a robust understanding of geomaterial reactivity can be obtained spanning from the nanoscale to the meso- and macroscales. Central to this pursuit is a new deterministic understanding of the reactivity of natural samples that will relate observed behavior to actual structures (e.g., pore throats of a particular dimension) instead of statistical measures of the

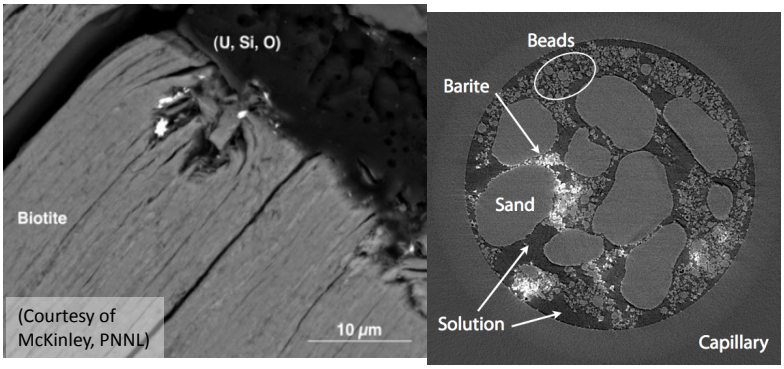

Fig. 7. Nucleation of (*left*) uranium precipitates in Hanford sediments and (*right*) barium sulphate within a simulated sandstone matrix (bright regions are the precipitates). Note the extreme spatial variation of the deposited material.[60]

structure (e.g., average pore sizes and pore-size distributions). It is widely observed, as shown in Fig. 7, that reactions in complex matrices proceed in a highly heterogeneously manner, but in a manner that is poorly understood.[60] That is, we do not understand the principles that govern the nucleation process in these materials, and in particular the contributing roles of confinement and fluid flow.

We can better understand the nucleation and evolution of reactions in complex matrices directly and in real-time using various forms of CDI, in both transmission[61, 62] and Bragg-CDI geometries,[63] and by using ptychographic imaging approaches that APS-U enables.[64,65] That is, we can observe the real-time, *in situ* evolution of heterogeneous reactivity in these systems, and relate specific reactions to structural features such as matrix strain, particle and pore sizes, and flow patterns to understand critical controls over elemental mobility in natural systems (e.g., as related to the sequestration of energy related by-products). Similar measurements also can be used to investigate NP structure and reactivity for a range of materials within their natural settings. Such observations, especially when coupled to parallel measurements of spatially resolved signals (e.g., fluorescence[66]) and through the use of larger-scale imaging modalities (i.e., tomographic approaches), will enable robust observations of structure and composition to provide a complete understanding of reactivity spanning length scales from nanometers to millimeters.

Scientific Objectives

The objective of this research is to understand the thermodynamic and kinetic controls over reactivity in geomaterials that exhibit significant heterogeneity in structure and composition. How do reactions take place in situations where interfacial energies are complex functions of the crystalline matrix orientation, composition, roughness, and curvature? The central theme is to enable observations that will reveal mineral-water reactivity in materials that are representative of those found in natural systems. Examples include confined fluids in nanoporous matrices; reactions at topographically rough surfaces; individual nanoparticle structure and reaction; the evolution of mineral morphology in the presence of externally applied stress (e.g., pressure solution); as well as the role of internal strain on reactivity (e.g., epitaxial strain associated with inter-particle interactions).

Experimental Details

The ability to image complex structures is enabled by the high x-ray beam coherence available with the APS-U. Of particular interest for this work is the use of hard x-rays (e.g., with photon energies in the range of 15 to 35 keV) that have sufficient penetration to probe structures for *in situ* observations. Given the broad range of interesting systems, we anticipate two general classes of measurements will be needed that will complement the currently available toolset (x-ray spectroscopy, microprobes, x-ray diffraction, and interfacial x-ray scattering), as follows:

Nanoprobe Imaging by Scanned Coherent Beams (Transmission Coherent Diffractive Imaging/Ptychography (CDI/P)): In such measurements, a coherent beam is raster-scanned across the sample in a manner that is similar to present microprobes. The transmitted beam is imaged by an area detector so that the local structure can be reconstructed within each beam illumination. The use of ptychographic imaging (i.e., using overlapping illuminated regions) enables vastly improved resolution with a reconstruction of the sample morphology having a resolution that is smaller than the beam size (ideally with few nm spatial resolution). When extended to tomographic modalities, such measurements can provide a full 3D image of the nano/micro porous matrix. Simultaneous measurements of secondary signals (e.g., x-ray fluorescence) coupled with the reconstruction of the beam profile enables the parallel reconstruction of the elemental- (and, in principle, oxidation-state-) specific distributions in the sample. Such measurements therefore have the ability to substantially enrich our understanding of reactions in heterogeneous materials, with a spatial resolution finer than can be currently achieved by microprobe systems. Tomographic reconstructions using incoherent illumination can be meshed with the smallest-scale images to extend this understanding to substantially larger (micrometer to millimeter) length scales.

Bragg-CDI/P: The internal strains within defective crystalline materials can be imaged using Bragg CDI/P. Here, the scattering intensity is measured near the Bragg peak of the material of interest, and structural distortions (e.g., lattice strain, morphology, and vacancies) are imaged through the shape of the near-Bragg diffraction pattern and its variation with beam position. Such measurements have the potential to extend the molecular-scale understanding that can be currently achieved only for single crystal mineral-water interfaces (i.e., with interfacial x-ray reflectivity) to more complex mineral topographies. In particular, such measurements can clarify the role of shape and strain on the reactivity of individual nanoparticles.

6.3.E. Unraveling Controls on Ocean Productivity by Trace Metal Micronutrients

Background and Motivation

The availability of trace metal micronutrients—such as iron, zinc, cobalt, and manganese—controls primary production (i.e., photosynthesis) in approximately 30% of the global ocean.[67, 68] Past variations in iron delivery to the ocean are thought to have contributed to glacial climate cycles over the past 800,000 years.[69] The cycling of metals on Earth fundamentally controls climate on a global scale, and metal fluxes to the ocean and atmosphere are complexly interrelated. Global iron budgets reflect land surface and dust availability, atmospheric aerosol loading, geologic fluxes, marine productivity, and climatic state.[70] For example, increased atmospheric aerosol loading can lead to increased marine productivity, which in turn can result

in lower CO_2 levels and a colder climate. Given likely variations in iron delivery and ocean nutrient cycling with changing climate conditions, it is critical to develop a mechanistic understanding of how competition for iron and other metals by ocean phytoplankton will alter marine productivity and the ocean's role in the global carbon cycle.

Scientific Objectives

One of the central parameters that must be experimentally constrained in order to create accurate ocean biogeochemical models are the metal contents, or quotas, of the dominant plankton groups in the ocean.[71] The vast majority of microbial ocean life cannot be cultured in the laboratory, so environmental measurements are necessary. But microbial diversity and the presence of co-occurring abiotic material severely limit the value of traditional elemental analysis approaches. High-brightness, micro-focused x-rays provide the only existing approach to measure metal quotas of ocean phytoplankton; over the past decade, many advances have been made using x-ray fluorescence microscopy.[72] However, the flux and focus of existing third-generation hard x-ray microprobe beamlines limit analyses to larger eukaryotic phytoplankton, leaving us largely ignorant of the metal contents and requirements of the smallest prokaryotes that dominate primary production in the vast mid-ocean gyres.

Experimental Details

Prochlorococcus is the most numerically abundant alga on Earth, responsible for almost 40% of the primary production in the tropical and sub-tropical oceans.[73] However, this keystone ocean species is too small (approximately 500 nm) to determine its metal content and distribution with existing capabilities. Present capabilities are likewise inadequate to study the heterotrophic bacteria, archaea, and viruses that dominate nutrient cycling and sub-surface biogeochemistry in the ocean. The APS Upgrade will provide order-of-magnitude increases in flux, accompanied by improved focused spot sizes, that will enable first-ever measurements of metals in representatives of the vast microbial ecosystems that largely control the metabolism of our planet.

Existing focused photon fluxes available at synchrotrons today require imaging dwell times of several seconds at each pixel for metal-poor cells from the open ocean – some of which may contain only a few thousand atoms of each metal per cell – resulting in extremely limited sample throughput. This severely limits the number and types of cells that can be analyzed, and hence the scientific questions that can be addressed with adequate statistical rigor. A 100- to 1,000-fold increase in the focal flux of nanoprobes will dramatically increase sample throughput and thereby open up entirely new avenues of research. Environmental single-cell metallomic analyses would be able to serve as needed complements to next-generation proteomic, transcriptomic, and metabollomic studies that are being developed to answer questions of plankton physiology, ecology, and ocean and global biogeochemistry. The techniques developed for this project, measuring metal content and speciation within oceanic single-cell organisms, will broadly impact similar studies by related user communities that require high-brightness fluorescence and spectroscopy beamlines to understand metal cycling on a global scale. This includes analysis of deep-sea hydrothermal plume particles that are known to sequester seawater trace elements and influence ocean-scale biogeochemical budgets [74] and analysis of metals bound to fine- and ultrafine particles in aerosol samples.[75, 76]

6.4 Operational and Instrumentation Needs

For the scientific community to successfully conduct the new E^3 experiments described here, the successful implementation of a new MBA lattice storage ring at the APS is clearly key. Yet it is also clear that these studies using the APS-U require development and implementation of optimized timing modes, high-resolution beamline optics, high-precision energy scanning capabilities, and advanced detector systems.

The operational needs for the proposed high-pressure experiments require a superconducting insertion device that can provide high-brightness, high-energy x-rays, preferably in the range from 30 to 80 keV, with capabilities for sub-micron focusing at all wavelengths and ultimate focusing down to 100 to 200 nm. (The focal flux and other parameters of high-photon energy focused x-rays beams are described in detail in the Operational Needs section of the Mesoscale Engineering and Advanced Materials chapter.)

For Mössbauer spectroscopy of iron, tin, europium, and dysprosium an appropriate time structure is essential. A fast chopper can, in principle, enable the use of non-singlet time structures, but this will require significant further development. Experience at several present-generation synchrotron lightsources suggests the capabilities for frontier extreme conditions science is optimized by development of high-pressure cells in parallel with source conceptualization, design, and construction. This tradition will continue, and accelerate, over the period prior to the APS-U.

The proposed x-ray fluorescence and x-ray spectroscopy experiments described for cosmochemical and environmental sciences require undulator insertion device sources that can provide x-rays in the range from 2.3-20 keV with 100-nm achromatic focusing at all energies. A critical requirement is positional stability between the sample and x-ray beam at the 10 nm scale as the undulator and monochromator (Si 111 and Si 311) are scanned in unison over 1 keV. Significant advances are being made in focusing hard x-rays to sub-30 nm spots using diffractive optics. Achromatic focusing to extend x-ray absorption studies to the highest spatial resolutions requires new beamline designs that incorporate new state-of-the-art reflective x-ray focusing mirrors. New undulator designs that can rapidly scan gaps synchronous to the monochromator are required. Maintaining the required spatial registry during energy scanning becomes exceedingly difficult as spot size decreases. For detection, a multichannel, energy-dispersive detector is required with the highest possible output count-rate capability, of at least several Mcps.

The improved brightness provided by the APS Upgrade may allow high-resolution x-ray emission spectroscopy techniques, currently only accessible in exceptionally difficult experiments, to become more routinely applicable for the spectroscopic analyses described. Such methodologies can potentially yield speciation information analogous to that provided by x-ray absorption spectroscopies, including chemical/spin state determination, but without scanning the energy of the incident x-ray beam. Optimal use of emission spectroscopy requires new high-energy resolution XRF detectors with resolutions of on the order of 1 eV at 6 keV. Coupled to the high brightness provided by APS-U, such detectors would allow determination of chemical state information for all elements in an illuminated spot simultaneously. Experiments today rely on crystal analyzers that have low efficiency, that are slow and photon

flux-limited, and that can only measure one element at a time. Recent developments at APS and NIST with superconducting XRF detectors promise 1-eV resolution at count rates up to 10^5 Hz. Coupled with a high-flux, reflective-mirror based nanobeam beam from the APS-U, this will allow chemical state determination for multiple elements simultaneously, without moving anything, and analyses that are much less susceptible to radiation damage.

For the described studies of ENM's in the environment and marine organisms there are additional requirements that data will need to be collected in a high-throughput fashion to enable measurement of a large number of samples to provide statistically significant experimental results and to reduce x-ray exposure to the samples which may be sensitive to radiation damage. These experiments are expected to generate many terabytes of data daily. Therefore, infrastructure to handle these massive datasets will be needed. Similarly, near-real-time reconstruction of the tomographic data will be necessary to provide feedback to the experimentalists during their experiments so that they can optimize their productivity during beam runs.

The proposed experiments studying heterogeneous interfaces in natural systems require an insertion device that can provide coherent, hard x-ray beams (photon energies of 15 to 35 keV) with the ability to control the beam footprint on the sample, area detectors, as well as sample environmental control (air, fluids, pressure, and temperature). The measurements require the robust use of coherent x-ray beams with controlled illumination area, beam divergence and photon energy. The instrumentation needs may be distinct for the transmission- and Bragg-CDI/P measurements. While the former requires the ability to illuminate a sample with nm-precision while measuring transmitted beams, the latter also requires precision angular manipulation of the sample (i.e., to perform rocking curves of the Bragg reflection) while measuring the Bragg-reflected beam. This will likely involve substantial improvements over current facilities. Also, the use of high energy density beams in such measurements for *in situ* environments will perturb the sample (e.g., through photon-induced radical species, especially for *in situ* observations in the presence of fluids), and a concerted research program to understand and control such perturbations will be needed to avoid imaging artifacts.

6.5 References

[1] Image adapted from NASA, earthobservatory.nasa.gov.

[2] Image adapted from Marcellus Center for Outreach and Research, http://www.marcellus.psu.edu/resources/maps.php.

[3] P. Wood, GEOExPro, **10**, 18 (2013).

[4] C. Park, P A. Fenter, K. L. Nagy, and N. C. Sturchio, Phys. Rev. Lett. **97**, 016101 (2006).

[5] J. Hemminger, G. Crabtree, and J. Sarrao, Rep. Basic Energy Sci. Advis. Comm. Tech. 1601 (2012).

[6] S. M. Benson, W. Chandler, J. Edmonds, J. Houghton, M. Levine, L. Bates, H. Chum, J. Dooley, D. Grether, J. Logan, G. Wiltsee, and L. Wright, "*Assessment of Basic Research Needs for Greenhouse Gas Control Technologies*," Lawrence Berkeley National Laboratory, LBNL-42398 (1998).

[7] D. J. DePaolo, and F. M. Orr, "*Basic Research Needs for Geosciences: Facilitating 21st Century Energy Systems*," U.S. Department of Energy, Office of Basic Energy Sciences (2007).

[8] J. C. S. Long and R. C. Ewing, Annu. Rev. Earth Pl. Sc. **32**, 363 (2004).

[9] A. Vengosh, N. Warner, R. Jackson, and T. Darrah, Proc. Earth Pl. Sc. **7**, 863 (2013).

[10] C. A. Goodrich, S. R. Sutton, S. Wirick, and M. J. Jercinovic, Geochim. Cosmochim. Ac. **122**, 280 (2013).

[11] P. Fenter, C. Park, Z. Zhang, and S. Wang, Nat. Phys. **2**, 700 (2006).

[12] M. Schmidt, S. S. Lee, R. E. Wilson, K. E. Knope, F. Bellucci, P. J. Eng, J. E. Stubbs, L. Soderholm, and P. Fenter, Environ. Sci. Technol. **47**, 14178 (2013).

[13] M. V. Holt, S. O. Hruszkewycz, C. E. Murray, J. R. Holt, D. M. Paskiewicz, and P. H. Fuoss, Phys. Rev. Lett. **112**, 165502 (2014).

[14] S. O. Hruszkewycz, M. V. Holt, D. L. Proffit, M. J. Highland, A. Imre, J. Maser, J. A. Eastman, G. R. Bai, and P. H. Fuoss, AIP Conf. Proc. **1365**, 235 (2011).

[15] C. I. Steefel, D. J. DePaolo, and P. C. Lichtner, Earth Planet. Sc. Lett. **240**, 539 (2005).

[16] P. G. Falkowski, T. Fenchel, and E. F. Delong, Science **320**, 1034 (2008).

[17] L. Dubrovinsky, N. Dubrovinskaia, V. B. Prakapenka, and A. M. Abakumov, Nat. Comm. **3**, 1163 (2012).

[18] H. K. Mao, R. J. Hemley, L. C. Chen, J. F. Shu, L. W. Finger, and Y. Wu, Science **246**, 649 (1989).

[19] J. M. Jackson, W. Sturhahn, M. Lerche, J. Zhao, T. S. Toellner, E. E. Alp, S. V. Sinogeikin, J. D. Bass, C. A. Murphy, and J. K. Wicks, Earth Planet. Sc. Lett. **362**, 143 (2013).

[20] T. S. Toellner, E. E. Alp, T. Graber, R. W. Henning, S. D. Shastri, G. Shenoy, and W. Sturhahn, J. Synchrotron Radiat. **18**, 183 (2011).

[21] S. Anzellini, A. Dewaele, M. Mezouar, P. Loubeyre, and G. Morard, Science **340**, 464 (2013).

[22] C. A. Murphy, J. M. Jackson, and W. Sturhahn, J. Geophys. Res.-Sol. Ea. **118**, 1999 (2013).

[23] W. Sturhahn and J. M. Jackson, Geol. S. Am. S. **421**, 157 (2007).

[24] J. K. Wicks, J. M. Jackson, and W. Sturhahn, Geophys. Res. Lett. **37**, L15304 (2010).

[25] D. Zhang, J. M. Jackson, J. Zhao, W. Sturhahn, E. E. Alp, T. S. Toellner, and M. Y. Hu, Rev. Sci. Instrum. **86**, 013105 (2015).

[26] M. I. Eremets and I. A. Troyan, Nat. Mater. **10**, 927 (2011).

[27] C.-S. Zha, R. E. Cohen, H.-K. Mao, and R. J. Hemley, P. Natl. Acad. Sci. USA **111**, 4792 (2014).

[28] C.-S. Zha, Z. Liu, M. Ahart, R. Boehler, and R. J. Hemley, Phys. Rev. Lett. **110**, 217402 (2013).

[29] R. T. Howie, C. L. Guillaume, T. Scheler, A. F. Goncharov, and E. Gregoryanz, Phys. Rev. Lett. **108**, 125501 (2012).

[30] R. A. Fischer, Y. Nakajima, A. J. Campbell, D. J. Frost, D. Harries, F. Langenhorst, N. Miyajima, K. Pollok, and D. C. Rubie, Geochim. Cosmochim. Acta **167**, 177 (2015).

[31] Y. Amelin, A. N. Krot, I. D. Hutcheon, and A. A. Ulyanov, Science **297**, 1678 (2002).

[32] K. D. McKeegan and A. M. Davis, Treatise Geochem. **1**, 431 (2003).

[33] G. J. MacPherson, Treatise Geochem. **1**, 201 (2003).

[34] D. S. Ebel, Meteor. Early Sol. Syst. II **1**, 253 (2006).

[35] H. C. Connolly Jr, in "*Chondrites and the Protoplanetary Disk*," A. N. Krot, E. R. D. Scott, and B. Reipurth, eds., Astronomical Society of the Pacific (2005), p. 215.

[36] S. B. Simon, A. M. Davis, L. Grossman, and K. D. McKeegan, Meteorit. Planet. Sci. **37**, 533 (2002).

[37] C. A. Goodrich, S. R. Sutton, S. Wirick, and M. J. Jercinovic, Geochim. Cosmochim. Acta **122**, 280 (2013).

[38] D. Brownlee, P. Tsou, J. Aléon, C. M O'd Alexander, T. Araki, S. Bajt, G. A Baratta, R. Bastien, P. Bland, P. Bleuet, J. Borg, J. P Bradley, A. Brearley, F. Brenker, S. Brennan, J. C Bridges, N. D Browning, J. R Brucato, E. Bullock, M. J Burchell, H. Busemann, A. Butterworth, M. Chaussidon, A. Cheuvront, M. Chi, M. J. Cintala, B. C. Clark, S. J Clemett, G. Cody, L. Colangeli, G. Cooper, P. Cordier, C. Daghlian, Z. Dai, L. D'Hendecourt, Z. Djouadi, G. Dominguez, T. Duxbury, J. P Dworkin, D. S Ebel, T. Economou, S. Fakra, S. A. J. Fairey, S. Fallon, G. Ferrini, T. Ferroir, H. Fleckenstein, C. Floss, G. Flynn, I. A. Franchi, M. Fries, Z. Gainsforth, J.-P. Gallien, M. Genge, M. K. Gilles, P. Gillet, J. Gilmour, D. P. Glavin, M. Gounelle, M. M. Grady, G. A Graham, P. G. Grant, S. F Green, F. Grossemy, L. Grossman, J. N Grossman, Y. Guan, K. Hagiya, R. Harvey, P. Heck, G. F. Herzog, P. Hoppe, F. Hörz, J. Huth, I. D. Hutcheon, K. Ignatyev, H. Ishii, M. Ito, D. Jacob, C. Jacobsen, S. Jacobsen, S. Jones, D. Joswiak, A. Jurewicz, A. T. Kearsley, L. P. Keller, H. Khodja, A. L. D. Kilcoyne, J. Kissel, A. Krot, F. Langenhorst, A. Lanzirotti, L. Le, L. A. Leshin, J. Leitner, L. Lemelle, H. Leroux, M.-C. Liu, K. Luening, I. Lyon, G. Macpherson, M. A Marcus, K. Marhas, B. Marty, G. Matrajt, K. McKeegan, A. Meibom, V. Mennella, K. Messenger, S. Messenger, T. Mikouchi, S. Mostefaoui, T. Nakamura, T. Nakano, M. Newville, L. R Nittler, I. Ohnishi, K. Ohsumi, K. Okudaira, D. A. Papanastassiou, R. Palma, M. E. Palumbo, R. O. Pepin, D. Perkins, M. Perronnet, P. Pianetta, W. Rao, F. J. M. Rietmeijer, F. Robert, D. Rost, A. Rotundi, R. Ryan, S. A. Sandford, C. S. Schwandt, T. H. See, D. Schlutter, J. Sheffield-Parker, A. Simionovici, S. Simon, I. Sitnitsky, C. J. Snead, M. K. Spencer, F. J. Stadermann, A. Steele, T. Stephan, R. Stroud, J. Susini, S. R. Sutton, Y. Suzuki, M. Taheri, S. Taylor, N. Teslich, K. Tomeoka, N. Tomioka, A. Toppani, J. M. Trigo-Rodríguez, D. Troadec, A. Tsuchiyama, A. J. Tuzzolino, T. Tyliszczak, K. Uesugi, M. Velbel, J. Vellenga, E. Vicenzi, L. Vincze, J. Warren, I. Weber, M. Weisberg, A. J. Westphal, S. Wirick, D. Wooden, B. Wopenka, P. Wozniakiewicz, I. Wright, H. Yabuta, H.

Yano, E. D. Young, R. N. Zare, T. Zega, K. Ziegler, L. Zimmerman, E. Zinner, and M. Zolensky, Science **314**, 1711 (2006).

[39] L. Grossman, Geochim. Cosmochim. Acta **36**, 597 (1972).

[40] K. Lodders, Astrophys. J. **591**, 1220 (2003).

[41] NASA optical micrograph.

[42] S. B. Simon, D. J. Joswiak, H. A. Ishii, J. P. Bradley, M. Chi, L. Grossman, J. Aléon, D. E. Brownlee, S. Fallon, and I. D. Hutcheon, Meteorit. Planet. Sci. **43**, 1861 (2008).

[43] S. B. Simon, S. R. Sutton, and L. Grossman, Geochim. Cosmochim. Acta **71**, 3098 (2007).

[44] R. Hooke, "*Micrographia*," James Alleftry, London (1665).

[45] M. Vos, A. B. Wolf, S. J. Jennings, and G. A. Kowalchuk, FEMS Microbiol. Rev. **37**, 936 (2013).

[46] T. Rennert, K. U. Totsche, K. Heister, M. Kersten, and J. Thieme, J. Soil. Sediment. **12**, 3 (2012).

[47] S. W. Rogers, T. B. Moorman, and S. K. Ong, Soil Sci. Soc. Am. J. **71**, 620 (2007).

[48] K. M. Kemner, W. Yun, Z. Cai, B. P. Lai, H.-R. Lee, D. G. Legnini, W. Rodrigues, J. D. Jastrow, R. M. Miller, S. T. Pratt, M. A. Schneegurt, C. F. Kulpa, Jr., and A. J. M. Smucker, SPIE Proc. Ser. **3449**, 45 (1998).

[49] I. M. Young and J. W. Crawford, Science **304**, 1634 (2004).

[50] V. L. Bailey, L. A. McCue, S. J. Fansler, M. I. Boyanov, F. DeCarlo, K. M. Kemner, and A. Konopka, Soil Biol. Biochem. **65**, 60 (2013).

[51] J. Unrine, P. Bertsch, and S. Hunyadi, in "*Nanoscience and Nanotechnology: Environmental and Health Impacts*," edited by V. H. Grassian, John Wiley & Sons, Inc. (2008), 345.

[52] National Research Council, "*Research Progress on Environmental, Health, and Safety Aspects of Engineered Nanomaterials*," The National Academies Press (2013).

[53] I. M. Young, J. W. Crawford, N. Nunan, W. Otten, and A. Spiers, Adv. Agron. **100**, 81 (2008).

[54] N. Fierer, M. Breitbart, J. Nulton, P. Salamon, C. Lozupone, R. Jones, M. Robeson, R. A. Edwards, B. Felts, and S. Rayhawk, Appl. Environ. Microbiol. **73**, 7059 (2007).

[55] E. Lombi, E. Donner, E. Tavakkoli, T. W. Turney, R. Naidu, B. W. Miller, and K. G. Scheckel, Environ. Sci. Technol. **46**, 9089 (2012).

[56] J. H. Priester, Y. Ge, R. E. Mielke, A. M. Horst, S. C. Moritz, K. Espinosa, J. Gelb, S. L. Walker, R. M. Nisbet, and Y.-J. An, P. Natl. Acad. Sci. USA **109**, E2451 (2012).

[57] W. Stumm, "*Chemistry of the Solid-Water Interface*," John Wiley & Sons, Inc. (1992).

[58] G. E. Brown, V. E. Henrich, W. H. Casey, D. L. Clark, C. Eggleston, A. Felmy, D. W. Goodman, M. Grätzel, G. Maciel, and M. I. McCarthy, Chem. Rev. **99**, 77 (1999).

[59] See for example, "*Applications of Synchrotron Radiation in Low-Temperature Geochemistry and Environmental Science*," P. Fenter, M. Rivers, N. C. Sturchio and S. Sutton, eds., Rev. Mineralogy and Geochem. **49**, Geochemical Soc. (2002).

[60] J. McKinley, private communication (2015).

[61] J. Miao, T. Ishikawa, T. Earnest, and Q. Shen, Ann. Rev. Phys. Chem. **59**, 387 (2008).

[62] H. N. Chapman, A. Barty, S. Marchesini, A. Noy, S. P. Hau-Riege, C. Cui, M. R. Howells, R. Rosen, H. He, J. C. Spence, U. Weierstall, T. Beetz, C. Jacobsen, and D. Shapiro, J. Opt. Soc. Am. A **23**, 1179 (2006).

[63] R. Harder, M. Liang, Y. Sun, Y. Xia, and I. K. Robinson, New J. Phys. **12**, 035019 (2010).

[64] J. M. Rodenburg, A. C. Hurst, A. G. Cullis, B. R. Dobson, F. Pfeiffer, O. Bunk, C. David, K. Jefimovs, and I. Johnson, Phys. Rev. Lett. **98**, 034801 (2007).

[65] H. M. L. Faulkner and J. M. Rodenburg, Phys. Rev. Lett. **93**, 023903 (2004).

[66] J. Deng, D. J. Vine, S. Chen, Y. S. G. Nashed, Q. Jin, N. W. Phillips, T. Peterka, R. Ross, S. Vogt, and C. Jacobsen, Proc. Natl. Acad. Sci. USA **112**, 2314 (2015).

[67] C. M. Moore, M. M. Mills, K. R. Arrigo, I. Berman-Frank, L. Bopp, P. W. Boyd, E. D. Galbraith, R. J. Geider, C. Guieu, and S. L. Jaccard, Nat. Geosci. **6**, 701 (2013).

[68] J. K. Moore, S. C. Doney, D. M. Glover, and I. Y. Fung, Deep-Sea Res. Pt. II **49**, 463 (2001).

[69] A. Martínez-García, D. M. Sigman, H. Ren, R. F. Anderson, M. Straub, D. A. Hodell, S. L. Jaccard, T. I. Eglinton, and G. H. Haug, Science **343**, 1347 (2014).

[70] T. D. Jickells, Z. S. An, K. K. Andersen, A. R. Baker, G. Bergametti, N. Brooks, J. J. Cao, P. W. Boyd, R. A. Duce, and K. A. Hunter, Science **308**, 67 (2005).

[71] B. S. Twining and S. B. Baines, Ann. Rev. Mar. Sci. **5**, 191 (2013).

[72] B. S. Twining, S. B. Baines, N. S. Fisher, J. Maser, S. Vogt, C. Jacobsen, A. Tovar-Sanchez, and S. A. Sañudo-Wilhelmy, Anal. Chem. **75**, 3806 (2003).

[73] Z. I. Johnson, E. R. Zinser, A. Coe, N. P. McNulty, E. Malcolm S. Woodward, and S. W. Chisholm, Science **311**, 1737 (2006).

[74] J. A. Breier, B. M. Toner, S. C. Fakra, M. A. Marcus, S. N. White, A. M. Thurnherr, and C. R. German, Geochim. Cosmochim. Acta **88**, 216 (2012).

[75] S. Utsunomiya, K. A. Jensen, G. J. Keeler, and R. C. Ewing, Environ. Sci. Technol. **36**, 4943 (2002).

[76] S. Utsunomiya, K. A. Jensen, G. J. Keeler, and R. C. Ewing, Environ. Sci. Technol. **38**, 2289 (2004).

7 Frontiers of Condensed Matter Physics

Oleg Shpyrko, *University of California, San Diego*
John W. Freeland, *Argonne National Laboratory*

Daniel Haskel, John F. Mitchell, Jonathan Logan, Ian McNulty, G. Brian Stephenson, Haidan Wen, *Argonne National Laboratory*; Chris Marianetti, *Columbia University*; Steven May, *Drexel University*; N. Peter Armitage, *Johns Hopkins University*; Stephen D. Kevan, *Lawrence Berkeley National Laboratory*; Rafael Jaramillo, *Massachusetts Institute of Technology*; Mark Sutton, *McGill University*; N. Laanait, *Oak Ridge National Laboratory*; Luc Patthey, *Paul Scherrer Institute;* Vladimir Stoica, *Pennsylvania State University;* Richard Averitt, *University of California, San Diego*; Jordi Cabana, *University of Illinois at Chicago*; Robert Maass, *University of Illinois at Urbana-Champaign*; Gang Cao, *University of Kentucky*; Gregory Fiete, *University of Texas at Austin*; Paul G. Evans, *University of Wisconsin-Madison*;

7.1 Executive Summary

Condensed matter physics is fundamentally a quest to create and to test quantitative models for explaining and controlling the behavior of large ensembles of atoms and electrons. In the most scientifically and technologically compelling cases, these elementary building blocks of matter act not as individuals but rather as entangled collectives that evolve together to express many familiar cooperative phenomena, such as magnetism, superconductivity, and ferroelectricity. These cooperative behaviors are a manifestation of emergence, referring to the complex, dynamic, many-body states that materialize from an ensemble of quantum mechanical particles. Such emergent phenomena comprise a major focus of the challenges in condensed matter physics for which the APS-U will have the greatest impact.

Emergence is the process by which individual particles cooperate, becoming linked together across lengthscales and timescales characteristic of their underlying many-body forces. Emergence can be familiar. In ferromagnets, for example, magnetism emerges from a random collection of electron spins (a paramagnet) when the exchange interaction among them is strong enough to overcome the disordering effects of temperature. More importantly, emergence lies at the frontier of new physics: A magnetic skyrmion emerges as a topological defect in an antiferromagnet under the influence of spin-orbit coupling,[1] potentially opening a route to low-power information technologies beyond silicon. Recently discovered Weyl fermions behave as massless quasiparticles, a missing link foundational to quantum field theory.[2] When compressed to 150 GPa, gaseous H_2S, becomes a superconducting solid.[3] With a world-record T_c = 203 K, well beyond that of other "conventional" phonon-mediated

superconductors, H_2S again raises the possibility of room-temperature lossless power transmission.

Condensed matter physics asks what lies behind emergent phenomena such as these: What are the microscopic drivers for collective, mesoscale behavior? What causes the atoms and electrons to function cooperatively? And can we control these phenomena? The attention of condensed matter physicists has rightfully focused on competing interactions and frustration as conceptual organizing frameworks with which to address these challenges. By carefully choosing crystal structure or elemental composition, vastly different and competing phases (e.g., metallic and insulating) can be brought to near degeneracy, and the ground state balance can be tipped by small perturbations including magnetic field, temperature, and pressure. Similarly, by creating lattice geometries that confuse the interactions among spins so that long-range magnetic order is frustrated, exotic spin-liquid states can be preserved that can shed light on problems from magnetic monopoles to quantum computers.

But several persistent questions remain: How do the competing or frustrated phases grow? What controls the lengthscales and timescales of emergent matter? In what ways does imperfection influence the outcome of phase competition? Discovering and exploiting the new rules under which collective states of matter self-organize, how they reconfigure, and how they respond to their environment defines a central intellectual challenge of condensed matter physics today and inspires pathways to a host of future technological breakthroughs in energy and information technology. This is the landscape in which the APS-U, with its unprecedented ability to explore spin, charge and lattice correlations in small, inhomogeneous samples, under complex environments or extreme conditions, will play a foundational role in charting the course of condensed matter physics.

7.2 New Opportunities in Condensed Matter Physics at APS-U

The APS-U will open new windows on emergent phenomena in condensed matter physics by offering capabilities anchored by dramatically enhanced coherent x-ray flux and high photon energy. With these advances, it will become possible to explore small, heterogenous sample regions, to penetrate complex environments, and to decode the self-organization and spatio-temporal characteristics of complex and competing phases. For instance, the search for quantum spin liquids, lattices decorated by spin-1/2 ions that escape long-range order due to geometric frustration, can be accelerated by using extreme conditions such as pressure to modify competing magnetic exchange pathways. Small samples, complex environments, and the weak magnetic scattering inherent to spin-1/2 systems are challenges to such experiments that will be addressed by the advances that the APS-U brings.

As another example, we hypothesize today that nanoscale separation of charges leads to the dramatic susceptibility of complex transition metal oxides to weak perturbations such as field and pressure, but the challenge remains to systematically follow the creation and evolution of such structures. Nanofocused beams from the APS-U with 100 to 1,000 times the intensity of the current APS will bring such features into focus, shedding light on emerging phases in frustrated quantum magnets (e.g., iridates) and in charge- and orbital-ordered magnetic oxides.

Importantly, APS-U will enable exploration of the hidden excitations, or fluctuations, of these nanoscale features, allowing quantitative understanding and model-building of the emergence, stability, and evolution of these and related quantum phases. Directly accessing fluctuations in a highly local fashion, with nanoscale sensitivity, is a major scientific problem that coherent x-ray scattering, including XPCS, can solve. The 100-to-1,000-fold increase in coherent x-ray flux at the APS Upgrade will result in a more than 10,000-fold increase in the fluctuation timescales accessible with XPCS, resulting in sub-microsecond temporal resolution. While extremely challenging technically, it also is possible that some experiments can achieve measurements of correlations probed by two sequential pulses, i.e., at 100-ns timescales, or even within a correlation time corresponding to the duration of just a single bunch.

With intense coherent x-ray beams, the role of imperfections and interfaces can be explored at a far more fundamental level. Until recently, condensed matter physics owed its remarkable success to a hypothesis of perfection, i.e., that ideal crystalline lattices with idealized electronic structures tied to the atomic arrangement were the key to novel and potentially useful phenomena. Physicists now must go further to embrace the absence of perfection, such as the role of defects within and interfaces between emergent phases, and to recognize that these deviations from order are intrinsic tools both for probing and for manipulating the underlying physics. The vastly enhanced microscopy and XPCS capabilities foundational to the APS-U will unravel how chemical or electronic inhomogeneity influence emergent behavior by mapping the three-dimensional distribution of structural and electronic features and will probe their dynamics and response functions. The nano- to micrometer lengthscale, i.e., the mesoscale gap, is the crucial and most difficult lengthscale for these studies, and the one that will be addressed by the APS-U.

The descriptions in this chapter of early condensed matter physics activities at the APS-U are intended to inspire the kinds of questions, systems, and approaches that will be well-matched to the new capabilities of the APS-U. Here we highlight three examples of challenging and important problems:

1) *Quantum Phases under Extreme Conditions*: The recent identifications of quantum magnetism and signatures of possible superconductivity in iridates have opened many questions about the underlying physics of these materials. Of particular interest is whether quantum phases, including a quantum spin liquid, can be discovered and tuned. Novel experimental tools are emerging to do this via fine-tuning the free-energy landscape using pressure. The APS-U will enable the extension of coherent x-ray techniques to move beyond simply measuring structure and allow visualization of ordered phases via resonant techniques.

2) *Fluctuations in Correlated Electron Systems*: The inhomogeneity of correlated electron systems has long been recognized as having an extremely important role in determining their properties. At the shortest lengthscales, this randomness is beginning to be understood, such as the key role that chemical doping plays in the development of new ordered phases. At larger scales, however, the evolution of electronic and magnetic phases is spontaneous and exhibits long-range. The APS-U will allow the fluctuations of correlated systems to be fully explored using hard x-ray coherent scattering.

3) *Dynamic Control of Novel Ferroelectric Polarization States*: As our understanding of condensed matter evolves, it becomes possible to drive these systems far from equilibrium in specific ways to seek out new phases. External optical, chemical, electric, and magnetic driving forces, among others, can drive matter into states that are not stable in thermodynamic equilibrium. Once discovered, such phases can in principle be stabilized using doping, pressure, or synthetic thin-film heterostructures. The latter strategy is particularly important in ferroelectrics and other materials that have wide potential applications in the form of thin films. The case of ferroelectrics is highlighted below, spurred by the recent discovery that one can stabilize ferroelectric flux closure states, which are often seen in magnetic systems but which have only recently been observed in ferroelectric heterostructures.[4] The average dynamics of these states can be probed with present techniques, but little is known about their microscopic dynamics.[5] With the APS-U, the nanoscale dynamics and non-equilibrium states of ferroelectric vortices can be probed and used to design new materials and devices.

7.3 Early Condensed Matter Physics Experiments at APS-U

7.3.A. Quantum Phases of Magnetic Iridates under Extreme Conditions

Background and Motivations

Theory predicts that many emergent phases of matter are accessible by tuning the interaction of electron correlations (U) and the spin-orbit interaction (λ).[6] Furthermore, if the quantum states possess a topological property, the states of matter are distinguished not only by their broken symmetries but also by mathematical structures in their wave functions. With this insight, there is tremendous interest in insulating quantum magnets (systems with local magnetic moments) that do not order at zero temperature. In some systems, instead of reaching ordered magnetic states, the stable low temperature state is thought to be a quantum spin-liquid (QSLs).[7,8] In analogy to a structural liquid phase, these systems are distinguished by possessing dynamic short-range magnetic correlations but no long-range order. The key is that the spin 1/2 moment of the ions enables unusual quantum phenomena such as Majorana fermions and fractional statistics to emerge. To date, however, there is no definitive discovery of such a quantum spin liquid; given questions of how to define and measure such correlations together with the lack of conventional order, unambiguous identification remains a critical experimental challenge.

While geometrical frustration of exchange interactions in triangular and Kagome lattices containing 3d transition metals have been heavily studied for their potential to harbor quantum spin liquid ground states, recent attention has expanded to iridium-oxide 5d transition metal oxides, known as iridates. In the iridium oxides, the large spin-orbit interaction intrinsic to the j_{eff}=1/2 state of Ir^{4+} introduces bond-directional magnetic anisotropy as an alternative route to magnetic frustration on specific lattices with three-fold symmetric nodes, such as the honeycomb lattice.[6] When only bond-directional magnetic interactions are considered in the honeycomb lattice, a spin-liquid ground state should emerge as a result of multiple configurations presented to each individual spin.[9] The spin at any honeycomb lattice site can

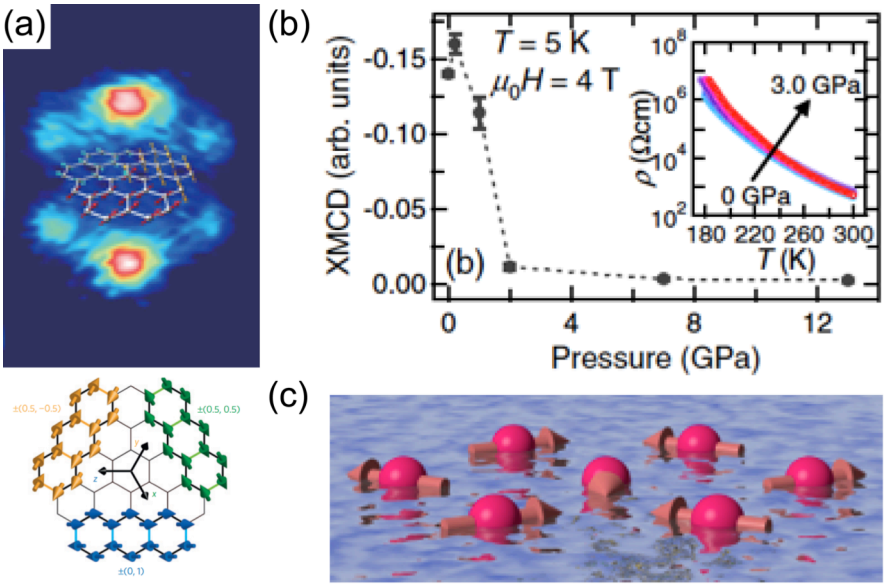

Fig. 1. (a) X-ray resonant magnetic scattering from zig-zag magnetic domains in Na_2IrO_3 above its ordering temperature. (b) Suppression of magnetic ordering with pressure in Li_2IrO_3. (c) Schematic of quantum spin liquid.[11]

point along any one of the three bond directions, and there are thus six possible configurations of "up" and "down" spins.

The experimental realization of such a Kitaev spin liquid remains elusive because other, competing exchange mechanisms between spins can lift the macroscopic degeneracy. The honeycomb-lattice oxide Na_2IrO_3 comes close to a spin-liquid state, but instead it orders below 13 K and adopts a "zig-zag" magnetic structure as a result of isotropic exchange interactions.[10] Diffuse x-ray resonant magnetic scattering studies above the magnetic ordering temperature, however, reveal the presence of three symmetry-related magnetic domains with nanoscale correlations indicating strong entanglement between spins and lattice and the dominance of

bond-directional Kitaev exchange interactions, as in Fig. 1.[11] Pressure can be used to tune exchange interactions and possibly drive the honeycomb system into a spin-liquid state. Indeed, recent x-ray magnetic circular dichroism experiments in the related Li_2IrO_3 hyper-honeycomb structure show collapse of magnetic order under pressure but do not yet offer proof for the existence of the quantum spin liquid.[12]

More generally, understanding the magnetism of the iridates provides insight into a class of materials in which there is a rapid pace of discovery. The layered iridates offer potential new phases besides the QSL states. Magnetism disappears when doping with impurities, creating either holes or electrons, accompanied by a simultaneous insulator to metal transition.[13,14] Given the similarities with cuprates in the magnetic excitation spectra,[15] there have been several predictions of a superconducting phase with high doping concentrations.[16,17,18,19] To overcome the challenge of doping by chemical means,[20] which has proved challenging beyond concentrations of approximately 10%, recent photoemission experiments have used dosing with alkali metals to push to large electron doping levels at the surface. At this doping level, there are clear cuprate-like Fermi arcs in the band structure,[21] although there has been some debate over the interpretation.[22] Recently, an extension of these experiments showed the

opening of a gap with d-wave symmetry at low temperatures;[23] while this does not constitute direct proof of superconductivity, it is certainly strongly suggestive and consistent with predictions. Probing the possible QSL state, as described in detail below, is a key step toward understanding the superconducting phase, since theory has highlighted the fluctuating magnetism as crucial to the pairing mechanism.

Scientific Objectives

The APS Upgrade presents unique opportunities to study the frustration of magnetic interactions and to use pressure, rather than chemical doping alone, as an additional means to drive frustrated systems into either fully ordered or disordered states, including the possible emergence of the long-sought-after spin-liquid states and associated new electronic phases. It is equally interesting to drive these spin-liquid phases by doping or external forces and attempt to discover new emergent phases, such as high-temperature superconductivity. The iridates are only one example of the many materials that can be expected to demonstrate new phases under pressure and for which precise new probes can provide answers to these fundamental questions.

Experimental Details

In the example of Li_2IrO_3, shown above in Fig. 1, pressure leads to the disappearance of magnetic order, but little is known about the nature of the high-pressure phase. Preliminary scattering evidence shows that the high-pressure phase exhibits residual magnetic order, even at the highest pressures reached in experiments to date. The important question to be answered now is whether there exist liquid-like correlations and fluctuations in this state of quenched magnetism. In liquids, such correlations will display a local antiferromagnetic (AFM) arrangement, as in Fig. 1, but are inherently dynamic and thus can be probed through XPCS techniques using magnetic resonant scattering contrast. The resulting temporal signatures of the magnetic fluctuations can be compared directly with theory, which can predict how the fluctuations evolve during the collapse of magnetic order. In the case of the QSL, there are clear predictions for how the quantum nature of the fluctuations will manifest.[24] The key experiment in identifying whether this state is indeed the QSL is to establish that expected differences between the evolution of the fluctuations in transitions driven by pressure and those driven by temperature occur as predicted by theory.

Due to small sample volumes and strong neutron absorption,[25] tools to probe the continuum of excitations associated with a spin-liquid are currently limited, making novel x-ray tools particularly important.[26] Using the short wavelengths of hard x-rays, it is possible to use the x-ray scattering associated with the short-range AFM order to explore the magnetic order. The inhomogeneity in the electronic and magnetic phases of iridates spans distance scales from the atomic to macroscopic, which can be probed by a combination of XPCS and inelastic scattering experiments.[27,28]

The key experiments to track the collapse of long-range magnetic order and evolution of frustrated magnetic phases in iridates require the significant increase in coherent x-ray flux provided by the APS Upgrade. Definitive experiments must employ two approaches: 1) imaging the correlation of structural, electronic, and magnetic order under the influence of pressure and

2) tracking the spatial frequency and time dependence of fluctuations of the magnetic state when crossing the quantum phase transition associated with the disappearance of the long-range magnetic order. Electronic and magnetic resonant spectral features can be explored in both absorption and scattering and are applicable to imaging and scattering in the iridates.[29,37]

Imaging of magnetic phases with hard x-rays offers the ability to penetrate into complex sample environments, but have to date typically been limited to the micron scale,[30,31,32,33,34] largely due to the small signal levels associated with magnetic contrast. The crucial advance enabled by the APS-U lies in merging nanoscale x-ray probes with resonant enhancements of scattering signals from electronic and magnetic order.[35,36] Non-resonant magnetic scattering cross sections are extremely small in comparison with charge scattering. This is not only because the interactions leading to magnetic scattering are weak but also because magnetic form factors reflect the wide spatial distribution of magnetism around atoms and because magnetic moments are at most one Bohr magneton per atom. Together these effects reduce the intensity of non-resonant magnetic scattering by a factor of approximately 10^8 with respect to structural (i.e., Thomson scattering) x-ray reflections. Resonant scattering at the Ir L_3 edge at a photon energy of 11.21 keV provides enhancement of the magnetic signal by a factor of 100,[37,38] somewhat simplifying experiments, but this is not sufficient to enable magnetic coherent scattering at present sources. The high coherent flux of APS-U resolves this problem and uniquely enables hard x-ray coherent magnetic scattering.

Recently, sub-micron-scale structural imaging in high-pressure environments has been demonstrated; however, this work demanded the use of high-intensity structural Bragg peaks rather than comparatively weak magnetic reflections.[39] As will be highlighted below, the factor of 100 increase in coherent flux opens the ability to simultaneously improve spatial resolution and enable experiments that would otherwise involve prohibitively small signals. A second aspect of the use of coherent x-ray beams is to probe spatial and temporal fluctuations using XPCS. There are only a few reported studies of magnetism using hard x-ray XPCS,[40,41] limited largely because the signal with today's level of x-ray source coherence is prohibitively small.

The APS-U will enable the use of high-pressure sample environments in coherent scattering and imaging experiments. Spatially resolved studies of complex magnetic phases will become possible under simultaneous extremes of high pressure (up to 3 Mbar) and high magnetic field (14 T) at low temperature (1 K), as in Fig. 2. The small sample size required for such environments at present makes such experiments impossible with today's sources. A further important enabling advance of the APS-U is full polarization control of the x-rays generated by undulator insertion devices, which simplifies magnetic scattering experiments by enabling rapid and precise variation of the helicity of the incident beam. New strategies for the design of undulator insertion devices can be employed to create fast polarization switching sources, including

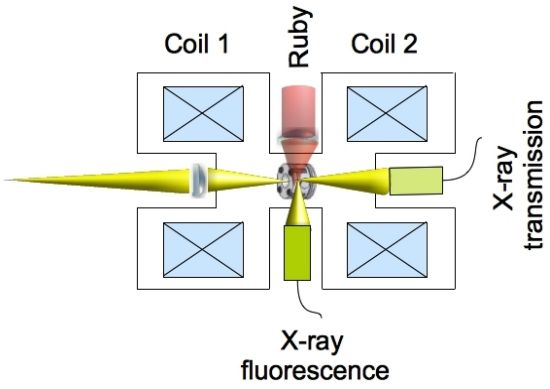

Fig. 2. High-magnetic-field/high-pressure study of quantum magnetism using x-ray dichroism contrast in absorption, imaging, and scattering.

helical superconducting undulators.[42] The use of lock-in detection in combination with novel insertion devices allows improved signal-to-background in experiments. Together, these advances in storage ring design and insertion devices will provide, for the first time, the ability to view the emergence and collapse of new magnetic and electronic phases in the iridates.

The feasibility of new types of experiments using resonant scattering coupled to coherent x-ray beams can be considered using the following estimates of magnetic scattering intensities in the iridates. Today, the intensity of a structural Bragg reflection of an iridate crystal is typically 10^8 photons/s, and the intensities of x-ray resonant magnetic scattering reflections are on the order of 10^2-10^3 photon/s. At present, reaching even these intensities requires using the full "incoherent" x-ray beam produced by the APS, consisting of about 10,000 coherent modes. To use a coherent beam today, extracting the coherent fraction would require a 10×10 μm^2 pinhole, reducing the overall flux by a factor of 10^4 from a 1×1 mm starting beam. At this point the count rate on the Bragg peak count is just 10^4 photons/sec and the peaks from charge, orbital, and magnetic order drop to 10^{-2} to 0.1 photons/sec. The APS-U will increase the coherent fraction to on the order of 10% in this energy range, bringing the Bragg peak count rate with a coherent beam to on the order of 10^6-10^7 cts/s and peaks from ordered electronic and magnetic phases up to 1 to 10 counts/sec. While the gain may not sound dramatic, this is in fact a dramatic game-changer that takes the scattering signals above the noise floor and makes feasible these types of experiments, which are impossible today.

7.3.B. Fluctuations in Correlated Electron Systems

Background and Motivations

Correlated electronic and magnetic materials often exhibit relationships between magnetic and electronic order parameters, resulting in a variety of emergent phenomena, such as superconductivity, magnetism, metal-insulator transitions, ferroelectricity, and orbital ordering. The competition between these order parameters also can lead to phase coexistence, between, for example, metallic and insulating phases, charge-ordered and superconducting phases, or ferromagnetic metal and antiferromagnetic insulator phases, as shown in Fig. 3. The resulting coexisting domains are typically nanoscale, often referred to as nanoscale inhomogeneities or nanoscale phase separation. Measurements of telegraph noise and other transport techniques indicate that many materials exhibit electronic fluctuations, or intermittent "avalanches," across a wide range of timescales, extending down to microseconds and nanoseconds, with timescales naturally becoming faster as the individual fluctuating domains become smaller, as for example in the magnetic critical fluctuations.[43] This size-dependence appears in the experimental results as the q-dependence of the dynamic structure factor $S(q,\omega)$.

One of the most famous examples of nanoscale electronic order is the ordering of hole carriers in underdoped cuprate superconductors into periodic conducting stripes in otherwise insulating host material.[44,45,46] There has been a recent surge of interest in understanding the mechanisms and energetics of these stripes and their formation, because doing so is likely to reveal how electronic correlations form in complex materials. The nature of the nanoscale fluctuating charge stripes in high-T_c superconductors can be probed by a combination of XPCS in the time domain and resonant inelastic x-ray scattering in the frequency domain. The characteristic excitation energy scale associated with stripe fluctuations is expected to be at the sub-10-meV

level, consistent with the observation of picosecond-scale dynamics of stripe fluctuations in ultrafast optical studies.[47] Therefore, extending resonant XPCS temporal resolution toward picosecond timescales is one of the most promising pathways for addressing the spatial component of this grand challenge.

The fluctuation approach applies to many other collective excitations, such as Goldstone modes in charge- or spin-density wave systems, Dirac excitations, superconducting vortices, Kondo resonances, and orbitons. Studying fluctuations of stripes and other collective phenomena by coupling directly to the dynamic structure factor $S(q,\omega)$ over a wide range of lengthscales and timescales is crucial to our understanding of the energetics involved in formation of these complex quantum phases of correlated matter. Several examples of phase separation and ordering phenomena are illustrated in Fig. 3.[48,49,50,51,52,53] Understanding fluctuations more completely eventually will provide guidance as to how these order parameters can be controlled to arrive at a given domain structure or to create specific dynamics to obtain some desired functionality. As a representative example of this class of questions, we here describe in detail a first experimental study of orbital order dynamics in doped manganites.

Scientific Objectives

Current studies of correlated electron system fluctuations are typically limited to timescales on the order of 10 ms and slower, constrained primarily by the lack of coherent flux and the weakly scattering nature of charge-, spin-, and orbital-order parameters, even if coupled to via a resonant enhancement.[54,30,] This is too slow to resolve much of the interesting dynamics in correlated electron systems, since characteristic "electronic" dynamics happens at nanosecond timescales or faster. As a result, XPCS and other coherent scattering techniques to date have largely targeted the "glassy", very slow relaxations that occur after very large collective states are formed—for example, macroscopic (tens of microns) charge-ordered or orbitally ordered domains that exhibit dynamics in the millisecond to kilosecond timescale range.

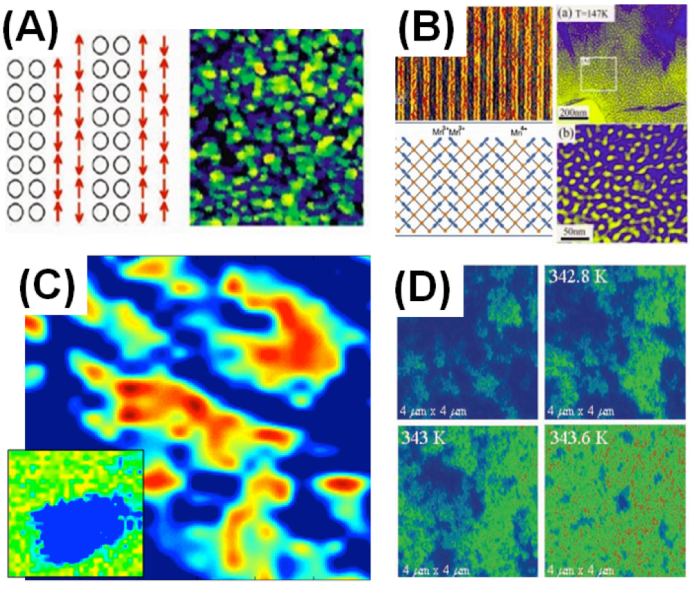

Fig. 3. Examples of nanoscale inhomogeneities in a variety of strongly correlated systems. (A) Scanning tunneling spectroscopy of the inhomogeneous super-conducting gap distribution as well as stripe (or checkerboard) patterns in underdoped high-T_c super-conductors. (B) Phase separation in colossal magnetoresistive (CMR) manganites. (C) Charge-density wave and spin-density wave (inset) domains in Cr. (D) Coexistence of conducting and insulating domains in VO_2 at the onset of the metal-insulator transition.

Experimental Details

Fluctuations in the orbital order of manganite oxides illustrate the potential of x-ray coherence to extend how we use dynamical information to understand phase transitions in systems with complex degrees of freedom. The 3d electrons of Mn ions in the perovskite manganites exhibit directional ordering in certain regimes of doping, temperature, and mechanical stress.[55] The properties of these orbital ordering phases and the "orbital physics" associated with their fluctuations have posed persistent challenges with long-recognized consequences for electronic and magnetic phenomena.[56] Fluctuations and short-range orbital order are important even in regimes of temperature and doping at which the orbital ordered phase is not stable.

X-rays are uniquely sensitive to orbital ordering via photon polarization analysis in resonant scattering experiments conducted with photon energies near the Mn K-edge near 6.55 keV. The scattering at these resonances is sufficiently strong to allow the basic phase diagram of orbital ordering to be determined with present-generation x-ray sources, including transition temperatures and doping and field-dependences, as in (Pr,Ca)MnO_3. [57] However, the mechanisms of phase transitions to the orbitally ordered phase, the scaling of fluctuation phenomena with temperature or doping, and the development of mesoscale spatial separation of charge and orbital domains have remained unknown, because answering such questions requires insight into the fluctuations of the orbital order. Other dynamical phenomena in manganite materials can be probed via inelastic techniques, which provide insight into spin wave and phonon dispersions. The highly coherent x-ray beams available from APS-U will provide insight into manganite orbital fluctuations and allow the development of orbital order within competing phases to be probed. Doing this will resolve the long-standing uncertainty associated with the role of orbital phenomena in the properties of manganites and will more generally demonstrate how understanding previously difficult-to-observe fluctuations addresses important physical problems.

Orbital order produces relatively strong scattering in comparison with that arising from other order parameters. High count rates will make it possible to study correlations at very short times, perhaps as short as times within the duration of a single pulse. Correlations within one pulse can be studied at the signal-to-noise statistics as correlations between two individual pulses.[58] With this approach, it will be possible to track the local evolution of $S(q,\omega)$ at unprecedented timescales, down to 100 ps; this corresponds to fluctuations far from the critical temperatures of the phase transition. This would imply potentially getting to 100 ps temporal resolution, enabling measurements of collective excitation in charge-stripe or magnetic or orbital domain systems over temporal scales extending across more than 13 orders of magnitude (from 100 ps to hours and beyond).

7.3.C. Dynamic Control of Novel Ferroelectric Polarization States

Background and Motivations

In the time domain, complex materials exhibit a time-dependent, free-energy surface that generally has a large number of non-equilibrium minima, as in Fig. 4(a), representing new states that do not exist under steady-state conditions. It remains challenging to systematically drive materials into these states so that they can be fully characterized and rational paradigms developed to stabilize them. The APS-U will offer new capabilities to visualize dynamic phenomena at nanometer lengthscales over timescales ranging from tens or hundreds of picoseconds to hours, making it possible to accurate follow condensed matter systems as they traverse a non-equilibrium energy landscape and providing crucial insights that will better allow us to intelligently manipulate and stabilize novel states.

One of the most powerful stabilization approaches is the use of interfacial stress and bonding as additional degrees of freedom in synthesis (Fig. 4(b)).[59,60] A powerful example of such strain engineering is the creation of novel polarization states in ferroelectric superlattices.[61] The boundary-avoiding vortex domain is a long sought-after topological defect possible in nanoscale ferroelectrics, but not in the bulk. Vortex states are of general interest in condensed matter because similar geometric motifs appear in magnetism,[62] superconductivity,[63] and polar materials.[64] A recently discovered ferroelectric vortex-like state occurs as an ordered lattice of nanoscale polar vortices in the $PbTiO_3$ layers of a $PbTiO_3/SrTiO_3$ superlattice heterostructure.[4] By confining an array of ferroelectric vortex states with alternating chirality within the $PbTiO_3$ layers, well-ordered arrays of confined vortices with sizes in the range of 10 nm are stabilized throughout the individual layers of such superlattices, in agreement with phase-field simulations shown in Fig. 5(a). The domains in such heterostructures can be manipulated with applied electric fields, including via a transition to a uniform polarization state. Metastable structural configurations can be induced during such a transformation.[5,65]

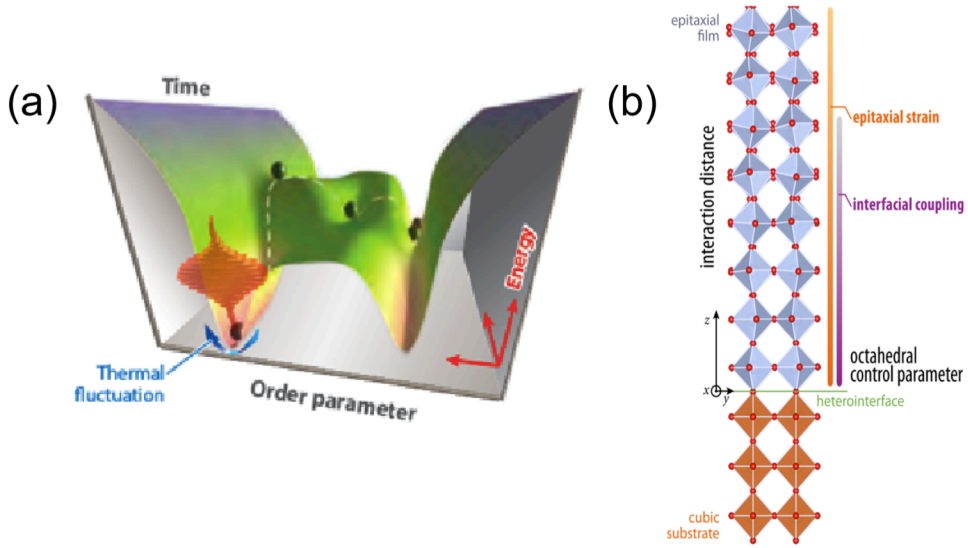

Fig. 4. (a) Complex non-equilibrium landscape and local minima accessible for complex systems.[53] (b) Strain imposed via epitaxy enables access to distinct crystalline phases and subsequent properties.[59,59]

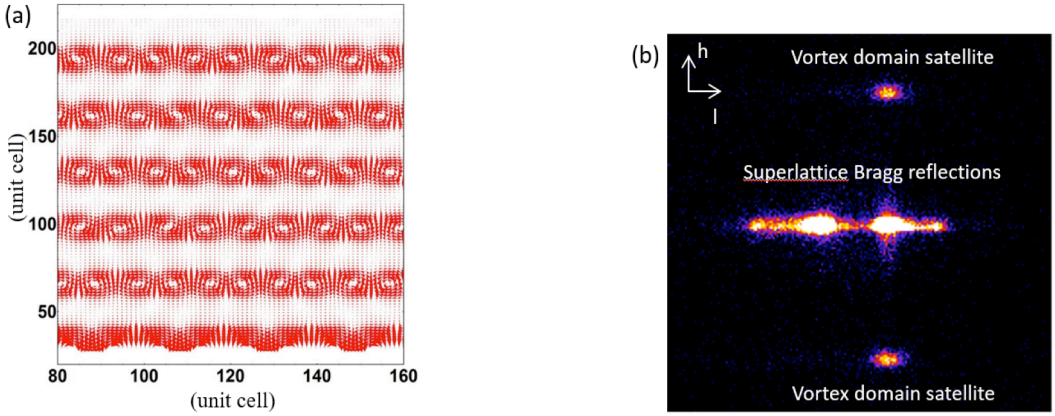

Fig. 5. (a) Phase field simulation of confined vortex states in a $PbTiO_3)_{16}/(SrTiO_3)_{16}$ superlattice heterostructure indicating the local polarization vector versus unit cell dimensions. (b) Reciprocal space image near the (002) Bragg reflection showing superlattice reflections and diffuse scattering satellites arising from vortex domain scattering.

While the local static structure of ferroelectric vortices has recently been a subject of intense study,[4,61,66,67,68] the *in situ* determination of their behavior under external stimuli has been a challenge. Understanding how to control these ferroelectric states at the nanometer scale, where confined atomic scale interactions can generate new properties, may reveal their potential for a plethora of possible applications, such as dense non-volatile memory, based on new mechanisms and novel ultrafast responses such as domain reorientation through motion of chiral walls through chiral fields, unusual transport behavior through the cores of vortices[69], and low-field switching[70]. Such vortices also may prove useful as templates for rational fabrication targeting high-efficiency photovoltaics,[71,72] or ultrafast photodetectors.[73]

Scientific Objectives

The intrinsic response of topological defects when driven into a non-equilibrium state is largely unknown today. Quantitative analysis of time-dependent coherent diffraction experiments will answer the following questions: 1) What is the intrinsic timescale and response of unit cells and vortex domains upon ultrafast excitation? What is the role of domains in non-equilibrium structural states? 2) Are the vortex domains topologically protected against an external perturbation? Are there engineered optical excitations that can effectively control this ordered state? 3) What is the relation between the ferroelectric polarization and the local strain, in a case such as this in which mean-field descriptions of order parameter coupling are expected to fail? The enhanced brightness of the APS-U will enable the new tools needed to greatly advance our knowledge of topological defects and will allow us to harness their potential for applications.

Experimental Details

High-resolution ptychographic techniques recently have been demonstrated for imaging strain[74] and ferroelectric[75] nanodomains hidden within a larger measurement volume. However, state-of-the-art coherent x-ray diffractive imaging is able to retrieve the spatial distribution of domains only in limited model systems, due to the lack of coherent flux.[75] The quantitative measurement of more complex or unknown domain structures remains prohibitively difficult at the APS today,

let alone imaging the dynamics of ferroelectric vortices. These new sets of experiments will be enabled by the APS-U.

This improvement in coherent flux is critical for quantitative studies of thin film ferroelectric samples using x-ray Bragg projection ptychography. Smaller features and more complex structures can be imaged after the upgrade to the MBA lattice. X-ray diffraction at the APS with a 10-μm-diameter x-ray beam (Fig. 5(b)) shows that the scattering efficiency of the diffuse scattering arising from the vortex domains is 10^{-6} with respect to the Bragg peak.

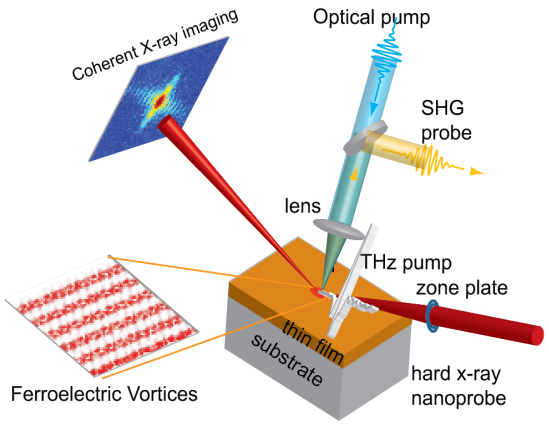

Fig. 6. Time-resolved coherent x-ray scattering and imaging experiment in combination with selective excitation at optical or THz frequencies.

Using a Fresnel zone plate-focused x-ray probe, there are 10^3 photons/sec arriving at the x-ray detector at the current APS. This flux is two orders of magnitude smaller than that used in the recent coherent x-ray imaging of standard ferroelectric domains, increasing the nominal data collection time from hours to weeks; a study of this length simply is not feasible, given instrumental instability such as mechanical and thermal drift and the noise level of today's detectors. The APS-U will increase the scattering signal from vortex domains to 10^5 photons/sec, providing sufficient signal-to-noise ratio to image ferroelectric vortices. In addition, to utilize the bunch structure of the APS-U for time-resolved studies, pump-probe techniques can be employed to capture the evolution of the vortex state at a 6.5-MHz repetition rate. The excitation can be either above-band-gap optical pulses or picosecond electric field pulses in the form of broadband THz radiation that directly couples to the ferroelectric polarization (Fig. 6). A sequence of snapshots of ferroelectric vortices imaged by coherent x-ray pulses will reveal the local strain state due to chiral polarization rotation and therefore the anisotropic response of the lattice upon excitation.

7.4 Operational and Instrumentation Needs

In addition to the necessary beamline optics upgrades essential to preserve the coherence of x-rays made by the upgraded MBA lattice and the enhanced detectors needed for fast readout, reduced pixel size, and increased sensitivity (all of which are discussed in detail in the previous chapters), condensed matter physics has some specific needs connected to the APS-U.

Polarized Superconducting Undulator Sources

A key requirement for the study of magnetic materials is the ability to generate x-rays with left- or right-circular polarization and to switch easily between the two. Such tunable polarization in the hard x-ray regime is usually achieved either with phase-retarding optics or Apple-II type undulators, both of which have significant drawbacks. One potential solution is the universal helical superconducting undulator, Fig. 7, which allows for full polarization control directly at the source, delivers equal intensities of LCP and RCP (or L-H and L-V) beams, and has the potential to allow for fast (> 10 Hz) polarization switching.[76] The helical undulator device uses

bifilar windings in inner and outer coils, with the oppositely circulating currents in each coil resulting in very low self-inductance, facilitating fast polarization switching. Magnetic simulations of helical devices confirm that necessary peak field (K) values and optimal tuning curves can be achieved with realistic parameters for inner and outer winding bores and available (low-T_c) superconducting wire.[77] Prospects for using high-T_c superconducting wire to increase switching frequency are being explored. A double helical superconducting device was built for early free-electron laser research.[42]

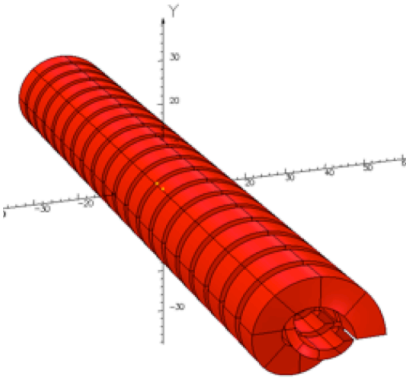

Fig 7. Model of helical super-conducting undulator: peak current 1000 A/mm^2 and peak field of 1.36 T are achievable with 6-mm and 11-mm winding bores.[77]

High Pressure Environments for Magnetism and Scattering

To date there have been impressive technical achievements in the use of x-ray techniques to study magnetism in high-pressure environments. Low-temperature polarized x-ray spectroscopy has been developed as a probe of ferromagnetic order to 0.8 Mbar,[78,79,80] and non-resonant x-ray magnetic scattering has been used to probe antiferromagnetic ordering in materials carrying large magnetic moments to 0.16 Mbar.[81] So far, however, it has not been possible to address simultaneously two important challenges: (1) reaching pressures into the several Mbar range and (2) mapping electronic/magnetic nano- and mesoscale inhomogeneity at high pressures in real space using resonant scattering and polarized spectroscopy techniques. Impediments to reaching high pressures include x-ray attenuation in diamond anvil cells (DACs) at the resonant energies of interest (3-15 keV energy range) and constraints imposed by the large angular apertures needed to access significant swaths of reciprocal space at these energies. The use of perforated DACs together with panoramic DACs with large optical access offers opportunities to bypass these limitations (Fig. 8).[81, 82, 83, 84] However, anvil perforation reduces the strength of diamond and limits ultimate pressures to about a factor of 2-3 lower than achievable with full anvils of the same culet size (area of maximal pressure).

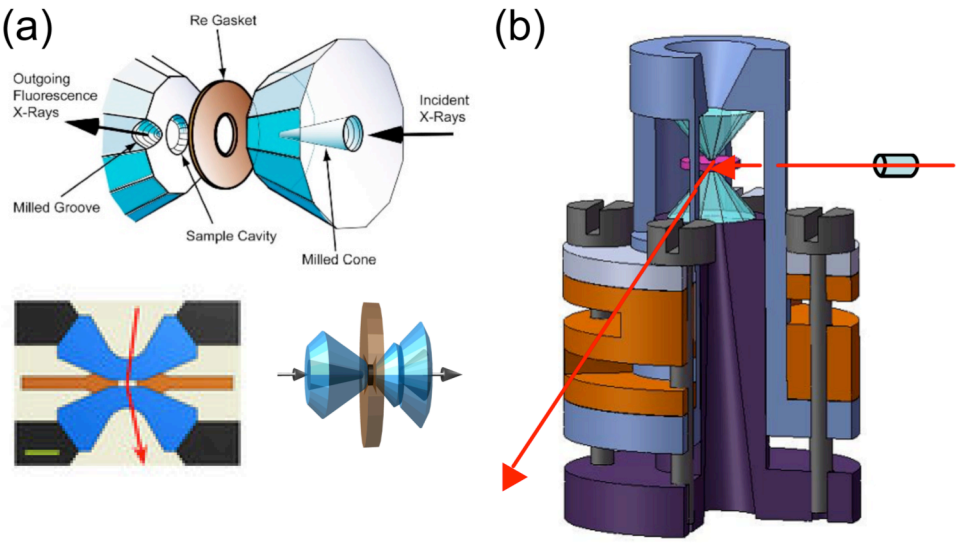

Fig. 8. (a) Diamond anvil perforations reduce attenuation and background in absorption and scattering experiments.[82] (b) Panoramic DAC allows access to large swaths of reciprocal space.[81]

Two sets of magnets are required. For mapping electronic/magnetic inhomogeneity in single crystals using resonant scattering, simultaneous conditions of high pressure (~1 Mbar), low temperature (~1.5 K), and modest magnetic fields (~1 T) can be achieved with small, short-working-distance magnets. The limited magnetic field is necessary to preserve a small working distance to the x-ray optics (~100 mm), which is required to enable maximum spatial resolution (~50 nm). Mapping electronic/magnetic inhomogeneity in other less ideal systems requires simultaneous extremes of high pressure (up to 3 Mbar) and high magnetic field (14 T), at low temperature (~1 K). Two large-bore, cryogenic superconducting magnets with horizontal and vertical fields, respectively, will be used for these studies. The spatial resolution is expected to be in the 200-nm range, a result of the longer working distance (~400 mm) required to accommodate the large superconducting magnets.

Time-Resolved Multimodal Imaging

The incorporation of time-resolved techniques requires the design and creation of x-ray nanobeam instruments incorporating optical and THz excitation. Such an instrument can, in principle, include time-resolved near-field THz imaging, an optical microscope, and a versatile atomic-force microscope-based imaging system to identify regions of interest for further study.[85,86] Time-resolved hard x-ray imaging techniques will include the full-field reflective x-ray microscope[87,88] and coherent x-ray imaging,[89] as well as scanning fluorescence and diffraction.

7.5 References

[1] W. Jiang, P. Upadhyaya, W. Zhang, G. Yu, M. B. Jungfleisch, F. Y. Fradin, J. E. Pearson, Y. Tserkovnyak, K. L. Wang, O. Heinonen, S. G. E. te Velthuis, and A. Hoffmann, Science **349**, 283 (2015).

[2] S.-Y. Xu, I. Belopolski, N. Alidoust, M. Neupane, G. Bian, C. Zhang, R. Sankar, G. Chang, Z. Yuan, C.-C. Lee, S.-M. Huang, H. Zheng, J. Ma, D. S. Sanchez, B. Wang, A. Bansil, F. Chou, P. P. Shibayev, H. Lin, S. Jia, and M. Z. Hasan, Science **349**, 613 (2015).

[3] A. P. Drozdov, M. I. Eremets, I. A. Troyan, V. Ksenofontov, and S. I. Shylin, Nature **525**, 73 (2015).

[4] Y. L. Tang, Y. L. Zhu, X. L. Ma, A. Y. Borisevich, A. N. Morozovska, E. A. Eliseev, W. Y. Wang, Y. J. Wang, Y. B. Xu, Z. D. Zhang, and S. J. Pennycook, Science **348**, 547 (2015).

[5] J. Y. Jo, P. Chen, R. J. Sichel, S. J. Callori, J. Sinsheimer, E. M. Dufresne, M. Dawber, and P. G. Evans, Phys. Rev. Lett. **107**, 055501 (2011).

[6] W. Witczak-Krempa, G. Chen, Y. B. Kim, and L. Balents, Ann. Rev. Cond. Mat. Phys. **5**, 57 (2014).

[7] L. Balents, Nature **464**, 199 (2010).

[8] F. L. Pratt, P. J. Baker, S. J. Blundell, T. Lancaster, S. Ohira-Kawamura, C. Baines, Y. Shimizu, K. Kanoda, I. Watanabe, and G. Saito, Nature **471**, 612 (2011).

[9] A. Kitaev, Ann. Phys.-New York **321**, 2 (2006).

[10] X. Liu, T. Berlijn, W.-G. Yin, W. Ku, A. Tsvelik, Y.-J. Kim, H. Gretarsson, Y. Singh, P. Gegenwart, and J. P. Hill, Phys. Rev. B. **83**, 220403 (2011).

[11] S. H. Chun, J.-W. Kim, J. Kim, H. Zheng, C. C. Stoumpos, C. D. Malliakis, J. F. Mitchell, K. Mehlawat, Y. Singh, Y. Choi, T. Gog, A. Al-Zein, M. Moretti Sala, M. Krisch, J. Chaloupka, G. Jackeli, G. Khaliullin, and B. J. Kim, Nat. Phys. **11**, 462 (2015).

[12] T. Takayama, A. Kato, R. Dinnebier, J. Nuss, H. Kono, L. S. I. Veiga, G. Fabbris, D. Haskel, and H. Takagi, Phys. Rev. Lett. **114**, 077202 (2015).

[13] M. Ge, T. F. Qi, O. B. Korneta, D. E. De Long, P. Schlottmann, W. P. Crummett, and G. Cao, Phys Rev B **84**, 100402 (2011).

[14] X. Chen, T. Hogan, D. Walkup, W. Zhou, M. Pokharel, M. Yao, W. Tian, T. Z. Ward, Y. Zhao, D. Parshall, C. Opeil, J. W. Lynn, V. Madhavan, and S. D. Wilson, Phys. Rev. B **92**, 075125 (2015).

[15] J. Kim, D. Casa, M. H. Upton, T. Gog, Y.-J. Kim, J. F. Mitchell, M. Van Veenendaal, M. Daghofer, J. van den Brink, G. Khaliullin, and B. J. Kim, Phys. Rev. Lett. **108**, 177003 (2012).

[16] F. Wang and T. Senthil, Phys. Rev. Lett. **106**, 136402 (2011).

[17] Y.-Z. You, I. Kimchi, and A. Vishwanath, Phys. Rev. B **86**, 085145 (2012).

[18] H. Watanabe, T. Shirakawa, and S. Yunoki, Phys. Rev. Lett. **110**, 027002 (2013).

[19] Z. Y. Meng, Y. B. Kim, and H.-Y. Kee, Phys. Rev. Lett. **113**, 177003 (2014).

[20] J. F. Mitchell, APL Mater. **3**, 062404 (2015).

[21] Y. K. Kim, O. Krupin, J. D. Denlinger, A. Bostwick, E. Rotenberg, Q. Zhao, J. F. Mitchell, J. W. Allen, and B. J. Kim, Science **345**, 187 (2014).

[22] J. He, H. Hafiz, T. R. Mion, T. Hogan, C. Dhital, X. Chen, Q. Lin, M. Hashimoto, D. H. Lu, Y. Zhang, R. S. Markiewicz, A. Bansil, S. D. Wilson, and R.-H. He, Sci. Rep. **5**, 8533 (2015).

[23] Y. K. Kim, N. H. Sung, J. D. Denlinger, and B. J. Kim, arXiv: 1506.06639v2 (2015).

[24] J. Knolle, G.-W. Chern, D. L. Kovrizhin, R. Moessner, and N. B. Perkins, Phys. Rev. Lett. **113**, 187201 (2014).

[25] M. C. Shapiro, S. C. Riggs, M. B. Stone, C. R. de la Cruz, S. Chi, A. A. Podlesnyak, and I. R. Fisher, Phys. Rev. B **85**, 214434 (2012).

[26] T.-H. Han, J. S. Helton, S. Chu, D. G. Nocera, J. A. Rodriguez-Rivera, C. Broholm, and Y. S. Lee, Nature **492**, 406 (2012).

[27] C. Dhital, T. Hogan, W. Zhou, X. Chen, Z. Ren, M. Pokharel, Y. Okada, M. Heine, W. Tian, Z. Yamani, C. Opeil, J. S. Helton, J. W. Lynn, Z. Wang, V. Madhavan, and S. D. Wilson, Nature Comm. **5**, (2014).

[28] S. Tardif, S. Takeshita, H. Ohsumi, J.-I. Yamaura, D. Okuyama, Z. Hiroi, M. Takata, and T.-H. Arima, Phys. Rev. Lett. **114**, 147205 (2015).

[29] M. Laguna-Marco, D. Haskel, N. Souza-Neto, J. Lang, V. Krishnamurthy, S. Chikara, G. Cao, and M. Van Veenendaal, Phys. Rev. Lett. **105**, 216407 (2010).

[30] P. G. Evans, E. D. Isaacs, G. Aeppli, Z. Cai, and B. Lai, Science **295**, 1042 (2002).

[31] P. G. Evans and E. D. Isaacs, J. Phys. D: Appl. Phys. **39**, R245 (2006).

[32] J. M. Logan, H. C. Kim, D. Rosenmann, Z. Cai, R. Divan, O. G. Shpyrko, and E. D. Isaacs, Appl. Phys. Lett. **100**, 192405 (2012).

[33] R. D. Johnson, P. Barone, A. Bombardi, R. J. Bean, S. Picozzi, P. G. Radaelli, Y. S. Oh, S.-W. Cheong, and L. C. Chapon, Phys. Rev. Lett. **110**, 217206 (2013).

[34] M. Suzuki, N. Kawamura, M. Mizumaki, Y. Terada, T. Uruga, A. Fujiwara, H. Yamazaki, H. Yumoto, T. Koyama, Y. Senba, T. Takeuchi, H. Ohashi, N. Nariyama, K. Takeshita, H. Kimura, T. Matsushita, Y. Furukawa, T. Ohata, Y. Kondo, J. Ariake, J. Richter, P. Fons, O. Sekizawa, N. Ishiguro, M. Tada, S. Goto, M. Yamamoto, M. Takata, and T. Ishikawa, J. Phys.: Conf. Ser. **430**, 012017 (2013).

[35] J. P. Hill and D. F. McMorrow, Acta Cryst. A **52**, 236 (1996).

[36] T. Matsumura, H. Nakao, and Y. Murakami, J. Phys. Soc. Jpn. **82**, 021007 (2013).

[37] B. J. Kim, H. Ohsumi, T. Komesu, S. Sakai, T. Morita, H. Takagi, and T. Arima, Science **323**, 1329 (2009).

[38] D. Haskel, G. Fabbris, M. Zhernenkov, P. P. Kong, C. Q. Jin, G. Cao, and M. van Vennendaal, Phys. Rev. Lett. **109**, 027204 (2012).

[39] Y. Ding, Z. Cai, Q. Hu, H. Sheng, J. Chang, R. J. Hemley, and W. L. Mao, Appl. Phys. Lett. **100**, 041903 (2012).

[40] F. Yakhou, A. Létoublon, F. Livet, M. de Boissieu, and F. Bley, J. Magn. Magn. Mater. **233**, 119 (2001).

[41] J. A. Lim, E. Blackburn, G. Beutier, F. Livet, N. Magnani, A. Bombardi, R. Caciuffo, and G. H. Lander, J. Phys.: Conf. Ser. **519**, 012010 (2014).

[42] L. R. Elias and J. M. Madey, Rev. Sci. Instrum. **50**, 1335 (1979).

[43] H. Sato and K. Maki, Int. J. Magn. **6**, 183 (1974).

[44] J. M. Tranquada, B. J. Sternlieb, J. D. Axe, Y. Nakamura, and S. Uchida, Nature **375**, 561 (1995).

[45] P. Abbamonte, A. Rusydi, S. Smadici, G. D. Gu, G. A. Sawatzky, and D. L. Feng, Nat. Phys. **1**, 155 (2005).

[46] G. Ghiringhelli, M. Le Tacon, M. Minola, S. Blanco-Canosa, C. Mazzoli, N. B. Brookes, G. M. De Luca, A. Frano, D. G. Hawthorn, F. He, T. Loew, M. Moretti Sala, D. C. Peets, M. Salluzzo, E. Schierle, R. Sutarto, G. A. Sawatzky, E. Weschke, B. Keimer, and L. Braicovich, Science **337**, 821 (2012).

[47] D. H. Torchinsky, F. Mahmood, A. T. Bollinger, I. Bozovic, and N. Gedik, Nature Mater. **12**, 387 (2013).

[48] T. Hanaguri, C. Lupien, Y. Kohsaka, D.-H. Lee, M. Azuma, M. Takano, H. Takagi, and J. C. Davis, Nature **430**, 1001 (2004).

[49] S. Mori, C. H. Chen, and S.-W. Cheong, Nature **392**, 473 (1998).

[50] M. Uehara, S. Mori, C. H. Chen, and S.-W. Cheong, Nature **399,** 560 (1999).

[51] F. Ye, J. A. Fernandez-Baca, P. Dai, J. W. Lynn, H. Kawano-Furukawa, H. Yoshizawa, Y. Tomioka, and Y. Tokura, Phys. Rev. B **72**, 212404 (2005).

[52] M. M. Qazilbash, M. Brehm, B.-G. Chae, P.-C. Ho, G. O. Andreev, B.-J. Kim, S. J. Yun, A. V. Balatsky, M. B. Maple, F. Keilmann, H.-T. Kim, and D. N. Basov, Science **318**, 1750 (2007).

[53] J. Zhang and R. D. Averitt, Ann. Rev. Mater. Res. **44**, 19 (2014)

[54] O. G. Shpyrko, E. D. Isaacs, J. M. Logan, Y. Feng, G. Aeppli, R. Jaramillo, H. C. Kim, T. F. Rosenbaum, P. Zschack, M. Sprung, S. Narayanan, and A. R. Sandy, Nature **447**, 68 (2007).

[55] J. F. Mitchell, D. N. Argyriou, and J. D. Jorgensen, "*Structural Response to Orbital, Spin, and Charge Ordering in Colossal Magnetoresistive Materials*," in *Colossal magnetoresistive oxides*, Y. Tokura, ed. Gordon and Breach (2000).

[56] Y. Tokura and N. Nagaosa, Science **288**, 462 (2000).

[57] S. Grenier, J. P. Hill, D. Gibbs, K. J. Thomas, M. v. Zimmermann, C. S. Nelson, V. Kiryukhin, Y. Tokura, Y. Tomioka, D. Casa, T. Gog, and C. Venkataraman, Phys. Rev. B **69**, 134419 (2004).

[58] J. Wingert, A. Singer, and O. G. Shpyrko, J. Synchrotron Rad. **22**, 1141 (2015).

[59] J. Rondinelli, S. May, and J. Freeland, MRS Bull. **37**, 261 (2012).

[60] J. Chakhalian, J. W. Freeland, A. J. Millis, C. Panagopoulos, and J. M. Rondinelli, Rev. Mod. Phys. **86**, 1189 (2014).

[61] D. Lee, R. K. Behera, P. Wu, H. Xu, Y. L. Li, S. B. Sinnott, L. Q. Chen, and V. Gopalan, Phys. Rev. B, **80**, 060102 (2009).

[62] S. Mühlbauer, B. Binz, F. Jonietz, C. Pfleiderer, A. Rosch, A. Neubauer, R. Georgii, and P. Böni, Science **323**, 915 (2009).

[63] D. F. Agterberg and H. Tsunetsugu, Nature Phys. **4**, 639 (2008).

[64] C. T. Nelson, B. Winchester, Y. Zhang, S. J. Kim, A. Melville, C. Adamo, C. M. Folkman, S. H. Baek, C. B. Eom, D. G. Schlom, L. Q. Chen, and X. Q. Pan, Nano Lett. **11**, 828 (2011).

[65] P. Chen, M. P. Cosgriff, Q. Zhang, S. J. Callori, B. W. Adams, E. M. Dufresne, M. Dawber, and P. G. Evans, Phys. Rev. Lett. **110**, 047601 (2013).

[66] C. M. Wu, W. J. Chen, Y. Zheng, D. C. Ma, B. Wang, J. Y. Liu, and C. H. Wood, Sci. Rep. **4**, 3946 (2014).

[67] M. G. Stachiotti and M. Sepliarsky, Phys. Rev. Lett. **106**, 137601 (2011).

[68] C.-L. Jia, K. W. Urban, M. Alexe, D. Hesse, and I. Vrejoiu, Science **331**, 1420 (2011).

[69] N. Balke, B. Winchester, W. Ren, Y. H. Chu, A. N. Morozovska, E. A. Eliseev, M. Huijben, R. K. Vasudevan, P. Maksymovych, J. Britson, S. Jesse, I. Kornev, R. Ramesh, L. Bellaiche, L. Q. Chen, and S. V. Kalinin, Nat. Phys. **8**, 81 (2012).

[70] E. K. H. Salje and J. F. Scott, Appl. Phys. Lett. **105**, 252904 (2014).

[71] S. Y. Yang, J. Seidel, S. J. Byrnes, P. Shafer, C. H. Yang, M. D. Rossell, P. Yu, Y. H. Chu, J. F. Scott, J. W. Ager, L. W. Martin, and R. Ramesh, Nat. Nanotechnol. **5**, 143 (2010).

[72] A. Zenkevich, Y. Matveyev, K. Maksimova, R. Gaynutdinov, A. tolstikhina, and V. Fridkin, Phys. Rev. B **90**, 161409 (2014).

[73] D. Daranciang, M. J. Highland, H. Wen, S. M. Young, N. C. Brandt, H. Y. Hwang, M. Vattilana, M. Nicoul, F. Quirin, J. Goodfellow, T. Qi, I. Grinberg, D. M. Fritz, M. Cammarata, D. Zhu, H. T. Lemke, D. A. Walko, E. M. Dufresne, Y. Li, J. Larsson, D. A. Reis, K. Sokolowski-Tinten, K. A. Nelson, A. M. Rappe, P. H. Fuoss, G. B. Stephenson, and A. M. Lindenberg, Phys. Rev. Lett. **108**, 087601 (2012).

[74] S. O. Hruszkewycz, M. V. Holt, C. E. Murray, J. Bruley, J. Holt, A. Tripathi, O. G. Shpyrko, I. McNulty, M. J. Highland, and P. H. Fuoss, Nano Lett. **12**, 5148 (2012).

[75] S. O. Hruszkewycz, M. J. Highland, M. V. Holt, D. Kim, C. M. Folkman, C. Thompson, A. Tripathi, G. B. Stephenson, S. Hong, and P. H. Fuoss, Phys. Rev. Lett. **110**, 177601 (2013).

[76] D. F. Alferov, Y. A. Bashmakov, and E. G. Bessonov, Zh. Tkh. Fiz **46**, 2392 (1976).

[77] Y. Ivanyushenkov, private communication (2015).

[78] W. Bi, N. M. Souza-Neto, D. Haskel, G. Fabbris, E. E. Alp, J. Zhao, R. G. Hennig, M. M. Abd-Elmeguid, Y. Meng, R. W. McCallum, K. Dennis, and J. S. Schilling, Phys. Rev. B **85**, 205134 (2012).

[79] D. Haskel, Y. C. Tseng, J. C. Lang, and S. Sinogeikin, Rev. Sci. Instrum. **78**, 083904 (2007).

[80] D. Haskel, Y. C. Tseng, N. M. Souza-Neto, J. C. Lang, S. Sinogeikin, Y. Mudryk, K. A. Geschneider, and V. K. Pecharsky, High Press. Res. **28**, 185 (2008).

[81] Y. J. Feng, J. Y. Yang, A. Palmer, J. A. Aguiar, B. Mihalia, J. Q. Yan, P. B. Littlewood, and T. F. Rosenbaum, Nat. Comm. **5**, 4218 (2014).

[82] R. A. Mayanovic, A. J. Anderson, W. A. Bassett, and I.-M. Chou, Rev. Sci. Instrum. **78**, 053904 (2007).

[83] A. Dadashev, M. P. Pasternak, G. K. Rozenberg, and R. D. Taylor, Rev. Sci. Instrum. **72**, 2633 (2001).

[84] A. G. Gavriliuk, A. A. Mironovich, and V. V. Struzkhin, Rev. Sci. Instrum. **80**, 043906 (2009).

[85] A. J. Huber, F. Keilmann, J. Wittborn, J. Aizpurua, and R. Hillenbrand, Nano Lett. **8**, 3766 (2008).

[86] J. Levy, V. Nikitin, J. M. Kikkawa, A. Cohen, N. Samarth, R. Garcia, and D. D. Awschalom, Phys. Rev. Lett. **76**, 1948 (1996).

[87] P. Fenter, C. Park, Z. Zhang, and S. Wang, Nat. Phys. **2**, 700 (2006).

[88] N. Laanait, Z. Zhang, C. M. Schlepütz, J. Vila-Comamala, M. J. Highland, and P. Fenter, J. Synchrotron Radiat. **21**, 1252 (2014).

[89] S. O. Hruszkewycz, M. J. Highland, M. V. Holt, D. Kim, C. M. Folkman, C. Thompson, A. Tripathi, G. B. Stephenson, S. Hong, and P. H. Fuoss, Phys. Rev. Lett. **110**, 177601 (2013).